Emilie Beaudon

GLACIOCHEMICAL EVIDENCE OF SPATIAL AND TEMPORAL ENVIRONMENTAL VARIABILITY ACROSS SVALBARD

Supervised by
Professor John Moore
Professor Paavo Perämäki

Opponent
Adjunct professor Christian Zdanowicz

Examiners
Professor Karl Kreutz
Doctor Valérie Masson-Delmotte

Publisher
Lapland University Press

Series editor
Jukka Jokimaki

Cover photos
Front: IPY KINNVIKA/ Emilie Beaudon
Back: Didier Boutonnet (Adélie Land)

Layout
Annika Hanhivaara
(Cover: Iines Partanen)

Sales
Academic and Art Bookshop Tila
University of Lapland
P.O.Box 8123
FI-96101 Rovaniemi
phone +358 40 821 4242
fax +358 16 362 932

publications@ulapland.fi
www.ulapland.fi/lup

University of Lapland Printing Centre, Rovaniemi 2012

ISNN 1235-0583
ISBN 978-952-484-562-5 (printed)
ISBN 978-952-484-563-2 (pdf)

Arctic Centre Reports 58

Emilie Beaudon

GLACIOCHEMICAL EVIDENCE OF SPATIAL AND TEMPORAL ENVIRONMENTAL VARIABILITY ACROSS SVALBARD

Faculty of Science, Department of Chemistry, University of Oulu

Academic Dissertation to be presented with the assent of the Faculty of Science, University of Oulu, for public discussion in Arktikum (Polarium), Rovaniemi, on September 14th, 2012, at 12 noon.

P.O. Box 3000
FI-90014
University of Oulu
Finland

Arctic Centre
University of Lapland
PO Box 122
FI-96101 Rovaniemi
Finland

LAPLAND UNIVERSITY PRESS
LAPIN YLIOPISTOKUSTANNUS
ROVANIEMI 2012

“Ceux qui lisent dans la glace y croisent
le passé et l’avenir du monde. Ecoutons-les.”

Isabelle Autissier

Emilie Beaudon:
Jäätikköjään kemiallinen koostumus Huippuvuorten
ympäristöolosuhteiden ajallisten ja paikallisten vaihteluiden ilmentäjänä

Oulun yliopiston luonnontieteellinen tiedekunta,
Kemian laitos, PL 3000, FI-90014, Oulun yliopisto.

TIIVISTELMÄ

Huippuvuorten lakijäätiköiltä kairatut jäänäytteet ovat osoittautuneet hyödyllisiksi arkistoiksi, jotka kattavat useita vuosisatoja ja kertovat Barentsin alueen paleoympäristöstä sekä alueen ilmaston kytköksistä Euroopan arktisiin alueisiin. Länsi-Huippuvuorten Holtedahlfonna-jäätiköltä ja Nordaustlandetin Vestfonna-jäätiköltä otetuista lumi-, firn- ja jääkairasydännäytteistä analysoitiin vesiliukoisten ionien pitoisuuksia (Na^+, NH_4^+, K^+, Mg^{2+}, Ca^{2+}, $CH_3SO_3^-$, Cl^-, SO_4^{2-}, NO_3^-) ja hapen isotooppikoostumus, ja tulosten avulla tutkittiin ympäristöolosuhteiden vaihtelua Huippuvuorilla ajallisesti ja paikallisesti. Vertaamalla systemaattisesti eri tutkimuskohteiden paikallisia kerrostumisenjälkeisiä olosuhteita ja prosesseja (tuuliolosuhteet, eroosio, sulaminen, vesihöyryn diffuusio), niiden vaikutus pystyttiin erottamaan puhtaasti ilmastollisista tekijöistä.

Holtedahlfonnan 125 metriä pitkä jääkairanäyte on toistaiseksi kattavin glasiokemiallinen arkisto läntisiltä Huippuvuorilta. Vaurioituneet vuosikerrokset ja tuntematon jäätikön paksuus aiheuttivat kuitenkin ongelmia jääkairasydämen ajoituksessa. Tämän takia kehitettiin uusi ajoitusmenetelmä, jossa eroteltiin tilastollisesti vulkaanisperäisen sulfaatin osuus kokonaissulfaatin määrästä. Menetelmää testattiin Holtedahfonnan jääkairasydämeen ja neljään polaarialueen ulkopuolelta kairattuun jääkairasydämeen. Menetelmä poistaa havaittujen sulfaattipiikkien vulkaanisen/ei-vulkaanisen alkuperän määrittämiseen liittyvät epävarmuudet, ja toimii erityisen hyvin silloin, kun vulkaanisperäistä sulfaattia on huomattavasti enemmän kokonaismäärästä kuin antropogeenistä eli ihmisen toiminnasta syntynyttä sulfaattia. Menetelmän avulla Holtedahlfonnan 305 vuotta (1700-2005) kattavasta jääkairasydämestä, joka ulottuu pienen jääkauden loppuun, saatiin viisi ajoitusta (mukaan lukien 103 metrin syvyydessä sijaitseva Laki-horisontti vuodelta 1783) huolimatta siitä, että vain 1,4 % sulfaatista on vulkaanista alkuperää. Holtedahfonnan jäätikkö altistuu voimakkaalle vuodenaikaissulamiselle, joka on kiihtynyt vuodesta 1850 lähtien. Se häivyttää ca. 50%:a jään sisältämästä kemiallisesta ilmastosignaalista, minkä vuoksi menneistä ilmasto-olosuhteista voidaan tehdä tulkintoja vain karkeammalla, usean vuoden resoluutiolla.

Holtedahlfonnan ja Lomonosovfonnan (itäiset Huippuvuoret) kemiallisten aikasarjojen huolellinen vertailu paljastaa, että Grönlannin meri on ollut todennäköisin kosteuden, lämmön, merisuolan ja biogeenisen rikin lähde läntisillä Huippuvuorilla viimeisen 300 vuoden aikana. Huomiota kiinnitettiin erityisesti ammoniumin lähteen määrittämiseen ja siihen, miksi sen määrä Holtedahlfonnalla on kolminkertaistunut vuodesta 1880, 60 vuotta myöhemmin kuin Lomonosovfonnalla. Moninkertaisen lineaarisen regressioanalyysin innovatiivinen käyttö ammonium-aikasarjojen yhteydessä osoittaa, että talveen ja kevääseen ajoittuva saasteiden kulkeutuminen (Arctic haze -ilmiö) on todennäköisin syy pitoisuuksien kasvulle. Lämmön siirtyminen jäättömänä pysyvästä Grönlannin merestä edistää paksumman lämpötilan inversiokerroksen syntymistä, mikä mahdollisesti aiheuttaa pH-arvoltaan neutraalimpien saasteiden kulkeutumisen korkeammalle merenpinnasta läntisillä Huippuvuorilla.

Lumen kemiallisen koostumuksen ja akkumulaatiomäärän suuret paikalliset ja ajalliset vaihtelut, jotka johtuvat pääosin etäisyydestä avomereen, ovat havaittavissa myös lakijäätikön mittakaavassa.

Lumen ja firn-lumen kemialliset analyysit Vestfonnan kahdelta päähuipulta tulkittiin hyödyntäen saatavilla olevia sää- ja glasiofysikaalisia parametreja (jääkairasydänten stratigrafia, paikallisten automaattisten sääasemien havainnot, kaukokartoitushavainnot tai uudelleen analysoitu kaukokartoitusdata). Korkeat merellisten suolojen pitoisuudet ja matala sulfaattikonsentraatio läntisellä huipulla tavatussa talvilumikerroksessa viittaavat kuurankukkien (frost flower) ja uuden merijään muodostumiseen talvisin Nordaustlandetia ympäröivissä vesissä, Hinlopenin salmessa.

Molemmissa Vestfonnan huipuilta kairatuissa jääsarjoissa havaittiin hapen ^{18}O-isotoopista voimakkaasti köyhtynyt kerros. Isotooppiarvoltaan matalan kerroksen arvioitiin edustavan talvea 1994/1995, ja heijastavan merijään laajuusanomaliaa Barentsin merellä, joka sai aikaan poikkeuksellisen pohjoisen ilmavirtauksen ja ^{18}O-köyhtyneen vesihöyryn kulkeutumisen alueelle Arktikselta. Matalan $\delta^{18}O$-arvon sisältämän kerroksen syntyajankohdan määrittäminen mahdollisti 17 ja 13 vuotta pitkien akkumulaatioaikasarjojen rekonstruoimisen läntisellä ja itäsellä Vestfonnalla. Huomattavasti alhaisempi nettoakkumulaatio itäisellä puolella kertoo todennäköisesti paikallisesti vaihtelevista tuuliolosuhteista lakijäätiköllä.

Emilie Beaudon:
Glaciochemical evidence of spatial and temporal environmental variability across Svalbard

Faculty of Science, Department of Chemistry,
University of Oulu, P.O. Box 3000, FI-90014, University of Oulu, Finland.

ABSTRACT

Ice cores extracted from Svalbard ice caps have proved to be useful multi-century paleoenvironmental archives for the Barents region and its climatic connection with the broad European Arctic sector. Concentration measurements of water soluble ions (Na^+, NH_4^+, K^+, Mg^{2+}, Ca^{2+}, $CH_3SO_3^-$, Cl^-, SO_4^{2-}, NO_3^-) along with isotopic analysis of oxygen were carried out on snow, firn and ice samples from Holtedahlfonna (western Spitsbergen) and Vestfonna (Nordaustlandet) ice caps in order to investigate Svalbard climate variability over diverse spatial and temporal scales. Local environmental patterns were inferred from site comparative studies with a systematic and careful distinction between the signal proportions induced by post-depositional processes (wind drift, erosion, melt, diffusion of water vapor) from that related solely to climatic factors.

The 125 m long Holtedahlfonna core is, to date, the most extensive glaciochemical archive for western Spitsbergen. Disrupted seasonal cycles and the unknown glacier thickness presented obstacles in dating the core which led to the development of a new dating method aimed at statistically extracting the volcanic fraction from the total sulfate budget dominated by other sources. This method, tested on Holtedahlfonna and four other non-polar ice cores, dispels ambiguities about the volcanic nature of sulfate concentration peaks and proves to work particularly well when, for instance, volcanic sulfate is overwhelmed by anthropogenic sulfate. Despite only 1.4 % of sulfate being defined as volcanic, five signatures (including the Laki horizon (1783) at 103 m depth) were found in Holtedahlfonna records dating back to the end of the Little Ice Age and spanning 305 years (1700-2005). Strong seasonal melting, intensifying since 1850, affects Holtedahlfonna and blurs ca. 50% of the climatic signal contained in ionic records which are thus interpretable at a multi-year resolution only.

The thorough comparison of Holtedahlfonna and Lomonosovfonna (eastern Spitsbergen) chemical time series reveals the Greenland Sea as the most plausible source of moisture, warmth, sea-salt and biogenic sulfur for western Spitsbergen over the last three centuries. Particular attention was paid to determining the possible ammonium sources and understanding its threefold concentration rise starting in 1880, i.e. 60 years earlier than observed in Lomonosovfonna core. The innovative application of multiple linear regression to the ammonium time series yields winter-spring pollution events (Arctic haze) as the most likely contributors to the post-1880 increase. A thicker temperature inversion layer, favored by oceanic heat advection from the year round open Greenland Sea, is suggested as the phenomenon facilitating transport of more pH-neutral pollution to higher elevations in western Spitsbergen.

The high spatial and temporal variability of snow chemistry and accumulation rates mostly induced by the distance to open sea is also visible at the scale of the ice cap. Chemistry analysis of snow and firn cores from the main summits of Vestfonna were interpreted in the light of all weather and glaciophysical parameters available for that remote region (core stratigraphy, in situ AWS data, remote sensing observations or reanalysis data). A sea-salt enriched and sulfate depleted layer de-

tected in the western summit winter snow pack inferred that young sea ice and frost flowers can form around Nordaustlandet (in Hinlopen strait) in winter. A highly ^{18}O-depleted layer measured in all shallow cores from the two Vestfonna summits was dated as 1994/95 winter when Barents Sea ice extent anomaly induced northerly wind and ^{18}O-depleted moisture advection from the Arctic. Dating the low $\delta^{18}O$ value horizon enabled the reconstruction of 17 and 13 year long time series of net accumulation at western and eastern Vestfonna. The much lower average net accumulation rate on the eastern side probably unveils a heterogeneous wind drift regime over the ice cap.

Key words: Svalbard, ions, ice core dating, volcanic sulfate, oxygen isotopes, frost flower, spatial variability, paleoclimate.

LIST OF ORIGINAL PAPERS

I **Beaudon, E.** and Moore, J. (2009), Frost flower chemical signature in winter snow on Vestfonna ice cap (Nordaustlandet, Svalbard), The Cryosphere, 3 (2), 147–154, doi: 10.5194/tc-3-147-2009.

II **Beaudon, E.**, Arppe, L., Jonsell, U., Martma, T., Möller, M., Pohjola, V.A., Scherer, D. and Moore, J.C. (2011), Spatial and temporal variability of net accumulation from shallow cores from Vestfonna ice cap (Nordaustlandet, Svalbard), Geografiska Annaler: Series A, Physical Geography, 93, 287–299. doi: 10.1111/j.1468-0459.2011.00439.

III Moore, J. C., **Beaudon, E.**, S. Kang, D. Divine, E. Isaksson, V. A. Pohjola, and R. S. W. van de Wal (2012), Statistical extraction of volcanic sulphate from non-polar ice cores, Journal of Geophysical Research, doi:10.1029/2011JD016592. *Reproduced by permission of American Geophysical Union*.

IV **Beaudon, E.**, Moore, J.C., Martma, T., Pohjola, V.A., Van de Wal, R., Kohler, J., Isaksson, E., A 300 years environmental and climate archive for western Spitsbergen from Holtedahlfonna ice core, manuscript.

THE AUTHOR'S CONTRIBUTION TO THE PUBLICATIONS

The author planned and conducted the experimental work in all four papers. Most of the data analyses, the interpretation of results and writing of the manuscripts were accomplished by the author for papers I, II, IV.

I The fieldwork campaign (2007) was planned by J. Moore. Sampling and chemical analyses were performed by E. Beaudon. Both authors jointly interpreted the data and wrote the article.

II Fieldwork campaigns were planned by J. Moore (2007) and E. Beaudon (2009) who extracted the shallow cores with the help of V. Pohjola. E. Beaudon made the density measurements and the digital pictures of the cores and performed the chemical analyses. The isotopic analyses were carried out by T. Martma (cores 2007) and L. Arppe (core 2009). U. Jonsell provided the AWS data. M. Möller produced the downscaled temperature time series and D. Scherer provided the NCEP/NCAR reanalysis data. E. Beaudon prepared the manuscript to be edited by the other authors.

III The study is based on an idea developed by J. Moore who performed the data analyses and wrote the manuscript. E. Beaudon produced part of the chemical data, participated to the interpretation and to the editing of the manuscript. The other authors provided background information relevant to the study site.

IV The study was planned by E. Isaksson, who together with R. van de Wal and V. Pohjola collected the ice core. T. Martma carried out the isotopic analyses. J. Kohler provided the radar measurements figure. E. Beaudon processed and analyzed the samples, interpreted the results and wrote the manuscript. J. Moore took part in the data analyses and to interpretation of the results.

CONTENT

1 INTRODUCTION

1.1 Climatological context

The last 130 years (1880-2011), have been marked by a strong increase of global surface air temperature (+ 0.8°C, Hansen et al., 2010) which was unambiguously forced by the exponential increase of anthropogenic greenhouse gases emissions to the atmosphere (IPCC AR4, 2007) since the beginning if the Industrial Revolution around 1850, also referred as the "Anthropocene" (Creutzen, 2010; Steffen et al., 2011). This warming, accompanied by the accelerated Arctic rivers discharge (Wagner et al., 2011), the thawing of permafrost and the melting of polar and mountain glaciers (Morison et al., 2000), results in increased sea level (Grinsted et al., 2008, 2009; Jevrejeva et al., 2009, 2010; Moore et al., 2011; Day et al., 2012) which generates an influx of fresh water to the ocean that may affect the thermohaline circulation (Peterson et al., 2002; Wu et al., 2004; Comiso, 2006). De facto, understanding the mechanisms governing exchanges between the atmosphere, the cryosphere and the ocean was one of the major axes of the 4th IPY (2007-2009) dedicated to quantifying past and present natural environmental variations in polar regions to improve projection of future changes (Holland, 2003).

The Arctic region is where the observed warming rate is greatest (+1.35°C.decade^{-1} for 2000-2010) (Deser et al., 2000; Bekryaev et al., 2010) with, for instance, a temperature anomaly over Greenland (+1.5°C) twice as large as the global value (+0.7°C) over the period 2005-2007 relatively to the 1951-1980 reference period (AMAP, 2011). The strongly amplified response of surface air temperature in the Arctic is mainly explained by the positive albedo feedback exerted by the Arctic sea ice thinning and retreat itself intimately related to the atmospheric warming (Koenigk et al., 2009; Day et al., 2012). In addition the Arctic haze, containing light-absorbing aerosols transported from sub-Arctic and mid-northern latitudes within the lower troposphere in winter (Quinn et al., 2007), also perturbs the surface radiative budget and contributes to the warming of the Arctic (Shaw, 1995; Law and Stohl, 2007; Fisher et al., 2011).

As sea ice influences air-sea energy exchange over large regions; it is a key component of the global system. The ongoing lengthening of the melt season, the warmer winters and advection of warm and salty water from the North Atlantic to the Arctic ocean are likely the cause of the extreme sea ice lows reached recently with an absolute minimum seen in 2007 when the North-West passage was free of ice in September for the first time during at least 1450 years (Kinnard et al., 2011). While many climate projection models agree on the total disappearance of the permanent Arctic Ocean ice pack sometime over the years 2026-2046 (Stroeve et al., 2007) foretelling for instance the opening of new Arctic maritime routes and the growth of shipping emissions (Corbett et al., 2010), it remains nonetheless very difficult to predict exactly what the environmental, climatic and thus societal consequences of an ice-free North Pole in summer will be. These difficulties include, for example, the incomplete understanding of the complex feedback mechanisms of the whole cryosphere in the context of changing climate (Francis et al., 2005). In addition, discerning the natural part of climate mechanisms' variability from the part forced by human activities remains a challenge for climatologists. It is therefore essential to improve the knowledge of what regulates the Arctic sea ice extent variations.

The Arctic Oscillation (AO) and the North Atlantic Oscillation (NAO) dictate the climate variability of the Northern Hemisphere and the North Atlantic on annual to multidecadal time scales.

The NAO, defined by a seesaw of atmospheric mass between the Icelandic Low and the Azores High (Hurrell et al., 2003), is already known to correlate with Nordic Sea ice variations (Isaksson et al., 2005; Sorteberg and Kvingedal, 2006; Macias Fauria et al., 2010; Kinnard et al., 2011) However, for a given NAO phase, sea ice extent positive and negative anomalies can occur simultaneously in different regions of the Arctic (Dickson et al., 2000; Sorteberg and Kvingedal, 2006; Koenigk et al., 2009). For instance, positive sea ice extent anomalies in Baffin Bay and Labrador Sea are associated with positive NAO phases (Grumet et al., 2001; Holland, 2003), whereas similar analysis for the Barents Sea and the Greenland Sea ice extent shows the inverse relationship. This stresses the need to define regional sea-ice/NAO relationship and assess current and future Arctic climate variability on regional scales.

Mass balance estimates of land-based glaciers and ice sheets also focus considerable attention because of their primary contribution to the current sea-level change (Arendt et al., 2002; Jevrejeva et al., 2008; Nicholls and Cazenave, 2010, Moore et al., 2011). Ice loss from the Greenland Ice Sheet is currently contributing to 10% to 20% of the observed and estimated global sea level rise (respectively 1.74 mm a^{-1} for the period 1955-2000 (Jevrejeva et al., 2006) and 2.4±1.0 mm a^{-1} for the period 1993–2000 (Moore et al., 2011)), though discharge of mass from marine-terminating Arctic glaciers and ice caps outside the large ice sheets, representing only 0.5% of the Earth's terrestrial cryosphere, is more especially targeted as it is thought to dominate to the current and near future eustatic rise (Meier et al., 2007; Radíc and Hock, 2011, Jacob et al., 2012) (0.64 mm a^{-1} for the period 1993-2006 (Dyurgerov et al., 2010)).

In these respects, the Barents Sea ice cover and Svalbard glaciers are of particular interest. The Barents Sea connects the Arctic Ocean and the North Atlantic. Observational datasets show the largest seasonal to interannual sea ice variability occurs in this sector of the Arctic Ocean (Koenigk et al., 2009; Divine and Dick, 2006; Petoukhov and Semenov, 2011). This is also where the largest decrease of sea ice extent (-10% $decade^{-1}$ for the Barents-Kara Seas; -3% $decade^{-1}$ for the whole Arctic Ocean) has been observed since the late 1970's (Johannessen et al., 1999; Parkinson et al., 1999) due to enhanced atmospheric and oceanic heat transport. More precisely, the variation of the Barents Sea ice cover is determined by the oceanic volume inflow from the West (Bengtsson et al., 2004, Kvingedal, 2005). Considering this reduction trend, numerical simulations predict the Barents Sea will be within the next decades the first Arctic region without winter sea ice (Holland and Bitz, 2003) which would in turn certainly affect the ocean-atmosphere heat exchanges and thus impact large-scale atmospheric circulation (Holland, 2003). These regional changes in ocean surface energy flux are expected to have feedback on the lower atmosphere moisture (Day et al., 2012), the precipitation regimes over Svalbard and, therefore, on the surface mass balance of Svalbard glaciers and ice caps (Day et al., 2012). The direct relationships between the NAO, the position of the Barents Sea ice edge and glaciers mass balances make Svalbard a key location to understand and predict future Arctic climate.

1.2 Svalbard: a key location for Arctic climate research

An extension of the warm North Atlantic current bordering the western coast of Svalbard, the Norwegian current, (Figure 1) is responsible for the relatively cool summer seasons and warm winter seasons considering the high latitude of the archipelago (Loeng, 1991).The convergence of warm

air masses advected from the Southwest and the cold masses originating from North and the Arctic Ocean leads to highly disparate and variable climatic conditions across Svalbard which induces a significant spatial snow accumulation variability (Sand et al., 2003; Grabiec et al., 2011). For instance, a high Arctic climate and the influence of colder Arctic air masses rather than westerlies characterize Nordaustlandet and the northeastern part of Spitsbergen where the largest ice fields and ice caps of

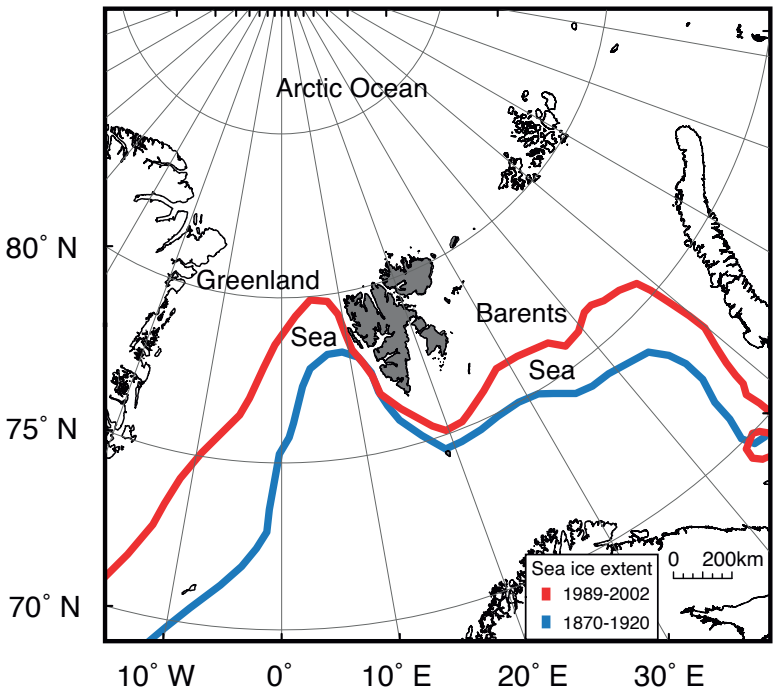

Figure 1: Map of the European Arctic sector showing April mean sea ice edge positions during the periods 1870-1920 (blue dotted line) and 1989-2002 (red dotted line) (Divine and Dick, 2006).

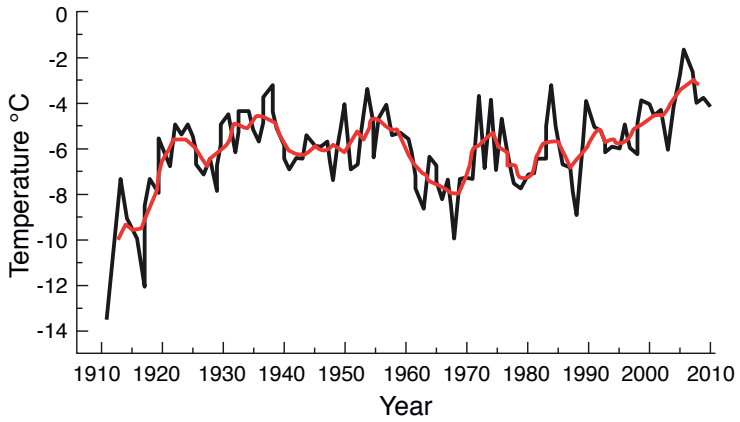

Figure 2: Annual mean (black) and 5-year running average (red) air temperature recorded at Longyearbyen airport weather station (78.25 °N, 15.47°E, 29 m a.s.l.) between 1911 and 2011. (source: http://climexp.knmi.nl/)

the archipelago lie. On the whole, 60% of the total land area of Svalbard is covered by low lying ice caps and tide water glaciers (Hagen et al., 1993).

Besides its suitable geographical setting and its vast glacierized expanses to conduct Arctic climate research, Svalbard benefits from a long history of occupation that generated highly valuable documentary and observational climate data. Since their first exploration in 1596 by the Dutch navigator Willem Barentsz, Svalbard region and the Nordic seas were visited from the 17th to the 19th century by Norwegian and Russian whalers and sealers who collected ship logs and meteorological observations. The compilation of these historical data and maps led, for example, to the reconstruction of the Nordic seas ice margins since 1850 (Figure 1; Vinje, 2001). Continuous atmospheric temperature and precipitation observational records exist since 1911 for the main town of Longyearbyen. They indicate that since the beginning of the observation period, annual mean temperature has varied from -13.7°C to -2.54°C (Figure 2). Svalbard settlements were first established with the beginning of coal mining activities in 1906. Nowadays, mining is confined to a few larger mines around the town of Longyearbyen, Svea and Barentsburg (western Spitsbergen). Other mining settlements were either abandoned (e.g. Pyramiden) or converted into research stations (e.g. Ny-Ålesund). Coal mining caused a local pollution visible in ice chemical records. This adds to contaminants coming from the close Eurasian continent and makes the west Barents region the area of the Arctic the most affected by anthropogenic pollution. That pollution is delivered to the Barents region and the Arctic through sea ice, rivers, ocean and especially the atmosphere in the form of Arctic haze (Barrie, 1986, 1990; Ottar, 1989). The Arctic haze affects Svalbard in late winter-early spring (February to April) when the extended polar high pressure cell isolates the lower troposphere from the rest of the atmosphere and provides conditions for poleward transport of pollutants from the western Eurasia sector (Stohl, 2006). Sulfate aerosols originating from industrial areas of northern Europe and Russia dominate the Arctic haze chemical fingerprint (Rahn, 1981; Iversen and Joranger, 1985; Shaw, 1995; Tuovinen et al., 1993). Ammonium, nitrate, dust and black carbon (BC) particles, volatile organic compounds (VOCs), trace metals and ozone precursors (NO_x) emitted by boreal forest/agricultural fires, fuel burning or shipping traffic, are also conveyed to Svalbard with enhanced northward meridional transport (Simoes, 2001; De Caritat, 2005; Stohl et al., 2007). Aerosol measurements in Zeppelin (western Spitsbergen) coupled with a backtrajectory analysis have shown that air masses contain two and a half times higher BC concentration when arriving from the East compared with air coming from the West (Forsström et al., 2008). Ice core chemical measurements across Svalbard reveal that acidity and sulfate levels during the last 50 years are highest in Nordaustlandet (Simoes, 2001).

1.3 The last millennium

Climate change is amplified in the Arctic and for instance, the average temperature increase observed in the Arctic during the 20th century exceeded that of the whole northern hemisphere (Overpeck et al., 1997). Yet, that modern warming trend and the environmental changes in the Arctic should be envisaged in the long-term context to distinguish anthropogenic forcing from the natural factors such as solar irradiation, volcanic activities, and the internal variability of the climate system. Therefore, the current warming trend must be interpreted in the context of the past. This task is inseparable from understanding regional patterns of past climate changes and the dynamical processes involved. In fact, more accurate regional projections under future conditions seek for higher

temporal and spatial resolution paleo-data. Since reliable instrumental records rarely extend back for more than a century, knowledge of past climates inevitably rely upon proxy records which include evidence obtained from natural archives such as ice cores. Given its data coverage, the last millennium is obviously the most appropriate time period to study phenomena at an annual to decadal resolution (Jones and Mann, 2004).

The compiling of information extracted from diverse sources of proxy data enabled the reconstruction of the main climatic trends for the Arctic region over the last several thousands of years. Starting from the Holocene thermal maximum (between about 10 000 and 6 000 years ago), proxy data indicate that Arctic summer temperatures were 1.6°C higher than the average of the 20th century which was likely driven by the Earth's orbital precession creating an insolation anomaly of +1.4% relative to present at 65°N (Masson-Delmotte, 2005; Kaufman et al., 2009; Helama et al., 2010). Decreases in summer insolation led to cooler summer temperatures in the late Holocene and during the Medieval Warm Period (AD 950 to 1200) the Arctic was not anomalously warm (Hughes and Diaz, 1994). The coldest period of the past 800 years occurred between 1600 and 1850 – the so-called Little Ice Age (LIA) which culminated between 1800 and 1840 in the Arctic (Overpeck et al., 1997). After 1840, a weakening of the global volcanic activity and the increase of solar irradiance led to a warming of 1.5°C across the Arctic that accelerated from 1920 (Yamanouchi et al., 2011) due to the exponential rise of trace gases concentrations in the atmosphere and to the wind-driven oceanic inflow into the Barents Sea with an associated sea ice retreat (Bengtsson et al., 2004). The 1920's warming thus marks the end of the LIA in Svalbard (Vinje, 2001). During the 1950-70's the Arctic warming marked a slowdown forced by the increasing input of aerosols in the troposphere. Today, the warming of the Arctic is dominated by greenhouse gases forcing (ACIA, 2005).

1.4 Ice cores: paleo environmental archives

Ice cores are wonderful archives of past climate and environmental changes as they contain physical and chemical records of variable length (from decades to some hundred thousand years) and time resolution (from seasonal to decadal) (Delmas, 1992; O'Brien et al., 1995; Legrand and Mayewski., 1997; Petit et al., 1999; Masson, 2000; Rasmussen et al., 2006) making them cornerstones of global change research. Snow scavenges impurities from the atmosphere hence the analysis of water soluble chemical particles stored in glaciers constitutes a powerful tool for studying short or long-term variations of the past atmospheric aerosol load.

1.4.1 Ion sources

Among the various chemical components (e.g. isotopes of oxygen and hydrogen in water, gases, ions, organic compounds) that can be determined from ice cores, ions are the most commonly studied. Ions in ice come from solid or liquid airborne particles (aerosols) which are generated directly from the surface of oceans and continents or by chemical reaction in the gas phase during transport. Therefore, ions can have multiple origins: either natural or anthropogenic or both, for example SO_4^{2-}.

Na^+, Cl^-, SO_4^{2-}, Mg^{2+}, Ca^{2+} and K^+ are the main soluble ions originating from oceanic sea spray. These ions also have terrestrial sources; however Na^+ and Cl^-, in the form of NaCl salt, is the most representative of the marine source. While Na^+ may be dry deposited in remote, inland, low accumulation and high elevation sites (in central Antarctica for instance), these sites are different from mari-

time, high accumulation sites such as the Svalbard low-lying ice caps where Na^+ is considered as the more reliable indicator for marine aerosol. However, this assumption must be systematically checked because evaporite deposits are present in Svalbard (Sørbel et al., 1990) and could have modified the Cl^-/Na^+ ratio (weight ratio) in snow relative to the bulk sea-salt ratio. Cl^- is usually a less relevant sea-salt indicator because NaCl can be subjected to fractionation when it gets in contact with atmospheric acids, for example H_2SO_4, or HNO_3, leading to the displacement of chloride ("dechlorination") by sulfate or nitrate (Legrand and Delmas, 1988) following the reactions:

$$2NaCl + H_2SO_4 \rightarrow Na_2SO_4 + 2HCl \quad (1)$$
$$NaCl + HNO_3 \rightarrow NaNO_3 + HCl \quad (2)$$

The Na^+/Cl^- ratio, when compared with that of the Standard Mean Ocean Water (SMOW) (0.86) (Wilson, 1975), is an indicator of the intensity of the fractionation. Besides sea-salt dechlorination by acidification of the atmosphere, HCl is primarily emitted from industrialized region of the northern hemisphere (coal burning, waste incineration), by volcanoes or by biomass burning (Legrand et al., 2002). The non-sea-salt (nss) fraction of SO_4^{2-}, Mg^{2+}, Ca^{2+} and K^+ is normally calculated using the following equation in which Na^+ functions as the reference component:

$$[nss\text{-}X] = [X]\text{-}(([X]/[Na^+])_{SMOW} * [Na^+]) \quad (3)$$

Where [nss-X] is the non-sea-salt fraction of species X, [X] is the total fraction of species X, and $([X]/[Na^+])_{SNOW}$ is the ratio of the species compared to sodium in standard mean ocean water. This is how nssMg and more especially nssCa can be used as chemical tracers of mineral particles, as the terrestrial source for Ca^{2+} (and for Mg^{2+} to less extent) is dominant (Delmas, 1992).

However, calculating its non-sea-salt fraction is not sufficient to determine the source of SO_4^{2-}. Since sulfur is present in all large natural reservoirs, SO_4^{2-} can have marine, terrestrial, anthropogenic, biogenic and volcanic sources (Legrand and Mayewski, 1997; Fisher et al., 1998). Sulfur is emitted in the atmosphere in the form of aerosols, essentially sea spray (Na_2SO_4) and more or less oxidized gases (Kerminen et al., 1998). Its atmospheric cycle is largely dominated by anthropogenic (fossil fuel combustion) and volcanic SO_2 that is the main precursor of SO_4^{2-} which inventory has been described in details for Lomonosovfonna ice core by Moore et al. (2006). Oxidation of SO_2 occurs either in the liquid phase with H_2O_2 and O_3 or in the gas phase with radical $^{\bullet}OH$. These reactions rapidly produce H_2SO_4. Sulfuric acid participates in the acidification of precipitation or is neutralized by NH_3 to form ammonium salts (NH_4HSO_4 or $(NH_4)_2SO_4$) (Jickells et al., 2003). Langner and Rodhe (1991) found that 81% of the total sulfate in the northern hemisphere has an anthropogenic source. The oxidation of dimethyl sulfide (DMS) released by marine biota as DMSP constitutes the biologic source of SO_4^{2-} (Hynes et al., 1986; Saigne and Legrand, 1987; Saltzman, 1995; O'Dwyer et al., 2000).

CH_3SO_3H (MSA) is with SO_2 and SO_4^{2-}, the other final product of the DMS oxidation (Dacey and Wakeham, 1986, Davis et al., 2011). This reaction is the unique source of MSA that is therefore naturally assimilated as the indicator of biospheric sulfur emissions (Legrand et al., 1991; Teinilä et al., 2004). MSA concentrations depend on the DMS oxidation efficiency and on DMS emission related to the primary productivity which is closely linked to temperature and sea ice conditions as biogenic

productivity is the highest around sea ice margins (Strass and Nothig, 1996; Sakshaug and Walsh, 2000; Jourdain and Legrand, 2001).

NO_3 is the principle sink for the atmospheric NO_x (Whung et al., 1994; Honrath et al., 1999; Burkhart et al., 2004) which is emitted from biotic activity in soils, biomass burning, lightning, stratospheric oxidation of N_2O, ionospheric dissociation of N_2 (Legrand and Kirchner, 1990), fossil fuel combustion and oxidation of NH_3 (resulting in the formation of NH_4NO_3). NO_3^- is present in the polar atmosphere as gaseous HNO_3 (Dibb et al., 1998) which after deposition in snow can be partly reemitted to the atmosphere (De Angelis and Legrand, 1995). The relatively limited knowledge of its air/snow transfer and the multiple post-depositional processes (photochemical reactions, high elution rate, and displacement by reaction with H_2SO_4) complicate the interpretation of nitrate records in ice cores (Röthlisberger et al., 2000; Savarino et al., 2007; Jarvis et al., 2008; Wolff et al., 2008). Despite the multiplicity of nitrate sources, NO_3^- ice core records mirror the anthropogenically induced emissions changes after the mid-20th century and give evidence that anthropogenic NO_3^- dominates the NO_3^- budget. Recently, isotopic-signature based methods have been developed to identify NO_3^- sources (Morin et al., 2008). With NO_3^- , NH_4^+ is the other nitrogenous species measured in snow and ice. NH_3 released in the atmosphere from bacterial decomposition in soil and by vegetation, wild fires and anthropogenic sources such as industrial combustions (e.g. coal burning), sewage treatments and agriculture (fertilizers application, livestock wastes). NH_3 is one of the most abundant base in the atmosphere and thus takes part in the neutralization of sulfate and controls the acidity of the atmosphere when converted in $(NH_4)_2SO_4$, NH_4HSO_4 and NH_4NO_3 by reaction with H_2SO_4 and HNO_3 respectively (Battye et al., 2003). Biological marine emissions, and rotting sea ice (emitting NO_x and halogens) to a lesser extent, have been suggested as a net natural source of ammonia (Quinn et al., 1990; Liss and Galloway, 1993; Galloway et al., 1995) although net flux from sea to land has now been reversed by anthropogenic emissions (Spokes et al., 2000).

1.4.2 Svalbard ice cores

The geographical location of Svalbard (section 1.2; Figure 1) makes it particularly relevant for studying the anthropogenic impact on the European Arctic environment. However, attempting to extract usable paleo-environmental information from Svalbard ice caps can be quite challenging because of the complicating effect of melt that tends to obscure part of the environmental signals. Despite that, several deep ice cores have been drilled on the main ice fields (Figure 3) of the archipelago in the 1970-80's by Soviet-Russian groups (Gordiyenko et al., 1981; Punning et al., 1986; Vaikmäe, 1990; Tarussov, 1992) who published only low resolution chloride and sulfate data. During the 1990's, new deep ice cores were drilled by Japanese teams on Vestfonna (Matoba et al., 2002; Motoyama et al., 2008), Austfonna (Watanabe et al., 2001) and Snøfjellafonna (Kameda et al., 1993; Goto-Azuma et al., 1995) which provided times series for a larger (though incomplete) panel of ions. Among all Svalbard cores, the deep ice core drilled in 1997 at the summit of the highest Svalbard ice field (Lomonosovfonna, 1250 m a.s.l.) presents the best preserved stratigraphy and the most reliable time scale. Lomonosovfonna high resolution records (multi-annual until 18th century) for nine major water-soluble ions span the last 800 years (Isaksson et al., 2001; Kekonen et al., 2005a). Only the ice core drilled in 1999 on Austfonna, the largest Svalbard ice cap, covers about the same period but its chemical

record resolution is lower (annual to decadal) than those of Lomonosovfonna (Isaksson et al., 2005). These ice cores have proven their suitability for paleoclimate reconstructions (Pohjola et al., 2002; Isaksson et al., 2003). Moreover, the study of Svalbard ice cores has induced the development of ion based proxies and statistical tools (Moore et al., 2005) to decipher climatic signals disrupted by melting; the definition of a good washout index (Log([Na^+]/[Mg^{2+}])) (Izuka et al., 2002; Grinsted et al., 2006), based on the specific elution propensity of each ion, is one good example. Ion sources have been assigned and discussed in detail for Lomonosovfonna core (Kekonen et al., 2002). Climatic periods such as the Warm Medieval Period and the LIA could be detected from the analysis of MSA that was found to reflect sea ice variability for instance (Isaksson et al., 2006). The industrialization and the 20th century anthropogenic pollution impact are also captured in NO_3^-, NH_4^+ and SO_4^{2-} records which sources for Lomonosovfonna have been thoroughly inventoried by Moore et al. (2006).

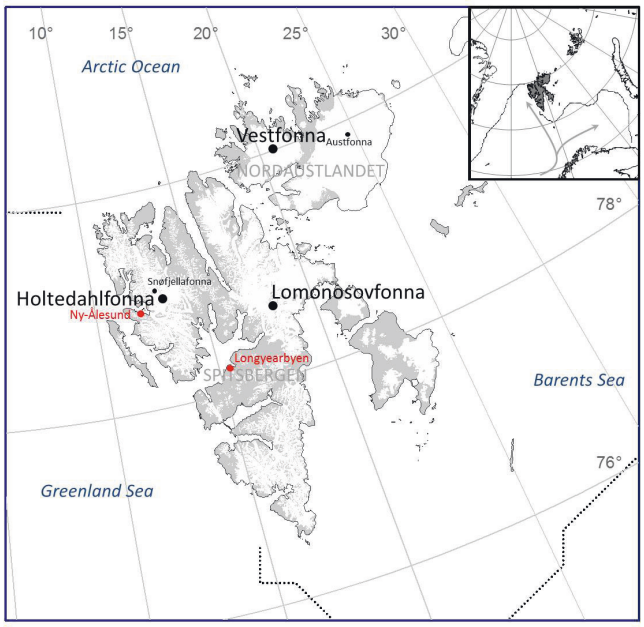

Figure 3: Map of Svalbard showing the drilling sites on Holtedahlfonna and Vestfonna and the two other main Svalbard ice caps: Austfonna and Lomonosovfonna. The dotted line is the median spring sea ice extent over the period 1979-2000 (source: http://nsidc.org/data/seaice_index/archives/index.html).

1.5 Objectives of the thesis

Climate data are scarce in poorly documented remote High Arctic regions such as Nordaustlandet though they help provide more comprehensive view of the climatic and environmental change. This work is aimed at closing this geographical gap in the current knowledge of Svalbard ice masses, glaciochemistry and climate variability by investigating different types of data (with a focus on chemical data) with statistical tools. The more specific objectives are:

To assess the magnitude of post-depositional processes impact on ion distribution within the snow and ice and retrospectively infer meteorological/climate patterns from disruption of ice chemical records.

To document Vestfonna snow chemical composition and its variability within the ice cap. This would constitute valuable in situ information for modelers and various remote sensing applications.

Provide a new 300 years glaciochemical archive for western Spitsbergen and discuss the relative contributions of major sources of impurities to define the role of the Greenland Sea in the spatial variability of Svalbard climate over the end of the LIA and the industrial period.

2 SPECIFIC ISSUES REGARDING THE STUDY AREAS IN SVALBARD

2.1 Holtedahlfonna

Holtedahlfonna ice cap is located at 79°N on Spitsbergen, the biggest island of Svalbard (Figure 3). Covering an area of 370 km^2 (including Kronebreen, its tidewater outlet glacier), Holtedahlfonna is the largest ice field of western Spitsbergen (Nuth et al., 2010) and one of the highest (1150 m a.s.l.). To date, the ice depth in the summit area (Snøfjellafonna) remains unknown as radar surveys conducted there reported thicknesses ranging from 150 to 300 m (Kohler et al., 2007). Holtedahlfonna is a polythermal glacier (Hagen et al., 1993) with firn thickness of about 15 m (Kameda et al., 1993). Because of the proximity of the research station of Ny-Ålesund operated since 1968 and the closely monitored surge glacier of Kronebreen (Lefauconnier et al., 2001), extensive research have been carried out in the Kongsfjorden area but paradoxically, chemistry of Holtedahlfonna ice cap remains poorly documented and has not been subject to a particular focus during the IPY.

2.2 Nordaustlandet, Vestfonna

In contrast to a variety of extensive research and monitoring activities in southern and western Svalbard, very little research has focused on Nordaustlandet (the northeasternmost island of Svalbard archipelago) during the last decades (Figure 4). This is probably due to difficult access and logistics issues. It is well known that changing sea ice conditions around Svalbard also induce regional disparities of accumulation and thus surface mass balance (Bamber et al., 2004). Nordaustlandet is almost year round surrounded by sea ice and receives moisture originating mostly from the Southeast and the open areas of the Barents Sea (Førland et al., 1997; Niedwiedz, 1997; Dagestad et al., 2006; Taurisiano et al., 2007). Several studies described how the complex accumulation patterns on Nordaustlandet ice caps are affected by coastal sea ice variability (Möller et al., 2011; Bamber et al. 2004). With their regional climate model, Day et al. (2012) investigated the impact of a future seasonally ice free Arctic Ocean on Svalbard hydrological cycle, temperature and surface mass balance. They suggest that sea ice decline would increase poleward moisture transport but the induced positive surface mass balance over the archipelago would not be sufficient to balance the enhanced melt due to increased temperature.

Vestfonna ice cap (Figure 5) at 80°N stretches over an area of 2340 km^2 (Braun et al, 2011) of Nordaustlandet making it one of the largest Arctic ice masses and the second largest in the European Arctic after the adjacent Austfonna (8120 km^2) (Dowdeswell, 1986; Hagen, 1993; Taurisiano, 2007). The geometry of Vestfonna consists of two ridges, East-West and North-South oriented, converging at the eastern summit (630 m a.s.l.) and which sides are essentially the drainage basins of outlet glaciers. Recent ground-based radar surveys (Pettersson et al., 2011), showing pockets of temperate ice near the surface and cold ice at a greater depth, confirmed the polythermal structure of the ice cap (Palosuo, 1987a; Pälli et al., 2003; Jania et al., 2005) and also enabled the new estimate of its thickness (185 m in average, 413 m at the central summit) and total volume (442 ± 0.6 km^3). The firn layer on Vestfonna is about 15-20 m thick (Vaykmyae, 1985, Schytt, 1964; Palosuo, 1987b; Pettersson, 2011) and has rather heterogeneous densities (0.6 kg m^{-3} on average, Watanabe et al., 2001, Paper II) because of the multiple

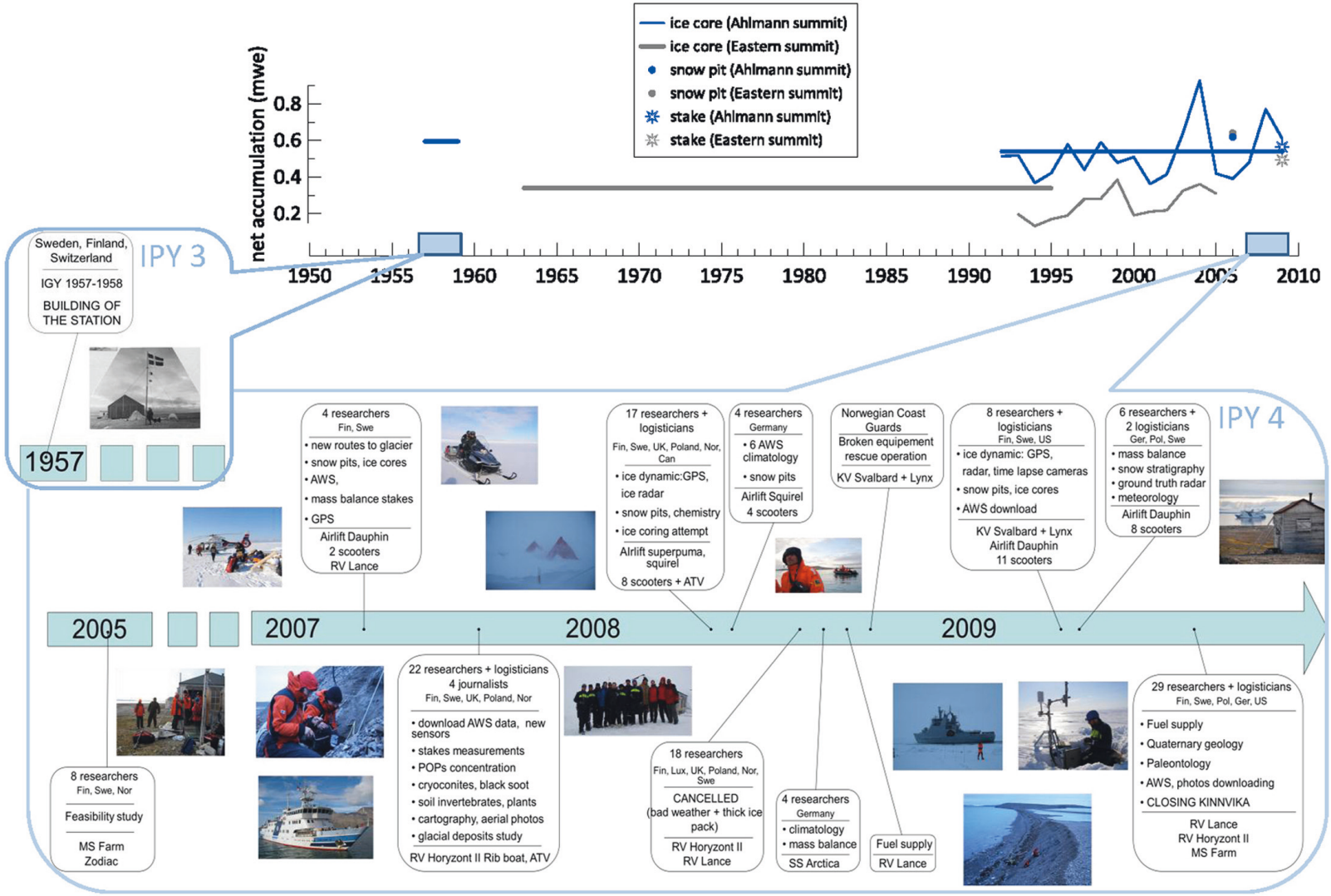

Figure 4: Timeline of research activities around Kinnvika station during the last two IPY. The graph displays the various snow accumulation rates obtained from snow pits, ice cores and accumulation stakes at summit Ahlmann (blue) and Eastern summit (grey).

layers of superimposed ice (~ 1-2 m thick) it contains. The ice temperature at 10 m, measured at the eastern summit in 1995 was -3.7 °C (Watanabe et al., 2001, Kotlyakov, 2004). This testifies that substantial seasonal melting of snow and refreezing occurs on Vestfonna similar to every other Svalbard glacier. It is assumed that percolating water refreezing within the underlying layers amounts to up to 60% of the current's year's winter accumulation beyond which runoff occurs (Pohjola et al., 2002; Samuelsson, 2001; Moore et al., 2005). Surface melting and water percolation cause the elution of ions and attenuates the original seasonal signal registered in snow and ice (Virkkunen et al., 2007, Moore and Grinsted, 2009) which results in difficulties of dating ice cores and extracting environmental information. The melt season, with positive daily mean surface temperature, extends from June to September but short term warming can also occur during winter (Matoba et al., 2002).

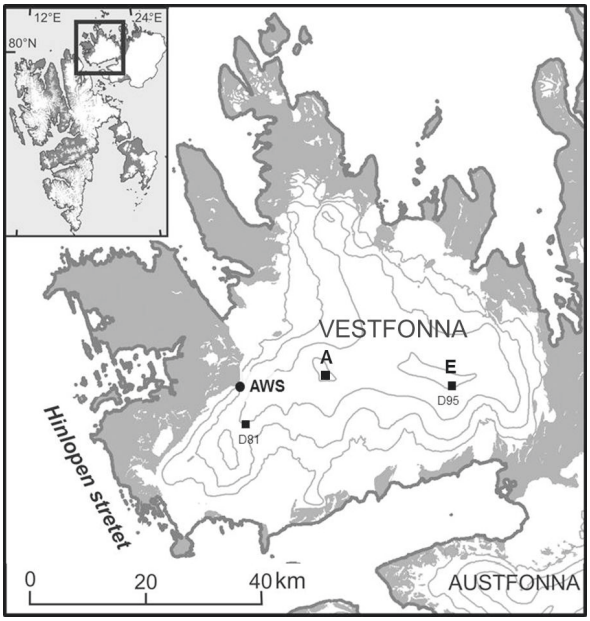

Figure 5: Vestfonna ice cap (Nordaustlandet) with locations of firn cores drilling sites (A: summit Ahlmann; E: Eastern summit), the previous deep drilling sites (D81: 1981; D95: 1995) and the Automatic Weather Station (AWS) installed in spring 2007.

3 MATERIAL AND METHODS

3.1 Sampling

The polar sunrise marks the beginning of the Arctic spring season that lasts from March to May. As the permanent daylight allows long working days on the glacier and since the still freezing temperatures limit the risk of getting the core drill stuck in the borehole, the spring period is the most appropriate to conduct ice core drilling campaigns and glaciology fieldwork in general. With the aim of getting a picture of present or past atmospheric conditions, snow and firn studies are the prerequisite to ice core investigation to better understand the air-to-snow and snow-to-ice transfer processes and post-depositional changes of snow chemistry. The results presented in this thesis rest on the analysis of these three types of samples (snow, firn and ice) collected during springs 2007, 2008, 2009 on three Svalbard ice caps: Vestfonna (within the frame of IPY-KINNVIKA project, Pohjola et al., 2011), Holtedahlfonna and Lomonosovfonna (Table 1)).

High elevated areas subject to minimal melting were preferably designated as sampling sites and care was taken that precise sampling spots would remain distant from any snowmobile tracks, footprints or other potential pollution sources. Moreover, pre-cleaned sampling tools were used and new ultraclean equipment (overall, gloves, facial mask) was wore throughout the entire sampling and processing phases, i.e. on the field and in the laboratory (cold room and clean room).

LOCATION		COORDINATES			SAMPLING				CHEMISTRY			INSOLUBLE PARTICLES	
ice cap	**sampling site**	**latitude N**	**longitude E**	**altitude (m a.s.l.)**	**date**	**type[1]**	**depth (m)**	**number of samples (n)**	**major ions (5 + 4)**	**Br^-, F^- and 3 carboxylic acids[2]**	**$\delta^{18}O$**	**$^{87}Sr/^{86}Sr$**	**size concentration EPMA**
Vestfonna (Nordaustlandet)	summit Ahlmann	79°59'22"	20°07'07"	622	4/28/2007	**snow pit (Pit 1)**	2,09	39	•				
		79°59'22"	20°07'07"	622	4/28/2007	**firn core (Ahl07)**	11,81	60	•		x		
		79° 58' 53.034"	20° 06' 50.76"	607	4/26/2009	**snow pit**	1,95	39	•	•			
		79°58'53"	20°06'51"	619	4/30/2009	**firn core (Ahl09)**	15,42	121	•	•	x	x	•
	Eastern summit	79°58	21°01	600	4/29/2007	**snow pit (Pit 2)**	2,02	12	•		x		
		79°58	21°01	600	4/29/2007	**firn core (E07)**	5,76	26	•		x		
		79° 56' 34.799"	21° 16' 32.88"	613	5/8/2009	**snow pit**	1,70	27	•	•	x		
Holtedahlfonna (Western Spitsbergen)	summit	79°14'	13°27'	1150	April 2005	ice core	124,45	740	•		x		
	stake 10	79° 08' 26.494"	13° 23' 36.481"	1126	March 2008	firn core	12,20	119	•		x		
Lomonosovfonna (Eastern Spitsbergen)	summit	78°51'53"	17°23'30"	1250	March 2008	firn core	10,57	97	•		x		

[1] sampled by the author (article designation)

[2] $HCOO^-$, CH_3COO^-, $C_2O_4^{2-}$

• analysis performed by the author

Table 1: Svalbard samples collected and analyzed by the author.

3.1.1 Snow

Each of the studied glaciers is subject to surface melting in summer resulting in the formation of a thick ice layer overlain by autumnal depth hoar (Cogley et al., 2011). Snow pits were excavated to the level of the previous summer surface or until below the previous summer surface when it was possible to dig through the ice layer using a pre-cleaned metallic spade or an ice axe. After the visual snow stratigraphy has been described in detail with depth, the snow wall was sampled vertically by pushing pre-cleaned plastic containers directly into the wall every 5 cm. Harder icy layer sample extraction sometimes called for a knife to be used to shape the sample to fit the container. On an adjacent vertical line, density measurements were performed at a 5 to 20 cm resolution using a stainless steel cylinder and a spring scale (Twickler and Whitlow, 1997). Snow extracted for density measurements was kept in clean ©Ziploc bags for supplementary ion chemistry analysis (reproducibility verification) and low vertical resolution chemical profiles.

3.1.2 Firn and ice cores

Shallow cores from Vestfonna were drilled from the bottom of snow pits using a portable electromechanical drill with a 1 m long barrel (diameter 9 cm). The drilling progress was slow in ice and faster in firn. Extra 1 m long drill extensions could be added between each coring runs when the two drill operators lifted the whole apparatus with the ice core piece. The weight of the full barrel plus ten extensions was the maximum that two strong persons could lift at once. Therefore the maximum core length we could get using that technique was not more than 10 m. Based on this experience, a lightweight Kovacs corer (attached to a 30 m long rope and operated by a winch and pulley) was brought to Vestfonna for the last spring campaign in 2009. However, that coring operation was stopped at 15.5 m depth when the corer got stuck in a thick ice lens. The core pieces extracted at each run were carefully packed in thermo-sealed clean polyethylene bags, measured in length and their stratigraphy was roughly described. The drill used to extract the long Holtedahlfonna ice core in the course of March 2005 (Millennium project) was made by University of Utrecht and British Antarctic Survey with a core diameter of 105 mm (Mulvaney et al., 2002). The core was retrieved in about 60 cm long sections, giving a total of 210 pieces. No drilling fluid was used.

3.2 Transportation, storage and processing samples

All snow samples in containers and bags as well as packed ice core pieces were placed carefully in cardboard boxes insulated with Styrofoam plates and buried in snow to insure they remained totally frozen until the end of the fieldwork campaign. Then, the boxes were placed in freezers and shipped to the mainland by cargo and transported with freezer trucks to the Finnish Forest Research Institute of Rovaniemi.

The cutting was proceeded in a cold room (-22°C) using a thin blade band saw. First, core pieces were cut longitudinally. Each core cutting follow a pre-designed plan (Figure 6) that assigns a specific ice portion as a function of the type of analysis it is intended. The prisms intended for ion and dust concentration measurements were always cut out of the inner part of the core, i.e. the best preserved from contamination generated during drilling and handling of the ice. A thin plate, adjacent to the ion section, was place on a light bench and photographed for a detailed description of ice facies and accurate calculation of the ice density. That part of the core was usually saved for oxygen isotopic measurements. The remaining outer pieces were packed back into the polyethylene plastic bags and archived. Then the prisms were cut transversally to reach the final desired sample resolution for chemical measurements by ion chromatography. With that analytical technique (see section 3.3), the

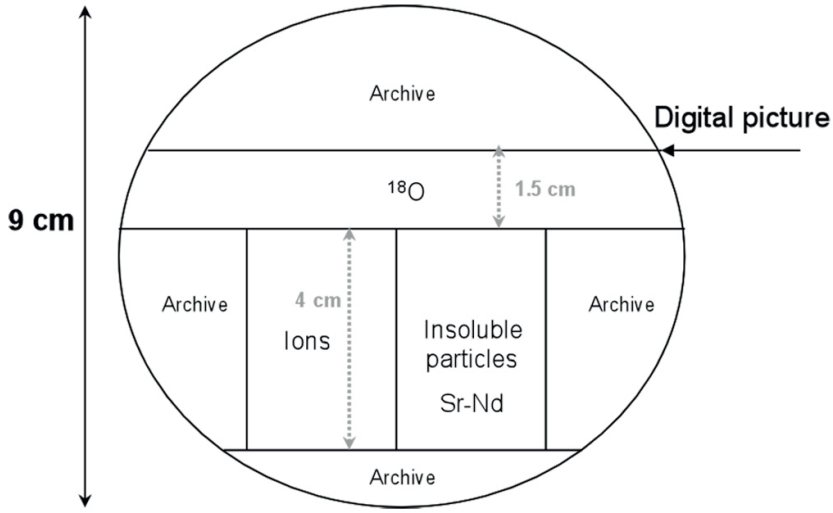

Figure 6: Transversal view and cutting plan of Ahl09 firn core (Vestfonna 2009, summit Ahlmann).

minimum volume necessary for both anion and cation analysis is 10 ml per sample. Considering the ice density and facies and with the aim of getting at least 4 samples per annual layer, the length of firn and ice samples ranged between 5 and 20 cm. Under a laminar bench, each surface of the samples prism were scrapped with a clean stainless steel knife before the samples were placed in pre-cleaned plastic containers and taken to the clean room where they were melted and poured into 5 ml sample vials (two vials per sample: one for anion, one for cation measurements).

3.3 Chemical analysis

Ion chromatographs involves separating different ionic species of a liquid solution and evaluating their concentration by conductivity. If the principle is simple, the experimental realization is more difficult as drastic precautions must be taken to avoid contamination and we must operate in the cleanest environment. Ion chromatography is an instrumental technique for the separation and determination, at low detection limits, of many ions in the same run (concentrations as low as ppb or even ppt); hence this technique is the most commonly used in glaciochemical studies. Details concerning the instrumentation used by our group and the operative protocol followed for the analysis of Svalbard snow and ice samples and have been the object of numerous publications already (Foley and Dorsey., 1984; Legrand et al., 1993; Jauhiainen et al., 1999; Kekonen et al., 2004; Virkkunen et al., 2007). Consequently, its thorough description will not be dealt with again in this thesis and only the main apparatus characteristics and analytical uncertainties are summed up in Tables 2a and 2b respectively. Nine calibration standard solutions were prepared every week by diluting 1000 $mg.l^{-1}$ commercial stock standard solutions (Alfa Aesar®) with ultrapure water (MilliQ resistivity > 18 mΩ). The precision (RSD) and the within-run repeatability is based on mixed control solutions (combining five anion/cation standards) analyzed five times a day (Table 2b).

Ion chromatograph data are heteroscedastic, i.e. in this case the relative standard deviation of the results (random errors) will increase for lower concentrations, and therefore the data underwent a log-transformation prior to any statistical analysis carried out in this work (Paper III and IV).

All snow and ice samples from Svalbard have been analyzed for nine major ions (Na^+, NH_4^+, K^+, Mg^{2+},

	ANIONS		CATIONS
	$CH_3SO_3^-$, Cl^-, NO_3^-, SO_4^{2-}	F^-, CH_3COO^-, $HCOO^-$, $CH_3SO_3^-$, Cl^-, Br^-, NO_3^-, SO_4^{2-}, $C_2O_4^{2-}$	Na^+, NH_4^+, K^+, Mg^{2+}, Ca^{2+}
Chromatograph	DX 120	DX 120	ICS 1000
guard column	AG15 (4 x 50 mm)	AG17 (4 x 50 mm)	CG12a (4 x 50 mm)
separator column	AS15 (4 x 250 mm)	AS17 (4 x 250 mm)	CS12a (4 x 250 mm)
neutralisation column	ASRS	ASRS 300 hydroxyde	CSRS
eluent	NaOH (34 mM)	KOH (gradient 11 to 50 mM)	MSA (14 mM)
regenerant	H_2SO_4 (36 mM)		
injection volume		2 mL	0.5 mL

Table 2a: Analytical conditions and equipment used for ion chromatography measurements (©Dionex devices).

	$CH_3SO_3^-$	Cl^-	NO_3^-	SO_4^{2-}	Na^+	NH_4^+	K^+	Mg^{2+}	Ca^{2+}
mean blank (ng.g^{-1})	0.13 ± 0.01	0.53 ± 0.08	0.84 ± 0.79	0.31 ± 0.05	0.23 ± 0.22	1.49 ± 0.54	1.82 ± 0.17	0.06 ± 0.14	0.32 ± 0.30
detection limit[a] (Skoog, 1995) (ng.g^{-1})	0,17	0,77	3,22	0,47	0,88	3,12	2,33	0,49	1,22
RSD (%)	2,29	5,44	7,65	0,92	1,98	1,50	1,91	2,45	0,48
repeatability error (%)	1,17	0,49	0,20	0,08	1,25	0,40	0,56	0,27	0,08

[a]sum of the mean blank and 3 times the standard deviation of the mean blank

Table 2b: Sampling characteristics for firn core ion analysis.

Ca^{2+}, $CH_3SO_3^-$, Cl^-, SO_4^{2-}, NO_3^-). Chromatographs are housed in a clean laboratory (clean room class 1000) of the Finnish Forest Institute (METLA) in Rovaniemi. For prospective purpose, initiative was taken to measure three supplementary organic ions (formate, acetate, oxalate) and two halogen ions (fluoride, bromide) in Vestfonna shallow core 2009 (Ahl09). For this, chromatographs were subject to some adjustments. Mainly, a Reagent-Free-Controller (RFC) was installed on the Dionex-120 to perform a gradient elution and obtain a better peak selectivity with a reasonable retention time. A carbonate removal device has also been connected to the anion chromatograph in order to eliminate carbonate originating from dissolved carbon dioxide from the air and that can interfere with the accurate determination of certain analytes of interest (here sulfate for instance). Results from these supplementary analyses are not presented in this thesis.

$\delta^{18}O$ is defined as the per mil difference between the sample composition and the Vienna Standard Mean Ocean Water (VSMOW):

$$\delta^{18}O = [((^{18}O/^{16}O)_{sample} - (^{18}O/^{16}O)_{SMOW}))/ (^{18}O/^{16}O)_{SMOW}] * 1000 ‰ \quad (4)$$

As $\delta^{18}O$ values contain climatic information and are commonly used as temperature proxy (Dansgaard, 1964), determination of the isotopic composition of oxygen in our ice cores has systematically gone along with that of ions concentration. All isotope samples from shallow cores LF08, HF08 (not shown), Ahl09 (Paper II) and the long core HDF05 (Divine et al., 2011a; Paper III, IV) were processed at the University of Technology in Tallinn on a Gasbench II with Delta V Advantage mass spectrometer and a reproducibility of replicate analysis of ± 0.1‰. The $\delta^{18}O$ records from Ahl07 and E07 discussed in Paper II arise from measurements performed at the Laboratory for Geochemistry of the Department of Geosciences and Geography, University of Helsinki, with a ThermoFinnigan Gasbench II coupled to a ThermoFinnigan DeltaPlus Advantage continuous flow mass spectrometer with a reproducibility of ± 0.1‰ indicated by replicate measurements of in-house water standards.

4 RESULTS AND DISCUSSION

4.1 Ice core dating (Paper II, III)

Owing to their fairly large snow accumulation rates (ranging from 0.38 to 0.82 m w.e. yr^{-1} (Pinglot et al., 1999)), Svalbard glaciers have the potential to provide high resolution (up to seasonal resolution records) paleoclimate archives from ice cores (Isaksson et al., 2003). This cannot be achieved without the most accurate dating of the cores (Kaspari et al., 2008). However this task is sometimes rendered arduous by a lack of identifiable reference horizons (usually volcanic sulfate or conductivity peak, a volcanic tephra layer or radioactivity peak (tritium or cesium)) or by post-depositional disruptions of annual layers caused by melt and refreezing or wind scouring that can prevent chemical cycles counting (Fisher et al., 1983, 85). Therefore, the main Svalbard ice cores dating have always involved as many available independent methods as possible to get the most precise chronology. So far the Lomonosovfonna core drilled in 1997 is considered as the best dated Svalbard ice core (Kekonen et al., 2005a-b; Moore et al., 2006; Divine et al., 2008). The ice thickness at the drill site was precisely determined, thus the simple Nye ice flow model (Nye et al., 1963) could be constrained by several well identified reference horizons (i.e. the 1963 radioactive layer and the 1783 Laki sulfate peak). Furthermore, the Lomonosovfonna age scale was checked with automated seasonal counting in stable isotopes and ions (Pohjola et al., 2002) so that the upper part of the core benefits from direct dating and a 3-year dating accuracy could be reached for the 20th century.

4.1.1 Holtedahlfonna ice core

Unfortunately, the dating of long Holtedahlfonna core was far more problematic since the bedrock was not reached by drilling and the bedrock depth at the drill site, an essential parameter to use in the Nye model, could not be categorically determined from radar sounding. The extremely rugged basal topography and the proximity of the steep rock cliff would produce erroneous bottom returns and weak reflectors. An additional difficulty for dating Holtedahlfonna lies in the fact that no obvious horizon, besides the 1963 tritium peak (van der Wel et al., 2011), could be found from the conductivity profile or from sulfate concentrations which volcanic fraction, drowned by marine and anthropogenic sources contributions is lower than 5% and half of that of Lomonosovfonna (Moore et al., 2006). Holtedahlfonna dating strategy therefore consists in a 3-steps approach involving separate dating methods:

1. Determine an idoneous ice thickness which:
   - *gives the best fit between the Nye model constrained with the 1963 tritium horizon and the automatic counting of annual layers in the isotopic series,*
   - *fits statistically with the well dated Lomonosovfonna ionic time series (Figure 7),*
2. Verify that thickness matches the observed thinning rate of the annual layers and the borehole temperature profile to produce a preliminary dating.
3. Refine the dating using an independent statistical method to find volcanic reference horizons in sulfate record, based on the assumption that Holtedahlfonna ice cap, in the same capacity as the other Svalbard glaciers (Kekonen et al., 2005b), should have inevitably recorded some volcanic chemical signals.

The new volcanic sulfate extraction method presented in Paper III is based on a statistical approach, i.e. a Multiple Linear Regression (MLR) described by Moore et al. (2006), that estimates the contribution to sulfate budget of chemical impurities other than sulfate to determine the general impurity level from non-volcanic sources. After subtracting the non-volcanic background signal, the residual sulfate is assumed to be stochastic and mainly of volcanic origin and statistically significant (95% confidence level) volcanic spikes are identified. The method is applied to three Svalbard ice cores and one core from Mount Everest (Kang et al., 2002; Kaspari et al., 2007; Xu et al., 2009), all of which having significant non-volcanic sulfate loads and are difficult to date by conventional means. The method is also tested with one well-dated core from the Altai (Eichler et al., 2009, 2011) and proves to work best at extracting volcanic spikes for periods when sulfate budget is dominated by anthropogenic sulfate emissions, typically after 1940. Yet, the analysis exerted on the Altai core also revealed that a too extensive percolation as well as a too low data resolution would limit the applicability of the volcanic sulfate residual method. The Holtedahlfonna core age-depth scale was refined with the identification by volcanic sulfate residual of five volcanic signatures, significant at 95%. This way it was found that Holtedahlfonna core spans 305 years (Figure 8). Four spikes were detected in Vestfonna 95 core whereas up to nine markers were found in Lomonosovfonna 97 core for the 1700-2000 time-period. Besides reemphasizing the stochastic nature of volcanic deposition process (Robock et al., 2000), this difference between neighbor Svalbard ice caps highlights a site specific capacity of glaciers for capturing and preserving volcanic fallouts. Considering the impact of volcanic sulfate aerosols in terms

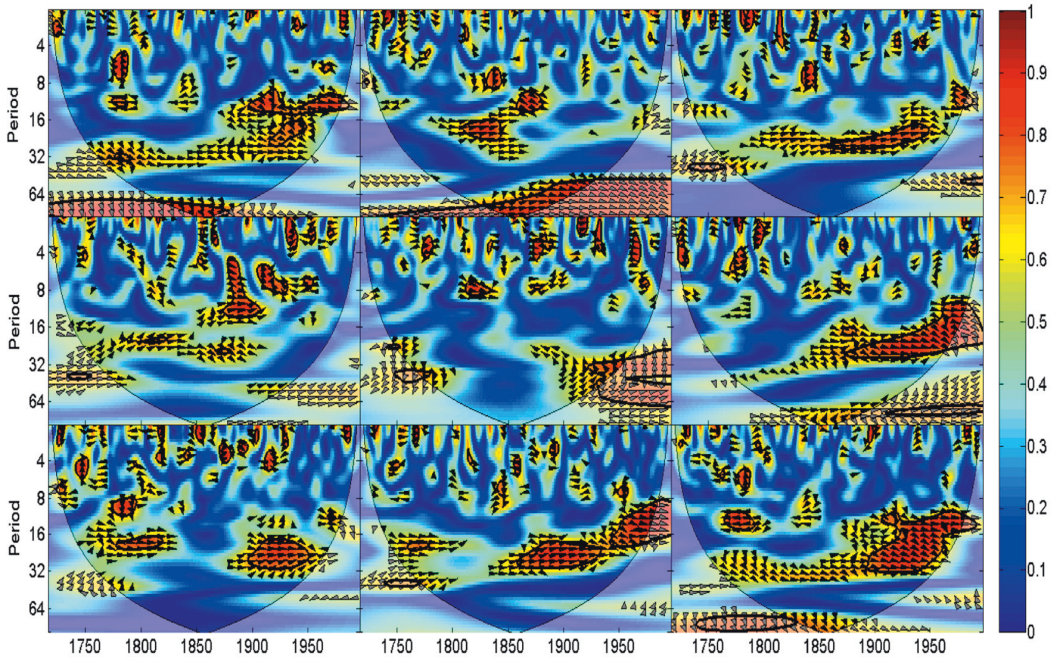

Cl^-	NO_3^-	SO_4^{2-}
MSA	NH_4^+	K^+
Ca^{2+}	Mg^{2+}	Na^+

Figure 7: Wavelet coherence (WTC) between the different ions (see the grid key) in Holtedahlfonna and Lomonosovfonna (Grinsted et al., 2004). Inside the subplots arrows pointing to the right indicate in-phase relationship between the two sites.

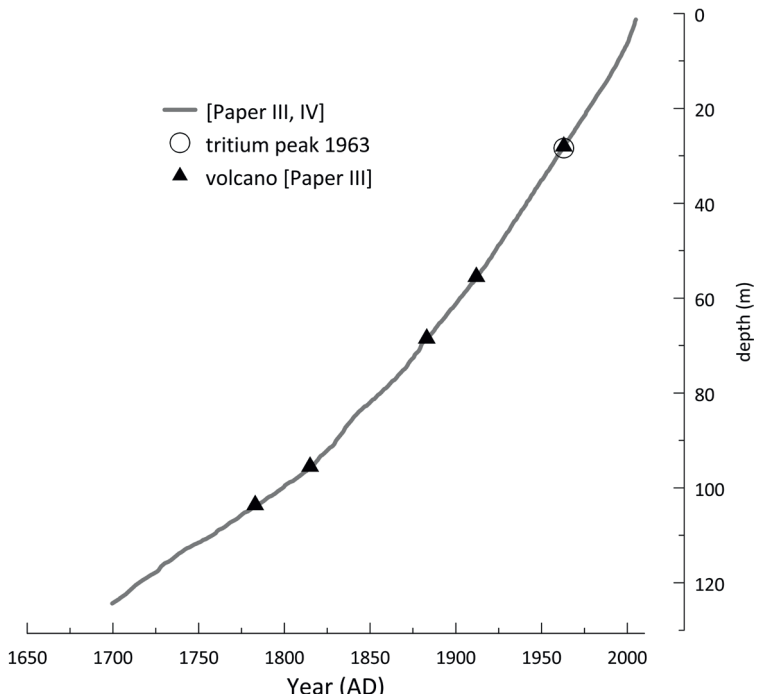

Figure 8: Age scale of Holtedahlfonna ice core.

of radiative forcing (Gao et al., 2008), it appears judicious to apply the method to geographically diverse core sites and thus better estimate the climate importance of different eruptions. This could be accomplished by combining the sulfate residual method with another multivariate mathematical approach. For instance, the method proposed by Gazeaux et al. (2012) is a joint extraction aimed at providing a sound amplitude estimate of volcanic events sometimes hidden in noisy background. This is based on the joint extraction of volcanic signal from multiple ice cores which chronologies are assumed to be perfectly dated and synchronized.

4.1.2 Vestfonna firn core

The establishment of an accurate chronology can be equally difficult for short firn cores that experience substantial seasonal melting and which $\delta^{18}O$ annual cycles are blurred by diffusion (Johnsen et al., 2000) or substantial depth percolation (Taylor et al., 2001). Obviously firn cores are so short that the application of any thinning model for dating is pointless. Because percolation length and melt features thickness are highly variable in Vestfonna shallow cores, the melt index described as a proxy for summer extreme temperature by Koerner (1977) for Canadian Arctic (Grumet et al., 1998; Kinnard et al., 2008) and Alaska (Kelsey et al., 2010) ice cores could not be either used to count annual layers. However, the detection of just one reference layer proved to be crucial for dating the three Vestfonna shallow cores (Paper II) whose $\delta^{18}O$ annual cycles were clearly countable only in the upper 3 m part. Below that, $\delta^{18}O$ cycle counting becomes more subjective but luckily, at the bottom of a 5 m thick ice lens the $\delta^{18}O$ records displayed a "cold isotopic feature" (a ^{18}O-depleted layer) common to the three firn cores (down to -18‰ in Ahl09) as well as to the long Vestfonna 95 core (Watanabe

et al., 2001). The combination of a thorough visual stratigraphy description, involving the complete inventory of ice layers, with model derived Nordaustlandet temperature (Möller et al., 2011a) and wind reanalysis data (Kistler et al., 2001) led to prove the ^{18}O-depleted layer was not the manifestation of post-depositional processes but actually linked to a specific climatologic configuration during winter 1994/95 when considerably reduced Barents Sea ice cover induced cold air and ^{18}O-depleted moisture advection from the Arctic. Ahl09, Ahl07 and E07 were found to span 17, 12, 13 years respectively.

4.2 What do we learn about post-depositional processes? (Paper I, II, IV)

Svalbard snow and ice chemical investigations imply careful preliminary impact study of post-depositional processes whose magnitude varies temporally and spatially. Holtedahlfonna ice core analysis (Paper IV) and Vestfonna snow chemistry (Paper I, II) presented in this thesis, implement knowledge on both dimensions.

4.2.1 Holtedahlfonna

At a larger regional scale, East-West differences within Spitsbergen arise when comparing seasonal melting on Holtedahlfonna (West) and Lomonosovfonna (East) with firn temperature at 15 m depth of -0.4°C (Paper IV) and -2.8°C (van de Wal et al., 2002) respectively. Accordingly, heat diffusion from percolation-refreezing has a greater influence on Holtedahlfonna glaciochemical records which, for the 20th century, capture local summer air temperatures much better than does Lomonosovfonna (Paper IV) which records a more regional signal (Paper III). The EOF analysis performed on the whole Holtedahlfonna core ion data, indicates that 51% of the ion concentration variance is not induced by melt and potentially contains paleoclimate information at a multi-annual resolution. Elution of ions is limited to the percolation depth and on average its decay is exponential from one year to another. Therefore, with a melt index of 50%, only 3% of the signal would be eluted deeper than five years. In fact, a five-year resolution reading of Holtedahlfonna records could be claimed though it was cautiously chosen to base the discussion on 10-year averaged time series. The relatively good preservation of the chemical signal in Holtedahlfonna is attributed to the multiple icy layers encountered in the firn limiting percolation depth and diffusion (Paper IV). Tritium (van der Wel et al., 2011) and cesium (Pinglot et al., 1999) isotope studies from both glaciers showed the same peak amplitudes and which are also similar to other cores at different locations, hence wind scouring was considered to have only a minor effect on chemistry at Holtedahlfonna and Lomonosovfonna.

4.2.2 Vestfonna

Thin ice layers were found in the Vestfonna eastern summit winter snow pack whereas no stratigraphic sign of melt-refreezing was detected in winter snow at the western summit, though culminating at a similar altitude (about 600 m a.s.l.). The increase of the washout index Log($[Na^+]/[Mg^{2+}]$) (Grinsted et al., 2006) in Pit 2 (eastern summit, 79°58'N, 21°01'E, 600 m a.s.l.) (Table 1) confirmed that melt events have an impact on ion redistribution in snow. Based on a single snow pit campaign, it is nonetheless impossible to thoroughly conclude that short melt events affects more specifically the eastern part of Vestfonna during the accumulation season (i.e. winter-spring). However, the shallow cores density profiles (Paper II) from the same locations as the snow pits, also revealed the more

frequent occurrence of thick ice lenses in the E07 core (eastern summit). Infiltration ice layer formation depends on the microstructure of the snow, which is initially largely determined by wind action (Fisher and Koerner, 1988). The question is whether this spatial variability in the position and thickness of these infiltration ice layers on Vestfonna is due to a zonal variation in climatic or atmospheric processes. The much lower average net accumulation rates deduced from the E07 core (0.25 ± 0.08 m w.e. yr^{-1}) with respect to the Ahl09 core (0.52 ± 0.15 m w.e. yr^{-1}) suggest that a probably more efficient remobilization of snow by wind scour takes place on that part of the glacier which is more under the influence of Austfonna ice cap (foehn effect) (Taurisiano et al., 2007). A snow pit based analysis of Vestfonna snowpack density carried out by Möller et al. (2011b) do not show any statistically significant zonal accumulation variability across the ice cap. Increasing snow accumulation with altitude is the only significant correlation found by Möller et al. (2011b) who also invoked snow deposition wind reworking to explain that discrepancy with the shallow cores study. An alternative explanation may be inherent to the differential outflow glacier dynamics with, for instance, Franklinbreen draining more mass out of the western watershed than southeastern outlet glaciers (Pohjola et al., 2011b).

A variable intensity of wind removal of snow and a fluctuable percolation depth are suspected to partially account for the high snow accumulation interannual variability. This shows in the discrepancies between the climatic mass balance calculated by Möller et al. (2011b) and the accumulation series inferred from the shallow cores. If a warming trend is observed in the $\delta^{18}O$ series (1995-2006), no significant correlations were found between the 17-year long accumulation time series and averaged air temperatures or any other climate indexes such as NAO or sea ice extent anomalies for instance. However, low $\delta^{18}O$ amplitudes were noticed to be associated with easterly surface wind whereas years with strong northerly wind would match the coldest winters in the downscaled temperature time series. Although these observations cannot be assimilated as reliable climate patterns, they at least provide tangible indications for future Vestfonna climate investigations. For instance, it could be profitable to assess the consistency between these remarkable ice core signals and the REMOiso simulations of precipitation isotopic composition and surface air temperature in Svalbard (Divine et al., 2011b). Also, future ice core measurements may include deuterium excess as a supplementary tracer particularly sensitive to moisture origin in the Arctic.

4.3 Sea ice impact on Svalbard snow and ice chemistry (Paper I, II, IV)

Holtedahlfonna ion records (Paper IV) shed light on the sea ice secular trend of reduction. More precisely, insights into the distance to the marine source and the biogenic source productivity, all driven by sea ice conditions around Svalbard, show through changes of sea-salt and biogenic fractions of ions. Sea-salt ions (Na^+, Cl^-, K^+, Mg^{2+}) represent 80% of the total Holtedahlfonna ionic budget. With the exception of magnesium between 1920 and 1950, their concentrations surpass those of Lomonosovfonna throughout all periods and the non-sea-salt fractions of calcium (nssCa) and sulfate (nss-SO_4) in Holtedahlfonna remain lower than these of Lomonosovfonna. Together with the higher $\delta^{18}O$ values measured in the Holtedahlfonna core, these results reflect the obvious fact that the Lomonosovfonna site is rendered relatively more continental than Holtedahlfonna by the more extensive Barents Sea ice cover compared with the Greenland Sea. Holtedahlfonna ice records confirm this has been the case for the last 300 years at least. Moreover, MSA averaged concentration in Holtedahlfonna remains lower than that measured in Lomonosovfonna over the common period spanned

by the two cores and suggests this more proximal marine source is also less biologically productive. The biogenic fraction of non-sea-salt sulfur (MSA/MSA+nssSO_4), is lower in Holtedahlfonna than in Lomonosovfonna before 1880 and a significant correlation between MSA and nssSO_4 from 1700 to 1880, also make the Greenland Sea being the most likely source of biogenic compounds for western Spitsbergen prior to 1880. However, due to the input of anthropogenic sulfate dominating the non-sea-salt budget, MSA/MSA+nssSO_4 becomes a poorer indicator of biogenic MSA productivity since 1880. Nevertheless, no decrease of MSA related to the rise of NO_3^- (NO_x) concentration is observed throughout the whole record suggesting that NO_x did not control MSA levels. Hence, the direct influence of the sharp Greenland Sea ice decline on the drop of MSA concentration in Holtedahlfonna ice around 1880 can be confirmed.

Performing a Multiple Linear Regression analysis (MLR) between ammonium and the other ions is an innovative way to estimate the different contributions to the ammonium budget along the core (the method was designed for sulfate in Lomonosovfonna core by Moore et al. (2006)). This analysis shows that before 1880 and the industrial period, ammonium was principally associated with nitrate which indicates a natural (either continental or oceanic) source of ammonium nitrate (NH_4NO_3). In the case of a contribution from the sea, since less NH_x (NH_4^+ and NO_3^-) are emitted from a low-productivity ocean (Johnson et al., 2008), the lower ammonium concentration in Holtedahlfonna would corroborate that the Greenland Sea was the marine source of impurities for western Spitsbergen during the colder 18th and 19th centuries. There again, it is not possible to draw any conclusion from the MLR about Holtedahlfonna ammonium sources during the 20th century because the post 1880 period is the interval in the core where the chemical washout index (Log[Na^+]/[Mg^{2+}]) is the highest and where the different elution rates are most likely to obscure the true relationship between ions. Yet, a comparison of Holtedahlfonna and Lomonosovfonna records allows detection of a striking difference in the timing of the ammonium 20th century concentration rise. In Holtedahlfonna ammonium starts rising with the beginning of the European industrial revolution and simultaneously to the very first observation of the Arctic haze by Arctic explorers around 1880 while in Lomonosovfonna ice ammonium concentration is decreasing. An alternative could be that ammonium in Holtedahlfonna has either an additional source relative to Lomonosovfonna or is more efficiently conveyed to the western ice cap. The lack of paludological (wetland) data for Svalbard prevents the proposition of any argument in favor of the development of ammonia-source ecosystems subsequent to the ending of the LIA in Svalbard and the retreat of glaciers. Notwithstanding, pollution derived ammonium has been detected in Holtedahlfonna snow while no such Arctic haze signature was found in the corresponding layer of Lomonosovfonna snowpack (Virkkunen et al., 2007). In addition, aerosol measurements carried out at the western Spitsbergen station of Zeppelin have shown a well-marked stratification of winter Arctic haze compounds with more neutralized aerosols (more ammonium) within the tropospheric boundary layer than the free troposphere (then more acidic) (Fisher et al., 2011). This supports the option of a better facilitated transport of low latitude ammonium towards Holtedahlfonna. Once more, the zonal difference of sea ice coverage around Spitsbergen is logically suspected to create asymmetric tropospheric conditions that would work on the thermal inversion layer's vertical thickness (Solberget et al., 1996; Treiffeisen et al., 2007) during polar night. Basically, the extensive Barents Sea ice cover would not only restrict the oceanic heat advection but would also stabilize the lower tropospheric layer. Hence, the thermal inversion layer on the eastern side of Svalbard and within which pollution travels, would not always be thick enough to exceed the altitude of Lomonosovfonna ice cap.

Comparing glacier snow chemical budgets also highlights site-specific influence of the surrounding sea ice on sea/air exchanges. Paper I describes spatial differences of the ionic seasonal sequence in Vestfonna snow. Sea-salt species concentrations at Ahlmann summit surpass sea-salt content of eastern summit snow unveiling a generally greater marine input on the western part of the ice cap. Besides, a particularly sea-salt enriched layer is the most striking feature observed in Ahlmann 2006/2007 winter snow. In this 30 cm thick layer, both sodium and sulfate are depleted compared with bulk sea water in such proportions that are typical of a frost flower signature: basically SO_4/Na in frost flower (0.092) equals one third SO_4/Na in bulk sea water (0.27) (Rankin et al., 2000, 2002). Frost flowers grow on newly formed sea ice (Wolff et al., 2003) and are associated with the crystallization of mirabilite ($Na_2SO_4.10H_2O$) within the supersaturated sea ice brine layer. As displayed in Figure 9, mirabilite ideally crystallizes between -8.2°C and -22°C (Marion et al., 1999) hence frost flowers can develop on sea ice in winter and be blown to Vestfonna by moderate winds. Radar satellite observation showing young sea ice areas, with high backscatter coefficients (Ulander et al., 1995), around Nordaustlandet converge with temperature measurements to confirm the conditions were propitious to the formation of frost flowers in Hinlopen strait during winter 2006/2007.

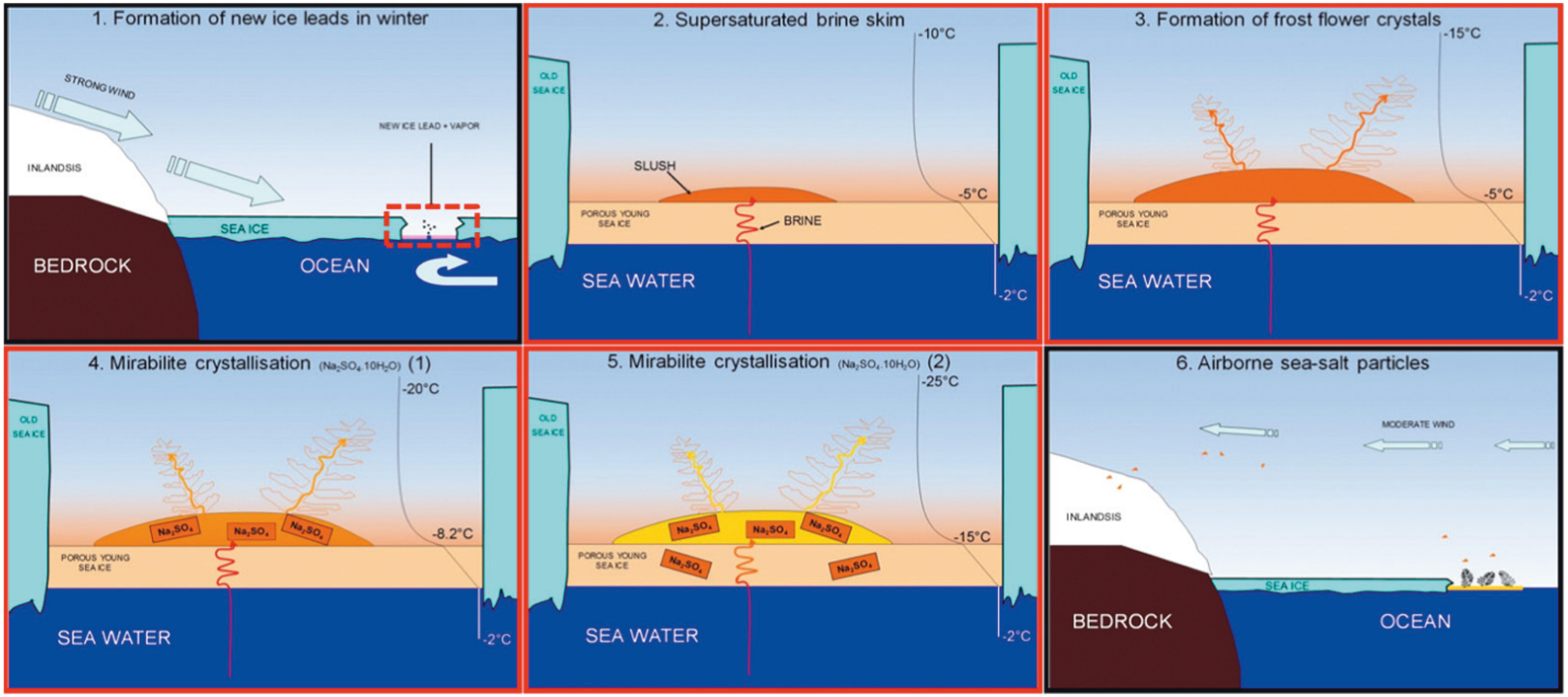

Figure 9: Formation and transport of mirabilite aerosols.

5 CONCLUDING REMARKS

The research presented in this thesis and the original papers is a contribution to the understanding of Svalbard regional climate variability through new knowledge of local climate-glaciological proxy data relationships. The work, based on new snow and ice ion datasets from Holtedahlfonna (western Spitsbergen) and Vestfonna (western Nordaustlandet), extends the spatial array of Svalbard environmental records covering the last centuries. Particular efforts were placed on the dating of the shallow and deep ice cores and in the careful distinction between climate signal and noise. This led to a reassertion of the potential of glaciochemical records contained in those problematic ice fields suffering from summer melting to provide valuable paleoclimate information. Although this work does not extend further back in time and neither reaches a higher temporal resolution in the history of Svalbard climate, it however provides new essential keys for future ice core based environmental reconstructions and model projections for the Barents region.

Holtedahlfonna perceives and records slight changes in the moisture, warmth and biologic productivity of the Greenland Sea since the 18th century at least. The end of the LIA and the transition to year round ice free ocean condition is particularly visible in the isotopic records, the washout index, sea-salt (and biogenic sulfur) concentration which all start to rise (decrease) after 1815. This indicates that a longer Holtedahlfonna ice core (possibly twice as long) could help to refine the reconstruction of Greenland Sea ice edges as far back as the 17th century. This will be possible provided this new core is extracted from where the glacier ice thickness is well known and the time scale suffers less uncertainties. The increasing trends of ammonium concentration starting around 1880 and about 60 years earlier than in other Svalbard cores, is another indication that Holtedahlfonna captures a more local climatic signal. It is not relevant to draw conclusions on wider geographical scale from this ice core, however Holtedahlfonna chemistry may give insights into what Lomonosovfonna may be like when the Barents Sea ice has disappeared and triggered a spatial/temporal shift of ions sources and transport (via the thickening of the thermal inversion layer for instance). This could lead to a modification of the degree of sulfate aerosol neutralization impacting directly the aerosol radiative forcing. Again, before thoroughly concluding that western Spitsbergen trends precede those of Svalbard and the Barents region, archives must rely on an accurate time scale. Tackling the problematic dating of Holtedahlfonna core allowed development of a powerful method to detect chemical signature of past volcanic eruptions. The statistical regression is applied to sulfate but could as well be implemented and adjusted to work on volcanic fluoride for instance or on ammonium to reconstruct the history of Eurasian forest fires. In addition to helping with the need to improve timescales of Arctic ice core records, the method, if systematically tried, could contribute to a global impact survey of every eruption in terms of chemical fallout. This would constitute a highly valuable database for atmospheric circulation model simulation and solar radiative forcing balance calculation.

Overall this thesis re-emphasizes the crucial role of surrounding sea ice cover on Svalbard climate and defines its local impact on snow and ice chemistry of formerly less documented ice caps. Unlike western Spitsbergen, western Nordaustlandet is still most of the time surrounded by sea ice during the year. Yet, shallow cores from Vestfonna extending old ice core records to the 21st century, also show the imprint of increasing warming in their stratigraphy. For this major Arctic ice cap, the shallow cores provide among the first ground based glaciological data that can be interpreted in the light of modern remote sensing tools. The latter combination revealed to be essential to categorically identify a frost flower chemical signature for the first time in Arctic terrestrial snow. This identification of a frost flower signature in a zone dominated by anthropogenic sulfate suggests its potential value in the interpretation of ice core data for local climatological conditions (provided it is possible to track the signal down the core). In other Arctic areas that are dominated by multi-year ice, for example northern Ellesmere Island, such a layer would make a good indicator of a period of reduced multiyear ice.

ACKNOWLEDGEMENTS

The many mysteries of the High Arctic do not easily let themselves be unraveled. In the 21st century still, any scientific activity in these regions is a challenge. For the humble contribution of this thesis to the knowledge about the European Arctic, it has taken no less than the 4th International Polar Year, the IPY-KINNVIKA project and the full enthusiasm and experience of glaciology "old stagers".

Among them, Professor John Moore let me take my place in this adventure, granting me from the start unwavering support and trust necessary for the development and independent expression of my scientific thinking. Throughout this doctorate, and despite the distance to Beijing, I benefited from his scientific dynamism and his always frank and constructive reviews. On the ice cap, I would almost blindly (also literally) trust in Professor Veijo Pohjola from whom I learnt a huge part of my field skills. Veijo and all my Kinnvika fieldwork colleagues share credit for the success of the sampling campaigns on Vestfonna. I cannot name them all but I address them a great thank you. I acknowledge the Finns who had the wonderful idea to build the world northernmost sauna in the 50's: it saved my mind.

I am grateful to Dr. Elisabeth Isaksson who put me in charge of the analysis of the first Holtedahlfonna deep ice core which turned out to be the longest glacial archive presented in this thesis. Also, I would like to thank all my glaciologists colleagues and especially Dr. Laura Arppe, Dr. Dmitry Divine, Dr. Ulf Jonsell, Dr. Shichang Kang, Dr. Jack Kohler, Dr. Tõnu Martma, Dr. Marco Möller, Professor Dieter Scherer and Dr. Roderik van de Wal for co-authorship. I am very inspired by the research and the scientific path of Dr. Anna Sinisalo. I am lucky that she took me to the top of the icy slopes of Jan Mayen in the best company of John Hulth and Johan Snygg.

I warmly thank the welcoming staff of the Rovaniemi unit of the Finnish Forest Institute for the rental of laboratory and cold room facilities. I am particularly in debt to Kristiina Penttilä who got me started with the measurements and Arja Hangasvaara whose infinite patience made me put our hard times with the machines ("hullut koneet") into perspective.

Obviously this work would not have been possible without financial support from the Academy of Finland, the ARKTIS doctoral programme and the University of Oulu with whom my co-supervisor Professor Paavo Perämäki, Dr. Päivi Soppela and Professor Kari Strand greatly facilitated exchanges: thank you so much.

I acknowledge the two pre-examiners of this thesis: Dr. Valérie Masson-Delmotte and Professor Karl Kreutz for their reviews and inspiring comments.

I sincerely thank all my co-workers at the Arctic Centre, my home institute. I would not have spent more time within these walls than in my home if the atmosphere they created was not warm and friendly. I refer of course to my fellow doctoral students with whom we happily haunted the institute late at night and on weekends. I also wish to thank our director Dr. Paula Kankaanpää, the most enthusiastic communication and science centre teams, the senior researchers and more particularly Professor Bruce Forbes for his advice, availability and mentoring. I would have succumbed to nervous without fairies like Tuija, Arto, Kari (H. and J.), Raija to guide me through the Finnish administration or solve computer problems.

All my dear friends in Finland (I include my glorious FCVS team mates!) who made my PhD-student life much lighter are warmly thanked. My deepest gratitude goes to Laura, Françoise and Nicolas (and pikku Arto) for their unconditional friendship and for simply making me feel at home in Finland.

Above all, I would like to pay tribute to my parents, and to my brother Julien who always encouraged me to live my dreams in spite of their excessive anxiety over me exposing myself to polar dangers. In truth, from any corner of the planet, I remain "connected" with my mother (even without satellite phone). My father taught me that "If you want to, you can" and Julien, the real geographer of the family, has always led the way in my existence which he made especially funny. Amazingly, together we understood why by -30°C, with frozen feet and head in a blizzard, it feels so good.

REFERENCES

ACIA (2005), Arctic Climate Impact Assessment, 1042 pp., Cambridge Univ. Press, New York.

AMAP (2011) Snow, water, ice and permafrost in the Arctic (SWIPA). Arctic Monitoring and Assessment Programme (AMAP), Oslo.

Arendt, A. A., Echelmeyer, K. A., Harrison, W. D., Lingle, C. S., and V.B., Valentine (2002) Rapid wastage of Alaska glaciers and their contribution to rising sea level, Science 297, 382–386.

Bamber, J., W. Krabill, V. Raper and J. Dowdeswell (2004) Anamolous recent growth of part of a large Arctic ice cap: Austfonna, Svalbard, Geophysical Research Letters, 31, L12402.

Barrie, L. A. (1986) Arctic air chemistry: an overview, edited by: Stonehouse, B., Arctic air pollution, Cambridge, Cambridge University Press, 5-23.

Barrie, L., and M. Barrie (1990) Chemical components of lower tropospheric aerosols in the high Arctic: Six years of observations, J. Atmos. Chem., 11(3), 211–226.

Battye, W., V.P. Aneja, P.A. Roelle (2003) Evaluation and improvement of ammonia emissions inventories, Atmos. Environ., 37, 3873-3883, doi:10.1016/S1352-2310(03)00343-1.

Bekryaev, R.V., I.V. Polyakov, V.A. Alexeev (2010) Role of Polar Amplification in Long Term Surface Air Temperature Variations and Modern Arctic Warming. J. Climate, 23, 3888–3906. doi: http://dx.doi.org/10.1175/2010JCLI3297.1.

Bengtsson, L., V. A. Semenov, and O. M. Johannessen (2004) The early twentieth-century warming in the Arctic- A possible mechanism, J. Clim., 17, 4045-4057.

Braun, M., V.A. Pohjola, R. Pettersson, M. Möller, R. Finkelnburg, U. Falk, D. Scherer, and C. Schneider (2011) Changes of glacier frontal positions of Vestfonna (Nordaustlandet, Svalbard). Geografiska Annaler: Series A, Physical Geography, 93, 301–310. DOI:10.1111/j.1468-0459.2011.00437.

Burkhart, J. F., M. Hutterli, R.C. Bales, and J.R. McConnell (2004) Seasonal accumulation timing and preservation of nitrate in firn at Summit, Greenland, J. Geophys. Res., 109, D19302, doi:10.1029/2004JD004658.

Caritat, P., G. Hall, S. Gìslason, W. Belsey, M. Braun, N.I. Goloubeva, H.K. Olsen, J.O. Scheie, J.E. Vaive (2005) Chemical composition of arctic snow: concentration levels and regional distribution of major elements. Sci.Total Environ. 336, 183-199.

Cogley, J.G., R. Hock, L.A. Rasmussen, A.A. Arendt, A. Bauder, R.J. Braithwaite, P. Jansson, G. Kaser, M. Möller, L. Nicholson, and M. Zemp (2011) Glossary of Glacier Mass Balance and Related Terms. IHP-VII Technical Documents in Hydrology No. 86, IACS Contribution No. 2, UNESCO-IHP, Paris.

Comiso, J.C. (2006) Abrupt decline in the Arctic winter sea ice cover, Geophysical Research Letter, 33, L18504, doi:10.1029/2006GL027341.

Corbett, J. J., D.A. Lack, J.J. Winebrake, S. Harder, J.A. Silberman, and M. Gold (2010) Arctic shipping emissions inventories and future scenarios, Atmos. Chem. Phys., 10, 9689–9704, doi:10.5194/acp-10-9689-2010.

Crutzen, P. J., and E.F. Stoermer (2000) The Anthropocene. Global Change Newsl. 41, 17–18.

Dacey, J.W.H., and S.G. Wakeham (1986) Oceanic Dimethylsulfide: Production During Zooplankton Grazing on Phytoplankton, Science, 223 (4770), 1314-1316, doi: 10.1126/science.233.4770.1314.

Dagestad, K. F., J. Johannessen, G. Hauge, V. Kerbaol, and F. Collard (2006) High-resolution Wind Field Retrievals off the Norwegian Coast: Comparing ASAR Observations and MM5 Simulations. Proceedings OceanSAR 2006 St. John's, NL, Canada.

Dansgaard W. (1964) Stable isotopes in precipitation. Tellus 14(4), 436-468.

Davis, D., G. Chen, P. Kasibhatla, A. Jefferson, D. Tanner, F. Eisele, D. Lenschow, W. Neff, and H. Berresheim (1998) DMS oxidation in the Antarctic marine boundary layer: Comparison of model simulations and Held observations of DMS, DMSO, $DMSO_2$, H_2SO_4(g), MSA(g), and MSA(p), J. Geophys. Res., 103(D1), 1657–1678, doi:10.1029/97JD03452.

Day, J. J., J.L. Bamber, P.J. Valdes, and J. Kohler (2012) The impact of a seasonally ice free Arctic Ocean on the temperature, precipitation and surface mass balance of Svalbard, The Cryosphere, 6, 141-141, doi:10.5194/tc-6-141-2012.

Delmas, R. J. (1992) Environmental information from ice cores, Rev. Geophys., 30(1), 1 – 21.

Deser, C., R. Tomas, M. Alexander, D. Lawrence (2010) The Seasonal Atmospheric Response to Projected Arctic Sea Ice Loss in the Late Twenty-First Century. J. Climate, 23, 333–351. doi: http://dx.doi.org/10.1175/2009JCLI3053.1.

Dibb, J. E., R. W. Talbot, J. W. Munger, D. J. Jacob, and S.-M. Fan (1998) Air-snow exchangeo f HNO_3 and NOy at Summit,Greenland, J. Geophys. Res., 103, 3475-3486.

Dickson R.R., T.J.Osborn, J.W. Hurrell, J. Meincke, J. Blindheim, B. Ådlandsvik, T. Vinje, G. Alekseev, W. Maslowski (2000) The Arctic Ocean response to the North Atlantic Oscillation. J. Clim 13:2671–2696.

Divine, D. and C. Dick (2006) Historical variability of sea ice edge position in the Nordic Seas, J. Geophys. Res., 111. C01001, doi:10.1029/2004JC002851.

Divine, D., E. Isaksson, V. Pohjola, H. A. J. Meijer, R. S. van de Wal, T. Martma, J. C. Moore, B. Sjögren, and F. Godtliebsen (2008) Deuterium excess record from a small Arctic ice cap, J. Geophys. Res., 113, D19104, doi:10.1029/2008JD010076.

Divine, D., E. Isaksson, F. Godtliebsen, T. Martma, H. A. J. Meijer, J. C. Moore, V. Pohjola, and R. S. van de Wal (2011a) Thousand years of winter surface air temperature variations in Svalbard and northern Norway reconstructed from ice core data, Polar Res. 30, 7379, doi: 10.3402/polar.v30i0.7379.

Divine, D. V., J. Sjolte, E. Isaksson, H. A. J. Meijer, R. S. W. van de Wal, T. Martma, V. Pohjola, C. Sturm and F. Godtliebsen (2011b) Modelling the regional climate and isotopic composition of Svalbard precipitation using REMOiso: a comparison with available GNIP and ice core data. Hydrol. Process., 25: 3748–3759. doi: 10.1002/hyp.8100.

Dowdeswell, J.A. (1986) Drainage-basin characteristics of Nordaustlandet ice caps, Svalbard, Journal of Glaciology, 32(110),31-38.

Dyurgerov, M., A. Bring, and G. Destouni (2010) Integrated assessment of changes in freshwater inflow to the Arctic Ocean, J. Geophys. Res.-Atmos., 115, D12116, 9 pp., doi:10.1029/2009JD013060.

Eichler, A., S. Brütsch, S. Olivier, T. Papina, and M, Schwikowski (2009) A 750 year ice core record of past biogenic emissions from Siberian boreal forests. Geophys. Res. Lett. 36, L18813. doi:10.1029/2009GL038807.

Eichler, A., W. Tinner, S. Brütsch, S. Olivier, T. Papina, and M. Schwikowski (2011) An ice-core based history of Siberian forest fires since AD 1250. Quat. Sci. Rev., 30, 1027-1034.

Engelsen, O., E. N. Hegseht, H. Hop, E. Hansen, and S. Falk-Petersen (2002) Spatial variability of chlorophyll-a in the Marginal Ice Zone of the Barents Sea, with relations to sea ice and oceanographic conditions, J. Marine Syst., 35, 70-97.

Fisher, D. A., R. M. Koerner, W. S. B. Paterson, W. Dansgaard, N. Gundestrup, and N. Reeh (1983) Effect of wind scouring on climatic records from ice-core oxygen-isotope profiles, Nature, 301, 205-209, doi:10.1038/301205a0.

Fisher, D. A., N. Reeh, and H. B. Clausen (1985) Stratigraphic noise in time series derived from ice cores, Ann. Glaciol., 7, 76–83.

Fisher, D.A., and R.M. Koerner (1988) The effects of wind on $\delta^{18}O$ and accumulation give an inferred record of δ seasonal amplitude from the Agassiz ice cap, Ellesmere Island, Canada. Annals of Glaciology, 10, 34–37.

Fisher, D. A., R.M. Koerner, J.C. Bourgeois, G. Zielinski, C. Wake, C.U. Hammer, H.B. Clausen, N. Gundestrup, S. Johnsen, K. Goto-Azuma, T. Hondoh, E. Blake, M. Gerasimoff (1998) Penny Ice Cap Cores, Baffin Island, Canada, and the Wisconsinan Foxe Dome Connection: Two States of Hudson Bay Ice Cover, Science, 279 (5351), 692-695, doi: 10.1126/science.279.5351.692.

Fisher, J.A., D. J. Jacob, Q. Wang, R. Bahreini, C. C. Carouge, M. J. Cubison, J. E. Dibb, T. Diehl, J. L. Jimenez, E. M. Leibensperger, Z. Lu, M. B. J. Meinders, H. O. T. Pye, P. K. Quinn, S. Sharma, D. G. Streets, A. van Donkelaar, R. M. Yantosca (2011) Sources, distribution, and acidity of sulfate-ammonium aerosol in the Arctic winter-spring, Atmos. Environ., 45, 7301-7318, doi:10.1016/j.atmosenv.2011.030.

Foley, P., J.G. Dorsey (1984) Clarification of the limit of detection in chromatography, Chromatographia 18,503.

Francis, J. A., E. Hunter, J. R. Key, and X. Wang (2005) Clues to variability in Arctic minimum sea ice extent, Geophys. Res. Lett., 32, L21501, doi:10.1029/2005GL024376.

Forsström, S., J.Strom, C. A. Pedersen, E.Isaksson, and S. Gerland (2009) Elemental carbon distribution in Svalbard snow, J. Geophys. Res., 114, D19112, doi:10.1029/2008jd011480.

Førland, E.J., I. Hanssen-Bauer, and P.Ø., Nordli (1997) Climate statistics and long-term series of temperatures and precipitation at Svalbard and Jan Mayen. Det Norske Meteorologiske Institutt, Oslo.

Galloway, J. N., W. H. Schlesinger, H. Levy, A. Michaels, and J. L. Schnoor (1995) Nitrogen fixation: Anthropogenic enhancement-environmental response, Global Biogeochem. Cycl., 9, 235–252.

Gao, C., A. Robock, and C. Ammann (2008) Volcanic forcing of climate over the past 1500 years: An improved ice-core-based index for climate models. J. Geophys. Res., 113, D23111, doi:10.1029/2008JD010239.

Gazeaux, J., D. Batista, C.M. Ammann, P. Naveau, C. Jégat, and C. Gao (2012) Extracting common pulse-like signals from multiple ice core time series, Comput. Stat. Data An., doi:10.1016/j.csda.2012.01.024.

Gordiyenko, F. G., V. M. Kotlyakov, Y.-K. M. Punning, and R. Vaikmäe (1981) Study of a 200-m core from the Lomonosov ice plateau on Spitsbergen and the paleoclimatic implications, Polar Geogr. Geol., 5(4), 242– 251.

Goto-Azuma, K., S. Koshima, T. Kameda, S. Takahashi, O. Watanabe, Y. Fujii, and J.-O. Hagen (1995) An ice-core chemistry record from Snøfjellafonna, northwestern Spitsbergen, Ann. Glaciol., 21, 213-218.

Grabiec, M., D. Puczko, T. Budzik, G. Gajek (2011) Snow distribution patterns on Svalbard glaciers derived from radio-echo soundings, Polish Polar Research, vol. 32, no. 4, pp. 393–421, doi: 10.2478/v10183–011–0026–4.

Grinsted, A., J.C. Moore and S. Jevrejeva (2004) Application of the cross wavelet transform and wavelet coherence to geophysical time series, Nonlinear Processes Geophys., 11, 561-566.

Grinsted, A., J. C. Moore, V. Pohjola, T. Martma, and E. Isaksson (2006) Svalbard summer melting, continentality and sea ice extent from the Lomonosovfonna ice core, J. Geophys. Res., 111, D07110, doi:10.1029/2005JD006494.

Grinsted, A., J. C. Moore, and S. Jevrejeva (2009) Reconstructing sea level from paleo and projected temperatures 200 to 2100AD, Clim. Dyn., doi:10.1007/s00382-008-0507-2.

Grinsted, A., J. C. Moore, and S. Jevrejeva (2010) Reconstructing sea level from paleo and projected temperatures 200 to 2100 AD, Clim. Dyn., 34, 461–472, doi:10.1007/s00382-008-0507-2.

Groves, D. G., and J. A. Francis (2002) Variability of the Arctic atmospheric moisture budget from TOVS satellite data, J. Geophys. Res., 107(D24), 4785, doi:10.1029/2002JD002285.

Grumet, N. S., C. P. Wake, G. A. Zielinski, D. Fisher, R. Koerner, and J. D. Jacobs (1998) Preservation of glaciochemical time-series in snow and ice from the Penny Ice Cap, Baffin Island, Geophys. Res. Lett., 25(3), 357-360, doi:10.1029/97/GL03787.

Grumet, N.S., C.F. Wake, P.A. Mayewski, G.A. Zielinski, S.I. Whitlow, R.M. Koerner, D.A. Fisher, and J.M. Woollett (2001) Variability of sea-ice extent in Baffin Bay over the last millennium. Clim. Change, 49:129–145.

Hagen, J. O., O. Liestøl, E. Roland, and T. Jørgensen (1993) Glacier atlas of Svalbard and Jan Mayen, Meddelelse 129, Norw. Polar Inst., Oslo.

Hansen, J., R. Ruedy, M. Sato, and K. Lo (2010) Global surface temperature change, Rev. Geophys., 48, RG4004, doi:10.1029/2010RG000345.

Helama, S., H., Seppä , H.J.B. Birks, and A.E. Bjune (2010) Reconciling pollen-stratigraphical and tree-ring evidence for high- and low-frequency temperature variability in the past millennium, Quaternary Sci. Rev., 29, 3905–3918.

Holland, M. M. (2003) The North Atlantic Oscillation–Arctic Oscillation in the CCSM2 and its influence on Arctic climate variability. J. Climate 16, 2767–2781.

Holland M., and C. Bitz (2003) Polar amplification of climate change in coupled models. Clim Dyn 21:221–232. doi:10.1007/s00382-003-0332-6.

Honrath, R. E., M.C. Peterson, S. Guo, J.E. Dibb, P.B. Shepson, and B. Campbell (1999) Evidence of NO_x production within or upon ice particles in the Greenland snowpack, Geophys. Res. Lett., 26, 695–698.

Hughes, M. K., and H. F. Diaz (1994) Was there a 'Medieval Warm Period' and if so, when and where?, Clim. Change, 26, 109–142.

Hurrell, J. W., Y. Kushnir, G. Ottersen, and M. Visbeck (2003) An overview of the North Atlantic Oscillation. The North Atlantic Oscillation: Climatic Significance and Environmental Impact, Geophys. Monogr., Vol. 134, Amer. Geophys. Union, 1–35.

Hynes, A.J., P.H. Wine, and D.H. Semmes (1986) Kinetics and mechanism of OH reactions with organic sulfides, J. Phys. Chem. 90, 4148-4156.

Iizuka, Y., M. Igarashi, K. Kamiyama, H. Motoyama, and O. Watanabe (2002) Ratios of Mg^{2+}/Na^{+} in snowpack and an ice core at Austfonna ice cap, Svalbard, as an indicator of seasonal melting, J. Glaciol., 48(162), 452-460.

Intergovernmental Panel on Climate Change (2007) Climate change 2007: synthesis report. Contribution of working groups I, II and III to the fourth assessment report of the Intergovernmental Panel on Climate Change. Core Writing Team. In: Pachauri, R.K., Reisinger, A. (Eds.). IPCC, Geneva, Switzerland, p. 104.

Isaksson, E., V. A. Pohjola, T. Jauhiainen, J. C. Moore, J-F. Pinglot, R. Vaikmäe, R. S. W. van de Wal, J-O. Hagen, J. Ivask, L. Karlöf, T. Martma, H.A.J. Meijer, R. Mulvaney, M. Thomassen, M. van den Broeke (2001) A new ice core record from Lomonosovfonna, Svalbard: Viewing the data between 1920– 1997 in relation to present climate and environmental conditions, J. Glaciol., 47(157), 335– 345, doi:10.3189/172756501781832313

Isaksson E., M. Hermansson, S. Hicks, M. Igarashi, K. Kamiyama, J. Moore, H. Motoyama, D. Muir, V. Pohjola, R. Vaikmäe, R. van de Wal, and O. Watanabe (2003) Ice cores from Svalbard – useful archives of past climate and pollution history. Phys Chem Earth 28: 1217-1228.

Isaksson, E., J. Kohler, V. Pohjola, J. C. Moore, M. Igarashi, L. Karlöf, T. Martma, H. A. J. Meijer, H. Motoyama, R. Vaikmäe, and R. S. van de Wal (2005) Two ice-core $\delta^{18}O$ records from Svalbard illustrating climate and sea-ice variability over the last 400 years, The Holocene, 15(4), 501-509.

Isaksson, E., T. Kekonen, J. C. Moore, and R. Mulvaney (2006) The methansulfonic acid (MSA) record in a Svalbard ice core, Ann. Glaciol., 42(1), 345-351.

Iversen, T. and E. Joranger (1985) Arctic air pollution and large scale atmospheric flows, Atmos. Environ., 19, 2099-2108.

Jacob, T., J. Wahr, W.T. Pfeffer, and S. Swenson (2012) Recent contributions of glaciers and ice caps to sea level rise. Nature, in press.

Jania, J., Y. Y. Macheret, F. J. Navarro, A. F. Glazovksy, E. V. Vasilenko, J. Lapazaran, P. Glowacki, K. Migala, A. Balut, and P. A. Piwowar (2005) Temporal changes in the radiophysical properties of a polythermal glacier in Spitsbergen, Ann. Glaciol., 42, 125–134.

Jarvis, J. C., E.J. Steig, M.G. Hastings, and S.A., Kunasek (2008) Influence of local photochemistry on isotopes of nitrate in Greenland snow, Geophys. Res. Lett., 35, L21804, doi:10.1029/2008GL035551.

Jauhiainen, T., J. Moore, P. Perämäki, J. Derome and K. Derome (1999) Simple procedure for ion chromatographic determination of anions and cations at trace levels in ice core samples. Anal. Chim. Acta, 389(1), 21–29.

Jevrejeva, S., A. Grinsted, J.C. Moore and S. Holgate (2006) Nonlinear trends and multi-year cycle in sea level records. J. Geophys. Res., 111(C9), C09012. (10.1029/2005JC003229.

Jevrejeva, S., J. C. Moore, and A. Grinsted (2008) Relative importance of mass and volume changes to global sea level rise, J. Geophys. Res., 113, D08105, doi:10.1029/2007JD009208.

Jevrejeva, S., A. Grinsted and J.C. Moore (2009) Anthropogenic forcing dominates sea level rise since 1850, Geophys. Res. Lett. doi:10.1029/2009GL040216.

Jevrejeva, S., J. C. Moore, and A. Grinsted (2010) How will sea level respond to changes in natural and anthropogenic forcings by 2100?, Geophys. Res. Lett., 37, L07703, doi:10.1029/2010GL042947.

Jickells, T. D., S. D. Kelly, A. R. Baker, K. Biswas, P. F. Dennis, L. J. Spokes, M. Witt, and S. G. Yeatman (2003) Isotopic evidence for a marine ammonia source, Geophys. Res. Lett., 30(7), 1374, doi:10.1029/2002GL016728.

Johannessen, O. L., E. V. Shalina, and M.W. Miles (1999) Satellite evidence for an Arctic sea ice cover in transformation, Science, 286, 1937– 1939.

Johnsen, S. J., H. B. Clausen, K. M. Cuffey, G. Hoffmann, J. Schwander, and T. Creyts (2000) Diffusion of stable isotopes in polar firn and ice: The isotope effect in firn diffusion, in Physics of Ice Core Records, edited by T. Hondoh, pp. 121–140, Hokkaido University Press, Sapporo.

Johnson, M. T., P. S. Liss, T. G. Bell, T. J. Lesworth, A. R. Baker, A. J. Hind, T. D. Jickells, K. F. Biswas, E. M. S. Woodward, and S. W. Gibb (2008) Field observations of the ocean-atmosphere exchange of ammonia: Fundamental importance of temperature as revealed by a comparison of high and low latitudes, Global Biogeochem. Cycles, 22, GB1019, doi:10.1029/2007GB003039.

Jones, P. D., and M. E. Mann (2004) Climate over past millennia, Rev. Geophys., 42, RG2002, doi:10.1029/2003RG000143.

Jourdain, B., and M. Legrand (2001) Seasonal variations of dimethyl sulfide, dimethyl sulfoxide, sulfur dioxide, methanesulfonate, and nonsea-salt sulfate aerosols at Dumont d'Urville (December 1998 - July 1999), J. Geophys. Res., 106, 14,391-14,408.

Kameda, T., S. Takahashi, K. Goto-Azuma, S. Kohshima, O. Watanabe, and J.-O. Hagen (1993) First report of ice core analyses and borehole temperatures on the highest ice field on western Spitsbergen in 1992, Bull. Glac. Res., 11, 51-62.

Kang S., P. A. Mayewski, D. Qin, Y. Yan, S. Hou, D. Zhang, J. Ren, K. Kreutz (2002) Glaciochemical records from a Mt. Everest ice core: relationship to atmospheric circulation over Asia. Atmos. Environ., 36: 3351-3361.

Kaspari, S., P.A. Mayewski, S. Hkang, S.B. Sneed, S. Hou, R. Hooke, K.J. Kreutz, D. Introne, M. Handley, K.A. Maasch, D. Qin, J. Ren (2007) Reduction in northward incursions of the South Asian Monsoon since ;1400 AD inferred from a Mt. Everest ice core. Geophys. Res. Lett., 34, L16701, doi:10.1029/2007GL030440.

Kaspari, S, R. Hooke, P. A. Mayewski, S. Kang, S. Hou, and D. Qin (2008) Snow accumulation rate on Qomolangma (Mount Everest), Himalaya: Synchroneity with sites across the Tibetan Plateau on 50-100 year timescales. J. Glaciol., 54, 343–352.

Kaufman, D.S. Schneider, D.P. McKay, N.P. Ammann, C.M. Bradley, R.S. Briffa, K.R. Miller, G.H. Otto-Bliesner, B.L. Overpeck, J.T. Vinther, Arctic Lakes 2k Project Members (2009) Recent warming reverses long term Arctic cooling. Science 325,1236–1239.

Kekonen, T., J. C. Moore, R. Mulvaney, E. Isaksson, V. Pohjola, and R. S. van de Wal (2002) A 800 year record of nitrate from the Lomonosovfonna ice core, Svalbard, J. Glaciol., 35, 261-265.

Kekonen, T., P. Perämäki, and J. C. Moore (2004) Comparison of analytical results for chloride, sulfate and nitrate obtained from adjacent ice core samples by two ion chromatographic methods, J. Environ. Monit., 2, 147–152, doi:10.1039/B306621E.

Kekonen, T., J. C. Moore, P. Perämäki, R. Mulvaney, E. Isaksson, V. Pohjola, and R. S. W. van de Wal (2005a) The 800 year long ion record from the Lomonosovfonna (Svalbard) ice core, J. Geophys. Res., 10, doi:1029/2004JD005223.

Kekonen, T., J.C. Moore, P. Perämäki and T. Martma (2005b) The Icelandic Laki volcanic tephra layer in the Lomonosovfonna ice core, Svalbard. Polar Research 24(1-2), 33-40.

Kelsey E.P, C.P Wake, K. Kreutz and E. Osterberg (2010) Ice layers as an indicator of summer warmth and atmospheric blocking in Alaska. J. Glaciol., 56(198), 715–722.

Kerminen, V.M., K. Teinila, R. Hillamo, T. Pakkanen (1998) Substitution of chloride in sea-salt particles by inorganic and organic anions Journal of Aerosol Science, 29, pp. 929–942.

Kinnard, C., R. M. Koerner, C. M. Zdanowicz, D. A. Fisher, J. Zheng, M. J. Sharp, L. Nicholson, and B. Lauriol (2008) Stratigraphic analysis of an ice core from the Prince of Wales Icefield, Ellesmere Island, Arctic Canada, using digital image analysis: High-resolution density, past summer warmth reconstruction, and melt effect on ice core solid conductivity, J. Geophys. Res., 113, D24120, doi:10.1029/2008JD011083.

Kinnard, C., C. M. Zdanowicz, D.A. Fisher, E. Isaksson (2011) Reconstructed changes in Arctic sea ice over the past 1,450 years, Nature 479(7374): 509-U231.

Kistler, R., E. Kalnay, W. Collins, S. Saha, G. White, J. Woollen, M. Chelliah, W. Ebisuzaki, M. Kanamitsu, V. Kousky, H. Van den Dool, R. Jenne, and M. Fiorino (2001) The NCEP–NCAR 50-Year Reanalysis: Monthly Means CD-ROM and Documentation. Bulletin of the American Meteorological Society, 82, 247–268.

Koenigk, T., U. Mikolajewicz, J. H. Jungclaus, A. Kroll (2009) Sea ice in the Barents Sea: seasonal to interannual variability and climate feedbacks in a global coupled model, Clim. Dyn., 32, 1119–1138, doi: 10.1007/s00382-008-0450-2.

Koerner, R.M. (1997) Some comments on climatic reconstructions from ice cores drilled in areas of high melt, J. Glaciol., 43, 90-97.

Kohler, J., T.D. James, T. Murray, C. Nuth, O. Brandt, N.E. Barrand, H.F. Aas, and A. Luckman (2007) Acceleration in thinning rate on western Svalbard glaciers, Geophys. Res. Lett., 34, L18502, doi:10.1029/2007GL030681.

Kotlyakov, V.M., Arkhipov, S.M. Henderson, K.A., and O. V. Nagornov (2004) Deep drilling of glaciers in Eurasian Arctic as a source of paleoclimatic records. Quaternary Science Reviews, 23, 1371–1390.

Kvingedal, B. (2005) Sea Ice Extent and variability in the Nordic Seas 1967-2002, The Nordic Seas: an integrated perspective, Helge Drange, AGU, ISBN-13:978-0-87590-423-8.

Langner, J., H. Rodhe (1991) A global three-dimensional model of the tropospheric sulfur cycle, Journal of Atmospheric Chemistry, 13, pp. 225–265.

Law, K. S., and A. Stohl (2007) Arctic air pollution: Origins and impacts, Science, 315(5818), 1537–1540, doi:10.1126/science.1137695.

Lefauconnier, B., J.-O. Hagen, and J.-P. Rudant (2001) Flow speed and calving rate of Kongsbreen glacier, Svalbard, using SPOT images, Polar Res., 59-65.

Legrand, M. R. and R.J. Delmas, (1988) Formation of HCl in the Antarctic Atmosphere, J. Geophys. Res. 93, 7153–7168.

Legrand, M. R. and S. Kirchner (1990) Origins and variations of nitrate in south polar precipitation, J. Geophys. Res., 95, 3493–3507.

Legrand, M., C. Feniet-Saigne, E.S. Saltzman, C. Germain, N.I. Barkov, and V.N. Petrov (1991) Ice-core record of oceanic emissions of dimethylsulphide during the last climate cycle. Nature 350, 144-146.

Legrand, M., M. DeAngelis, F. Maupetit (1993) Field investigation of major and minor ions along Summit (Central Greenland) ice cores by ion chromatography. J. Chromatogr. 460, 251–258.

Legrand, M., and P. Mayewski (1997) Glaciochemistry of polar ice cores: A review, Rev. Geophys., 35(3), 219– 243.

Legrand, M., S. Preunkert, D. Wagenbach, and H. Fischer (2002) Seasonally resolved Alpine and Greenland ice core records of anthropogenic HCl emissions over the 20th century, J. Geophys. Res., 107(D12), 4139, doi:10.1029/2001JD001165.

Liss, P. S., and J. N. Galloway (1993) Air-Sea exchange of sulphur and nitrogen and their interaction in the marine atmosphere, in: Interactions of C,N,P and S Biogeochemical Cycles and Global Change, edited by R. Wollast, F. T. Mackenzie, and L. Chou, Springer Verlag, Berlin.

Loeng, H. (1991) Features of the physical oceanographic conditions of the Barents Sea. In E. Sakshaug et al. (eds.): Proceedings of the Pro Mare Symposium on Polar Marine Ecology, Trondheim, Norway, 12–16 May 1990. Polar Res. 10, 5–18.

Macias-Fauria, M., A. Grinsted, S. Helama, J. Moore, M. Timonen, T. Martma, E. Isaksson, M. Eronen (2009) Unprecedented low twentieth century winter sea ice extent in the Western Nordic Seas since A.D. 1200. Climate Dynamics.

Marion, G., M.R.E. Farren, and A.J. Komrowski (1999) Alternative pathways for seawater freezing, Cold Reg. Sci. Technol., 29, 259--266.

Masson, V., F. Vimeux, J. Jouzel, V. Morgan, M. Delmotte, P. Ciais, C. Hammer, S. Johnsen, V. Lipenkov, E. Mosley-Thompson, J.-R. Petit, E.J. Steig, M. Stievenard, R. Vaikmae (2000) Holocene climate variability in Antarctica based on 11 ice-core isotopic records. Quaternary Research 54, 348–358.

Masson-Delmotte, V., J. Jouzel, A. Landais, M. Stievenard, S. J. Johnsen, J. W. C. White, M. Werner, A. Sveinbjornsdottir, and K. Fuhrer (2005) GRIP deuterium excess reveals rapid and orbital-scale changes in Greenland moisture origin, Science, 209, 118–121, doi:10.1126/science.1108575.

Matoba, S., H. Narita, H. Motoyama, K. Kamiyama, and O. Watanabe (2002) Ice core chemistry of Vestfonna ice cap in Svalbard, Norway. J. Geophys. Res.,107, doi:10.1029/2002JD002205.

Meier, M.F., M.B. Dyurgerov, U.K. Rick, S. O'Neel, W.T. Pfeffer, R.S. Anderson, S.P. Anderson, and A.F. Glazovsky (2007) Glaciers dominate eustatic sea-level rise in the 21st century. Science 317: 1064-1067.

Moore, J. C., A. Grinsted, T. Kekonen, and V. Pohjola (2005) Separation of melting and environmental signals in an ice core with seasonal melt, Geophys. Res. Lett., 32, L10501, doi:10.1029/2005GL023039.

Moore, J. C., T. Kekonen, A. Grinsted (2006) Sulfate source inventories from a Svalbard ice core record spanning the Industrial Revolution, J. Geophys. Res., 111, D15307, doi:10.1029/2005JD006453,.

Moore, J. C. and A. Grinsted (2009) Ion fractionation and percolation in ice cores with seasonal melting, Physics of Ice Core Records II, Supplement Issue of Low Temperature Science, 68.

Moore, J. C., S. Jevrejeva, and A. Grinsted (2011) The historical global sea level budget, Ann. Glaciol., 52(59), 8–14.

Morin, S., J. Savarino, M.M. Frey, N. Yan, S. Bekki, J.W. Bottenheim, and J.M.F. Martins (2008) Tracing the Origin and Fate of NO_x in the Arctic Atmosphere Using Stable Isotopes in Nitrate,Science, 322, 730–732, doi:10.1126/science.1161910.

Morison, J., K. Aagaard, M. Steele (2000) Recent environmental changes in the Arctic: A Review, Arctic, 53, 4, 359-371.

Motoyama, H, O. Watanabe, Y. Fujii, K. Kamiyama, M. Igarashi, S. Matoba, T. Kameda, K. Goto-Azuma, K. Izumi, H. Narita, Y. Iizuka, and E. Isaksson (2008) Analyses of ice core data from various sites in Svalbard glaciers from 1987 to 1999. NIPR Arctic data reports, NIPR, Tokyo.

Möller, M., R. Finkelnburg, M. Braun, R. Hock, U. Jonsell, V. Pohjola, D. Scherer, and C. Schneider (2011a) Climatic mass balance of the ice cap Vestfonna, Svalbard: a spatially distributed assessment using ERA-Interim and MODIS data. Journal of Geophysical Research, 116, F03009, doi:10.1029/2010JF001905.

Möller, M., R. Möller, É. Beaudon, O.-P. Mattila, R. Finkelnburg, M. Braun, M. Grabiec, U. Jonsell, B. Luks, D. Puczko, D. Scherer, and C. Schneider (2011b) Snowpack characteristics of Vestfonna and De Geerfonna (Nordaustlandet, Svalbard): a spatiotemporal analysis based on multiyear snow-pit data. Geografiska Annaler: Series A, Physical Geography. doi: 10.1111/j.1468-0459.2011.00440.

Mulvaney, R., S. Bremner, A. Tait and N. Audley (2002) A medium depth ice core drill. Nat. Inst. Polar Res. Mem., Special Issue, 56, 82–90.

Nicholls, R. J., and A. Cazenave (2010) Sea-level rise and its impact on coastal zones. Science 328,1517–1520. (doi:10.1126/science.1185782).

Niedzwiedz, T. (1997) Czastoea wystapowania typw cyrkulacji nad Spitsbergen (1951-1995). [Frequency of circulation patterns above Spitsbergen (1951–1995)]. Probl. Klimatol. Polarnerj, 7, 9–16.

Nuth, C., G. Moholdt, J. Kohler, J. Hagen, and A. Kääb (2010) Svalbard glacier elevation changes and contribution to sea level rise, J.Geophys. Res., 115, F01008, doi:10.1029/2008JF001223.

Nye, J. F. (1963) Correction factor for accumulation measured by the thickness of the annual layers in an ice sheet, J. Glaciol., 4(36), 785-788.

O'Brien, S. R., P. A. Mayewski, L. D. Meeker, D. A. Meese, M. S. Twickler, and S. I. Whitlow (1995) Complexity of Holocene climate as reconstructed from a Greenland ice core, Science, 270, 1962–1964.

O'Dwyer, J., E. Isaksson, T. Vinje, T. Jauhiainen, J. C. Moore, V. Pohjola, R. Vaikmäe, and R. S. van de Wal (2000) Methansulfonic acid in a Svalbard ice core as an indicator of ocean climate, Geophys. Res. Lett., 27(8), 1159-1162.

Ottar, B. (1989) Arctic air pollution: A Norwegian perspective, Atmos. Environ., 23, 2349–2356.

Overpeck, J., K. Hughen, D. Hardy, R. Bradley, R. Case, M. Douglas, B. Finney, K. Gajewski, G. Jacoby, A. Jennings, S. Lamoureux, A. Lasca, G. MacDonald, J. Moore, M. Retelle, S. Smith, A. Wolfe, and G. Zielinski (1997) Arctic environmental changes of the last four centuries. Science, 278, 1251–1256.

Palosuo, E. (1987a) A Study of Snow and Ice Temperatures on Vestfonna, Svalbard, 1956, 1957 and 1958, Geografiska Annaler: Series A, Physical Geography, 69A (3/4), 431-437.

Palosuo, E. (1987b) Ice layers and superimposition of ice on the summit and slope of Vestfonna, Svalbard. Geografiska Annaler: Series A, Physical Geography, 69 (2), 289–296.

Parkinson C.L., D.J. Cavalieri, P. Gloersen, H.J. Zwally (1999) Arctic sea ice extents, areas, and trends, 1978–1996. J Geophys Res-Oceans 104 (C9):20837–20856.

Peterson, B. J., R.M. Holmes, J.W. McClelland, C.J. Vörösmarty, R.B. Lammers, A.I. Shiklomanov, I.A. Shiklomanov, and S. Rahmstorf (2002) Increasing river discharge to the Arctic Ocean, Science 298, 2171–2173.

Petit JR, J. Jouzel, D. Raynaud, N. I. Barkov, J.-M. Barnola, I. Basile, M. Bender, J. Chappellaz, M. Davisk, G. Delaygue, M. Delmotte, V. M. Kotlyakov, M. Legrand, V. Y. Lipenkov, C. Lorius, L. Pépin, C. Ritz, E. Saltzmank and M. Stievenard (1999) Climate and atmospheric history of the past 4 20 000 years from the Vostok ice core, Antarctica. Nature, 399, 429–436.

Petoukhov, V. and V.A. Semenov (2010) A link between reduced Barents-Kara sea ice and cold winter extremes over northern continents. Journal of Geophysical Research, 115, doi:10.1029/2009JD013568.

Pettersson, R., P. Christoffersen, J.A. Dowdeswell, V. Pohjola, A. Hubbard, and T. Strozzi (2011) Ice thickness, thermal structure and basal conditions of the ice cap Vestfonna, eastern Svalbard, inferred from radio-echo sounding. Geog. Ann.

Pinglot, J. F., M. Pourchet, B. Lefauconnier, J. O. Hagen, E. Isaksson, R. Vaikmaë, and K. Kamiyama (1999) Investigations of temporal change of the accumulation in Svalbard glaciers deducted from nuclear tests and Chernobyl reference layers, Polar Res., 18, 315– 321, doi:10.1111/j.1751-8369.1999.tb00309.x.

Pohjola, V.A., J. C. Moore, E. Isaksson, T. Jauhiainen, R. S. van de Wal, T. Martma, H. A. J. Meijer, and R. Vaikmäe (2002a) Effect of periodic melting on geochemical and isotopic signals in an ice core from Lomonosovfonna, Svalbard, J. Geophys. Res., 107(04), 1-14.

Pohjola, V.A., T. Martma, H. A. J. Meijer, J. C. Moore, E. Isaksson, R. Vaikmäe and R. S. W. van de Wal (2002b) Reconstruction of three centuries of annual accumulation rates based on the record of stable isotopes of water from Lomonosovfonna, Svalbard. Ann. Glaciol., 35, 57-62.

Pohjola, V.A., P. Kankaanpää, J.C. Moore, and T. Pastusiak (2011a) Preface: The International Polar Year Project 'Kinnvika'– Arctic warming and impact research at 80° N. Geografiska Annaler: Series A, Physical Geography. doi: 10.1111/j.1468-0459.2011.00436.x.

Pohjola, V., P. Christoffersen, L. Kolondra, J.C. Moore, R. Pettersson, M. Schäfer, T. Strozzi, A. Hubbard, U. Jonsell, and C.H. Reijmer (2011b) Spatial distribution and change in the surface ice-velocity field of Vestfonna ice cap, Nordaustlandet, Svalbard, 1995–2010 using geodetic and satellite interferometry data. Geografiska Annaler: Series A, Physical Geography. doi: 10.1111/j.1468-0459.2011.00441.x.

Pälli, A., J. Kohler, E. Isaksson, J.C. Moore, J-F. Pinglot, V. Pohjola, and H. Samuelsson (2003) Spatial and temporal variability of snow accumulation using ground-penetrating radar and ice cores on a Svalbard glacier. J.fGlaciol. 48, 417-424.

Punning Y.-M.K., T.A. Martma, K.E. Tyugu, R.A. Vaykmyae, M. Pourchet and F. Pinglot (1986) Stratification in an ice core from Vestfonna, Nordaustlandet. Polar Geography and Geology 10, 39–43 (translated from Materialy Glyatsiologicheskikh Issledovanii 52, 202–205).

Quinn, P. K., T. S. Bates, J. E. Johnson, J. E. Covert, and R. J. Charlson (1990) Interactions between sulfur and reduced nitrogen cycles over the central Pacific Ocean, J. Geophys. Res., 95, 16,405– 16,416.

Quinn, P. K., G. Shaw, E. Andrews, E.G. Dutton, T. Ruoho-Airola, and S.L. Gong (2007) Arctic haze: current trends and knowledge gaps, Tellus, 59B, 99–114.

Radić V. and R. Hock (2011) Regionally differentiated contribution of mountain glaciers and ice caps to future sea-level rise. Nat Geosci 4:91–94.

Rahn, K. A. (1981) Relative importance of North America and Eurasia as sources of Arctic aerosol, Atmos. Environ., 15:1447–1455.

Rankin, A. M., V. Auld, and E. W. Wolff (2000) Frost flowers as a source of fractionated sea salt aerosol in the polar regions, Geophys. Res. Lett., 27(21), 3469–3472, doi:10.1029/2000GL011771.

Rankin, A. M., E. W. Wolff, and S. Martin (2002) Frost flowers: Implications for tropospheric chemistry and ice core interpretation, J. Geophys. Res., 107(D23), 4683, doi:10.1029/2002JD002492.

Rasmussen, S. O, K. K. Andersen, A. M. Svensson, J. P. Steffensen, B. M. Vinther, H. B. Clausen, M.-L. Siggaard-Andersen, S. J. Johnsen, L. B. Larsen, M. Bigler, R. Röthlisberger, H. Fischer, K. Goto-Azuma, M. E. Hansson and U. Ruth (2006) A new Greenland ice core chronology for the last glacial termination, J. Geophys. Res.,doi:10.1029/2005JD006079.

Robock, A. (2000) Volcanic eruptions and climate, Rev. Geophys., 38, 191– 219, doi:10.1029/1998RG000054.

Röthlisberger, R., M.A. Hutterli, S. Sommer, E.W. Wolff, and R. Mulvaney (2000) Factors controlling nitrate in ice cores: evidence from the Dome C deep ice core, J. Geophys. Res., 105, 20 565–20 572.

Sakshaug, E. and J. Walsh (2000) Marine biology: biomass, productivity distribution and their variability in the Barents and Bering Seas, Nuttall, M. and T.V. Callaghan, eds. The Arctic: environment, people, policy. Amsterdam, etc., Harwood Academic Publisher.: 161-196.

Samuelsson, H. (2001) Distribution of melt layers on the ice field Lomonosovfonna, Spitsbergen, M.S. thesis, Dep. of Earth Sciences, Uppsala Univ., Uppsala, Sweden.

Saigne,C ., and M. Legrand (1987) Methanesulfonic acid in Antarctic ice, Nature, 330, 240-242.

Saltzman, E. S. (1995) Ocean-atmosphere cycling of dimethylsulfide. In Ice core studies of global biogeochemical cycles (ed. R. Delmas), pp. 65±89. NATO ASI Series. New York: Springer-Verlag.

Sand, K., J. G. Winther, D. Marechal, O. Bruland, and K. Melvold (2003) Regional variations of snow accumulation on Spitsbergen, Svalbard, 1997– 99, Nord. Hydrol., 34(1– 2), 17–32.

Savarino, J., J. Kaiser, S. Morin, D.M. Sigman, and M.H. Thiemens (2007) Nitrogen and oxygen 30 isotopic constraints on the origin of atmospheric nitrate in coastal Antarctica, Atmos. Chem. Phys., 7, 1925–1945, http://www.atmos-chem-phys.net/7/1925/2007/.

Schytt, V. (1964) Scientific results of the Swedish glaciological expedition to Nordaustlandet, Spitsbergen, 1957 and 1958. Geografiska Annaler, 46 (3), 242–281.

Shaw, G. E. (1995) The arctic haze phenomenon, Bull. Am. Meteorol. Soc., 76, 2403–2413.

Simões, J. C. and V.S. Zagorodnov (2001) The record of anthropogenic pollution in snow and ice in Svalbard, Norway, Atmos. Environ., 35, 403--413.

Solberg, S., N. Schmidbauer, A. Semb, F. Stordal and Ø. Hov (1996) Boundary-layer ozone depletion as seen in the Norwegian Arctic in spring, J. Atm. Chem., 23(3),301-332, doi:10.1007/BF00055158.

Sorteberg, A. and B. Kvingedal (2006) Atmospheric forcing on the Barents sea winter ice extent, J. Clim., 19, 4772-4784.

Spokes, L.J., S.G. Yeatman, S.E. Cornell, T.D. Jickells (2000) Nitrogen deposition to the eastern Atlantic Ocean. The importance of south-easterly flow. Tellus 52B, 37–49.

Steffen, W., J. Grinevald, P. Crutzen, J. McNeill (2011) The Anthropocene: conceptual and historical perspectives, Phil. Trans. R. Soc. A, 369, 842-867, doi:10.1098/rsta.2010.0327.

Stohl, A. (2006) Characteristics of atmospheric transport into the Arctic troposphere, J. Geophys. Res., 111.

Stohl, A., T. Berg, J. F. Burkhart, A. M. Fraa, C. Forster, A. Herber, O. Hov, C. Lunder, W. W. McMillan, S. Oltmans M. Shiobara, D. Simpson, S. Solberg, K. Stebel, J. Strm, K. Tørseth, R. Treffeisen, K. Virkkunen, and K. E. Yttri (2007) Arctic smoke – record high air pollution levels in the European Arctic due to agricultural fires in Eastern Europe in spring 2006, Atmos. Chem. Phys., 7, 511–534, http://www.atmos-chem-phys.net/7/511/2007/.

Strass, V. H., and E-M. Nöthig (1996) Seasonal shifts in ice edge phytoplankton blooms in the Barents Sea related to the water column stability, Polar Biol., 16(6), 409-422, doi: 10.1007/BF02390423.

Stroeve, J., M. M. Holland, W. Meier, T. Scambos, and M. Serreze (2007) Arctic sea ice decline: Faster than forecast, Geophys. Res. Lett., 34, L09501, doi:10.1029/2007GL029703.

Sørbel, L., Høgvard, K., and J., Tolgensbakk (1990) Geomorphology and quaternary geology of Gipsdalen, Svalbard, in Environmental atlas Gipsdalen, Svalbard, B. Brekke and R. Hanson (eds.), vol. 2, Rapport 61, Norwegian Polar Research Institute, Oslo.

Tarussov, A. (1992) The Arctic from Svalbard to Severnaya Zemlya: climatic reconstructions from ice cores. In Bradley, R.S. and Jones, P.D., editors, Climate since A.D. 1500. London and New York:Routledge, 505/16.

Taurisano, A., T.V. Schuler, J.O. Hagen, T. Eiken, E. Loe, K. Melvold, and J. Kohler (2007) The distribution of snow accumulation across the Austfonna ice cap, Svalbard: direct measurements and modelling, Polar Res., 26, 7–13.

Taylor, S., X. Feng, J.W. Kirchner, R. Osterhuber, B. Klaue, C.E. Renshaw (2001) Isotopic evolution of a seasonal snowpack and its melt. Water Resour. Res. 37 (3), 759–769.

Teinilä, K., R. Hillamo, V.-M. Kerminen, and H. J. Beine (2004) Chemistry and modal parameters of major ionic aerosol components during NICE campaigns at two altitudes, Atmos. Environ., 38, 1481 1490.

Treffeisen, R., R. Krejci, J. Ström, A. C. Engvall, A. Herber, and L. Thomason (2007) Humidity observations in the Arctic troposphere over Ny-Ålesund, Svalbard based on 15 years of radiosonde data, Atmos. Chem. Phys., 7, 2721–2732.

Tuovinen, J.-P., Y. Laurila, H. Lättilä, A. Ryaboshapko, P. Brukhanov, S. Korolev (1993) Impact of the sulphur dioxide sources in the Kola peninsula on air qualityin Northern Europe. Atmospheric Environment 27A (9), 1379–1395.

Twickler, M. and S. Whitlow (1997) Appendix B, in: Guide for the collection and analysis of ITASE snow and firn samples, edited by: Mayewski, P. A. and Goodwin, I. D., International Trans-Antarctic Scientific Expedition (ITASE), Bern, Past Global Changes (97-1).

Ulander, L. M. H. A. Carlström, and J. Askne (1995) Effect of frost flowers rough saline snow and slush on the ERS-1 SAR backscatter of thin arctic sea ice, Int. J. Remote Sens., 16(17), 3287-3305.

Vaikmäe R. (1990) Isotope variations in the temperate glaciers of the Eurasian Arctic. Nuclear Geophys 4: 4-55.

Van de Wal, R. S. W., R. Mulvaney, E. Isaksson, J. C. Moore, J.-F. Pinglot, V. Pohjola, and M. P. A. Thomassen (2002) Reconstruction of the historical temperature trend from measurements in a medium-length borehole on the Lonomosovfonna Plateau, Svalbard, Ann. Glaciol., 35, 371–378.

van der Wel, L. G., H. J. Streurman, E. Isaksson, M. M. Helsen, R. S. van de Wal, T. Martma, V. Pohjola, J. C. Moore, and H. A. J. Meijer (2011) Using high resolution tritium profiles to quantify the effects of melt on two Spitsbergen ice cores, J. Glaciol.,57(206),1087-1096.

Vaykmyae, R.A., T.A. Martma, Ya.-M.K. Punning, and K.R. Tyugu (1985) Variations in $\delta^{18}O$ and Cl^- in an ice core from Vestfonna Nordaustlandet. Polar Geography and Geology, 9 (4), 329–333.

Vinje, T. (2001) Anomalies and trends of sea ice extent and atmospheric circulation in the Nordic seas during the period 1864–1998, J. Climate, 14,255– 267.

Virkkunen, K., J. C. Moore, E. Isaksson, V. Pohjola, P. Perämäki, A. Grinsted, and T. Kekonen (2007) Warm summers and ion concentrations in snow: comparison of present day with Medieval Warm Epoch from snow pits and an ice core from Lomonosovfonna, Svalbard, J. Glaciol., 53(183), 623-634.

Wagner A., G. Lohmann, M. Prange (2011) Arctic river discharge trends since 7ka BP Global and Planetary Change,79, 1–2, 48-60, 10.1016/j.gloplacha.2011.07.006.

Watanabe, O., H. Motoyama, M. Igarashi, K. Kamiyama, S. Matoba, K. Goto-Azuma, H. Narita, T. Kameda (2001) Studies on climatic and environmental changes during the last few hundred years using ice-cores from various sites in Nordaustlandet, Svalbard, National Institute of Polar Research Memoirs, 54 (special issue), 227–242.

Whung, P.-Y., E. S. Saltzman, M. J. Spencer, P. A. Mayewski, and N. Gundestrup (1994) Two-hundred-year record of biogenic sulfur in a south Greenland ice core (20D), J. Geophys. Res., 99(D1), 1147–1156, doi:10.1029/93JD02732.

Wilson, T. R. S. (1975) Salinity and the major elements of sea water, in Chemical Oceanography, edited by J. P. Riley and G. Skirrow, pp. 365–413, Academic, Elsevier, New York.

Wolff, E. W., A. M. Rankin, and R. Röthlisberger (2003) An ice core indicator of Antarctic sea ice production?, Geophys. Res. Lett., 30(22), 2158, doi:10.1029/2003GL018454.

Wolff, E. W., A.E. Jones, S. J.-B. Bauguitte, and R.A. Salmon (2008) The interpretation of spikes and trends in concentration of nitrate in polar ice cores, based on evidence from snow and atmospheric measurements, Atmos. Chem. Phys., 8, 5627–5634, 30 http://www.atmos-chem-phys.net/8/5627/2008/.

Wu, B., J. Wang, J. Walsh (2004) Possible Feedback of Winter Sea Ice in the Greenland and Barents Seas on the Local Atmosphere, Mon. Wea. Rev., 132,1868–1876, doi:10.1175/1520-0493(2004)132<1868:PFOWSI>2.0.CO;2

Xu J Z, S. Kaspari, S.G. Hou, S. Kang, D. Qin, J.W. Ren, and P. Mayewski (2009) Records of volcanic events since AD 1800 in the East Rongbuk ice core from Mt. Qomolangma. Chinese Sci Bull, 54, 1411-1416, doi: 10.1007/s11434-009-0020-y.

Yamanouchi, T. (2012) Early 20th century warming in the Arctic: A review, Polar Science, 5, 53-71, ISSN 1873-9652, doi:10.1016/j.polar.2010.10.002.

The Cryosphere, 3, 147–154, 2009
www.the-cryosphere.net/3/147/2009/

The Cryosphere

Frost flower chemical signature in winter snow on Vestfonna ice cap, Nordaustlandet, Svalbard

E. Beaudon[1] **and J. Moore**[1,2,3]

[1]Arctic Centre, University of Lapland, P.O. Box 122, 96101 Rovaniemi, Finland
[2]Thule Institute, University of Oulu, Finland
[3]College of Global Change and Earth System Science Beijing Normal University, 19 Xinjiekou Wai Street, Beijing, 100875 China

Received: 17 November 2008 – Published in The Cryosphere Discuss.: 2 February 2009
Revised: 18 June 2009 – Accepted: 18 June 2009 – Published: 2 July 2009

Abstract. The chemistry of snow and ice cores from Svalbard is influenced by variations in local sea ice margin and distance to open water. Snow pits sampled at two summits of Vestfonna ice cap (Nordaustlandet, Svalbard), exhibit spatially heterogeneous soluble ions concentrations despite similar accumulation rates, reflecting the importance of small-scale weather patterns on this island ice cap. The snow pack on the western summit shows higher average values of marine ions and a winter snow layer that is relatively depleted in sulphate. One part of the winter snow pack exhibits a $[SO_4^{2-}/Na^+]$ ratio reduced by two thirds compared with its ratio in sea water. This low sulphate content in winter snow is interpreted as the signature of frost flowers, which are formed on young sea ice when offshore winds predominate. Frost flowers have been described as the dominant source of sea salt to aerosol and precipitation in ice cores in coastal Antarctica but this is the first time their chemical signal has been described in the Arctic. The eastern summit does not show any frost flower signature and we interpret the unusually dynamic ice transport and rapid formation of thin ice on the Hinlopen Strait as the source of the frost flowers.

1 Introduction

Investigations focussing on the glaciology of Vestfonna glacier (Nordaustlandet, Svalbard) form a part of the IPY-Kinnvika project – an International Polar Year initiative aimed at understanding the past, present and future environmental changes in the high Arctic. This study results from preliminary work carried out on Vestfonna ice cap in spring 2007.

Nordaustlandet is the northernmost island of Svalbard archipelago (Fig. 1). With an area of 2623 km^2 (Schytt, 1964) and a maximum altitude of 622 m (Palosuo, 1987), Vestfonna is the second largest ice cap on Nordaustlandet, the adjacent Austfonna being the largest one. Like all the glaciers of Svalbard and almost everywhere in the Arctic (except on the highest part of Greenland), Vestfonna is subject to seasonal melting during most summers (nominally from June to September), though because of its maritime climate, sporadic melt can occur even during winter (here being nominally from December to March). The summer melting generally soaks a large part of the annual snow layer even though accumulation rates in Svalbard are relatively high compared to Greenland and other Arctic sites (Koerner, 1997).

The melt water percolation affects the temperature near the surface of the glacier and plays a major role in the firn/ice transition, which in Vestfonna occurs between 5 and 10 m depth (Watanabe et al., 2001). At this depth, the ice temperature is −3.7°C (Kotlyakov et al., 2004). However, despite melt rates of 30–50% on another Svalbard glacier (Lomonosovfonna), isotopic variations (Pohjola et al., 2002) and chemical records (Moore et al., 2005) of climate are well preserved on annual or multi-year scales. Vestfonna winter surface snow contains a record of chemistry that has not been altered by melting and the ice cap has provided reliable climatic and environmental information (Watanabe et al., 2001; Matoba et al., 2002). Preliminary studies of snow are essential to interpret the ice core records, and snowpack

Correspondence to: E. Beaudon
(ebeaudon@ulapland.fi)

Published by Copernicus Publications on behalf of the European Geosciences Union.

stratigraphy and chemistry can provide information on the annual accumulation rate at the drilling sites, the elution rates of chemical species, the formation mechanism of superimposed ice and other post-depositional phenomena.

Svalbard snow chemistry is also affected by anthropogenic pollution (Simões et al., 2001). In winter, Arctic haze from industrialized areas of Eurasia and North America (Barrie, 1986) can bring significant acidic and ammonium ions to the archipelago (Kekonen et al., 2005). For example Moore et al. (2006) calculated that the western European anthropogenic source represents 10 to 25% of the 20th century sulphate budget of Lomonosovfonna.

This article is based on the chemistry of snow pit samples from each end of the east-west summit ridge of the ice cap. Few chemical investigations have been conducted previously on Vestfonna (Schytt, 1964; Matoba et al., 2002). Earlier authors (e.g. Matoba et al., 2002) reported highly soluble ions (principally NO_3^- and non sea-salt (nss) SO_4^{2-}) concentrations in winter snow which they attributed to anthropogenic impurities advected with warm air masses coming from the south. This study concentrates on a particular layer of the winter snowpack with a high sea salt load that we propose to be of frost flower origin.

Frost flowers grow on a thin layer of supersaturated brine expelled from the refrozen surface of open leads (Rankin et al., 2002). Brine is drawn onto to the surface of frost crystals by capillary action, leading to large salinities in the frost flower. When sea ice surface temperatures are below −8°C, mirabilite ($Na_2SO_4{\cdot}10H_2O$) starts to precipitate from the brine and is incorporated into the sea ice matrix. Because of this fractionation, the brine and, thus, the frost flowers are depleted in sodium and sulphate. Due to their fragile structure, frost flowers are easily windblown and redistributed to the snow surface. From Antarctic observations, Wolff et al. (2003) and Rankin et al. (2002) hypothesized that frost flowers constituted a significant source of sea-salt to the atmosphere and snow in winter. However, to our knowledge, the frost flower signature in the winter snow layer has never been described on an Arctic ice cap.

2 Study site and methods

Sampling locations were selected as part of a "pre-site" survey for a future deep drilling campaign. Therefore, preferences were given to flat and high elevated areas subject to minimal melting. Snow samples were collected from two pits located on the main summit ridge of Vestfonna ice cap in April–May 2007. Pit 1 (79°59′ N, 20°07′ E, 622 m a.s.l.) is close to the western summit which we term "Ahlmann" where snow studies and meteorological measurements were carried out during the IGY 1957. Pit 2 is close to the Japanese drilling site of 1995 (79°58′ N, 21°01′ E, 600 m a.s.l). Figure 1 shows the locations of the sampling sites.

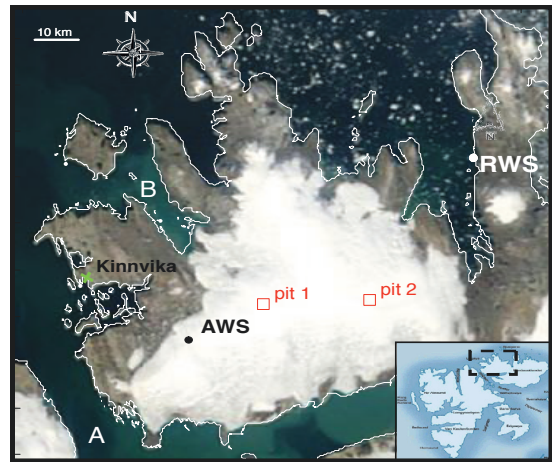

Fig. 1. Satellite image (image from NASA) of Western Nordaustlandet with location of Kinnvika station, snow-pit sampling sites (Pit 1 and Pit 2), Automatic Weather Station (AWS), Rijpfjorden Weather Station (RWS), Hinlopen strait **(A)** and Lady Franklinfjorden **(B)**.

2.1 Sampling

The samples were taken in accordance with the ITASE (International Trans-Antarctic Scientific Expedition) protocol (Twickler and Whitlow, 1997). The sampling equipment was cleaned in the laboratory with ethanol and packed in polyethylene (PE) sealed bags prior to the fieldwork using a technique described by Kekonen et al. (2004). Disposable face masks, powder-free vinyl gloves and full-body clean suits were worn throughout on-site and off-site activities in order to minimize contamination during sampling, manipulations and analyses. The pits were dug as small trenches in the snowpack down to the visually located hard and icy layers of firn corresponding to the previous summer or warm autumn surface. Snow samples from Pit 1 were taken continuously in 5 cm increments down to a depth of 220 cm by pushing clean plastic cups into the side-wall of the trench. In Pit 2 (180 cm deep), 20 cm vertical snow cores were retrieved using a clean metallic cylinder and placed into double PE bags. In the presence of ice layers, a sharp clean stainless-steel knife was used to cut sub-samples of 5 cm. The snow cores were also weighed for density measurements. After retrieval, the samples were stored and transported in insulated boxes to the laboratory where they were kept frozen until analysis.

2.2 Analyses

Ten major water-soluble ions were measured with a Dionex DX-120 suppressed ion chromatograph, at the Finnish Forest Research Institute (Rovaniemi Unit). The anions

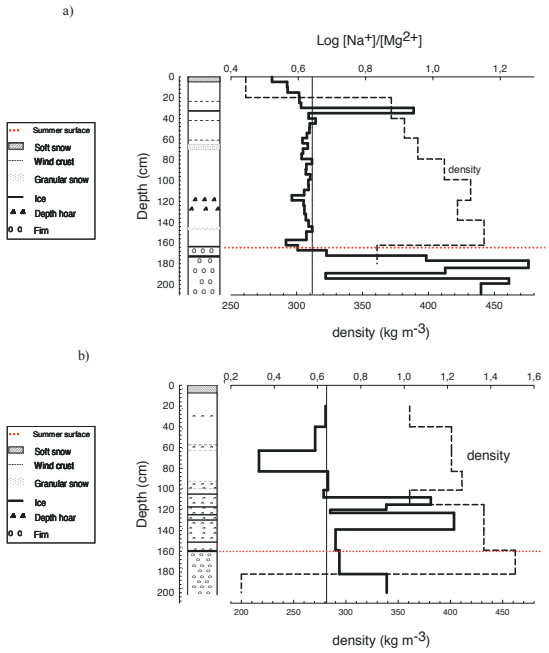

Fig. 2. Stratigraphy and depth profile of the melting indicator Log $[Na^+]/[Mg^{2+}]$ in μEql^{-1} (solid line) and density (dashed line) for **(a)** Pit 1 and **(b)** Pit 2.The black arrow points the melting indicator value for Standard Mean Ocean (SMOW).

(methanesulfonate acid MSA, Cl^-, SO_4^{2-}, NO_3^-) were determined using Dionex Ionpack AS15 columns. The cations (Na^+, NH_4^+, K^+, Mg^{2+}, Ca^{2+}) were determined using Dionex Ionpack CS12 columns. To minimize the effect of any systematic errors, samples were analyzed in a random depth order. The analytical method is described in detail by Virkkunen (2004). We estimate errors in ion measurements are <5% based on repeat measurements and calibration against standards. The $nssSO_4^{2-}$ and $nssCa^{2+}$ fraction have been calculated using sodium as the reference species assuming that all observed sodium originates from sea-salt: [nssX]=[X]−a [Na], where X is the fractionated species and a=[X]/[Na] in sea water.

3 Results

The samples of surface snow, i.e. the snow above the last summer layer, span the time period between the sampling time (April 2007) and the autumn of the previous year (2006). For each of the pits, Fig. 2 shows the stratigraphy and the vertical variance of snow density. Log $[Na^+]/[Mg^{2+}]$ ratio has been shown to be a good indicator of summer melting in Svalbard snow by Iizuka et al. (2002) and Grinsted et al. (2006).

In both sites, fresh snow, and wind packed snow layers, composed the upper parts of the sampling wall. At 35 cm depth in Pit 1, Log $[Na^+]/[Mg^{2+}]$ peaks and the stratigraphy shows an icy layer 0.5 cm thick. Below 120 cm in Pit 1 and below 130 cm in Pit 2 snow grains were coarser and depth-hoar layers were interleaved with thin ice layers (0.5 to 1 cm thick). In Pit 2, at the depth of these thin ice layers the value of the melt index, Log $[Na^+]/[Mg^{2+}]$, doubles. Below this section, a firn horizon with more frequently occurring melt ice layers was found from 160 cm to the bottom of the pits. The change in snow properties at 160 cm is accompanied by a rapid decline in density in both profiles. In Pit 1 the density drop is coupled with a doubling of the melt indicator Log $[Na^+]/[Mg^{2+}]$ (Fig. 2). We assume that this transition at the depth of 160 cm is the top of the 2006 summer layer. Based on the mean density of snow between 0–160 cm, we found that the accumulation rate was approximately 0.62 m w.e.yr^{-1} at Pit 1 and 0.64 m w.e.yr^{-1} at Pit 2. These estimates are similar to the 0.595 m w.e.yr^{-1} found during the IGY expeditions (Schytt, 1964).

Mean concentrations of the ionic species and the calculated $nssCa^{2+}$ and $nssSO_4^{2-}$, standard deviations (σ) and the coefficient of variation (CV=$\sigma/\bar{x}$) are presented in Table 1 for both pits. The concentrations of major ions (Cl^-, SO_4^{2-}, Na^+, Ca^{2+}, Mg^{2+}, K^+) range from 1.84 to 84 μEql^{-1} in Pit 1 and from 0.37 to 17.3 μEql^{-1} in Pit 2.

The concentration profiles for the cations and anions in the two pits are shown in Fig. 3. In the case of Pit 1, there is a concentration peak present at about 100 cm for Na^+, K^+, Mg^{2+}, Ca^{2+}, Cl^- and SO_4^{2-}. This snow layer between 95 cm and 115 cm presents ionic concentrations (except nitrate and MSA) from 4 to 6 times higher than the mean concentration for the snowpack above and below (excluding the firn layer starting at 160 cm). The absence of a peak in nitrate, which is eluted more easily than other ions, indicates that ions in this layer were not introduced by melting of layers above, such as the thin melt layer at 35 cm depth. Furthermore, the calculated concentration of $nssSO_4^{2-}$ (Fig. 3) in this layer was found to be clearly negative. This means that in this layer sulphate ions do not have an anthropogenic or terrestrial source, but must be marine in origin. Pit 2 displays a regular decrease in ionic concentrations from the surface of the pit to the summer snow surface with the exception of a small peak between 85 cm and 105 cm.

4 Discussion

A comparison of the snowpack ionic budgets between the sites (Table 1) reveals that Pit 1 has systematically higher concentrations than Pit 2 which probably represents a geographical trend across the ice cap. The major sources of these ions are marine (Matoba et al., 2002) and there is no topographical divide between the two sites. This indicates a variable geographical distribution of major marine ions on

Table 1. Mean concentrations ($\bar{x}$), standard deviations (σ) in μEql^{-1} and coefficients of variation, CV, in the entire surface snowpack of Pit 1 and Pit 2 and for the Frost Flower layer in Pit 1 (FF).

	Pit 1 (n=39)			FF (n=5)			Pit 2 (n=12)		
	$\bar{x}$	σ	CV	$\bar{x}$	σ	CV	$\bar{x}$	σ	CV
MSA	0.03	0.06	1.87	0.01	0.03	2.11	0.01	0.02	2.04
Cl^-	64.68	66.32	1.03	208.39	73.22	0.35	16.72	18.51	1.11
SO_4^{2-}	8.59	7.92	0.92	25.46	7.06	0.28	2.44	2.47	1.01
NO^{3-}	0.61	0.53	0.88	0.70	0.35	0.50	0.27	0.29	1.08
Na^+	75.15	85.83	1.14	262.57	103.02	0.39	17.30	18.94	1.09
NH^{4+}	0.75	0.42	0.56	0.67	0.62	0.93	1.14	0.56	0.49
K^+	1.65	1.94	1.17	5.88	2.34	0.40	0.38	0.40	1.08
Mg^{2+}	17.46	20.25	1.16	61.69	23.78	0.39	4.15	4.81	1.16
Ca^{2+}	3.56	3.82	1.07	11.97	4.67	0.39	2.55	1.76	0.69
$nssCa^{2+}$	0.25	0.43	1.69	0.41	0.76	1.88	1.79	1.33	0.74
$nssSO_4^{2-}$	−0.46	3.33	−7.20	−6.19	5.47	−0.88	0.36	0.51	1.42

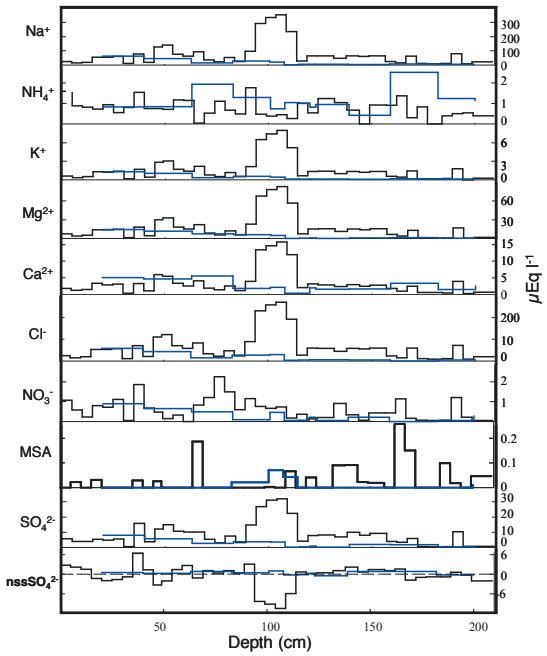

Fig. 3. Ion concentration (μEq l^{-1}) in Pit1 (black histogram) and Pit 2 (blue histogram).

Vestfonna, with summit Ahlmann under stronger marine influence. In addition, the lower $nssSO_4^{2-}$ and $nssCa^{2+}$ contents observed in Pit 1 also point towards higher oceanic inputs at Pit 1 compared to Pit 2. The snow stratigraphy and densities also support the chemical melt indicator in suggesting that the snow layer at the depth of 1 m in Pit 1 has not experienced melting.

Table 2. Weight ratios of ions in Halley station Frost Flowers, Antarctica (HFF), Frost Flowers Layer (FFL) and bulk sea water (SMOW).

	K/Na	Mg/Na	Ca/Na	Cl/Na	SO_4/Na
HFF	0.0389	0.1400	0.0441	2.0400	0.0853
FFL	0.0220	0.2360	0.0452	0.8120	0.0920
SMOW	0.0370	0.1200	0.0382	1.7900	0.2520

4.1 Frost flowers as a source of fractionated sea-salt in winter

At Antarctic coastal sites, high sea-salt concentrations and strong $nssSO_4^{2-}$ depletion found in winter snow have been described as evidence of an important sea ice surface source (Rankin et al, 2002). Other studies of Antarctic winter snow (e.g. Hall and Wolff, 1998) confirm that air coming from fresh sea ice covered with frost flowers has a high salinity and a negative $nssSO_4^{2-}$ signal. Based on the similar chemical characteristics found in the highly saline layer in Pit 1 winter snow, we propose these features represent a frost flower chemical fingerprint. Additionally, the sulphate to sodium ratio (SO_4^{2-}/Na^+) in this particular layer of the winter snowpack, 0.092, is about one third that of sea water (0.25) and very close to the SO_4^{2-}/Na^+ ratio measured by Rankin et al. (2002) in Antarctic frost flowers (0.085) and winter aerosols (0.1).

Earlier investigations on Vestfonna snow (Matoba et al, 2002) showed that peaks of $\delta^{18}O$, Na^+, Cl^- in winter snow were caused by advection of warm air masses with a high content of sea-salt. These winter warm events were also associated with high NO_3^-, NH_4^+ and $nssSO_4^{2-}$ peaks and the authors concluded in favour of both anthropogenic and sea water sources. The concentrations of NO_3^- and NH_4^+ do

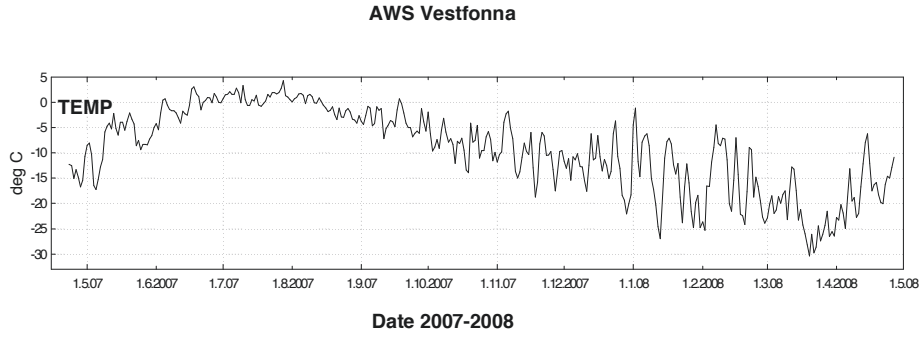

Fig. 4. Temperature (°C) plotted from AWS (Personal communication from Regine Hock & Ulf Jonsell 2008).

not exhibit peaks and $nssSO_4$ is clearly negative (Fig. 3) in the frost flower layer. We can therefore exclude anthropogenic contribution to the sulphate. In addition, the Mg/Na (0.236) and Ca/Na (0.045) weight ratios in the frost flower layer are slightly higher than those in bulk sea water (SMOW, Standard Mean Ocean Water) (0.12 and 0.038, respectively, Table 2), implying that sea-salt aerosols incorporated into the winter snow are depleted also in sodium. This is to be expected if we assume that the depletion of both sodium and sulphate is due to crystallization of mirabilite ($Na_2SO_4{\cdot}10H_2O$) from sea water at temperatures below −8.2°C. Simulations of sea water freezing along the Gitterman pathway by Marion et al. (1999) reveal that mirabilite is the only salt to precipitate out when sea ice is formed between −8.2°C and −22°C. Colder ice surfaces are generally associated with multiyear ice on which frost flowers do not form. The ions deposited in the frost flower layer clearly display a fractionated sea-salt signature and we can conclude that sodium is the cation depleted with sulphate.

According to Rankin et al. (2002) sodium and sulphate depletion due to mirabilite precipitation are expected in glacier snow if this snow has been affected by a frost flower wind deposition. Frost flowers grow on patches of thin slush layers on young sea-ice formed in leads of open water. To create these leads, appropriate meteorological conditions in terms of wind speed and direction are necessary and must be combined with sufficiently low temperatures (below −8°C) to allow fractionation to occur. Such cold temperatures are frequently reached during the winter in Nordaustlandet (Fig. 4). Once offshore winds open up a coastal lead, new sea ice is produced. Then, the wind direction must change to blow onshore in order to carry the aerosols derived from the frost flowers inland. Hall and Wolff (1998) show that strong winds are not associated with frost flower signatures perhaps because strong winds destroy the flower's fragile crystals and the thin surface skim of brine on which they form. So moderate winds and low temperatures are needed.

Patches of enriched brine on solid ice create an irregular surface with a greater roughness and backscatter coefficient at radar frequencies than ice without flowers. A synthetic aperture radar (SAR, carried by the ERS-1 satellite), which is sensitive to the nature of sea ice surface, has been used to identify leads covered by frost flowers in the Arctic (Melling, 1998; Ulander et al., 1995). In addition, a radar study conducted in Svalbard archipelago using the ERS-2 satellite in March-April 1998 (Augstein, 2000) registered strong reflectance of a $15\times15\,km^2$ area of the Arctic Ocean west of Nordaustlandet (80°42′ N, 8° E), which was interpreted as frost flowers by Kaleschke et al. (2004). These observations support our assumption that frost flowers can form around Nordaustlandet and constitute a potential source of fractionated aerosols for Svalbard winter snow.

Moreover, the snow layer affected by the frost flower peak is too thick (20 cm) to be formed by fog, which is also unsupported by the stratigraphy (Fig. 2). The importance of fog deposits (rime, hoar frost) has been overestimated in Nordaustlandet during the past; Schytt (1964) observed that the snow mass contributed by fog deposits amounts to roughly 3 percent of the total accumulation.

4.2 Hinlopen Strait: newly formed sea ice in winter

To locate the young winter sea ice formation area, we used the records from the weather station installed on the eastern coast of Rijpfjorden (80°13′ N, 22°31′ E) (see Fig. 1 for location). The wind data for the period 2007–2008 are plotted in Fig. 5. Two predominant wind directions are observed: one is 290 to 340° (from the Arctic Ocean, NW) and the other is 110 to 135° (from Austfonna ice cap, SE). These wind directions are consistent with the dominant regional easterly winds (Niedzwiedz, 1997; Dagestad et al., 2006) and with our field observations in spring 2007 and 2008 at summit Ahlmann where strong winds came most of the time from the Arctic Ocean channeled by Lady Franklinfjorden (Fig. 1). This suggests that the Arctic Ocean is not the frost flowers source area, since the frost flowers signature is not a continuous signal in the snow pack, but an infrequent event. The only plausible source is Hinlopen Strait (SSW).

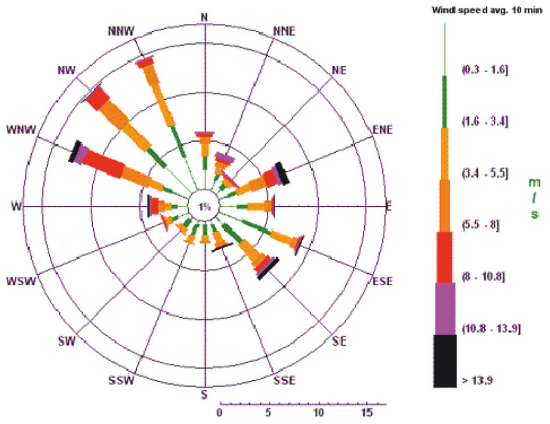

Fig. 5. Rose diagram showing wind direction (deg.) and speed (m/s) from August 2007 to August 2008 at Rijpfjorden Weather Station (source: http://158.39.11.101/command=RTMC\&screen=WindYear%20%20).

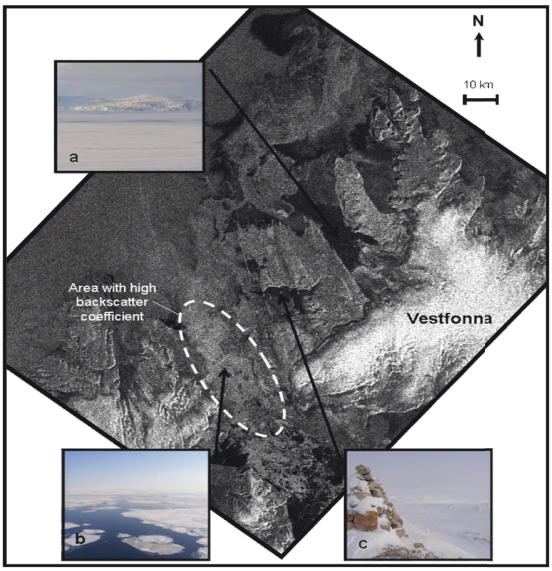

Fig. 6. ERS-2 SAR image of Hinlopen Strait and the western part of Nordaustlandet on 22 February 2007 compared with ground shots of **(a)** Lady Franklinfjorden (4th May 2007), **(b)** Hinlopen (19th April 2007), and **(c)** Murchinson Bay (5th May 2007) taken during the field campaign in spring 2007 (Source SAR image: ESA).

During the field campaigns we noted that Hinlopen Strait was partially covered with a thin slick of ice and partially ice free, whereas Lady Franklinfjorden was completely frozen. These observations from early spring corroborate those made by the satellite ERS-2 in February 2007: SAR images show a much higher backscatter coefficient in Hinlopen than in Lady Franklinfjorden or Murchinson Bay (Fig. 6). Strong currents in the Hinlopen Strait continuously create exposed areas of sea water which freeze rapidly in the winter and create areas of local, freshly formed ice with a surface cover of concentrated brine. Moreover, the decrease in sea-salt concentrations with distance across the ice cap (at Pit 2), indicates that the sea-salt source is closer to Pit 1 than to Pit 2. From these observations we can speculate that the principal source of saline air masses is most likely Hinlopen Strait (about 45 km from Pit 1 and about 60 km from Pit 2). Unlike in Pit 1, melting layers are present in the winter snowpack of Pit 2 while the frost flower chemical signature is absent in the pack. This shows evidence of locally variable atmospheric conditions at the two summits which are 20 km apart. We frequently experienced this local weather variability during our two field campaigns in 2007 and 2008 when snow was sometimes observed at one pit site but not the other.

Table 3. Concentration (μEql^{-1}) of ions in Halley station Frost Flowers, Antarctica (HFF), Frost Flowers Layer (FFL) and Bulk Sea water (SMOW).

	Na	K	Mg	Ca	Cl	SO_4
HFF	154	4	41	8	207	6
FFL	263	6	62	12	208	25
SMOW	468	10	107	21	553	56

4.3 Fractionated salt as a new sea ice production proxy

Wolff et al., 2003 have suggested that sea-salt concentrations in ice cores can be used to infer aspects of the marine environment in the past. Generally, such studies have assumed that the atmospheric sea-salt concentrations are related to a combination of sea ice extent and wind speed. Although Svalbard ice cores suffer from postdepositional percolation they have been proven to give reliable paleoinformation (Kekonen et al., 2005; Grinsted et al., 2006; Moore et al., 2009). Iizuka et al. (2002) successfully extracted information on environmental changes from chemical signals in a Nordaustlandet ice core. Also, Watanabe et al. (2001) reported that most of the chemical features contained in the initial snow of Austfonna still remained in the ice core. We could therefore expect that the preservation of the frost flower chemical signature in Vestfonna ice is possible. If the signal described in this paper is not disrupted by melt percolation, it might serve as a potential proxy for sea ice production (extent) in winter via the reconstruction of past atmospheric conditions. Additionally, if higher sea-salt levels measured in winter snow are systematically associated with moderate winds (and not strong winds), we could attribute high sea-salt concentrations (Table 3) seen in cold periods, such as the Little Ice Age, in coastal or maritime ice

cores to changes in sea ice production, rather than increased storminess and more efficient transport.

The apparent rarity of the frost flower signature in Arctic regions may be related to the quite different sea ice conditions in the Arctic Ocean compared with the seas surrounding Antarctica. Multi-year floes tend to be more common in the Arctic basin, while in the Southern Ocean the pack ice reforms each year, so there is more young and thin ice that provides suitable frost flower sites around Antarctica than in much of the Arctic. The Arctic is also much more affected by anthropogenic and terrestrial SO_4^{2-} input than Antarctica and large $nssSO_4^{2-}$ are typical. This would tend to disguise the characteristic SO_4^{2-}/Na^+ frost flower signature.

5 Conclusion

By comparing chemical analyses of the snowpack from two snow pits in Vestfonna ice cap, we show that the western side of Vestfonna receives a greater marine ionic contribution than the eastern edge, and that the winter snowpack at the western end (summit Ahlmann) is enriched in sea-salt fractionated in sodium and sulphate. As the particular nature of this saline content corresponds to a typical frost flower signature described in aerosols and snow from Antarctic coastal regions, we hypothesize that frost flowers, possibly formed in Hinlopen Strait, could form a significant source of sea-salt in winter snow in Vestfonna. However, to rigorously assess the reliability of the frost flower chemical signature as a proxy for winter sea ice production around Nordaustlandet, the annual snowpack needs to be analyzed at different locations on Vestfonna and more snow pit studies carried out along with continuous meteorological measurements should be performed. Studies of shallow ice cores drilled at the two summits and new snow analyses are currently underway. Frost flowers chemical signatures have not yet been reported at other locations in the Arctic. However, their detection in ice cores from areas that, at present, are usually surrounded by multi-year pack ice could indicate that, in earlier periods, young sea ice was present instead.

Acknowledgements. We thank the Finnish Forest Research Institute, Rovaniemi Research Unit for the use of cold-room and clean-room facilities. Financial support was provided by the Finnish Academy. We are grateful to Veijo Pohjola and Ulf Jonsell for their important assistance in the field. We also thank Regine Hock who provided the meteorological data from the AWS on Vestfonna.

Edited by: J. L. Bamber

References

Augstein, E.: Final report on the Arctic Radiation and Turbulence Interaction Study (ARTIST). Bremerhaven, Alfred-Wegener-Institut für Polar und Meeresforschung, 92–105, 2000.

Barrie, L. A.: Arctic air chemistry: an overview, edited by: Stonehouse, B., Arctic air pollution, Cambridge, Cambridge University Press, 5–23, 1986.

Dagestad, K. F., Johannessen, J. Hauge, G., Kerbaol, V., et al.: High-resolution Wind Field Retrievals off the Norwegian Coast: Comparing ASAR Observations and MM5 Simulations. Proceedings OceanSAR 2006 St. John's, NL, Canada, 2006.

Drinkwater, M. R. and Crocker, G. B.: Modeling changes in the dielectric and scattering properties of young snow-covered sea ice at GHz frequencies, J. Glaciol., 34, 274–282, 1988.

Grinsted, A., Moore, J. C., Pohjola, V., Martma, T., et al.: Svalbard summer melting, continentality and sea ice extent from the Lomonosovfonna ice core, J. Geophys. Res., 111, D07110, 10.1029/2005JD006494, 2006.

Hall, J. S. and Wolff, E. W.: Causes of seasonal and daily variations in aerosol sea-salt concentrations at a coastal Antarctic station, Atmos. Environ., 32, 3669–3677, 1998.

Iizuka, Y., Igarashi, M., Kamiyama, K., Motoyama, H., et al.: Ratios of Mg^{2+}/Na^+ in snowpack and an ice core at Austfonna ice cap, Svalbard, as an indicator of seasonal melting, J. Glaciol., 48(162), 452–460, 2002.

Kaleschke, L. and Heygster, G.: Towards multisensory microwave remote sensing of frost flowers on sea ice, Ann. Glaciol., 39, 219–222, 2004.

Kekonen, T., Perämäki, P., Moore, J. C., et al.: Comparison of analytical results for chloride, sulphate and nitrate obtained from adjacent ice core samples by two ion chromatographic methods, J. Environ. Monitor., 6, 147–152, 2004.

Kekonen, T., Moore, J. C., Perämäki, P., et al.: The 800 year long ion record from the Lomonosovfonna (Svalbard) ice core, J. Geophys. Res., 110, DO7304, doi:1029/2004JD005223, 2005.

Koerner, R. M.: Some comments on climatic reconstructions from ice-cores drilled in areas of high melt, J. Glaciol., 43(143), 90–97, 1997.

Kotlyakov, V. M., Arkhipov, S. M., Henderson, K. A., et al.: Deep drilling of glaciers in Eurasian Arctic as a source of paleoclimatic records, Quatern. Sci. Rev., 23, 1371–1390, 2004.

Marion, G., Farren, M. R. E., Komrowski, A. J., et al.: Alternative pathways for seawater freezing, Cold Reg. Sci. Technol., 29, 259–266, 1999.

Matoba, S., Narita, H., Motoyama, H., et al.: Ice core chemistry of Vestfonna Ice Cap in Svalbard, Norway, J. Geophys. Res., 107(D23), 4721, doi:10.1029/2002JD002205, 2002.

Melling, H.: Detection of features in first-year pack ice by synthetic aperture radar, Int. J. Remote Sens., 19(6), 1223–1249, 1998.

Moore, J. C., Grinsted, A., Kekonen, T., and Pohjola, V.: Separation of melting and environmental signals in an ice core with seasonal melt, Geophys. Res. Lett., 32, L10501, doi:10.1029/2005GL023039, 2005.

Moore, J. C., Kekonen, T., Grinsted, A., et al.: Sulfate source inventories from a Svalbard ice core record spanning the Industrial Revolution, J. Geophys. Res., 111, D15307, doi:10.1029/2005JD006453, 2006.

Moore, J. C. and Grinsted, A.: Ion fractionation and percolation in ice cores with seasonal melting, Physics of Ice Core Records

II, edited by: Hondoh, T., Hokkaido University Press, in press, 2009.

Niedzwiedz, T.: Czastoea wystapowania typw cyrkulacji nad Spitsbergen (1951–1995), [Frequency of circulation patterns above Spitsbergen (1951–1995)], Probl. Klimatol. Polarnerj, 7, 9–16, 1997.

Palosuo, E.: A Study of Snow and Ice Temperatures on Vestfonna, Svalbard, 1956, 1957 and 1958, Geogr. Ann. A, 69A(3/4), 431–437, 1987.

Pohjola, V. A., Moore, J. C., Isaksson, E., Jauhiainen, T., van de Wal, R. S. W., Martma, T., Meijer, H. A. J., and Vaikmäe, R.: Effect of periodic melting on geochemical and isotopic signals in an ice core from Lomonosovfonna, Svalbard, J. Geophys. Res., 107(D4), 4036, doi:10.1029/2000JD000149, 2002.

Rankin, A. M., Wolff, E. W., Auld, V., et al.: Frost Flowers as a source of fractionated sea salt aerosol in the polar regions, Geophys. Res. Lett., 27, 3469–3472, 2000.

Rankin, A. M., Wolff, E. W., Martin, S., et al.: Frost flowers: implications for tropospheric chemistry and ice core interpretation, J. Geophys. Res., 107(D23), 4683, doi:0.1029/2002JD002492, 2002.

Schytt, V.: Scientific Results of the Swedish Glaciological Expedition to Nordaustlandet, Spitsbergen, 1957 and 1958, Geografiska Annaler, 46(3), 242–281, 1964.

Simões, J. C. and Zagorodnov, V. S.: The record of anthropogenic pollution in snow and ice in Svalbard, Norway, Atmos. Environ., 35, 403–413, 2001.

Twickler, M. and Whitlow, S.: Appendix B, in: Guide for the collection and analysis of ITASE snow and firn samples, edited by: Mayewski, P. A. and Goodwin, I. D., International Trans-Antarctic Scientific Expedition (ITASE), Bern, Switzerland, Past Global Changes (PAGES report 97-1), 1997.

Ulander, L. M. H., Carlstrom, A., Askne, J., et al.: Effect of frost flowers rough saline snow and slush on the ERS-1 SAR backscatter of thin arctic sea ice, Int. J. Remote Sens., 16(17), 3287–3305, 1995.

Virkkunen, K.: Snow pit studies in 2001–2002 in Lomonosovfonna, Svalbard, MSc thesis, Univ. of Oulu, Finland, 26–34, 2004.

Virkkunen, K., Moore, J. C., Isaksson, E., et al.: Warm summers and ion concentrations in snow: present day and Medieval Warm Period comparisons from snow pits and an ice core from Lomonosovfonna, Svalbard, J. Glaciol., 53(183), 623–634, 2007.

Watanabe, O., Motoyama, H., Igarashi, M., et al.: Studies on climatic and environmental changes during the last few hundred years using ice-cores from various sites in Nordaustlandet, Svalbard, Nat. Inst. Polar Res. Mem., 54 (special issue), 227–242, 2001.

Wolff, E. W., Rankin, A. M., and Rothlisberger, R.: An ice core indicator of sea ice production?, Geophys. Res. Lett., 30(22), 2158, doi:10.1029/2003GL018454, 2003.

II

SPATIAL AND TEMPORAL VARIABILITY OF NET ACCUMULATION FROM SHALLOW CORES FROM VESTFONNA ICE CAP (NORDAUSTLANDET, SVALBARD)

BY
EMILIE BEAUDON[1], LAURA ARPPE[2], ULF JONSELL[3,6], TÕNU MARTMA[4], MARCO MÖLLER[5], VEIJO A. POHJOLA[6], DIETER SCHERER[7] AND JOHN C. MOORE[1,8]

[1]Arctic Centre, University of Lapland, Rovaniemi, Finland
[2]Department of Geosciences and Geography, University of Helsinki, Finland
[3]ETSI de Telecomunicación, Universidad Politécnica de Madrid
[4]Institute of Geology, Tallinn University of Technology, Estonia
[5]Department of Geography, RWTH Aachen University, Germany
[6]Department of Earth Sciences, Uppsala University, Sweden
[7]Department of Ecology, Technische Universität Berlin, Germany
[8]Colleges of Global Change and Earth System Science, Beijing Normal University, China

Beaudon, E., Arppe, L., Jonsell, U., Martma, T., Möller, M., Pohjola, V.A., Scherer, D. and Moore, J.C., 2011. Spatial and temporal variability of net accumulation from shallow cores from Vestfonna ice cap (Nordaustlandet, Svalbard). *Geografiska Annaler*: *Series A, Physical Geography*, 93, 287–299. DOI: 10.1111/j.1468-0459.2011.00439.x

ABSTRACT. We analyse ice cores from Vestfonna ice cap (Nordaustlandet, Svalbard). Oxygen isotopic measurements were made on three firn cores (6.0, 11.0 and 15.5 m deep) from the two highest summits of the glacier located on the SW–NE and NW–SE central ridges. Sub-annual $\delta^{18}O$ cycles were preserved and could be counted visually in the uppermost parts of the cores, but deeper layers were affected by post-depositional smoothing. A pronounced $\delta^{18}O$ minimum was found near the bottom of the three cores. We consider candidates for this $\delta^{18}O$ signal to be a valuable reference horizon since it is also seen elsewhere in Nordaustlandet. We attribute it to isotopically depleted snow precipitation, which NCEP/NCAR reanalysis shows was unusual for Vestfonna, and came from northerly air during the cold winter of 1994/95. Finding the 1994/95 time marker allows establishment of a precise depth/age scale for the three cores. The derived annual accumulation rates indirectly fill a geographical gap in mass balance measurements and thus provide information on spatial and temporal variability of precipitation over the glacier for the period spanned by the cores (1992–2009). Comparing records at the two locations also reveals that the snow net accumulation at the easternmost part of Vestfonna was only half of that in the western part over the last 17 years.

Key words: accumulation rate, firn core, oxygen isotope ratio, sea ice, wind anomaly, Vestfonna

Introduction

Firn and ice core studies are key tools to reconstruct regional characteristics of glacier processes and climatic and environmental changes. The retrieval of three shallow firn cores from Vestfonna ice cap (Nordaustlandet, Svalbard) was carried out during the IPY-KINNVIKA project whose main objective was to enhance the understanding of the Arctic system, to monitor Arctic climate change and to study effects of human activity on Arctic islands (Pohjola *et al*. 2011).

Svalbard is in an interesting geographical position surrounded by the Arctic Ocean, the Barents Sea, and at the southerly edge of the permanent Arctic sea ice. In addition, it is near to the overturning point of the North Atlantic thermohaline circulation whose warm waters contribute to high average winter temperatures. Vestfonna ice cap is located in the western part of Svalbard's northernmost island (Nordaustlandet) whose atmospheric circulation is dominated by easterly winds bringing moisture from the Barents Sea (Førland *et al*. 1997). Due to its maritime climate and its low altitude (from sea level to 630 m a.s.l.), Vestfonna experiences seasonal melting during most summers and occasional melting during winter. However, glaciers that are subject to moderate melt can provide valuable ice core records (Pohjola *et al*. 2002; Moore *et al*. 2005).

DOI: 10.1111/j.1468-0459.2011.00439.x

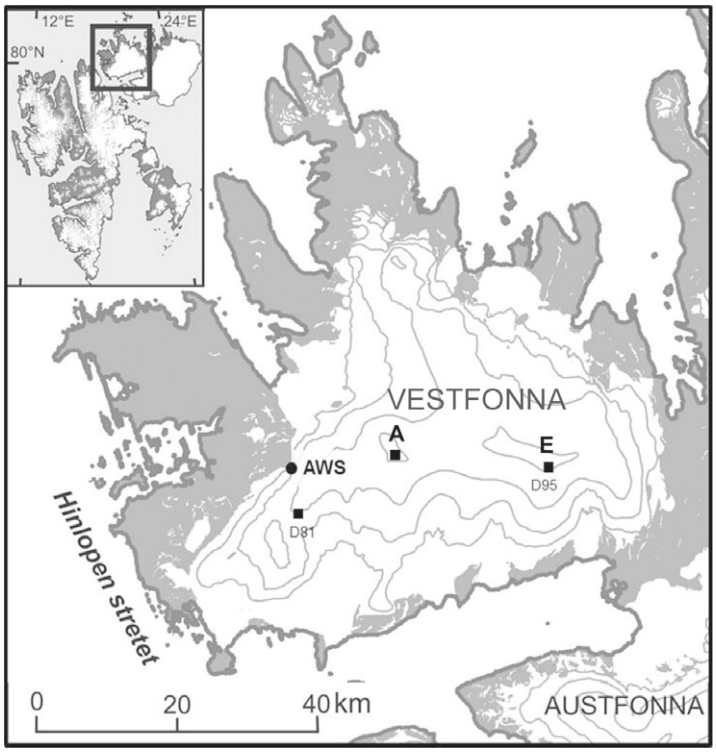

Fig. 1. Map of Western Nordaustlandet with locations of the drilling sites (Ahlmann summit as A and Eastern summit as E), Automatic Weather Station (AWS) and previous deep drilling sites in 1981 (D81) and in 1995 (D95).

Two deep ice cores have already been drilled on Vestfonna in the past (Kotlyakov *et al*. 2004): the first was extracted in July 1981 from the northwestern part of the ice dome (Vaykmyae *et al*. 1985), and the last one was drilled in May–June 1995 at the eastern peak (Watanabe *et al*. 2001) (Fig. 1, Table 1). Both ice cores provided regional low temporal resolution paleoclimate records spanning several centuries. This was achieved by measuring the isotopic composition of oxygen in ice which is controlled by the atmospheric deposition conditions, especially temperature, and the associated air mass trajectories from the source region (Matoba *et al*. 2002). The $\delta^{18}O$ records were found to correlate well with historical temperature records.

In this work, using high resolution $\delta^{18}O$ and density profiles, we use firn cores from two different locations on Vestfonna in order to extract recent climate information missing for the last 20 years and compare precipitation regimes and provenance at the two sites. The new data can be used to extend the data from the earlier deeper cores into the twenty-first century.

Materials and methods

Firn core retrieval

During the first IPY-KINNVIKA spring campaign on Vestfonna ice cap in April–May 2007, two shallow firn cores were retrieved from the two highest summits of the West–East ridge at 79° 59′ 22″ N and 79° 56′ 58″ N, respectively (Fig. 1). Percolation processes and ice flow are assumed to be less problematic for ice core studies at the ridges than at lower elevations and in local depressions where the role of melting and liquid precipitation is more important (Kotlyakov *et al*. 2004). At these sites, hereafter named Ahlmann and Eastern summits and respectively labelled 'Ahl07' and 'E07', cores were taken with a portable electro-mechanical corer. The coring was started from the summer 2006 surface layer, i.e., from the bottom of 1.9 m deep snow pits which have been previously described in terms of stratigraphy and chemistry by Beaudon and Moore (2009).

Table 1. Summary of firn and ice core information, average isotope values and annual accumulation rates calculated from the three shallow firn cores (this work) and compared with older Vestfonna 95 ice core.

Drilling site	Reference	Latitude (N)	Longitude (E)	Elevation (m a.s.l.)	Drill depth (m)	Time span (year)	Average[1] δ^{18}O (‰) (±σ)	Average[2] accumulation (m w.e. yr^{-1}) (±σ)
Ahl07	this study	79°59′22″	20°07′07″	622	11.81	12	−15.0 (1)	0.54 (0.16)
Ahl09	this study	79°58′53″	20°06′51″	619	15.42	17	−14.9 (1.1)	0.52 (0.15)
E07	this study	79°58′	21°01′	600	5.76	13	−15.5 (0.9)	0.25 (0.08)
Vestfonna 95	(Watanabe *et al. 2001*)	79°58′	21°01′	600	210	>210	−17.2	0.34
Austfonna 99	(Watanabe *et al. 2001*)	79°50′	24°01′	750	289	800	−16.7	0.45

[1] 1996-2006 for Ahl09, Ahl07 and E07, 1985-1995 for Vestfonna 95, 1989-1999 for Austfonna.
[2] over the entire time span for this study and 1963-1995 for Vestfonna 95 and Austfonna.

In April–May 2009, a new 15.4 m long core 'Ahl09' was drilled at Ahlmann summit using a lightweight Kovacs corer, which was also capable of drilling through the many thick ice layers encountered. The firn-glacier ice transition was not reached in either core. The stratigraphic melt index for the Ahl09 core is 46%, which is lower than in the 1990s in other Svalbard cores (Pohjola *et al*. 2002).

Laboratory analyses

The cores were processed in the cold room (−22°C) of the Finnish Forest Institute in Rovaniemi. The diameter, length and weight of each core section were first measured for density calculations. The entire density profiles of the cores are shown in Fig. 2. After removing the outer part of the core with a band saw, a 20 mm thick plate cut along the core length and placed on a light bench was photographed in order to accurately determine ice facies and calculate high resolution density profiles following the method proposed by Pohjola *et al*. (2002). For purposes of oxygen isotopic analysis, prisms were cut from the inner part and sub-sampled in 10 to 15 cm long increments for Ahl07 and E07, and in 2 to 5 cm long increments for Ahl09. The samples were then melted in closed vials and the water was analysed for the isotopic composition of oxygen.

Ahl07 and E07 isotope samples were processed at the Laboratory for Geochemistry of the Department of Geosciences and Geography, University of Helsinki, where the oxygen isotope ratios were measured on a ThermoFinnigan Gasbench II coupled to a ThermoFinnigan Delta^{Plus} Advantage continuous flow mass spectrometer. Replicate measurements of in-house water standards indicate a reproducibility of ±0.1‰. Analysis of Ahl09 samples were carried out at the University of Technology in Tallinn on a Gasbench II with Delta V Advantage mass spectrometer. The reproducibility of replicate analysis is ±0.1‰.

Mass balance survey and meteorological data

An array of 31 accumulation and ablation stakes was installed on the western slope of the ice cap during the 2007 spring campaign. The 2007 array was resurveyed during the two following fieldwork seasons, when new stake arrays were set up

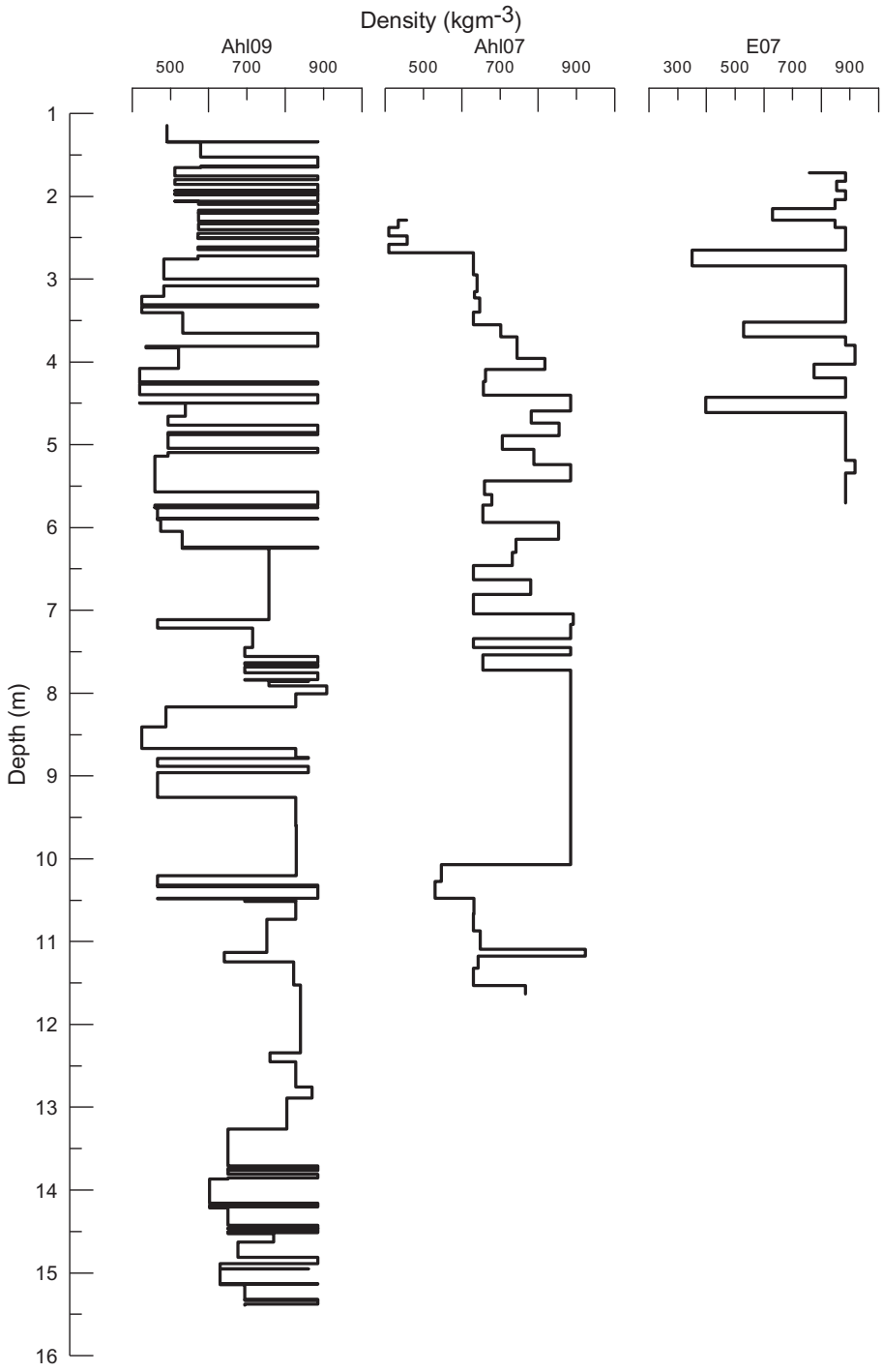

Fig. 2. Density depth profiles of the three shallow firn cores.

in the Ahlmann and Eastern summit areas. Repeat readings were carried out during spring and summer campaigns from 2007 to 2010. Stake surveys are described in detail by Pohjola *et al*. (2011).

The surface air temperature data used to identify the sub-annual $\delta^{18}O$ cycles and to establish a precise chronology for the uppermost firn and ice layers of the Ahl09 core were measured from April 2007 to May 2009 by an *automatic weather station* (AWS) set up on the western slope of Vestfonna at 335 m a.s.l. (Fig. 1).

The ERA interim temperatures we use are 2 m air temperatures from a grid point located at 79° 5′ N; 19° 5′ E. These temperatures were statistically downscaled to match local conditions at summit Ahlmann on Vestfonna (Möller *et al*. 2011a). The wind data that are taken from the NCEP/NCAR reanalysis dataset (monthly mean values; Kistler *et al*. 2001) for the grid point 80° N; 20° E (close to summit Ahlmann) are representative of the synoptic-scale wind conditions near summit Ahlmann and are very similar to those of the entire Svalbard region.

Dating procedure

The preliminary dating of the three shallow cores we propose is based on visual counting of $\delta^{18}O$ (winter) minima with the addition of information from ERA-interim air temperatures and NCEP/NCAR reanalysis wind data. The three ice core timescales, adjusted to a common stratigraphic horizon, are used to calculate the net annual accumulation (or amount of water per reconstructed annual layer) at each site that are then compared with results of a climatic mass balance model for the period 2000–2009 (Möller *et al*. 2011b).

Results and discussion

Preliminary dating of the cores

Sub-annual $\delta^{18}O$ cycles In the first 6.3 m of the Ahl09 core, the $\delta^{18}O$ profile presents pronounced oscillations of high amplitude which, $\delta^{18}O$ being commonly used as a (condensation) temperature proxy in ice core studies, clearly correspond to seasonal variations. By matching the $\delta^{18}O$ minima measured in Ahl09 with the winter temperature minima recorded on the western slope of Vestfonna (AWS; Fig. 1) since 2007, it is possible to precisely date the uppermost part of the core.

Figure 3 shows this fitted dating, which is also partly constrained by stratigraphic features such as clear ice or depth hoar layers shown in pictures inserts in Fig. 3. The uppermost $\delta^{18}O$ minimum (−18.3‰) at 1.6 m depth, marked as (1), is associated with the winter temperature minimum that occurred in January 2009 (−28°C). The second $\delta^{18}O$ minimum (2) at 2.7 m is matched to the March 2008 winter temperature minimum (−26°C). We note that the small peaks, marked with yellow arrows, succeeding (in depth) the minimum in the temperature profile are also visible in the $\delta^{18}O$ profile. The same late autumn shoulder pattern is systematically observed in other Svalbard air temperature records for the past 10 years (Fig. 4b).The small local $\delta^{18}O$ peak corresponds to late autumn/early winter precipitation on Vestfonna. The relatively high $\delta^{18}O$ value of −13.9‰ at 2.3 m (3) is measured in the uppermost clear ice layer (5 cm thick at 0.91 m w.e.) of the core probably resulting from summer melting and refreezing of surficial snow layers. We suggest this layer was formed by percolation of part of the surface snow in June 2008 when the first positive temperatures of the year are measured. At 3.3 m depth, we find a depth hoar layer (4) filled with refrozen water ice, characteristic of an autumnal layer (Pohjola *et al*. 2002) and followed by clear ice at 3.7 m depth (5). The $\delta^{18}O$ values of samples taken in these layers are respectively attributed to August and June 2007. We suggest that the high positive correlation ($r^2 = 0.53$) between $\delta^{18}O$ and T (for the period 2007–2009) found with this method shows that depth-age is fairly well established for the two last years. Furthermore, it supports using the oxygen isotope ratios from Ahl09 firn core as a reliable indicator of air temperature variability for Vestfonna, which makes dating the firn cores possible as long as isotopic cycles are discernable. This is the case for the five first cycles in Ahl09 that are clearly visible, however the signal becomes more difficult to read with increasing depth as the amplitudes of the $\delta^{18}O$ fluctuations are smoothed by post-depositional processes. Simple visual counting in Ahl09 and Ahl07 gives 15–20 and 12–16 $\delta^{18}O$ cycles, respectively.

Finding a time marker to refine the dating A substantial averaging of the original isotopic signals, perhaps due to vapour diffusion and/or mixing of percolating melt water, is observed along all cores.

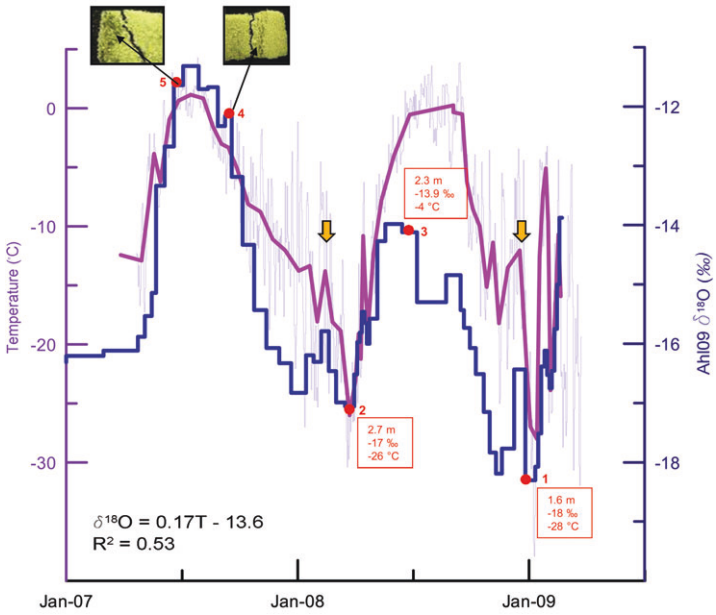

Fig. 3. Oxygen isotopic ($\delta^{18}O$) measurements (blue) on the upper 3 m (1.4 m w.e.) of the Ahl09 firn core matched with stratigraphy features (photographs of melt layers with corresponding depth (m) of the layer) and daily air temperature (°C; violet) recorded from April 2007 to May 2009 at the AWS. The dating of the isotopic profile is interpolated between stratigraphical tie points numbered in red. The pink curve is the averaged air temperature over each $\delta^{18}O$ sample increment. The yellow arrows point the small autumnal temperature peaks.

According to Johnsen (1977), vapour diffusion causes the annual cycle's amplitude to decay rapidly in the firn and much slower at deeper depths as vapour diffusion is slower in solid ice than in firn. The isotopic signal amplitude of the top firn layers of Ahl07 and E07 is lower than in the top firn layers of Ahl09 where the diffusion was probably limited by the formation of thin ice layers. For the 2007 cores we suspect that in addition to firn diffusion, the isotopes could have been redistributed within the top layers by melt water percolation or/and by mechanical mixing of snow and wind scouring (Fisher *et al*. 1988). However in our case it is impossible to evaluate the respective impact of these post-depositional processes in the alteration of the $\delta^{18}O$ seasonal records. All cores show a high degree of smoothing (Fig. 4 d–f, grey section) in a thick ice layer (between 5 m w.e. down to 7.5 m w.e. for Ahl09; Fig 4a), probably driven by warm summers (June to September) and winters (December to March). In this part of the $\delta^{18}O$ profiles, the identification of annual layers is almost impracticable or at least very subjective, while below 7.5 m w.e. (Ahl09 depth) the $\delta^{18}O$ signal is better preserved. In this part of the ice layer, the Ahl09, Ahl07, and E07 $\delta^{18}O$ records all show an absolute minimum of −17.6‰, −19.3‰ and −18.4‰ , respectively, above a $\delta^{18}O$ maximum measured in fine-grained firn lying below the ice.

Unlike the altered isotopic signal within melt layers, the minimum $\delta^{18}O$ value common to the three shallow cores cannot result from melt water infiltration. In fact, $\delta^{18}O$ values measured in layers affected by refrozen percolation tend to be higher than the original signal. Downward percolating fluid would more likely be enriched in ^{18}O since it results mostly from summer rain or melting of spring/summer snow, isotopically heavier than average pack (Pohjola *et al*. 2002). Therefore, we consider that the $\delta^{18}O$ minimum can be regarded as a climatological signal and its corresponding ice layer can be used as a dating reference horizon. More precisely, and based on the earlier assumption that precipitation $\delta^{18}O$ values on Vestfonna are a good proxy for air temperatures, with the lowest $\delta^{18}O$ values in winter, we suggest this ^{18}O-depleted snow layer at the two summits most likely results from the precipitation from a notably cold air mass, which additionally may have been affected by an

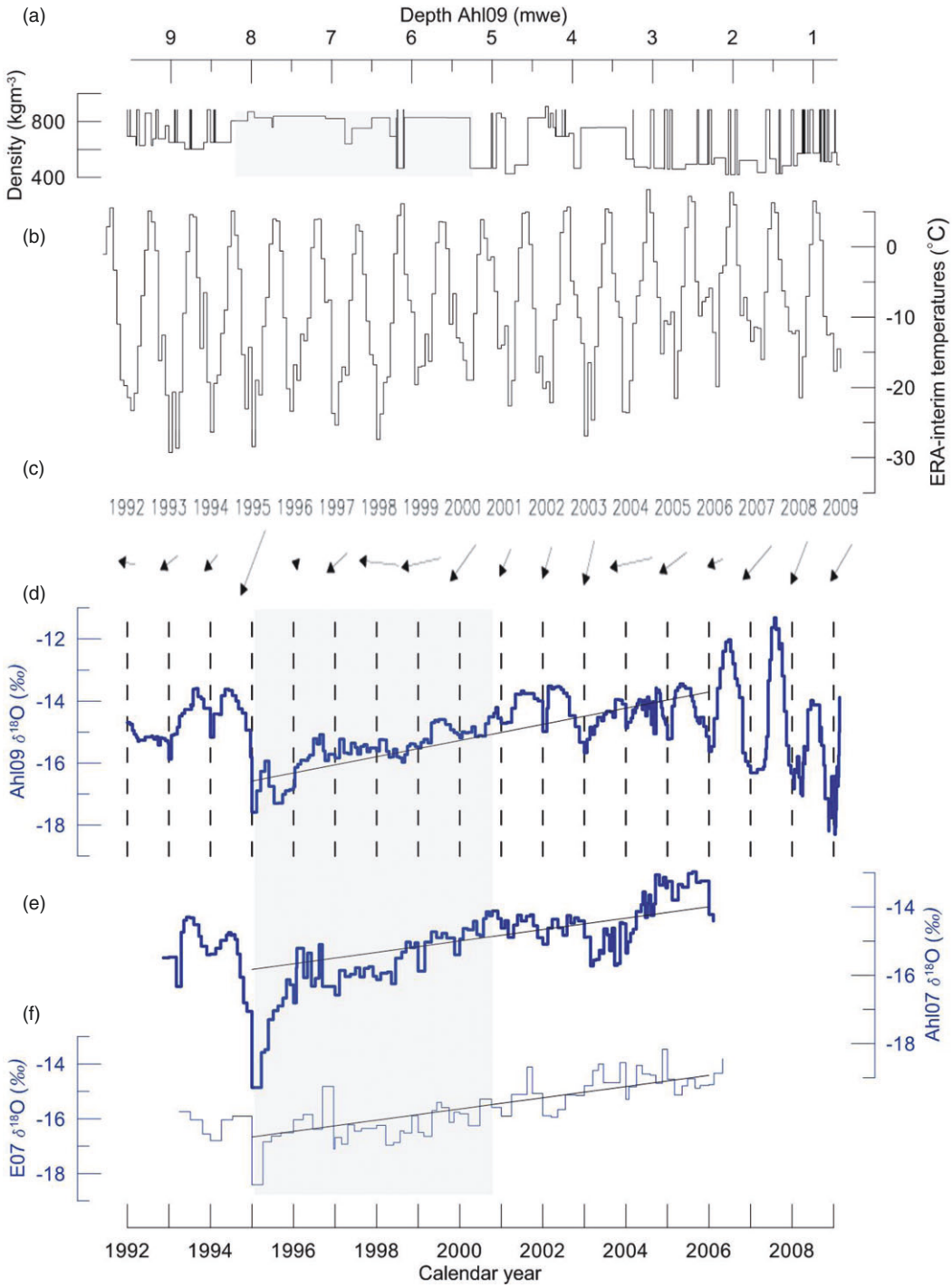

Fig. 4. Ahl09 densities plotted with depth (a), ERA-interim air temperatures downscaled to 600 m a.s.l. on Vestfonna (b), NCEP/NCAR reanalysis surface wind direction annual anomaly. The maximum wind is displayed as a fixed arrow length and used to scale the arrows (c), δ18O profiles of Ahl09 (d), Ahl07 (e) and E07 (f).The grey section marks the thick ice layer mentioned in the text.

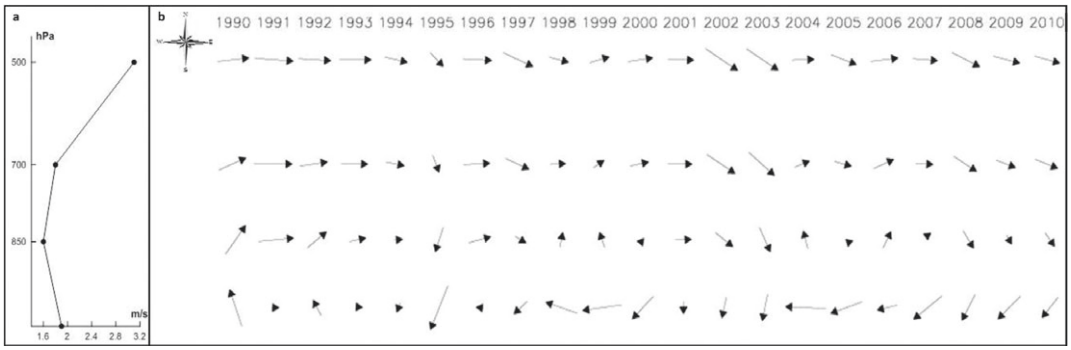

Fig. 5. (a) Wind speed in 1995 calculated from the NCEP/NCAR reanalysis dataset (data source: NCEP reanalysis produced at NOAA/ESRL PSD at http://www.esrl.noaa.gov/psd/data/timeseries/) at the grid point 80 N; 20 E, (b) 1990–2010 annual wind direction anomaly at 4 pressure levels (surface, 850 hPa, 700 hPa and 500 hPa). Time series of wind speed in each pressure level. The maximum wind is displayed as a fixed arrow length and used to scale the arrows.

advanced 'amount effect' (Rozanski *et al*. 1993), that is condensation-driven isotopic depletion and limited recycling of moisture. Owing to the lack of direct meteorological observations (temperature, precipitation) in Nordaustlandet area over the last 20 years, we compare the isotopic and stratigraphic data with ERA-Interim air temperatures downscaled to represent conditions at 600 m a.s.l. and NCEP/NCAR reanalysis time series of wind direction and speed in order to assign a date to the cold winter precipitation event and thus refine the shallow core time scale.

Figure 4 shows the Ahl09 density profile (a), the downscaled Vestfonna monthly temperatures since 1992 (b), the annual mean wind direction and speed at the surface (c) and the three complete $\delta^{18}O$ profiles (d–f). The pronounced negative $\delta^{18}O$ value could possibly correspond to one of the three coldest winters of the last two decades: 1992/93, 1994/95 and 1997/98 with respective average downscaled January temperatures of −29.2°C, −28.4°C and −27.4°C. The Vestfonna 95 isotope record contains the deepest winter minimum of the twentieth century at 1.2 m depth (Motoyama *et al*. 2008) that certainly corresponds to the previous winter (1994/95) since the summer 1994 surface was found below 1.5 m depth (Matoba *et al*. 2002). The NCEP/NCAR reanalysis for the grid point 80° N; 20° E (Fig. 4c) shows that 1995 (winter 1994/95) had an unusually strong Northern component. In the surface and the 850 hPa pressure levels (Fig. 5b), this is the most pronounced anomaly in the mean annual wind conditions since at least 1992 suggesting the source area of water vapour was shifted more to the North in 1995 compared to other years. The increase of the mean wind speed at the surface shown in Fig. 5a for 1995 also indicates a strong inversion keeping most of the water vapour in the *planetary boundary layer* (PBL) where most of its transport and condensation takes place. Similar pronounced wind-dynamic features associated with low surface temperatures are also observed in winter 2002/03, which is also characterized in the ice cores isotope profiles by notably lower $\delta^{18}O$ ratio (−15.7‰ for Ahl09). Furthermore, there is a clear relationship between the amplitude of the isotopic signal and the wind field, with low amplitude periods characterized by easterly air flow. No exceptional wind conditions favouring exceptionally depleted precipitation over Vestfonna ice cap are found for the winters 1992/93 and 1997/98, hence we choose to rule out these dates for the 'cold' isotopic signal.

Besides its thermodynamic impact on the lower troposphere, wind, depending on strength and direction, also affects the sea ice cover in various ways. Wind can cause ice floes to break into smaller pieces making them more vulnerable to melt. Wind induces sea ice drift to other regions, including warmer waters where the ice melts, and compaction of the ice cover through rafting and ridging (Comiso 2006). Because thermodynamic mechanisms are likely to be involved in the forcing of the sea ice anomalies, strong northern surface wind component calculated for 1995 could have forced the negative Barents sea ice extent observed in spring 1995 (Fig. 6). By blowing the sea ice out of the Barents Sea, and also presumably out of Hinlopen Strait between Nordaustlandet and Spitsbergen, we argue that the strong cold northerly wind may have caused

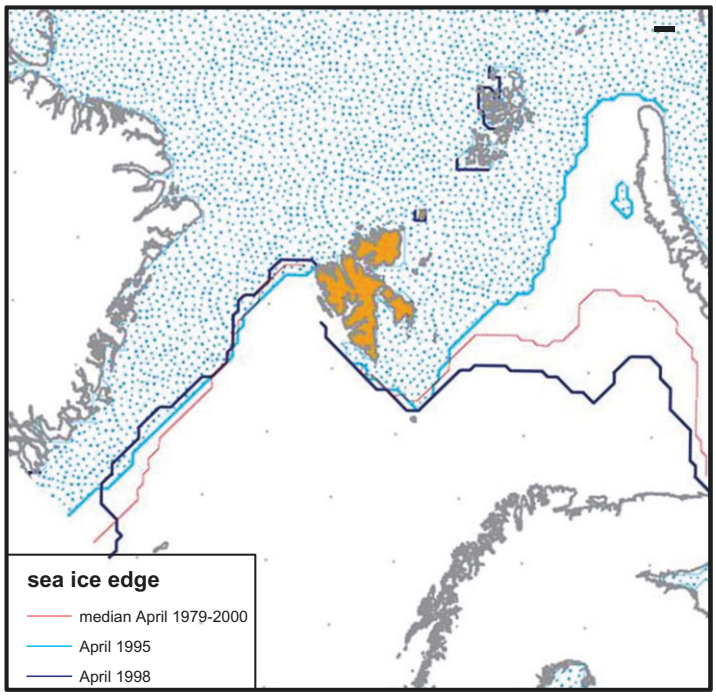

Fig. 6. Map of the Barents Sea area with indication of the April sea ice edge in 1993, 1995, 1998 and the median spring extent over the period 1979–2000.

the opening of sea ice leads (Bengtsson *et al*. 2004; Petoukhov and Semenov 2010) and the formation of frost flowers on young sea ice leading to the high marine salt concentrations (not shown) measured in the same ice layer as the $\delta^{18}O$ minimum (Beaudon and Moore 2009).

Consequently, winter 1994/95 is adopted as the most reasonable estimation of the cold event date. This time marker horizon allows for a more reliable layer counting to establish the chronology of the three shallow cores discussed in this paper (Fig. 4) and yields Ahl09, Ahl07 and E07 spanning respectively 17, 12 and 13 years (Table 1).

Spatial and temporal variability of snow accumulation rates and air mass influence

The mean oxygen isotope compositions over the 13 years are similar at the western and eastern part of the ice cap and are respectively −15.0‰ (±1) and −15.5‰ (±0.9). These values are higher than any 13 years block throughout the twentieth century reported by Watanabe *et al*. (2001) for the Eastern summit, suggesting the climate was cooler during the twentieth century over Nordaustlandet. In addition, the rapid increase of the $\delta^{18}O$ values in the profiles (Fig. 4 d–f) also characterizes a general warming trend at both sites from 1995 to 2007. The rise is so strong that it probably reflects an increase in percolating melt water that formed the thick ice layer between 5 and 8 m w.e. (Palosuo 1987).

For the period 1992-2009 covered by Ahl09, the mean annual accumulation is 0.52 m w.e. yr^{-1} (±0.15) (Table 1), close to the 0.53 m w.e. yr^{-1} found by Schytt (1964) at summit Ahlmann for the period 1957 to 1959. At the Eastern summit of the ice cap, the mean accumulation derived from E07 is 0.25 m w.e. yr^{-1} (±0.08) which is half that at Ahlmann summit. This result is somewhat lower than the 0.34 m w.e. yr^{-1} reported by Watanabe *et al*. (2001) for the eastern site for the period 1963 to 1999, and certainly lower than the 0.54 reported by Schytt (1964) for 1957–58. The location of western and eastern peaks of the ice cap at essentially the same elevation and latitude implies that the present day pronounced difference of accumulation rates is due to a longitudinal gradient in the precipitation regime over Vestfonna with a drier eastern side. At elevations above the PBL

(850–500 hPa and beyond) the circulation becomes increasingly westerly (Fig. 5b) such that precipitation is higher on the windward side, even when synoptic scale surface winds are different. However it would be surprising if this spatial precipitation gradient alone explains the net accumulation difference between the two summits that are only 20 km apart, and we speculate that wind scour and foehn effects caused by the Austfonna ice cap also contribute. With greater net accumulation in the West than in the East, the ice thickness at the western summit would be expected to grow faster unless mass loss compensates. The elevation across the summit ridge appears not to be significantly changing (Pohjola *et al*. 2011); hence the spatial and temporal accumulation trend may also result from outflow glacier dynamics, such as observed for Franklinbreen (Pohjola *et al*. 2011). This finding is seemingly not supported by the spatio-temporal snow-pit analysis of Möller *et al*. (2011b) that did not reveal statistically significant zonal variability of snow accumulation across the ice cap. However, to explain that discrepancy between our ice core study and their snow pits analysis Möller *et al*. (2011b) also invoked a spatial difference in the magnitude of the small-scale accumulation variability due to patchy deposition of wind-drift snow. Möller *et al*. (2011b) present a more detailed discussion of this topic.

Owing to the relatively high uncertainty associated with the dating of the cores, a calculation of snow accumulation at seasonal resolution is not possible. Hence, the discussion on the variability of the net accumulation rates is limited to a year-to-year (calendar years) comparison with the modelled *climatic mass balance* (CMB) data from Möller *et al*. (2011a). The complete time series of accumulation rates from Ahl09 and E07 with Vestfonna modeled CMB and measurements of stake arrays near the drilling sites in 2009 are shown in Fig. 7. Both Ahl09 and E07 cores display a high inter-annual variability in terms of net accumulation which ranges from respectively 0.36 and 0.77 m w.e., to 0.13 and 0.38 m w.e. Ahl09 values are in the same range as the modelled CMB and all time series covary well except for the year 2006. By definition, a climatic mass balance is a surface mass balance that includes internal accumulation, i.e. refreezing (Cogley *et al*. 2011). 2006 was one of the years with highest refreezing amounts within the last decades according to the CMB model (Möller *et al*. 2011a); hence the discrepancy with ice core data may reflect deep percolation processes or runoff. The net accumulation of 0.61 m w.e. at Ahlmann for the 2009 layer is in agreement with the 0.56 m w.e. measured from a nearby stake, although the latter only provides information about the winter and spring accumulation and not the whole calendar year. Therefore, considering dating uncertainties, the net accumulation data extracted from shallow core studies can be considered as useful climatological information. Furthermore, they constitute a valuable dataset for mass balance modelling of Vestfonna ice cap at Ahlmann summit where direct mass balance time series are still rare and Eastern summit where such records are completely lacking.

Conclusion

Densities and stable oxygen isotopes ratios measured in three shallow firn cores from Vestfonna ice cap have been jointly analysed in the light of measured and modelled surface air temperature data. The Vestfonna $\delta^{18}O$ record captures the recently discovered autumnal warming local maximum and is confirmed as a good proxy for local air temperatures for the uppermost well preserved layers. There is a strong correlation between amplitude of isotopic cycles and downscaled wind field over Vestfonna with northerly winds leading to high amplitude signals and easterlies to smoothed signals. The Vestfonna isotopic records show a warming trend as seen in instrumental records from Svalbard (Isaksson *et al*. 2001) and thus could be used to reconstruct long-term trends of past atmospheric parameters driving the isotopic composition of local precipitation. A pronounced low $\delta^{18}O$ value has been found in the three cores within the same facies arrangement. This signal was interpreted as an imprint of a winter 1994/95 cold air mass that brought ^{18}O-depleted precipitation following a N–S trajectory. The counting of isotope cycles and the dating of the common 'cold winter horizon' led to an acceptable dating of the cores.

By assigning a time scale to the cores, annual net accumulation time series could be calculated for the western and eastern summits of the ice cap over 17 and 13 years. Spatial and temporal variability of snow accumulation was found to be very high with the eastern side accumulating half the snow than the western part perhaps because of snow drift, or the impact of Austfonna on wind dynamics. The verification of these hypotheses,

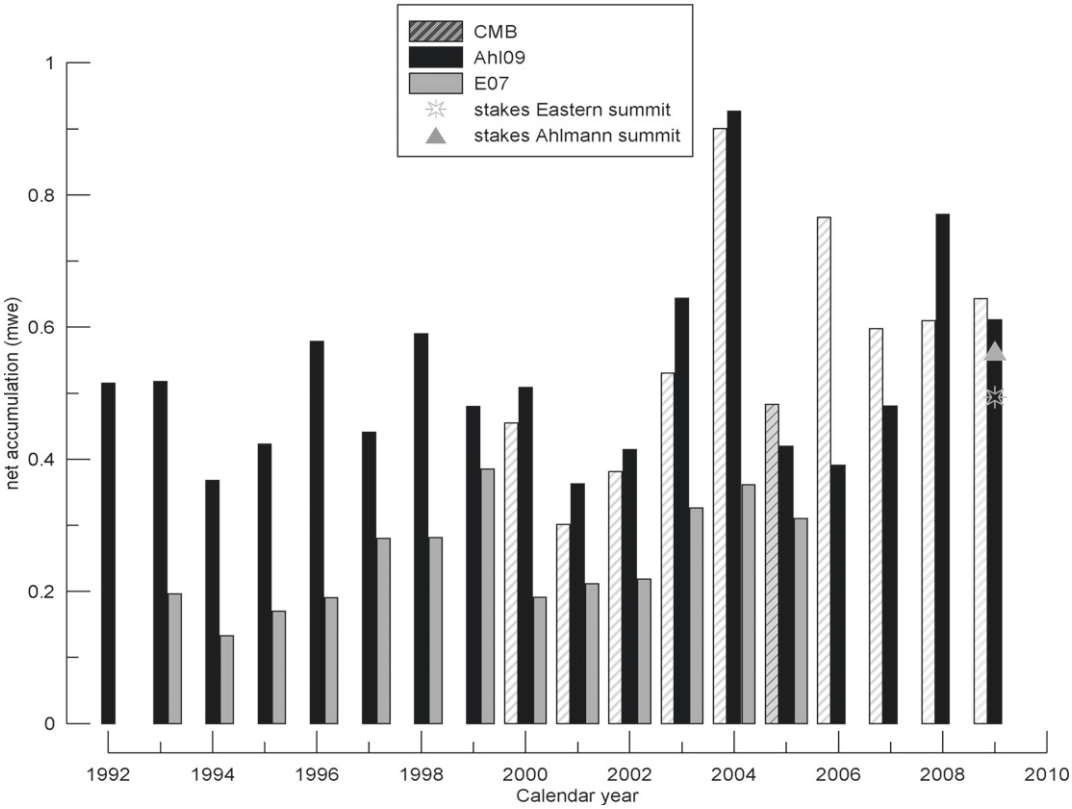

Fig. 7. Net annual accumulation calculated from the Ahl09 (black bars) and E07 (grey bars) cores dating proposed in this work and compared to modelled climatic mass balance (CMB) at Ahlmann summit (Möller *et al*. 2011a) and accumulation measurements at stakes near the drilling sites (2007–2010 averaged values).

however, requires further detailed investigations on wind fields, snow drift and resulting snow accumulation as well as a better characterization of spatial distribution of precipitation and moisture sources via the study of falling snow, snowpack and ice chemical compositions that is currently underway.

Acknowledgements

We thank the Finnish Forest Research Institute, Rovaniemi Research Unit for the use of cold-room and clean-room facilities for the cutting of the core. Financial support was provided by the Finnish Academy and by the Estonian Science Foundation through SvalGlac project and by The Nordic Council of Ministers and IPY-KINNVIKA. The German contribution to the research presented here was funded by the Deutsche Forschungsgemeinschaft (grants no. SCHE 750/3-1 and SCHN 680/2-1), and by the German Federal Ministry of Education and Research (grants no. 03F0623A and 03F0623B).

We acknowledge the Swedish Polar Research Secretariat for the logistic support within the SWEDARCTIC program and the University of Svalbard (UNIS) for the use of the cold room and vehicles. Special thanks to Janne Johansson, Lasse Tano and Åke Wallin for service in the field. We are grateful to Denis Samyn for his important assistance during the drilling operation and we also thank all people involved in IPY-KINNVIKA fieldwork and fieldwork planning: the ship and personnel of the Norwegian coast guard *Svalbard*, Naviga and Airlift A/S for their valuable services. The Governor of Svalbard is to be thanked for giving us permission to use the old IPY-3 station Kinnvika.

Emilie Beaudon, Arctic Centre, University of Lapland, P.O. Box 122, 96101 Rovaniemi, Finland
Email: ebeaudon@ulapland.fi

Laura Arppe, Department of Geosciences and Geography, P.O. Box 64, 00014 University of Helsinki,Finland.
Email: laura.arppe@helsinki.fi

Ulf Jonsell, Department of Earth Sciences, Uppsala University, Sweden; ETSI de Telecomunicación, Universidad Politécnica de Madrid, Avenida Complutense 30, City University, 28040 Madrid Spain.
Email: ulfygge@gmail.com

Tõnu Martma, Institute of Geology, Tallinn University of Technology, Ehitajate tee 5 19086 Tallinn, Estonia.
Email: martma@gi.ee

Marco Möller, Department of Geography, RWTH Aachen University, Templergraben 55, 52056 Aachen, Germany.
Email: marco.moeller@geo.rwth-aachen.de

Veijo A. Pohjola, Department of Earth Sciences, Uppsala University, Villavägen 16, S-752 36 Sweden.
Email: veijo.pohjola@natgeog.uu.se

Dieter Scherer, Department of Ecology, Technische Universität Berlin, Rothenburgstrasse 12, 12165 Germany.
Email: dieter.scherer@tu-berlin.de

John C. Moore, Colleges of Global Change and Earth System Science, Beijing Normal University, 19 Xinjiekou Wai street, Beijing, China,100875.
Email: john.moore.bnu@gmail.com

References

Beaudon, E. and Moore, J., 2009. Frost flower chemical signature in winter snow on Vestfonna ice cap (Nordaustlandet, Svalbard). *The Cryosphere*, 3 (2), 147–154, doi:10.5194/tc-3-147-2009.

Bengtsson, L., Semenov, V.A. and Johannessen, O.M., 2004. The early twentieth-century warming in the Arctic – a possible mechanism. *Journal of Climate*, 17, 4045–4057.

Cogley, J.G., Hock, R., Rasmussen, L.A., Arendt, A.A., Bauder, A., Braithwaite, R.J., Jansson, P., Kaser, G., Möller, M., Nicholson, L. and Zemp, M., 2011. *Glossary of glacier mass balance and related terms*. IHP-VII Technical Documents in Hydrology No. 86, IACS Contribution No. 2, UNESCO-IHP, Paris.

Comiso, J.C., 2006. Abrupt decline in the Arctic winter sea ice cover, *Geophysical Research Letter*, 33, L18504, doi:10.1029/2006GL027341.

Fisher, D.A. and Koerner, R.M., 1988. The effects of wind on $\delta^{18}O$ and accumulation give an inferred record of δ seasonal amplitude from the Agassiz ice cap, Ellesmere Island, Canada. *Annals of Glaciology*, 10, 34–37.

Førland, E.J., Hanssen-Bauer, I. and Nordli, P.Ø., 1997. *Climate Statistics and Long-Term Series of Temperatures and Precipitation at Svalbard and Jan Mayen*. Det Norske Meteorologiske Institutt, Oslo.

Isaksson, E., Pohjola, V.A., Jauhiainen, T., Moore, J., Pinglot, J.F., Vaikmäe, R., van de Wal, R.S.W., Hagen, J.O., Ivask, J., Karlöf, L., Martma, T., Meijer, H.A.J., Mulvaney, R., Thomassen, M. and van den Broek, M., 2001. A new ice core record from Lomonosovfonna, Svalbard: viewing the data between 1920–1997 in relation to present climate and environmental conditions. *Journal of Glaciology*, 47 (157), 335–345.

Johnsen, S.J., 1977. Stable isotope homogenization of polar firn and ice. Symposium at Grenoble 1975 – Isotopes and Impurities in Snow and Ice. *IAHS Publication*, 118, 210–219.

Kistler, R., Kalnay, E., Collins, W., Saha, S., White, G., Woollen, J., Chelliah, M., Ebisuzaki, W., Kanamitsu, M., Kousky, V., Van den Dool, H., Jenne, R. and Fiorino, M., 2001. The NCEP–NCAR 50-year reanalysis: monthly means CD-ROM and documentation. *Bulletin of the American Meteorological Society*, 82, 247–268.

Kotlyakov, V.M., Arkhipov, S.M., Henderson, K.A. and Nagornov. O.V., 2004. Deep drilling of glaciers in Eurasian Arctic as a source of paleoclimatic records. *Quaternary Science Reviews*, 23, 1371–1390.

Matoba, S., Narita, H., Motoyama, H., Kamiyama, K. and Watanabe, O., 2002. Ice core chemistry of Vestfonna ice cap in Svalbard, Norway. *Journal of Geophysical Research*, 107 (D23), 4721, doi:10.1029/2002JD002205.

Möller, M., Finkelnburg, R., Braun, M., Hock, R., Jonsell, U., Pohjola, V.A., Scherer, D. and Schneider, C., 2011a. Climatic mass balance of the ice cap Vestfonna, Svalbard: A spatially distributed assessment using ERA-Interim and MODIS data. *Journal of Geophysical Research*, 116, F03009, doi:10.1029/2010JF001905.

Möller, M., Möller, R., Beaudon, É., Mattila, O.-P., Finkelnburg, R., Braun, M., Grabiec, M., Jonsell, U., Luks, B., Puczko, D., Scherer, D. and Schneider, C., 2011b. Snowpack characteristics of Vestfonna and De Geerfonna (Nordaustlandet, Svalbard): a spatiotemporal analysis based on multiyear snow-pit data. *Geografiska Annaler: Series A, Physical Geography*. doi: 10.1111/j.1468-0459.2011.00440.x.

Moore, J.C., Grinsted, A., Kekonen, T. and Pohjola, V.A., 2005. Separation of melting and environmental signals in an ice core with seasonal melt. *Geophysical Research Letters*, 32, L10501, doi:10.1029/2005GL023039.

Motoyama, H, Watanabe, O., Fujii, Y., Kamiyama, K., Igarashi, M., Matoba, S., Kameda, T., Goto-Azuma, K., Izumi, K., Narita, H., Iizuka, Y. and Isaksson, E., 2008. *Analyses of ice core data from various sites in Svalbard glaciers from 1987 to 1999*. NIPR Arctic data reports, NIPR, Tokyo.

Palosuo, E., 1987. Ice layers and superimposition of ice on the summit and slope of Vestfonna, Svalbard. *Geografiska Annaler: Series A, Physical Geography*, 69 (2), 289–296.

Petoukhov, V. and Semenov, V.A., 2010. A link between reduced Barents-Kara sea ice and cold winter extremes over northern continents. *Journal of Geophysical Research*, 115, doi:10.1029/2009JD013568.

Pohjola, V.A., Christoffersen, P., Kolondra, L., Moore, J.C., Pettersson, R., Schäfer, M., Strozzi, T. and Reijmer, C.H., 2011. Spatial distribution and change in the surface ice-velocity field of Vestfonna ice cap, Nordaustlandet, Svalbard, 1995–2010 using geodetic and satellite interferometry data. *Geografiska Annaler: Series A, Physical Geography*. doi: 10.1111/j.1468-0459.2011.00441.x.

Pohjola, V.A., Moore, J.C., Isaksson, E., Jauhiainen, T., Van de Wal, R.S.W., Martma, T., Meijer, H.A.J. and Vaikmäe, R., 2002. Effect of period melting on geochemical and isotopic signals in an ice core from Lomonosovfonna, Svalbard. *Journal of Geophysical Research*, 107 (D4), 4036, doi:10.1029/2000JD000149.

Rozanski, K., Araguás-Araguás, L. and Gonfiantini, R., 1993. Isotopic patterns in modern global precipitation. In: Swart, P.K., Lohmann, K.L., McKenzie, J.A. and Savin, S. (eds), *Climate Change in Continental Isotopic Record: Geophysical Monograph Series*, 78, Washington, DC: American Geophysical Union, 1–37.

Schytt, V., 1964. Scientific results of the Swedish glaciological expedition to Nordaustlandet, Spitsbergen, 1957 and 1958. *Geografiska Annaler*, 46 (3), 242–281.

Vaykmyae, R.A., Martma, T.A., Punning, Ya.-M.K. and Tyugu, K.R., 1985. Variations in $\delta^{18}O$ and Cl^- in an ice core from Vestfonna Nordaustlandet. *Polar Geography and Geology*, 9 (4), 329–333.

Watanabe, O., Motoyama, H., Igarashi, M., Kamiyama, K., Matoba, S., Goto-Azuma, K., Narita, H. and Kameda, T., 2001. Studies on climatic and environmental changes during the last few hundred years using ice-cores from various sites in Nordaustlandet, Svalbard. *National Institute of Polar Research Memoirs*, 54 (special issue), 227–242.

Manuscript received Jan., 2011, revised and accepted Aug., 2011

JOURNAL OF GEOPHYSICAL RESEARCH, VOL. 117, D03306, doi:10.1029/2011JD016592, 2012

Statistical extraction of volcanic sulphate from nonpolar ice cores

J. C. Moore,[1,2,3] E. Beaudon,[2] Shichang Kang,[4,5] D. Divine,[6] E. Isaksson,[7] V. A. Pohjola,[3] and R. S. W. van de Wal[8]

Received 21 July 2011; revised 4 December 2011; accepted 15 December 2011; published 9 February 2012.

[1] Ice cores from outside the Greenland and Antarctic ice sheets are difficult to date because of seasonal melting and multiple sources (terrestrial, marine, biogenic and anthropogenic) of sulfates deposited onto the ice. Here we present a method of volcanic sulfate extraction that relies on fitting sulfate profiles to other ion species measured along the cores in moving windows in log space. We verify the method with a well dated section of the Belukha ice core from central Eurasia. There are excellent matches to volcanoes in the preindustrial, and clear extraction of volcanic peaks in the post-1940 period when a simple method based on calcium as a proxy for terrestrial sulfate fails due to anthropogenic sulfate deposition. We then attempt to use the same statistical scheme to locate volcanic sulfate horizons within three ice cores from Svalbard and a core from Mount Everest. Volcanic sulfate is <5% of the sulfate budget in every core, and differences in eruption signals extracted reflect the large differences in environment between western, northern and central regions of Svalbard. The Lomonosovfonna and Vestfonna cores span about the last 1000 years, with good extraction of volcanic signals, while Holtedahlfonna which extends to about AD1700 appears to lack a clear record. The Mount Everest core allows clean volcanic signal extraction and the core extends back to about AD700, slightly older than a previous flow model has suggested. The method may thus be used to extract historical volcanic records from a more diverse geographical range than hitherto.

Citation: Moore, J. C., E. Beaudon, S. Kang, D. Divine, E. Isaksson, V. A. Pohjola, and R. S. W. van de Wal (2012), Statistical extraction of volcanic sulphate from nonpolar ice cores, *J. Geophys. Res.*, *117*, D03306, doi:10.1029/2011JD016592.

1. Introduction

[2] Ice cores are wonderful archives of past environment and climate variations. However, to be useful a reliable dating for the ice in the core must be obtained. This has long been a major difficulty for ice cores located in low-lying ice caps or mountain glaciers where seasonal melting, and typically high concentrations of multiorigin impurities are the norm. Ice cores are often dated by reference horizons such as radioactivity from well dated bomb test fallout or acidic deposits from historically known volcanic eruptions [e.g., *Kekonen et al.*, 2005a, 2005b; *Palais et al.*, 1992], and some may also be dated by annual cycle counting [*Pohjola et al.*, 2002b; *Kaspari et al.*, 2008; *Kang et al.*, 2002; *Karlöf et al.*, 2005], or flow models [e.g., *Nye*, 1963; *Kaspari et al.*, 2008]. Reference horizons, particularly volcanic signatures are often assumed to be recorded as acidic sulfate [*Kekonen et al.*, 2005a], and more recently and rarely in the bismuth concentration record along a core [e.g., *Kaspari et al.*, 2007; *Xu et al.*, 2009]. The individual sulfate spikes are often accepted to be specific eruptions on the basis of other evidence leading to an approximate dating, but they are seldom proven to be specific eruption signatures since the evidence relies on finding volcanic tephra with a chemical signature that matches the known composition of the eruption in question. This is a time consuming task as often tephra particles are very rare in ice cores drilled at remote locations [*Palais et al.*, 1992], or the tephra may be outnumbered tens of thousands of times by local country rock swept into the atmosphere by the eruption [*Kekonen et al.*, 2005b].

[3] Major ionic impurities in ice cores may be categorized by their typical sources [e.g., *Legrand and Mayewski*, 1997; *Moore et al.*, 2006; *Moore et al.*, 2005; *Kekonen et al.*, 2005a; *Eichler et al.*, 2011; *Kaspari et al.*, 2007; *Kang et al.*, 2000; *Matoba et al.*, 2002]. Marine ions originating from oceanic sea spray are dominated by soluble salt derived ions, typically Na^+ and Cl^- with significant amounts of SO_4^{2-} and Mg^{2+}. Terrestrial ions come from

[1]College of Global Change and Earth System Science, Beijing Normal University, Beijing, China.
[2]Arctic Centre, University of Lapland, Rovaniemi, Finland.
[3]Department of Earth Sciences, Uppsala University, Uppsala, Sweden.
[4]Key Laboratory of Tibetan Environmental Changes and Land Surface Processes, Institute of Tibetan Plateau Research, Chinese Academy of Sciences, Beijing, China.
[5]State Key Laboratory of Cryospheric Sciences, Chinese Academy of Sciences, Lanzhou, China.
[6]Department of Mathematics and Statistics, University of Tromsø, Tromsø, Norway.
[7]Norwegian Polar Institute, Tromsø, Norway.
[8]Institute for Marine and Atmospheric Research, Utrecht University, Utrecht, Netherlands.

0148-0227/12/2011JD016592

wind blown dust and are dominated by Ca^{2+}, but also include Na^{+}, Mg^{2+}, SO_4^{2-} and K^{+}. Anthropogenic sources of ions have grown in importance since the industrial revolution and mainly affect concentrations of SO_4^{2-}, NO_3^{-}, and NH_4^{+}. Biogenic sources provide ions such as methane sulfonate ($CH_3SO_3^{-}$ or MSA), SO_4^{2-}, NH_4^{+}, and formate ($HCOO^{-}$). Volcanic emissions, while certainly complex, affect only concentrations of SO_4^{2-} in the set of ions routinely measured in ice cores. Though HF may be emitted, we do not measure F^{-} ions. HCl in ice cores is sometimes associated with reaction of NaCl with H_2SO_4 in the atmosphere during long-distance transport, hence is likely not significant except in fallout over the polar ice sheets. As large volcanic eruptions do not occur in most years, and since the volcanic SO_4^{2-} is removed from the atmosphere in the year or two after the eruption, a volcanic SO_4^{2-} signal appears as a narrow spike in concentrations. Hence volcanic eruptions are typically simply assumed to be the cause of peaks in sulfate. While this assumption may be true in central Antarctica [*Legrand and Mayewski*, 1997], in Svalbard and mountain glacier areas this is a very poor assumption since volcanic acids account for only 5–10% of sulfate in Svalbard [*Moore et al.*, 2006], and even less when terrestrial input is large, such as in Tibet [*Kang et al.*, 2000; *Cong et al.*, 2009]. In considering the sources of ions, sulfate from volcanic sources has two features that point to a less ambiguous way identifying volcanic markers: (1) the sulfate is not associated with any other ions, and (2) the signal appears as a sharp spike in concentrations.

[4] Sulfate measurements are typically done by ion chromatography which has heteroscedastic (that is systematically varying) errors, in this case proportional to the measured value, and simultaneously the sulfate concentrations tend to be Lognormally distributed, as is the case for the cores studied here. This means that elementary procedures such as determining a significant peak by testing if it stands 2 standard deviations above the mean sulfate level are statistically invalid.

[5] In this paper we present a more rigorous approach based on extracting spikes in the sulfate residual after fitting the sulfate to empirical regression, in log space, on all other measured ions. This process accounts for terrestrial, marine, biogenic and anthropogenic sulfate deposition fractions as well as postdepositional relocation of ions, leaving only stochastic sources, effectively volcanic fallout. We verify the procedure on ice cores from Svalbard and central Asia. These cores present similar problems in interpreting the sulfate profile, despite coming from very different environments: that is the sulfate signal has many additional sources rather than volcanoes. Additionally both regions experience large melt either prolonged through a polar day when temperatures may be at the melting point for 2 months, or daily freeze-thaw cycles. Although we anticipate that the method is most useful on ice cores from alpine or maritime sites, there are regions of the large ice sheets where ice cores are difficult to interpret such as coastal sites with large marine and biogenic sulfate inputs, or blue ice areas where local terrestrial sources are important.

2. Ice Cores

[6] In this paper we use ice collected from Svalbard, Altai mountains, and from Mount Everest (Figure 1). The core details are summarized in Table 1. The Svalbard cores come from: (1) Lomonosovfonna, central Spitsbergen, influenced by westerly and arctic airflow [*Kekonen et al.*, 2005a]; (2) Holtedahlfonna a western plateau site close to the Spitsbergen coast and subject to more westerly influences and with Arctic haze events [*Virkkunen et al.*, 2007; *Ruggirello et al.*, 2010]; and (3) Vestfonna ice cap in Nordaustlandet, a more high arctic site with dominant Arctic Ocean influence [*Matoba et al.*, 2002; *Beaudon and Moore*, 2009]. The three sites have distinct environmental chemistry, despite being located within a relatively small area, however they are conspicuous in their abundance of marine derived species [*Kekonen et al.*, 2005a, *Matoba et al.*, 2002, *Moore et al.*, 2006]. In contrast, the Mount Everest and Belukha (Altai mountains) cores come from central Asia far from marine sources of ions. At Everest impurities are deposited from mixed westerly and monsoon circulation regimes, and are dominated by terrestrially derived ion chemistry [*Kang et al.*, 2007; *Zhang et al.*, 2009]. The climatology of the Altai is dominated by the regular development of the Siberian High in winter, leading to extreme cold and dry conditions in this season. Humid air masses from the Atlantic Ocean as well as recycled moisture are the main sources of precipitation in summer [*Aizen et al.*, 2006]. This core has been exceptionally well dated using the sulfate and calcium ion concentrations from AD1250 to 1940 [*Eichler et al.*, 2009a], and we use it here to verify the volcanic sulfate extraction method, and then to extract volcanic signals in the post-1940 ice.

[7] The Lomonosovfonna core has been the subject of intense research on the influence of postdepositional processes on ion chemistry [*Moore et al.*, 2005] and structure [*Pohjola et al.*, 2002a], and dating [*Divine et al.*, 2011]. The Holtedahlfonna core was drilled 8 years after and has been much less reported. Dating of the Holtedahlfonna core is uncertain due to difficulties in determining bed depth and flow geometry in the saddle location [*Divine et al.*, 2011]. The Vestfonna core dating was reliant on 2 fixed horizons and no layer thinning model. The Everest core has been partially analyzed for bismuth, and several peaks in concentration have been tentatively assigned to eruptions over the last 200 years [*Xu et al.*, 2009], however for earlier periods the Mount Everest core dating has been largely reliant on a flow model and cycle counting [*Kaspari et al.*, 2007, 2008].

3. Methods

[8] All chemistry data discussed here were measured using ion chromatography. Postdepositional processes, basically seasonal melting, play a large role in Svalbard and low-latitude ice cores [*Koerner*, 1997; *Moore et al.*, 2005]. Postdepositional processes also affect high-altitude polar ice cores which never experience melting conditions [*Karlöf et al.*, 2005]. Postdepositional processes are chemical species dependent with some ions more conservative than others [*Karlöf et al.*, 2005; *Moore et al.*, 2005; *Goto Azuma et al.*, 2002]. These effects produce both small-scale disturbance due to local topography, and longer-range noise due to meteorology. For the Lomonosvfonna core, measurement and short range depositional noise errors are only about 8%. Longer-range noise may be estimated by the

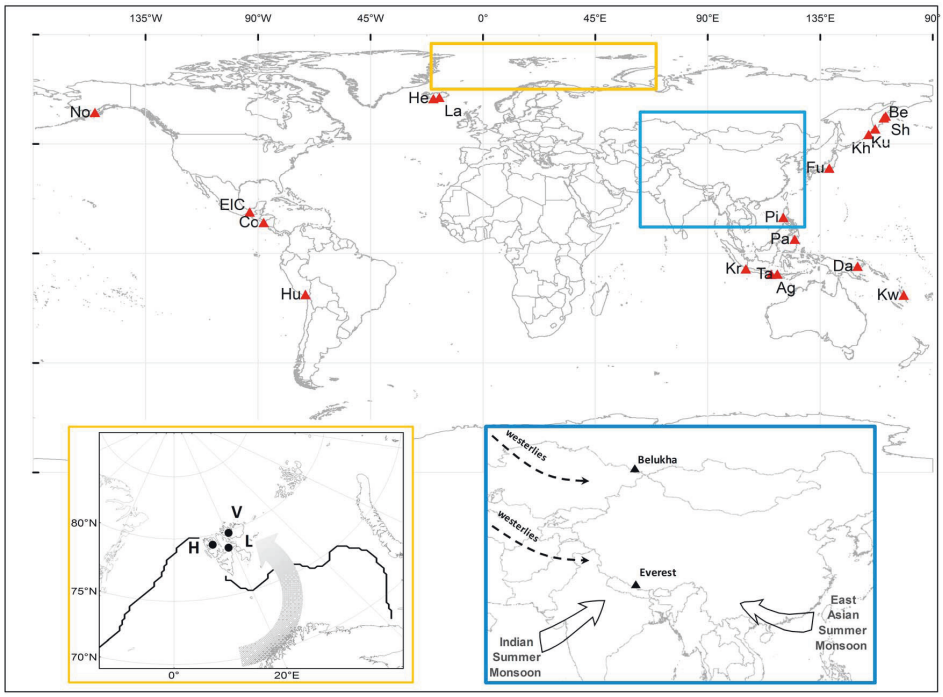

Figure 1. Map of ice core locations. Boxed insets show the Belukha, the Everest and 3 Svalbard core sites Lomonosovfonna (L), Holtedahlfonna (H) and Vestfonna (V), 1979–2000 monthly median sea ice position (black line) and principal wind directions. Also shown are the volcanoes detected in the ice cores in this paper (see Table 2 for details).

correlations of the climate related signals in cores over meters to kilometer scales, and observations from both the Canadian Arctic [*Goto Azuma et al.*, 2002], and Svalbard ice cores suggest noise may be as large as the climate signal. Hence we expect that the sulfate records will be a complex superposition of different environmental inputs and postdepositional processes. Figure 2 shows an illustrative set of ion concentrations of all 9 species measured along a 20 m long section of the Lomonosovfonna core from the early to mid 20th century. It is obvious that the sulfate profile is correlated with ions of various origins: marine, e.g., Na^+; terrestrial, e.g., Ca^{2+}; anthropogenic, e.g., NO_3^-; and biogenic, e.g., MSA ($CH_3SO_3^-$).

[9] *Moore et al.* [2006] showed that the different contributions to the sulfate budget along the core can be estimated based on multiple linear regression analysis, (MLR) between sulfate and the other ions in the core. The Lognormally distributed ion errors demand log transformation of concentrations before regression analysis. Because of the log transformation the regression coefficients are not simple multipliers of concentrations, but exponents (M_i) and the model residuals at any depth in the ice core are, R:

$$R = \log\left[SO_4^{2-}\right] - K - \sum_i^L M_i \log[s_i], \quad (1)$$

Table 1. Ice Core Characteristics[a]

Name	Latitude (°N)	Longitude (°E)	Altitude (m asl)	Drill Date	Ice Depth (m)	Drill Depth (m)	1963 Depth (m)	Mean Concentration (μEq/L)				
								SO_4^{2-}	NO_3-	Cl^-	NH_4^+	Ca^{2+}
Belukha	49.81	86.58	4062	2001	139	139	18.8	6.7	3.3	0.8	9.3	8.4
Lomonosovfonna	78.86	17.43	1250	1997	123	121	18.5	4.0	0.9	8.1	1.2	1.7
Mount Everest	28.03	86.98	6518	2002	108	108	31.5	1.3	1.9	0.5	N.A	8.9
Holtedahlfonna	79.14	13.27	1150	2005	180?	125	28.4	2.8	0.7	12.6	0.1.1	1.2
Vestfonna	79.97	21.02	600	1995	320	210	15.3	2.7	1.1	39.4	N.A	1.4

[a]NO_3^-, Cl^-, NH_4^+, and Ca^{2+} concentrations since 1800 are indicative of anthropogenic, marine, biogenic, and terrestrial SO_4^{2-} sources, respectively. An independent reference horizon comes from the radioactivity associated with the 1963 bomb fallout.

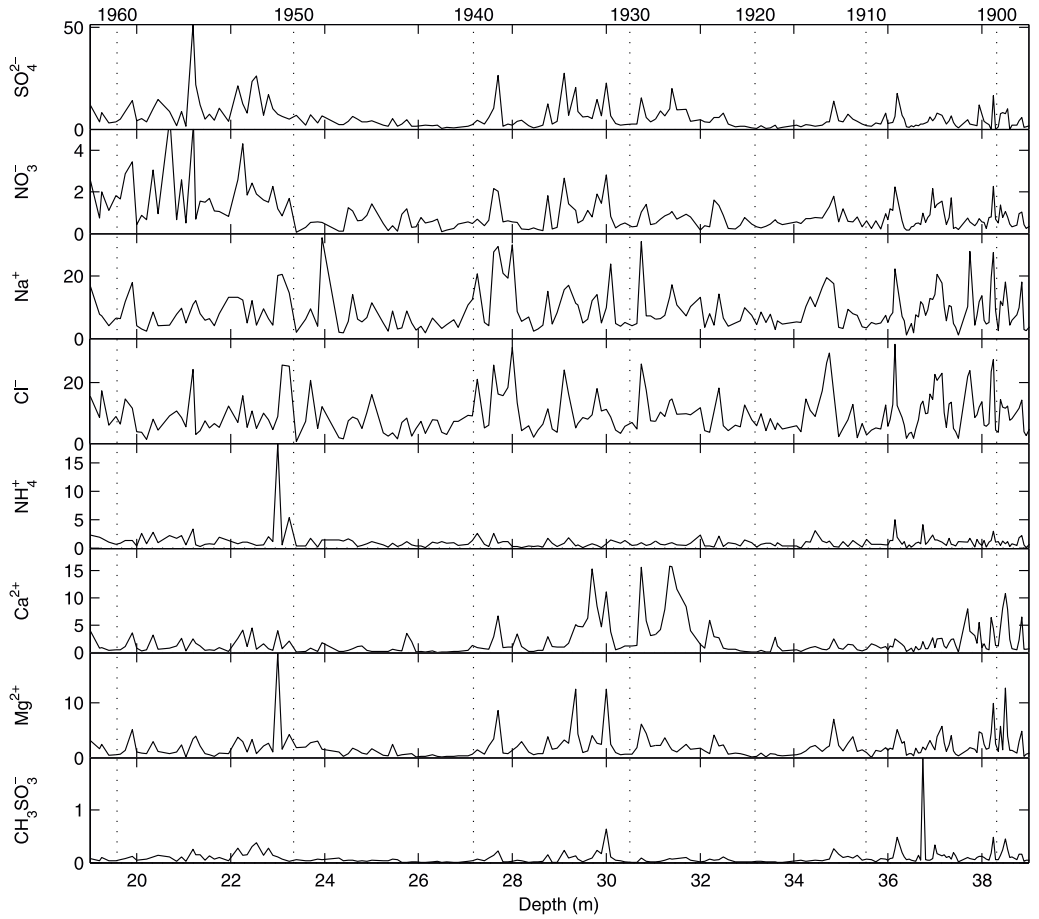

Figure 2. Ion concentration (in μEq/L) for all species measured profiles for 19–39 m depths of the Lomonosovfonna ice core with dates from *Divine et al.* [2011].

where K is the MLR intercept, $[s_i]$ denote the L other ionic species concentrations, $L = 8$ for Lomonosovfonna and Holtedahlfonna, and 6 for Everest and Vestfonna cores where NH_4^+ and MSA were not analyzed. In contrast to the approach used by *Moore et al.* [2006] where the best models were determined by the F statistic to avoid over fitting, here we are simply concerned with the residual, that is the part of the sulfate that cannot be related to any of the other ions—and which we expect to be stochastic or volcanic in origin. Hence we use all available ion species in the model fit, equation (1), even though most of the time several ions will make insignificant contributions to the model fit. We also allow both M and K to change over time (e.g., in response to climatic change) by running the MLR model in a moving window of data (e.g., 100 points long—we will show an example of how window length choice affects results in section 4.1). Thus a typical sulfate concentration at a given depth point of the ice core would have 100 models fit to it as the window moves past it. We smooth the ion data with 3-point running means to reduce short wavelength, species-dependent elution rate variations. By analyzing the time series in the original sampling intervals, we ensure that the MLR analysis window contains the same number of independent data points, and therefore allow the significance level of the fits to be comparable along the entire core.

[10] Estimating the significance level of a residual spike is possible in several ways. We can determine the 95% significance level in log space of each residual. This procedure effectively calculates the ratio of the measured SO_4^{2-} concentration relative to the model fit (e^R), hence a perfect model with no residual has an $e^R = 1$ and if $e^R > 2.72$ then there is more unexplained variance in sulfate concentration than modeled variance at that depth. Alternatively the absolute confidence interval of the residual in concentration space can be estimated. While the significance estimate from log space is more natural, it can be very sensitive to experimental errors, so that a small absolute sulfate concentration may be poorly fitted by the model and hence have a large

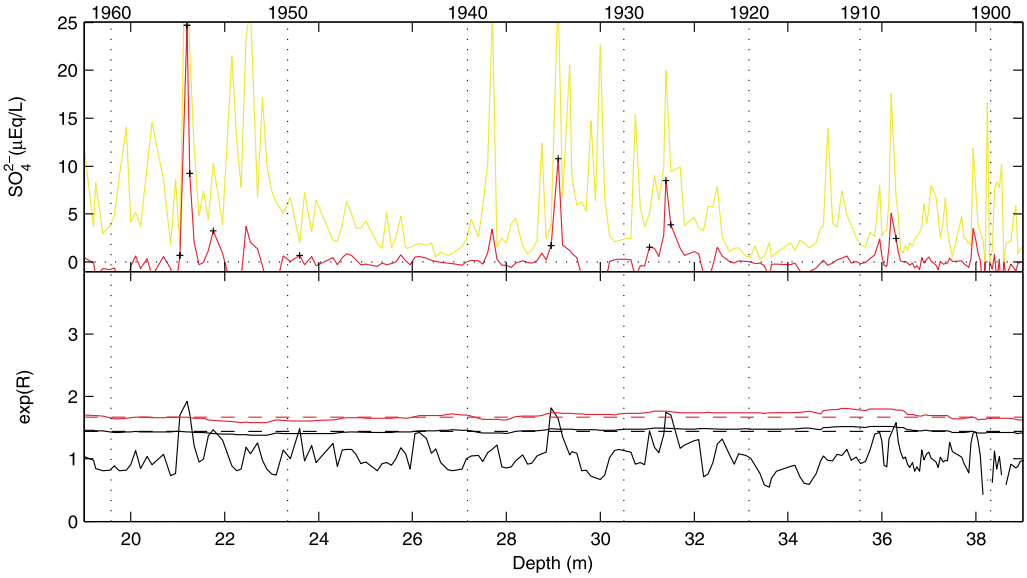

Figure 3. Sulfate (yellow) and residual (red) in uEq/L as a function of core depth. Bottom e^R (equation (2)) for the Lomonosovfonna ice core over the same depth range as in Figure 2. 99% and 95% significance levels are shown as red and black lines, with dashed lines based on the variance of the whole core, while solid lines are the based on variance within the 100 point window used for MLR fits in log space. Crosses indicate significant peaks at 95% level of residual of whole core or at 99% significance in the windowed test. Dates are from *Divine et al.* [2011]. Significant residuals correspond with Bezymianny 1956, Kharimokotan 1934, Kuril islands 1924–1929, and Novarupta 1912.

residual in log space, but amount to a only a few ppb in concentration space. The value of the residual $V[SO_4^{2-}]$ in concentration units is given at each measurement point along the core by:

$$V\left[SO_4^{2-}\right] = \left[SO_4^{2-}\right]\left(1 - 1/\left(e^R\right)\right). \quad (2)$$

[11] The size of the window used to determine the fit of SO_4^{2-} determines the size of the residual produced. A long window, say 400 points results in a less responsive fit, and hence stochastic peaks are less able to influence the fit, and so produce larger residuals than short windows, such as 50 points. While the longer windows produce more uniform background SO_4^{2-} levels for the core which is a positive feature, they are also less able to respond to changing environment or climate that can drive changes in the deterministic relationship between the ions in the core. Probably a better estimate of the significance of any peak comes from assessing the variance of the residuals within the sliding window used for the MLR, than using the variance of the residuals along the whole core. This compensates for large concentration peaks that bias the variance in quieter sections of core. Figure 3 shows results of the MLR analysis which can be compared with the ion concentration profiles in Figure 2. It should be obvious that $V[SO_4^{2-}]$ is a small fraction of the sulfate ion concentrations. Both the MLR models and the variance calculation are limited at the data boundary as the window starts to overlap, so that for the start and end points only one single MLR model is possible compared with typically 100 models per point if the window is 100 points long. At the data boundaries only half the usual number of residuals are available to compute the significance levels, since the window only exists within the data.

4. Results and Interpretation

4.1. Belukha Ice Core: Verification of the Method

[12] We make use of the well-dated Belukha ice core [*Eichler et al.*, 2009a] from the Altai Mountains (Figure 1) to verify our volcanic sulfate method. The ice core site is at high altitude and extremely continental, far from marine sources, but influenced by biogenic productivity over Southern Siberia and local dust sources [*Eichler et al.*, 2009b, Table 1]. Ion chemistry was performed at 3–4 cm (subseasonal to AD1800) resolution, for Na^+, Cl^- SO_4^{2-}, $HCOO^-$, Mg^{2+} Ca^{2+}, K^+, NO_3^-, and NH_4^+, [*Eichler et al.*, 2009a, 2009b, 2011] and all were used in the MLR analysis. The ratio of calcium to sulfate in the 1817–1899 interval is 0.21, and so an excess sulfate fraction $X[SO_4^{2-}]$, attributable to anthropogenic and volcanic sources was estimated to be $X[SO_4^{2-}] = [SO_4^{2-}] - 0.21[Ca^{2+}]$. This ice core shows a nice and simple series of spikes in $X[SO_4^{2-}]$ that can be easily identified with volcanic eruptions, from AD1250 to 1940 [*Eichler et al.*, 2009a]. After 1940 the rise in anthropogenic sulfate emissions means that volcanic sulfate is

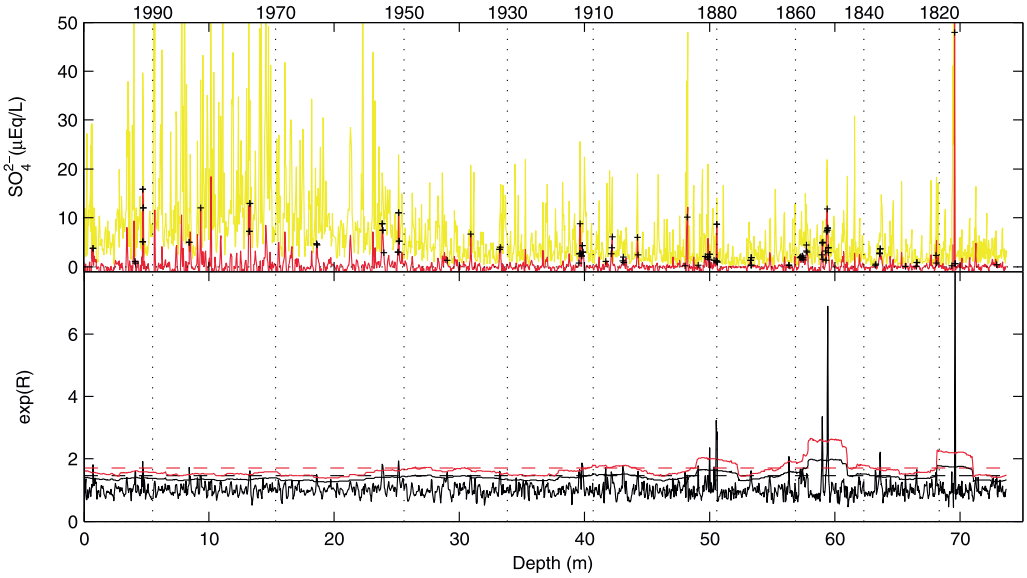

Figure 4. Same as for Figure 3 but for Belukha 2001 core sulfate from 1800 to 2001. Dates are from *Eichler et al.* [2009a, 2009b, 2011].

hidden. Therefore we can both test our data on a well dated and simple part of the ice core, such as that between 1800 and 1940, and examine how good the method is at extracting information when anthropogenic sulfate becomes increasingly important over the 20th century.

[13] Figure 4 shows the results of extracting volcanic sulfate spikes in the Belukha core from 1800 to 2001. *Eichler et al.* [2009a] identify volcanic signals from Tambora (1815), Shiveluch (1854), Novarupta (1912) and Kharimkotan (1932) between 1800 and 1940. All those peaks are clearly shown in Figure 4. In addition the third largest residual and significant e^R peak is at 50.5 m dated at 1880. This peak is assigned to Krakatau. It is noticeable that there is a larger peak in sulfate at 48.3 m depth, 1887 that may be misinterpreted as Krakatau (and may be Tarawera 1886), but there is only a single data point significant at the 95% level in e^R whereas we observe 4 data points above 99% significance level for the 1880 peak.

[14] In Figure 5 we compare the magnitude of $V[SO_4^{2-}]$ from equation (2) with $X[SO_4^{2-}]$ from *Eichler et al.* [2009a] for the period before significant anthropogenic sulfate deposition. The simple correlation coefficient is 0.91 between the 2 estimates of volcanic sulfate. Naturally the data should be regressed on a log plot so that the large magnitude and large uncertainty points from Tambora do not unduly affect the regression, but we want to show how the method compares in a simple way with an excess sulfate method. The result is essentially identical if those points are removed or a log plot is made. However, the slope of the linear regression line is only 0.42 implying that the $X[SO_4^{2-}]$ estimate based only on Ca^{2+} concentrations is twice the estimate from equation (2) found using all ion relationships to nonvolcanic sulfate sources. The contribution of other sulfate sources is also reflected in the higher correlation coefficient between $[SO_4^{2-}]$ and $X[SO_4^{2-}]$ of 0.95 compared with 0.87 between $[SO_4^{2-}]$ and $V[SO_4^{2-}]$.

[15] Since we find good correlation between our new method of extracting volcanic sulfate and the simpler method used by *Eichler et al.* [2009a], for the 1800–1940 period, we examine the peaks detected in the anthropogenic period post-1940 that *Eichler et al.* [2009a] could not find based simply on using Ca^{2+} as a SO_4^{2-} dust source proxy.

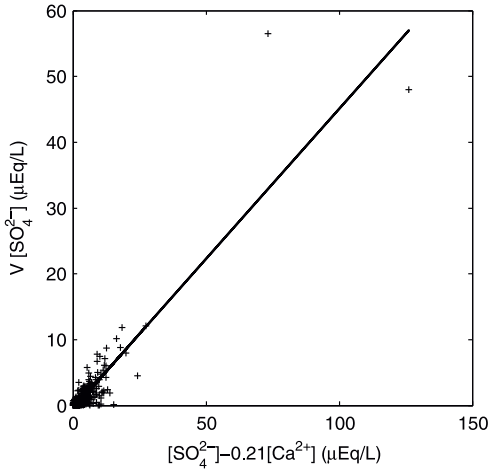

Figure 5. Relationship in Belukha ice core between volcanic sulfate estimated from equation (2) and that estimated by removing terrestrial sulfate from total sulfate. The regression line is $V[SO_4^{2-}] = 0.42\ X[SO_4^{2-}] - 0.46$. All data points where $V[SO_4^{2-}]$ and $X\ [SO_4^{2-}] > 0$ between 1800 and 1940, n = 561.

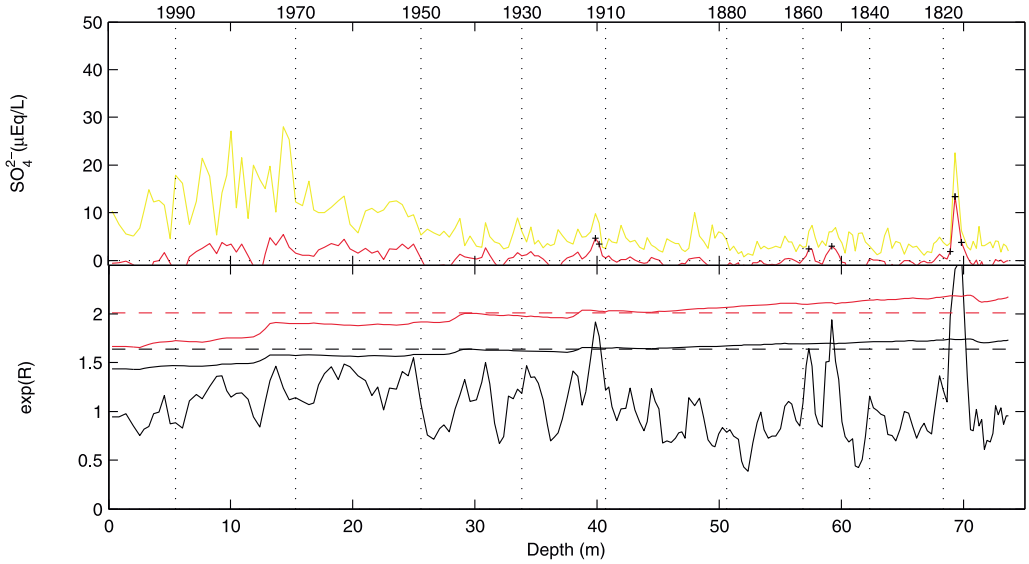

Figure 6. Same as Figure 4 but with a window length of 200 points, and with the original data down sampled to annual resolution.

There are 2 significant peaks at 23.7 and 25.1 m (1953 and 1951), and another at 18.5 m (1963). The 1963 horizon was confirmed with ^{3}H measurements indicating atmospheric nuclear fallout. Other peaks significant at the 95% level are at 13.3 m (1973), 9.4 and 8.4 m (1983.5 and 1984.5), and finally 4.6 m (1992). It is very tempting to assign three of these peaks to large well-known eruptions: Pinatubo (1991), El Chichón (1982) with fallout in 1983, and a second year of fallout in 1984, and Agung (1963). The Agung plume stayed almost exclusively in the Southern Hemisphere [*Robock*, 2000] and yet seems present and well dated. All these volcanic peaks appear within 3 years of the dates from *Eichler et al.* [2009a]. The peaks at 1951, 1953 and 1973 do not correspond to well known large eruptions, though several smaller candidates appear in the Global Volcanism Program (http://www.volcano.si.edu/world/largeeruptions.cfm).

[16] Finally we can illustrate the impact of low-resolution measurements, and changing the window width of the method by using the same post-1800 section of Belukha core but resampled to annual averages (Figure 6). The 200 point window in a sample size of only 202 points produces a very stiff response, which is essentially a linear significance level tilted by the Tambora high-magnitude points. There are far fewer significant eruptions, not due to the long window (a shorter window would produce even fewer significant points), but because the smoothing of the original sub-seasonal data to annual averages. This not only reduces the magnitude of volcanic peaks above background, but also modifies the correlation structure between SO_4^{2-} and all other ions. We return to this in section 5.

4.2. Volcanic Records From Nonpolar Cores

[17] The largest events recorded in ice cores from Antarctica and Greenland over the last millennium are the unknown eruption of 1259, Kuwae in 1453 and the 1815 Tambora eruption, and the event of unknown origin in 1809 [e.g., *Gao et al.*, 2008; *Gao et al.*, 2006]. It must however be emphasized that even in the dry snow regions far from large other sources of SO_4^{2-}, most ice cores typically lack 30% of volcanic signals that may be expected simply because of the stochastic nature of snow deposition and redistribution [*Legrand and Mayewski*, 1997; *Gao et al.*, 2008; *Moore et al.*, 2006, *Pälli et al.*, 2003; *Karlöf et al.*, 2005] this may also be seen in Figure 4 where the 1809 event is undetected both by *Eichler et al.* [2009a] and from the volcanic peak extraction method used here. Indeed *Robock* [2000] notes that for the northern hemisphere "the individual ice core records are, in general, not well correlated with each other or with any of the [volcanic] indices." Hence both the appearance of the volcanic spike and its relative magnitude may vary between ice cores. Since ice cores containing easily interpretable sulfate records have generally been confined to small geographical regions such as central Antarctica and Greenland ice sheets, estimates of fallout from ice cores in other regions may be valuable for atmospheric research.

[18] Preliminary timescales for all cores discussed below were made using the 1963 radioactive horizon (Table 1), and usually some seasonal layer counting based on variations in ions or stable isotopes of water. Inferred accumulation rates can be found using the simplest layer thinning model [*Nye*, 1963] based only on the core density profile, depth of the 1963 horizon at time of drilling, and estimates of total ice thickness (Table 1). We may expect variations in accumulation rates on decadal and century scales of 30% [e.g., *Pohjola et al.*, 2002b; *Kaspari et al.*, 2008].

4.3. Lomonosovfonna

[19] The 1997 Lomonosovfonna core is the best dated of the Svalbard cores [*Divine et al.*, 2011]. Ion chemical

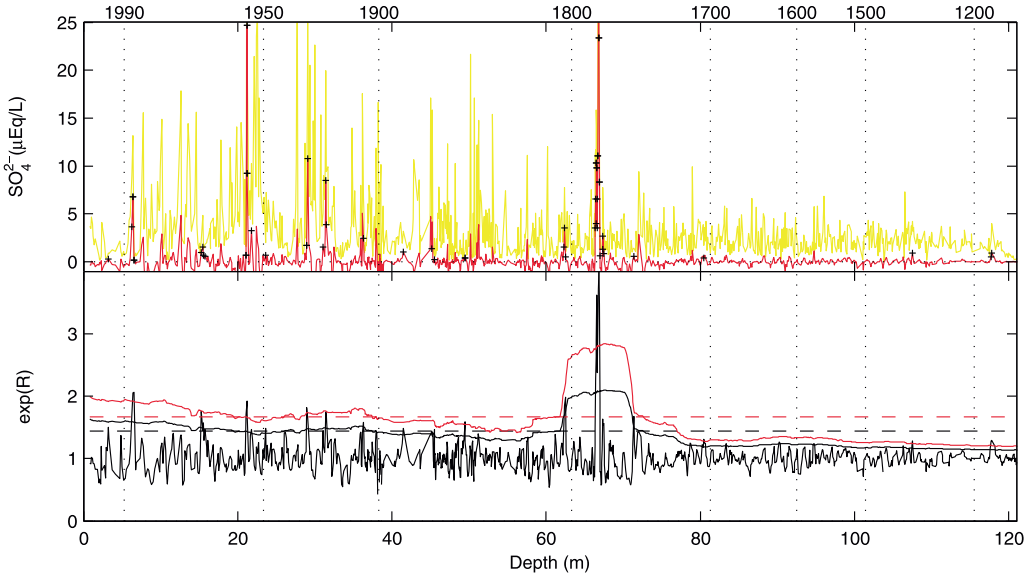

Figure 7. As for Figure 3 but for Lomonosovfonna 1997 core sulfate. Dates are from *Divine et al.* [2011] constrained by 1963 and 1783 horizons. Assignment to eruptions is discussed in the text.

analysis was done at 5–10 cm resolution along the core [*Kekonen et al.*, 2005a], corresponding to subseasonal resolution in the upper core, to approximately annual at 100 m depth. Below that depth some isolated core sections were not measured for chemistry due to bad core quality, [*Divine et al.*, 2011]. The ions measured were Na^+, Cl^- SO_4^{2-} MSA, Mg^{2+} Ca^{2+}, K^+, NO_3^-, and NH_4^+, and all were used in the MLR analysis. *Virkkunen et al.* [2007] show that 21st century summers are warmer than any in the ice core record since the 13th century. However, despite melt rates of 30–50%, isotopic variations [*Pohjola et al.*, 2002a] and chemical records [*Moore et al.*, 2005] of climate are well preserved on annual or multiyear scales. *Moore et al.* [2006] used a simplified version of the present scheme to find volcanic eruptions in the 1997 Lomonosovfonna core. Recently the timescale has been revised as updated ice thickness measurements and extended layer counting to 1613 [*Divine et al.*, 2011] became available. Unfortunately, the change in timescale leads to us to the conclusion that the 1259 eruption signal around 118 m depth may have been misidentified in the work of *Moore et al.* [2006], as it is quite likely the horizon was located in a badly damaged core section and was not found in the chemical analysis, instead this peak was suggested to be Hekla- 1104 or 1158. It is this revised timescale we use here. The 1783 Laki peak at 66.8 m is by far the largest in the core (Figure 7). Other signals clearly significant were discussed by *Moore et al.* [2006], however some small differences are noticeable in the new method of calculating the residual, with significant peaks deeper than Laki at 80.5 m (1705), which we have assigned previously to Fuji 1707. A peak at 107.5 m was assigned to Badarbunga 1477 in Iceland by *Moore et al.* [2006], however with the dating used here we feel it is more likely the 1453 eruption of Kuwae that is seen in many polar ice cores [*Gao et al.*, 2006]. The 117.7 m, peak dated at AD1100 in the *Divine et al.* [2011] dating was already discussed. A good candidate for Krakatau is at 45.5 m (Figure 7). Tambora, on the *Divine et al.* [2011] timescale at 1805, is a highly significant peak at 62.3 m.

[20] Figure 3 shows the period spanning the large Bezymianny 1956 signal at 21.1 m; and two significant peaks in 1934 and about 6 years previously that we consider to be the Kuril island eruption of Kharimokotan and one of several candidates in Japan and the Kuril islands that occurred between 1924 and 1929. The 1912 signature of Novarupta appears at 36.2 m (1909 on the *Divine et al.* [2011] timescale). It is worthwhile noting that tephra from the small Grimsvötn eruption of 1903 was found in the core at 37.3 m depth [*Wastegård and Davies*, 2009] but this corresponds with no significant sulfate residual and only a broad and modest sulfate concentration rise (Figure 3).

4.4. Mount Everest

[21] Mount Everest is a much different ice core location than Svalbard (Figure 1 and Table 1), and is another good test of our methodology since the ice has been subject to some independent dating and volcanic signal extraction. In addition the core presents some difficulties in volcanic sulfate extraction because of the domination of terrestrial sources in the sulfate budget (Table 1). Ion chemical analysis was done at 3–4 cm resolution along the core, corresponding to subseasonal resolution in the upper core, to approximately semiannual at 100 m depth. The ions measured [*Kaspari et al.*, 2007] were Na^+, Cl^-, SO_4^{2-}, Mg^{2+}, Ca^{2+}, K^+, and NO_3^- so no species traditionally representative of biogenic SO_4^{2-} (Table 1) was analyzed, but all available ions were used in the MLR analysis. Owing to the relatively high-accumulation rate (0.52 m w.e a^{-1}), seasonal variations in

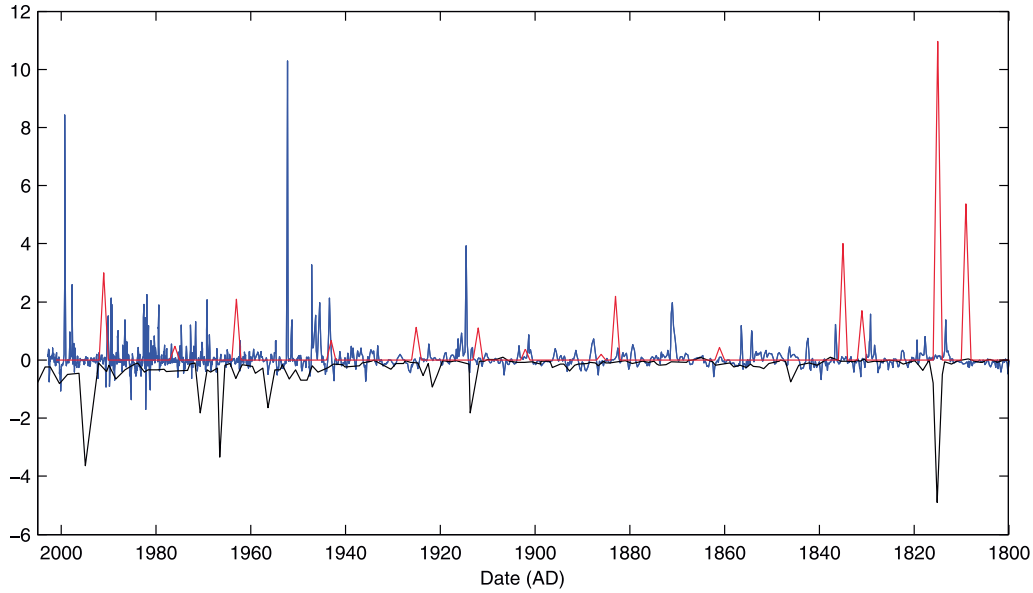

Figure 8. Comparison of the global ice core volcanic index [*Gao et al.*, 2008], red curve, $V[SO_4^{2-}]$ from the Mount Everest core (blue) and inverted Bi concentrations [*Xu et al.*, 2009], black curve. Data are arbitrarily scaled for clarity, time scale is from *Kaspari et al.* [2008].

water isotopes, soluble ions and trace elements are well preserved in the core, and were used to date ice in the core by counting annual layers [*Kaspari et al.*, 2008] to a depth of 86 m. The timescale was verified using high-resolution measurements of bismuth (Bi) to identify major volcanic horizons, including Pinatubo, Agung and Tambora [*Kaspari et al.*, 2007]. Other eruptions may be more tentatively assigned [*Xu et al.*, 2009], however Krakatau, 1883 is not present in the Bi profile. Dating uncertainties are estimated to be about 5 years at 1534, at 86.8 m depth. The method presented here based on ion concentrations has advantages because those data cover the whole length of the core, which was until now dated by cycle counting since 1534 and flow modeling with no fixed horizons beyond Tambora 1815 [*Kaspari et al.*, 2008].

[22] Figure 8 shows a comparison between the Bi profile [*Xu et al.*, 2009] and sulfate residual found from equation (2), and the averaged volcanic signature from polar ice cores [*Gao et al.*, 2008]. When comparing the ice core data with the volcanic index we use the published *Kaspari et al.*

Table 2. Volcanic Signatures Identified in Four Cores by Volcanic Sulfate Residual

			Lomonosovfonna			Everest			Holtedahlfonna			Vestfonna		
Eruption	Figure 1 Name	Year	Depth (m)	Model Date	Diff[a] (year)	Depth (m)	Model Date	Diff[a] (year)	Depth (m)	Model Date	Diff[a] (year)	Depth (m)	Model Date	Diff[a] (year)
Pinatubo	Pi	1991	6.5	1987.9	3.1	10	1990.1	0.9						
El Chichón	ElC	1982				13	1986.7	−4.7						
Agung	Ag	1963							28	1963.9	−0.9			
Bezymianny	Be	1956	21.1	1955.7	0.3	37.8	1952	4				18	1958.2	−2.2
Kharimkotan	Kh	1934	29	1935.4	−1.4									
Kuril	Ku	1928	31.5	1926.9	1.1									
Novarupta	No	1912	36.2	1907.4	4.6				55.5	1910.7	1.3	41.2	1907.7	4.3
Krakatau	Kr	1883	45.5	1871.3	11.7	56.2	1870.7	12.3	68.5	1873.4	9.6	55.5	1872.1	10.9
Coseguina	Co	1835				62.5	1836.2	−1.2						
Tambora	Ta	1815	62.3	1803.9	11.1				95.5	1805.8	9.2			
Laki	La	1783	67	1781.3	1.7				103.6	1781.9	1.1	86.8	1780.6	2.4
Fuji	Fu	1707	80.5	1706.8	0.2									
Parker	Pa	1641				90.8	1621.7	19.3						
Huaynaputina	Hu	1600										136.5	1617	−17
Kuwae	Kw	1453	107.5	1403.8	49.2	101.2	1490.9	−37.9						
Unknown	-	1259				105.1	1317.1	−58.1						
Hekla	He	1105?	117.7	1095.5	9.5									
Dakataua?	Da	738				107.8	861.3	−123.3						

[a]Diff is eruption date minus model dating.

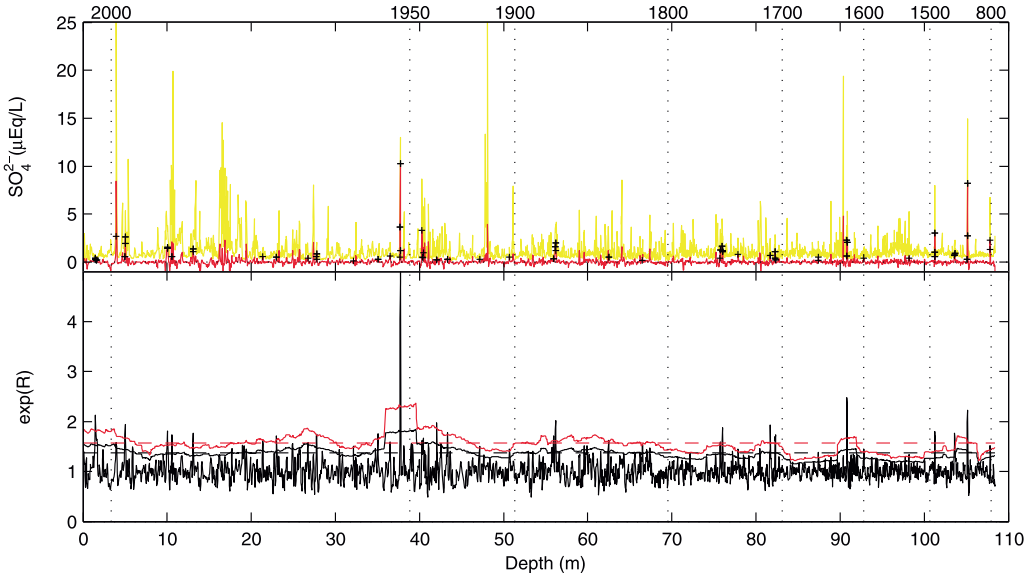

Figure 9. As for Figure 3 but for Everest 2002 core sulfate. Dates are from the *Kaspari et al.* [2008] model.

[2007] timescale, which was tied to the 1815 Tambora signal. For example it is tempting to align the peak dated at 1873 in the Everest core with the Krakatau eruption of 1883. Similarly peaks sulfate residual in the 1830 s may be linked to large eruptions recorded in polar ice cores (Table 2). It is clear that there are significant differences between the Bi and sulfate peaks, with only a few common signals, and in those cases the exact timing of the peak may differ by a year or two. This may be explained by different transport paths for Bi particles and aerosols. In several cases peaks in one method are completely absent or much smaller in the other.

[23] The whole record of volcanic sulfate is plotted in Figure 9. The recent large eruption of Pinatubo 1991 may be the signal at 10 m (1990), and El Chichón 1982 could be detected at 13 m (1986). Agung is not clearly seen in sulfate, though a peak at 1966 in Bi is associated with it by *Xu et al.* [2009]. A sulfate anomaly on the Kaspari *et al.* time scale at 1953 is dominant at 37.8 m and may be associated with a Bi peak at 1956 that *Xu et al.* [2009] assign to Kelut 1951 (Figure 8). We may tentatively reassign this peak to the Bezymianny (1956) eruption which as a high latitude, but very large eruption, and well recorded in several Arctic ice cores (e.g., Lomonosovfonna shown in Figure 3 [*Fritzsche et al.*, 2005]). This assignment of the peak to a large Kamchatka eruption is also consistent with the 1912 peak seen in SO_4^{2-} residual and Bi that *Xu et al.* [2009] assigns to Novarupta, Alaska 1912, a similarly large eruption from a similar location. However, the peaks at 1953 and 1951 in the well dated Belukha core (Figure 4) may have the same origin as those here, which tends to argue against the cause being Bezymianny (1956). The Krakatau eruption in 1883 is presumably the large residual peak at 56.2 m, 1872 in the Kaspari timescale, which was absent from the Bi analysis. The Tambora 1815 peak is significant at 99% level in e^R, at 66.5 m but has only a fairly modest residual of about 2 μEq/L. A clearer residual peak at 62.5 m (1836), is presumably the 1835 eruption of Coseguina. There are significant 18th century peaks at both 76 m (1758) and 82 m (1710), however the polar ice core volcanic records discussed by *Gao et al.* [2008] exhibit no large eruptions between Laki (1783) and Parker (1641), so assigning them to a specific volcano is problematic. Another large anomaly is seen around at 90.8 m (AD1620). This may be attributed to Huaynaputina (1600), however, possible a better candidate here is Parker (1641) in The Philippines which is much closer to Everest.

[24] One of the most obvious signals, even from the raw SO_4^{2-} profile is seen at 105.1 m, corresponding to about AD1310 in the Kaspari time scale. However, that is almost certainly the largest eruption signal of the last millennium: the unknown eruption seen in polar ice cores around 1259 [*Gao et al.*, 2008]. This signal must be from the tropics as it is seen in both polar ice sheets, hence it is also likely visible in Tibet. The 1453 eruption of Kuwae, again a very significant event globally [*Gao et al.*, 2006; *Gao et al.*, 2008], is likely the residual spike at 101.2 m dated just before 1500 on the Kaspari scale with a residual of 3 μEq/L, the dating difference is consistent with the offset for the large 1259 peak. There is one final signal at 107.8 m (0.6 m from the bottom of the core) that is highly significant around 450 years earlier than the 1259 peak, or about AD800. This may be the large eruption Dakataua in New Britain dated at 800 + −50 radiocarbon years, or 720 ± 80 calendar years. The largest signal in the polar ice cores between 540 and 1170 [*Gao et al.*, 2008] is dominant in Antarctic records at about AD738, and so consistent with the Dakataua eruption in an Everest core.

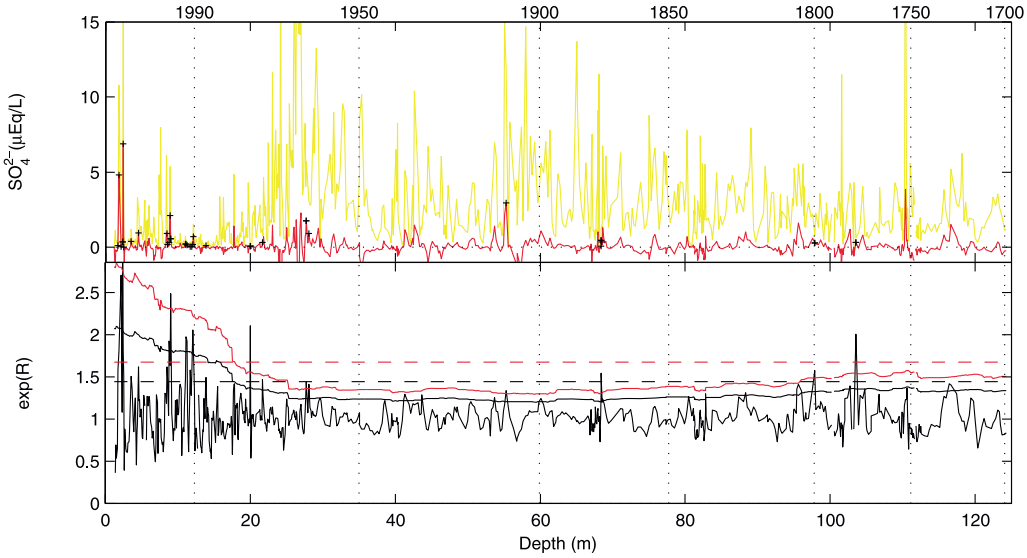

Figure 10. As for Figure 3 but for Holtedahlfonna 2005 core sulfate. Dates are from annual layer counting *Divine et al.* [2011] constrained by 1963 horizon.

4.5. Holtedahlfonna

[25] Having shown that the method appears to detect volcanic signals in settings as different as Altai, Everest and Svalbard, we now apply it to ice cores that have not been extensively studied to date, and which pose similar problems in dating as those found for Everest and Lomonosovfonna.

[26] In April 2005 an ice core was drilled at Holtedahlfonna on the west coast of Spitsbergen (Table 1). Ion chemical analysis was done at typically 10–25 cm resolution along the core, corresponding to seasonal resolution in the upper core, to approximately semiannual at 100 m depth. As with Lomonosovfonna, seasonal melt and percolation will act to reduce the useable resolution. The ions measured were Na^+, Cl^-, SO_4^{2-} MSA, Mg^{2+}, Ca^{2+}, K^+, NO_3^-, and NH_4^+, and all were used in the MLR analysis. Radar measurements showed that the ice depth in the area is highly variable and that it is approximately 150–250 m at the drill site. However, due to water-saturated ice layers and steep topography in the area, the exact depth from radar surveys is uncertain. Preliminary dating of the core can be based on a combination of counting summer peaks in the oxygen isotope stratigraphy [*Pohjola et al.*, 2002b], the tritium date at 1963, and a Nye model with the prescribed ice depth at the core site. Comparing layer counting with the Nye thinning model using 300 m bed depth gives ages of 1699 and 1740 at the core bottom, whereas a depth of 200 m gives model dates about 8 years different from counting dates. Although the 200 m depth model gives a closer match with counting dates, we prefer the 300 m depth model since it matches better the observed thinning rates of the annual layers, and gives a better statistical fit between the chemical series of the well dated Lomonosovfonna core and the Holtedahlfonna core. A depth of 300 m is also more consistent with the temperature profile along the borehole. The reason why the counting ages agree better with the 200 m depth model rather than 300 m depth model may be that some annual layers are miscounted. However, the dating issue cannot be resolved with the data and methods we have used, hence there is a need to explore the volcanic sulfate record in more detail.

[27] It is immediately clear from Figure 10 that, in contrast to Lomonosovfonna (Figure 7), there is no large peak which can be assigned to Laki 1783. The peak at 110 m depth (AD1755 in the preliminary dating) is not significant in the log ratio test despite it being the largest residual in the lower part of the core. The ionic chemical signature shows high levels of all species, which is very different from a typical eruption record in ice cores. Searching for a Laki eruption in the SO_4^{2-} residual is problematic, however, there is a large and highly significant peak in e^R with small absolute residuals values at 103.6 m, AD1780 in the tentative dating. There are 2 small peaks in absolute residual that are also significant at 95% on each side of the central highly significant peak in e^R. This feature at 103.6 m is our best candidate for Laki 1783. There is another significant peak at 116.5 m (AD1730), and there is a peak at 28 m close to the measured depth of the radioactive fallout layer in 1963 (Table 1), which is plausibly Agung, 1963. Similarly a peak in residual significant at 99% windowed test is observed at 55.5 m or 1910 that is plausibly Novarupta (1912). Another small peak at 95.5 m is dated at 1805 and is perhaps Tambora, and a similar peak at 68.5 m (1885), possibly Krakatau (1883).

4.6. Vestfonna

[28] Vestfonna is the second largest ice cap on Nordaustlandet, the adjacent Austfonna being the largest one. Vestfonna contains a record of chemistry that despite being altered by melting has provided reliable climatic and environmental information [*Watanabe et al.*, 2001; *Matoba*

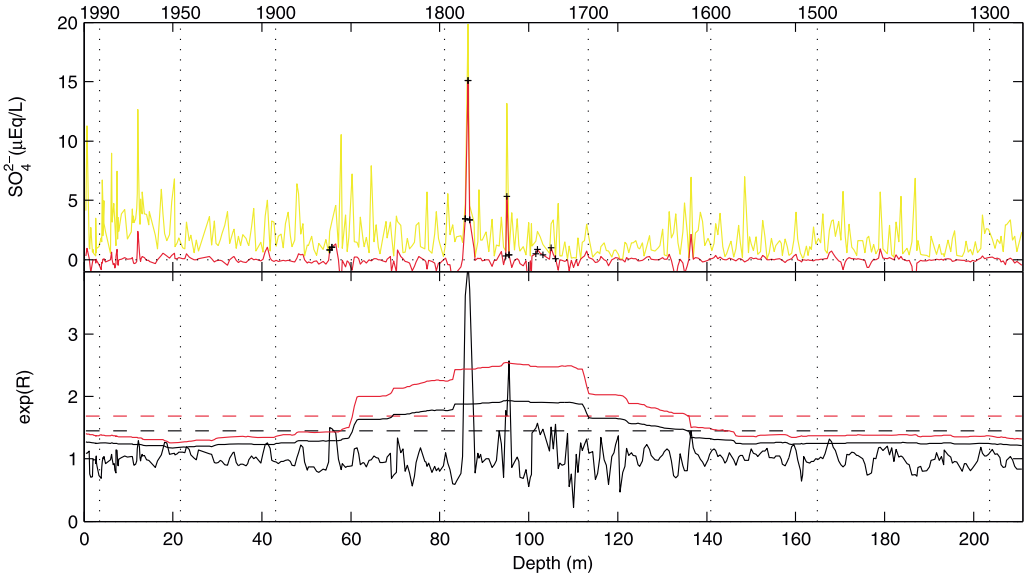

Figure 11. As for Figure 3 but for Vestfonna 1995 core sulfate. Dates are from the 1963 and 1783 horizons and a Nye thinning model with bedrock at 320 m.

et al., 2002]. Ion chemical analysis was done at typically 10–50 cm resolution along the core, corresponding to annual resolution in the upper core, to approximately biannual at 100 m depth. The ions measured were Na^+, Cl^-, SO_4^{2-}, Mg^{2+}, Ca^{2+}, K^+, and NO_3^- so no species traditionally representative of biogenic SO_4^{2-} (Table 1) was analyzed, but all available ions were used in the MLR analysis. The ice core was dated by *Matoba et al.* using the 1963 horizon, a prominent peak in SO_4^{2-} identified as 1783 Laki at 86.8 m (Figure 11) with interpolation between the dates and extrapolation to the bottom of the core. No flow model was made hence the dating was rather uncertain since the bedrock depth was not known in 2002 [*Watanabe et al.*, 2001]. In fact the depth at the drill site is about 320 m (Table 1) according to recent radar surveys [*Pettersson et al.*, 2011]. Using this bedrock depth, and the depths of the 1963 and obvious Laki peak we made a preliminary dating scale.

[29] Other significant peaks include one dated at 1873, presumably Krakatau 1883 at 55.5 m depth. Several peaks in the mid 18th century date around 1758 with smaller residuals in the 1720 s and 1730 s (insignificant in the windowed significance tests). It is possible that one of these may be the same 1730 peak seen in the Holtedahlfonna core. There is another peak significant at the 95% level dated at 1617 (136.5 m depth), which is plausibly the 1600 Huaynaputina signal seen in polar ice cores [*Gao et al.*, 2008]. The deepest signal of any note is at 167.5 m (AD1488), which we may tentatively suggest is Kuwae 1453 since below that depth very little is significant even in the windowed tests. The lack of peaks may be due to the low-resolution chemistry sampling available. Several residual peaks in the 20th century are significant in the windowed test: one dated at 1908 at 41.2 m depth, which may be Novarupta, 1912, and a very small residual at 1958 (18 m) that may be Bezymianny (1956), a very large signal at 1957 in the Lomonosovfonna core, and finally a peak in 1972, that we do not assign to any eruption.

5. Discussion and Conclusions

5.1. Dating Complex Ice Cores

[30] Many of the volcanic composite indicators [e.g., *Gao et al.*, 2008; *Robock*, 2000] dating to before 1880 are based on ice core records from the polar ice sheets. This is a relatively small region, 10%, of the Earth's surface. Here, we present some of the first time series of volcanic signatures in ice cores from outside the large ice sheets. The method, in common with all others, is however only useful used in combination with extra information such as annual layer counting since age—depth relations for ice cores can vary enormously between high accumulation rate and thin coastal glaciers, to thick dry interiors of ice sheets. Hence identification of a particular volcano is ambiguous. A comparison of the dating found from the 4 "complex" cores from the volcanic signals identified with the model dates extracted from earlier results or layer counting is shown in Figure 12. It is notable that despite the differences in the ice cores several eruptions signals are common to all the Svalbard cores: Krakatau, Tambora, Novarupta (Table 2 and Figure 1), despite the very low-level residuals in SO_4^{2-}. The 1956 Bezymianny eruption, which is seen as a small signal in Greenland ice cores [*Gao et al.*, 2008] is rather prominent in the Svalbard cores; in Lomonosovfonna it appears as the second largest signal. Atmospheric transport patterns will lead to quite different deposits from Icelandic eruptions in Greenland and Svalbard and the same appears true for a Kamchatka eruption since the 1956 signal is the largest in the Franz Josef Land Akadamii Nauk ice core [*Fritzsche*

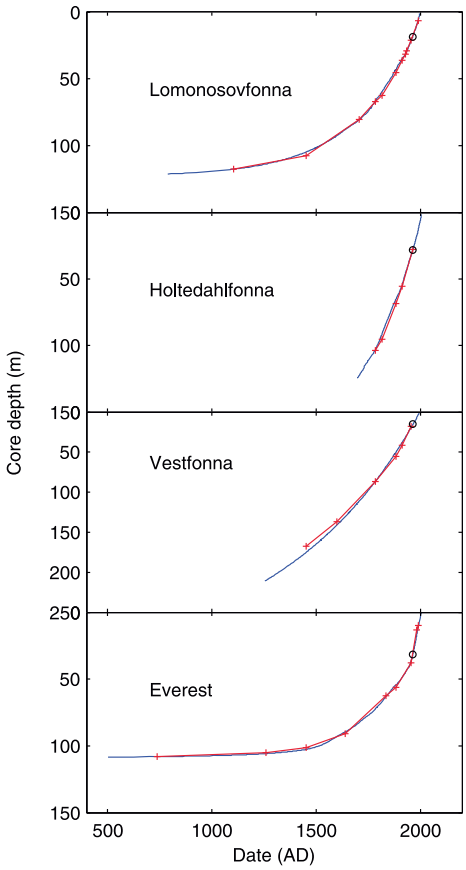

Figure 12. Dating models for the 4 ice cores studied here. Dating based on flow models constrained by layer counting and reference horizons are blue curves. The 1963 radioactivity layer depth is shown as a circle. "Plus" symbols are volcanic eruptions identified as significant in Figures 7, 9, 10, 11 and matched to plausible dated eruptions as discussed in the text; the eruptions are simply joined by red lines.

et al., 2005]. It is also common that cores contain a signal around 1730 that may be the 1732 Jan Mayen eruption. Both the Krakatau and the Tambora signals appear about 10 years prior to the dating model estimates while Laki is at its fixed date, which suggests that there may have been a period of relatively lower accumulation rates in 1783–1815 than the simple flow models use [*Pohjola et al.*, 2002b], and which may have been low enough to cause errors in layer counting. This would be consistent with extended disruption of North Atlantic oceanic circulation as noted by *Bjerknes* [1964] from British Admiralty data that northerly parts of the ocean were 2–3°C cooler and southerly parts 3°C warmer than normal from 1780 to 1820.

[31] The total fraction of the SO_4^{2-} extracted as residual from the MLR and defined to be volcanic is 4.5%, 1.4%, 1.7%, and 3.6% for Lomonosovfonna, Holtedahlfonna, Vestfonna, and Mount Everest, respectively. Comparing Figures 7, 10, and 11 and Table 2 it is very clear that the signals deposited in the cores are quite different. We may expect considerable variation, as has been noted previously; typically 30% of eruption signals may be missing from cores due to differences in local precipitation and postdepositional effects. However, the degree of dissimilarity (Table 2) is rather larger than that, especially between Lomonosovfonna and Holtedahlfonna, which are most similar in environment (Table 1 and Figure 1). This may be because of the vagaries of the local deposition regime in the two ice core locales: Lomonosovfonna is an ice cap frozen to bed with fairly gentle slopes at higher elevation than the local nunatak dust sources. The accumulation gradients in the region show a rising trend with elevation between 1000 and 1200 m, but then decreasing to lower accumulation above about 1200 m [*Pälli et al.*, 2003], which may suggest that wind scouring occurred at the drill site. However, *van der Wel et al.* [2011] show that the 1963 tritium peak from Holtedahlfonna and Lomonosovfonna has the same amplitude in both ice cores and is consistent with other radioactive measurements from Svalbard ice cores [*Pinglot et al.*, 1999]. Moreover ^{137}Cs on Lomonosovfonna has the same mean value at the summit drill site region and lower on the glacier ruling out significant removal of snow by wind scouring [*Isaksson et al.*, 2001]. On the other hand Holtedahlfonna drill site lies on a saddle and has a temperate rather than frozen bed. Holtedahlfonna is closer to the western fjords and seems to be within the air masses affected by Arctic haze [*Virkkunen et al.*, 2007], while Lomonosovfonna appears to sample more regional environmental signals, with much sulfate coming from Europe [*Moore et al.*, 2006]. Holtedahlfonna has only about 25% as much volcanic SO_4^{2-} as Lomonosovfonna, partly due to its higher sea salt loading, hence its poorer volcanic record.

[32] Vestfonna is significantly lower in elevation than either the other two Svalbard sites, but is well within the Arctic Ocean sphere of influence, hence it seems to suffer relatively little seasonal melt. The ice cap is frozen to the bed at the core site [*Watanabe et al.*, 2001], as is much of the central region of the ice cap [*Pettersson et al.*, 2011], so the site should be less influenced by melt processes and have a simpler flow pattern than the warm based Holtedahlfonna. Vestfonna and Holtedahlfonna are the warmest of the 4 sites studied, hence percolation and postdepositional impacts may be greater and make volcanic sulfate harder to identify. On the other hand the Vestfonna record studied here is relatively low resolution which may explain the low fraction of volcanic SO_4^{2-} since a smoothed volcanic spike will be harder to detect as an anomaly in the MLR. The detection of reasonable numbers of volcanic signals, however argues for a potentially good volcanic record if a higher-resolution record could be recovered.

[33] The Svalbard sites may well have volcanic records less reproducibly preserved than other ice core records with less seasonal melt. However, we also emphasize that even in Greenland, relative volcano magnitudes can vary, or be absent completely from the record due to stochastic processes [e.g., *Friedmann et al.*, 1995]. Of the 4 cores studies here, Everest has the cleanest volcanic record, and in many ways resembles the well preserved and high-altitude Belukha core. This may be because its location samples more of the better known tropical eruptions than the high-

latitude polar regions where historical eruption magnitudes are relatively less well reported than in the populated regions (Figure 1). The record is also high resolution in contrast to Vestfonna, easing the detection of anomalies in MLR. The site is much less dusty than central Tibet ice cores, but even there the volcanic SO_4^{2-} fraction was apparently less than at Lomonosovfonna, though greater than at the other Svalbard cores. It is interesting to note that there are some agreements with the Bi record of volcanism for the core (as far as the record extends), but several large signals are detected by the Bi method (such as Agung, 1963) that are absent in the sulfate analysis. Similarly we detected Krakatau clearly while it is absent in the Bi profile. Hence it is not immediately clear which locations will offer the best records of volcanic deposition since it is a combination of relative sulfate sources, volcanic plume chemistry and postdepositional effects that determine the final ice core record.

5.2. Remarks on the Methodology

[34] A key problem in interpreting sulfate records as a proxy for volcanic peaks in most ice cores is that there is significant deposition of sulfate from other sources: anthropogenic, marine, terrestrial or biogenic. This leads to the need for a more sophisticated approach in determining the origin of sulfate concentration spikes, a difficulty even in remote places as anthropogenic pollution grows, making small and moderate eruption signals hard to detect. This issue has restricted volcanic time series to mainly the central ice sheets, or to high-altitude ice caps. Our analysis of the Belukha ice core shows that the method we describe detects volcanic signatures well where sulfate sources from terrestrial dust have been easily corrected for by a simple regression on calcium. However, that simple method breaks down in the 20th century due to increased anthropogenic sulfate deposition. Our new method continues to function well and extracts the significant eruptions of the recent decades even when the volcanic fallout is much smaller than the background sulfate concentrations. Furthermore, comparison of the excess sulfate calculated by correcting for dust using calcium concentration leads to a high correlation with the $V[SO_4^{2-}]$ concentration from equation (2), but which is more than twice as large. The coefficient changes as a function of MLR variables, the fewer the ions used in the model, the closer the coefficient becomes to the simple $X[SO_4^{2-}]$ model. This is because more of the sulfate will be covarying with some particular ion or other, hence the more ions used the less stochastic sulfate residual will be left assigned to volcanoes.

[35] Limitations of the method are also highlighted in Belukha analysis. Transportation of impurities as well as sources and postdepositional effects change the association between ions. In running our analysis on individual samples we impose a varying sample rate along the core. This preserves as much information as possible, and the impact of lower resolution can be seen by comparing Figures 4 and 6. In particular, common seasonal transport of all the ions is important. In winter pollutants are trapped in a low-altitude boundary layer in the Arctic, but in summer there is much more mixing with the free troposphere. While in Alpine settings during summer stronger vertical transport of pollutants from the boundary layer produces higher concentrations than in the winter season that are more representative of the free troposphere. If measurement resolution is subseasonal near the surface but multiannual deeper then the transport factors become blurred. This can be seen in the correlation coefficient between SO_4^{2-} and $HCOO^-$ of 0.26 in the full resolution Belukha data compared with −0.003 in the annual down-sampled data. Postdepositional effects especially seasonal melt may produce similar smoothing of the original ionic covariation. Down sampling the data to annual or lower resolution would help to remove the effects of changing resolution along a core, however we think that the advantage of being able to use all the data points in the analysis is beneficial. In practice we suggest that the method is used with various input variables, window lengths and down sampling to common resolution to gain confidence in the robustness of peaks and hence volcanic signal identification. The method will also fail if there is an overwhelming dilution of volcanic sulfate, for example if there is simply too much dust so that any volcanic sulfate would be well within the experimental measurement of the sulfate concentration.

[36] In comparing our record of $V[SO_4^{2-}]$ with the volcanic proxy Bi in the Everest core we noticed quite low correlation: some eruption signals are present in $V[SO_4^{2-}]$ and not Bi, and vice versa. Given the success of $V[SO_4^{2-}]$ in matching the Belukha core signals, we argue that it is a good record of volcanic SO_4^{2-}, but it may not be the complete record of volcanic fallout at the core site. Bi is transported in the solid phase on dust particles, these may be rather heterogeneously dispersed following an eruption. Sulfate in contrast comes from gaseous aerosol precursors which would tend to be much better mixed. However, even these do depend on the initial plume trajectory in the first days of the eruption [*Robock*, 2000], and in the transfer of the sulfate from the stratosphere to troposphere which maybe by removal via steady sedimentation or by capture of material by "tropospheric folds" [*Sassen et al.*, 1995]. A further illustration of the differences between the dust and sulfate records can be seen in the Laki fallout at Lomonosovfonna [*Kekonen et al.*, 2005b] where the microparticle rich layer is separated from the sulfate deposit by 20 cm. Another example is the absence of any sulfate from the Grimsvötn eruption of 1903 despite tephra being found [*Wastegård and Davies*, 2009]. We should again note that individual ice core records—and it seems even volcanic proxies within the same ice core—are, in general, not well correlated with each other or with any of the composite volcanic indices. This is the result of stochastic variability associated with the transport and preservation of volcanic fallout to an ice core.

[37] Finally we point out that the method does not rely on measurement technique, so an ionic record from a continuous flow measurement system would be processed in exactly the same way as an ion chromatograph record since the errors are also proportional to magnitude. If errors differ between species then the species should be weighted accordingly in the MLR. Ice cores from regions such as Iceland where melting is severe may be problematic since the method relies on the correlation between ions being maintained to some degree. The method would fail if postdepositional processes move all ions to the same sample. However, where relationships between ions are not well understood the method can produce useful results since it requires no prespecified relations between ions, nor attempts

to find volcanic sulfate directly, rather the method simply tries to find the best explanation for sulfate in terms of other ions, and whatever is left is quite likely to be volcanic sulfate. Our method is reproducible and consistently applied, does not rely on dubious statistics, and does not arbitrarily correct only for, e.g., calcium ions. If it was applied to many cores it may give an indication of volcanic sulfate fallout which would in turn provide data for radiative forcing calculations which is a key element in climate change attribution studies [*Jansen et al.*, 2007; *Jevrejeva et al.*, 2009], and also give more geographic control for atmospheric transport models [e.g., *Gao et al.*, 2008].

[38] **Acknowledgments.** We thank three anonymous referees and Anja Eichler for constructive comments on the manuscript. This research is partially supported by China's National Key Science Program for Global Change Research (2010CB950504 and 2010CB951401) and NSFC 41076125.

References

Aizen, V. B., E. M. Aizen, D. R. Joswiak, K. Fujita, N. Takeuchi, and S. A. Nikitin (2006), Climatic and atmospheric circulation pattern variability from ice-core isotope geochemistry records (Altai, Tien Shan and Tibet), *Ann. Glaciol.*, *43*, 49–60, doi:10.3189/172756406781812078.

Beaudon, E., and J. C. Moore (2009), Frost flower chemical signature in winter snow on Vestfonna ice cap, Nordaustlandet, Svalbard, *Cryosphere*, *3*, 147–154, doi:10.5194/tc-3-147-2009.

Bjerknes, J. (1964), Atlantic air-sea interaction, *Adv. Geophys.*, *10*, 1–82, doi:10.1016/S0065-2687(08)60005-9.

Cong, Z., S. Kang, S. Dong, and D. Qin (2009), Seasonal features of aerosol particles recorded in central Himalayan snow and its environmental implications, *J. Environ. Sci.*, *21*, 914–919, doi:10.1016/S1001-0742(08)62361-X.

Divine, D., E. Isaksson, F. Godtliebsen, T. Martma, H. Meijer, J. C. Moore, V. Pohjola, and R. S. W. van de Wal (2011), A thousand years of winter surface air temperature variations in Svalbard and northern Norway reconstructed from ice core data, *Polar Res.*, *30*, 7379–7390, doi:10.3402/polar.v30i0.7379.

Eichler, A., S. Oliver, K. Henderson, A. Laube, J. Beer, T. Papina, H. W. Gäggeler, and M. Schwikowski (2009a), Temperature response in the Altai region lags solar forcing, *Geophys. Res. Lett.*, *36*, L01808, doi:10.1029/2008GL035930.

Eichler, A., S. Brütsch, S. Olivier, T. Papina, and M. Schwikowski (2009b), A 750 year ice core record of past biogenic emissions from Siberian boreal forests, *Geophys. Res. Lett.*, *36*, L18813, doi:10.1029/2009GL038807.

Eichler, A., W. Tinner, S. Brütsch, S. Olivier, T. Papina, and M. Schwikowski (2011), An ice-core based history of Siberian forest fires since AD 1250, *Quat. Sci. Rev.*, *30*, 1027–1034, doi:10.1016/j.quascirev.2011.02.007.

Friedmann, A., J. C. Moore, T. Thorsteinsson, and J. Kipfstuhl (1995), A 1200 year record of accumulation from North Greenland ice cores, *Ann. Glaciol.*, *21*, 19–25.

Fritzsche, D., R. Schütt, H. Meyer, H. Miller, F. Wilhelms, T. Opel, and L. M. Savatyugin (2005), A 275 year ice core record from Akademii Nauk ice cap, Severnaya Zemlya, Russian Arctic, *Ann. Glaciol.*, *42*, 361–366, doi:10.3189/172756405781812862.

Gao, C., A. Robock, S. Self, J. Witter, J. P. Steffenson, H. B. Clausen, M.-L. Siggaard-Andersen, S. Johnsen, P. A. Mayewski, and C. Ammann (2006), The 1452 or 1453 A.D. Kuwae eruption signal derived from multiple ice core records: Greatest volcanic sulfate event of the past 700 years, *J. Geophys. Res.*, *111*, D12107, doi:10.1029/2005JD006710.

Gao, C., A. Robock, and C. Ammann (2008), Volcanic forcing of climate over the past 1500 years: An improved ice core-based index for climate models, *J. Geophys. Res.*, *113*, D23111, doi:10.1029/2008JD010239.

Goto-Azuma, K., R. M. Koerner, and D. A. Fisher (2002), An ice-core record over the last two centuries from Penny Ice Cap, Baffin Island, Canada, *Ann. Glaciol.*, *35*, 29–35, doi:10.3189/172756402781817284.

Isaksson, E., et al. (2001), A new ice core record from Lomonosovfonna, Svalbard: Viewing the data between 1920–1997 in relation to present climate and environmental conditions, *J. Glaciol.*, *47*, 335–345, doi:10.3189/172756501781832313.

Jansen, E., et al. (2007), Palaeoclimate, in *Climate Change 2007: The Physical Science Basis. Contribution of Working Group I to the Fourth Assessment Report of the Intergovernmental Panel on Climate Change*, edited by S. Solomon et al., pp. 434–484, Cambridge Univ. Press, Cambridge, U. K.

Jevrejeva, S., A. Grinsted, and J. C. Moore (2009), Anthropogenic forcing dominates sea level rise since 1850, *Geophys. Res. Lett.*, *36*, L20706, doi:10.1029/2009GL040216.

Kang, S., C. P. Wake, D. Qin, P. A. Mayewski, and T. Yao (2000), Monsoon and dust signals recorded in Dasuopu Glacier, Tibetan Plateau, *J. Glaciol.*, *46*, 222–226, doi:10.3189/172756500781832864.

Kang, S., P. A. Mayewski, D. Qin, Y. Yan, S. Hou, D. Zhang, J. Ren, and K. Kruetz (2002), Glaciochemical records from a Mt. Everest ice core: Relationship to atmospheric circulation over Asia, *Atmos. Environ.*, *36*, 3351–3361, doi:10.1016/S1352-2310(02)00325-4.

Kang, S., Q. Zhang, S. Kaspari, D. Qin, Z. Cong, J. Ren, and P. A. Mayewski (2007), Spatial and seasonal variations of elemental composition in Mt. Everest (Qomolangma) snow/firn, *Atmos. Environ.*, *41*, 7208–7218, doi:10.1016/j.atmosenv.2007.05.024.

Karlöf, L., et al. (2005), Accumulation variability over a small area in east Dronning Maud Land, Antarctica, as determined from shallow firn cores and snow pits: Some implications for ice-core records, *J. Glaciol.*, *51*, 343–352, doi:10.3189/172756505781829232.

Kaspari, S., et al. (2007), Reduction in northward incursions of the South Asian Monsoon since ~1400 AD inferred from a Mt. Everest ice core, *Geophys. Res. Lett.*, *34*, L16701, doi:10.1029/2007GL030440.

Kaspari, S., R. Hooke, P. A. Mayewski, S. Kang, S. Hou, and D. Qin (2008), Snow accumulation rate on Qomolangma (Mount Everest), Himalaya: Synchroneity with sites across the Tibetan Plateau on 50–100 year timescales, *J. Glaciol.*, *54*, 343–352, doi:10.3189/002214308784886126.

Kekonen, T., J. C. Moore, P. Perämäki, R. Mulvaney, E. Isaksson, V. A. Pohjola, and R. S. W. van de Wal (2005a), 800 year long ion record from the Lomonosovfonna (Svalbard) ice core, *J. Geophys. Res.*, *110*, D07304, doi:10.1029/2004JD005223.

Kekonen, T., J. C. Moore, P. Perämäki, and T. Martma (2005b), The Icelandic Laki volcanic tephra layer in the Lomonosovfonna ice core, Svalbard, *Polar Res.*, *24*, 33–40, doi:10.1111/j.1751-8369.2005.tb00138.x.

Koerner, R. M. (1997), Some comments on climatic reconstructions from ice cores drilled in areas of high melt, *J. Glaciol.*, *43*, 90–97.

Legrand, M., and P. Mayewski (1997), Glaciochemistry of polar ice cores: A review, *Rev. Geophys.*, *35*, 219–243, doi:10.1029/96RG03527.

Matoba, S., H. Narita, H. Motoyama, K. Kamiyama, and O. Watanabe (2002), Ice core chemistry of Vestfonna Ice Cap in Svalbard, Norway, *J. Geophys. Res.*, *107*(D23), 4721, doi:10.1029/2002JD002205.

Moore, J. C., A. Grinsted, T. Kekonen, and V. Pohjola (2005), Separation of melting and environmental signals in an ice core with seasonal melt, *Geophys. Res. Lett.*, *32*, L10501, doi:10.1029/2005GL023039.

Moore, J. C., T. Kekonen, A. Grinsted, and E. Isaksson (2006), Sulfate source inventories from a Svalbard ice-core record spanning the Industrial Revolution, *J. Geophys. Res.*, *111*, D15307, doi:10.1029/2005JD006453.

Nye, J. F. (1963), Correction factor for accumulation measured by the thickness of the annual layers in an ice sheet, *J. Glaciol.*, *4*, 785–788.

Palais, J. M., M. S. Germani, and G. A. Zielinski (1992), Inter-hemispheric transport of volcanic ash from the 1259 A.D. volcanic eruption to the Greenland and Antarctic ice sheets, *Geophys. Res. Lett.*, *19*, 801–804, doi:10.1029/92GL00240.

Pälli, A., J. Kohler, E. Isaksson, J. C. Moore, J.-F. Pinglot, V. Pohjola, and H. Samuelsson (2003), Spatial and temporal variability of snow accumulation using ground-penetrating radar and ice cores on a Svalbard glacier, *J. Glaciol. 48*, 417–424.

Pettersson, R., P. Christoffersen, J. A. Dowdeswell, V. Pohjola, A. Hubbard, and T. Strozzi (2011), Ice thickness, thermal structure and basal conditions of the ice cap Vestfonna, eastern Svalbard, inferred from radio-echo sounding, *Geog. Ann.*, *93*, 311–322, doi:10.1111/j.1468-0459.2011.00438.x.

Pinglot, J. F., M. Pourchet, B. Lefauconnier, J. O. Hagen, E. Isaksson, R. Vaikmaë, and K. Kamiyama (1999), Investigations of temporal change of the accumulation in Svalbard glaciers deducted from nuclear tests and Chernobyl reference layers, *Polar Res.*, *18*, 315–321, doi:10.1111/j.1751-8369.1999.tb00309.x.

Pohjola, V. A., J. C. Moore, E. Isaksson, T. Jauhiainen, R. S. W. van de Wal, T. Martma, H. A. J. Meijer, and R. Vaikmäe (2002a), Effect of periodic melting on geochemical and isotopic signals in an ice core from Lomonosovfonna, Svalbard, *J. Geophys. Res.*, *107*(D4), 4036, doi:10.1029/2000JD000149.

Pohjola, V. A., T. Martma, H. A. Meijer, J. C. Moore, E. Isaksson, R. Vaikmäe, and R. S. W. van de Wal (2002b), Reconstruction of 300 years annual accumulation rates based on the record of stable isotopes of water from Lomonosovfonna, Svalbard, *Ann. Glaciol.*, *35*, 57–62, doi:10.3189/172756402781816753.

Robock, A. (2000), Volcanic eruptions and climate, *Rev. Geophys.*, *38*, 191–219, doi:10.1029/1998RG000054.

Ruggirello, R. M., M. H. Hermanson, E. Isaksson, C. Teixeira, S. Forsström, D. C. G. Muir, V. Pohjola, R. van de Wal, and H. A. J. Meijer (2010), Current use and legacy pesticide deposition to ice caps on Svalbard, Norway, *J. Geophys. Res.*, *115*, D18308, doi:10.1029/2010JD014005.

Sassen, K., D. O. Starr, G. Mace, M. R. Poellot, S. H. Melfi, W. L. Eberhard, J. D. Spinhirne, E. W. Eloranta, D. E. Hagen, and J. Hallett (1995), The 5–6 December 1991 FIRE IFO II jet stream cirrus case study: Possible influences of volcanic aerosols, *J. Atmos. Sci.*, *52*, 97–123, doi:10.1175/1520-0469(1995)052<0097:TDFIIJ>2.0.CO;2.

van der Wel, L. G., H. J. Streurman, E. Isaksson, M. M. Helsen, R. S. van de Wal, T. Martma, V. Pohjola, J. C. Moore, and H. A. J. Meijer (2011), Using high resolution tritium profiles to quantify the effects of melt on two Spitsbergen ice cores, *J. Glaciol.*, *57*, 1087–1096.

Virkkunen, K., J. C. Moore, E. Isaksson, V. Pohjola, P. Perämäki, and T. Kekonen (2007), Warm summers and ion concentrations in snow: Present day and Medieval Warm Period comparisons from snow pits and an ice core from Lomonosovfonna, Svalbard, *J. Glaciol.*, *53*, 623–634, doi:10.3189/002214307784409388.

Wastegård, S., and S. M. Davies (2009), An overview of distal tephrochronology in northern Europe during the last 1000 years, *J. Quat. Sci. 24*, 500–512, doi:10.1002/jqs.1269.

Watanabe, O., et al. (2001), Studies on climatic and environmental changes during the last few hundred years using ice-cores from various sites in Nordaustlandet, Svalbard, *Mem. Nat. Inst. Polar Res.*, *54*, 227–242.

Xu, J. Z., et al. (2009), Records of volcanic events since AD 1800 in the East Rongbuk ice core from Mt. Qomolangma, *Chin. Sci. Bull.*, *54*, 1411–1416, doi:10.1007/s11434-009-0020-y.

Zhang, Q., S. Kang, S. Kaspari, C. Li, D. Qin, P. A. Mayewski, and S. Hou (2009), Rare earth elements in an ice core from Mt. Everest: Seasonal variations and potential sources, *Atmos. Res.*, *94*, 300–312, doi:10.1016/j.atmosres.2009.06.005.

E. Beaudon, Arctic Centre, University of Lapland, PO Box 122, FI-96101 Rovaniemi, Finland.

D. Divine, Department of Mathematics and Statistics, University of Tromsø, N-9018 Tromsø, Norway.

E. Isaksson, Norwegian Polar Institute, N-9296 Tromsø, Norway.

S. Kang, Key Laboratory of Tibetan Environmental Changes and Land Surface Processes, Institute of Tibetan Plateau Research, Chinese Academy of Sciences, Beijing 100085, China.

J. C. Moore, College of Global Change and Earth System Science, Beijing Normal University, 19 Xinjiekou Wai St., Beijing 100875, China. (john.moore.bnu@gmail.com)

V. A. Pohjola, Department of Earth Sciences, Uppsala University, Villavägen 16, SE-75236 Uppsala, Sweden.

R. S. W. van de Wal, Institute for Marine and Atmospheric Research, Utrecht University, PO Box 80005, NL-3508 TA Utrecht, Netherlands.

IV

A 300 YEARS ENVIRONMENTAL AND CLIMATE ARCHIVE FOR WESTERN SPITSBERGEN FROM HOLTEDAHLFONNA ICE CORE

Emilie Beaudon[1], John C. Moore[1, 2, 3], Tõnu Martma[4], Veijo A. Pohjola[3], Roderik S.W. van de Wal[5], Jack Kohler[6], Elisabeth Isaksson[6]

[1] Arctic Centre, University of Lapland, P.O. Box 122, 96101 Rovaniemi, Finland.
[2] Colleges of Global Change and Earth System Science, Beijing Normal University, 19 Xinjiekou Wai Street, Beijing 100875, China.
[3] Department of Earth Sciences, Uppsala University, Villavägen 16, S-752 36 Uppsala, Sweden.
[4] Institute of Geology, Tallinn University of Technology, Ehitajate tee 5, 19086 Tallinn, Estonia.
[5] Institute for Marine and Atmospheric research Utrecht, Utrecht University, P.O. Box 80005, 3508 TA Utrecht, The Netherlands.
[6] Norwegian Polar Institute, Polar Environmental Centre, N-9296 Tromsø, Norway.

ABSTRACT

An ice core extracted from Holtedahlfonna ice cap, the most extensive in western Spitsbergen, was analyzed for major ions and spans the period 1700-2005. The leading EOF component is correlated with an indicator of summer melt (log ($[Na^+]/[Mg^{2+}]$)) from 1850 and shows that almost 50% of the variance can be attributed to seasonal melting since the beginning of the industrial revolution. Percolation or diffusion disturbs the annual stratigraphy allowing paleoclimate interpretation of the chemical record only at decadal resolution. The Holtedahlfonna $\delta^{18}O$ value is less negative than that in the more easterly Lomonosovfonna ice core suggesting that moist air masses originate from a closer source most likely the Greenland Sea. During the Little Ice Age lower methansulfonic acid (MSA) concentration and MSA non-sea salt sulfate fraction is consistent with the Greenland Sea as the main source for biogenic ions in the ice core. Ammonium concentrations rise from 1880, which may result from the warming of the Greenland Sea or from zonal differences in atmospheric pollution transport over Svalbard. During winter neutralized aerosols are trapped within the tropospheric inversion layer which is usually weaker over open seas than over sea ice placing Holtedahlfonna within the inversion more frequently than Lomonosovfonna.

Key words: Svalbard, Holtedahlfonna, ice core studies, major ions, melt, inversion layer.

1 INTRODUCTION

Sea ice cover is an important modulator of the decadal scale climate variability in the Arctic. The largest temperature changes associated with the high winter sea ice cover variability are observed in the Greenland-Barents-Kara seas (Bengtsson et al, 2004), which receive warm water driven by the southwestern to western winds between Svalbard and the northernmost Norwegian coast. The location of Svalbard, at the southern edge of the permanent sea ice cover of the Arctic Ocean, and on the pathway of both Arctic and North Atlantic cyclones, contributes to the relatively mild climate compared with most of the Arctic. Sea ice has been one of the main driving forces of the Svalbard climate over at least the last 500 years, (Grinsted et al., 2006; Isaksson et al., 2005), hence Svalbard is an interesting location to conduct climate studies in the European Arctic Ocean sector.

Previous Svalbard ice cores have proven the suitability of these records for paleoclimate investigations despite alteration by post-depositional processes, in particular seasonal melt (Pohjola et al., 2002a; Kekonen et al., 2005, van der Wel et al., 2011). Consequently, a panel of proxies and statistical tools useful in deciphering climatic signals disrupted by melting has been developed for these low altitude ice caps. For instance, Iizuka et al. (2002) and Grinsted et al. (2006) found good summer melting indicators based on ion concentrations of snow and ice from Austfonna (Nordaustlandet) and Lomonosovfonna (eastern Spitsbergen) (Figure 1). Moore et al. (2005) examined the impact of seasonal melt using Principal Component Analysis (PCA) on the complete Lomonosovfonna ion dataset. Environmental signals were separated from melting in Lomonosovfonna (Kekonen et al., 2005), Austfonna (Watanabe et al., 2001) and Vestfonna (Matoba et al., 2002) (Nordaustlandet) ice cores with detection of Medieval Warm Period (Kekonen et al., 2005) and Little Ice Age (LIA) at multi-year or multi-decadal resolution (Watanabe et al., 2001; Matoba et al., 2002).

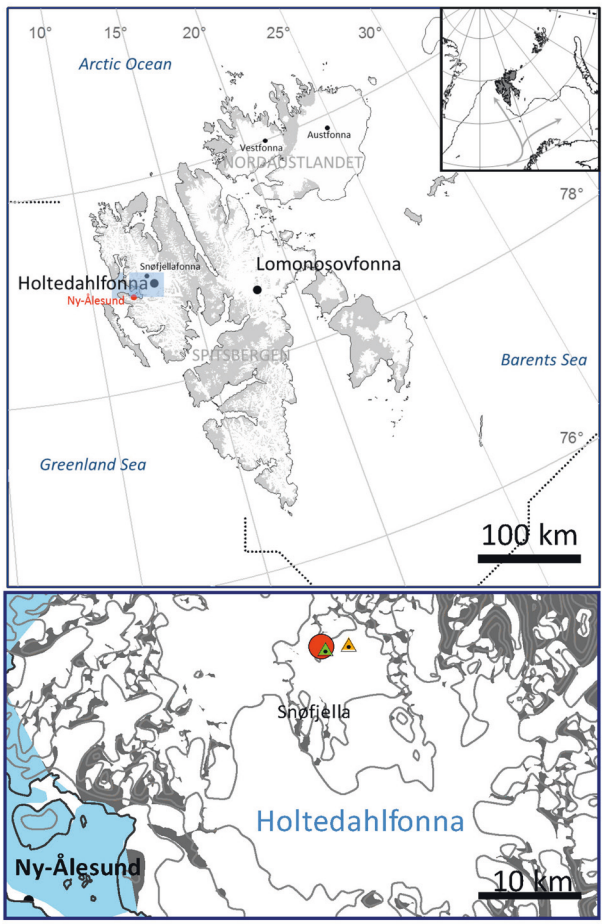

Figure 1.

a) Map of Svalbard showing Holtedahlfonna ice core site and Lomonosovfonna ice cap. The dotted line represents the median spring sea ice extent over the period 1979-2000 (source: http://nsidc.org/data/seaice_index/archives/index.html);

b) Holtedahlfonna with the location of the long 2005 core (red circle), the Snøfjellafonna core (Goto-Azuma et al., 1995) (green triangle) and the firn core 2008 (orange triangle) drilling sites.

The origins of major chemical species were discussed (Kekonen et al., 2002), and a regional scale picture of the anthropogenic pollution history has been composed, the 20th century sulfate sources in particular being inventoried by Moore et al. (2006) for the Lomonosovfonna ice cap.

North-South disparities across Svalbard in the influence of the Arctic front and the impact of the Barents Sea ice extent were identified by comparing the Austfonna ice core (Nordaustlandet) with Lomonosovfonna (Isaksson et al., 2005). However, glaciochemical references for western Spitsbergen are lacking, with the exception of Snøfjellafonna ice core drilled in 1995 with a published record spanning only 70 years (Kameda et al., 1993, Goto-Azuma et al., 1995; Goto-Azuma and Koerner, 2001). The new chemical dataset from a long ice core drilled on Holtedahlfonna presented here aims to fill this gap and provides the first century length paleo-environmental equivalent to the Lomonosovfonna core for western Spitsbergen. In this paper we compare the chemical dataset from these two glaciers throughout their overlapping time period and, by using statistical methods we discuss the differences in their respective ionic budget focusing on biogenic sulfur and ammonium.

2 SITE DESCRIPTION AND DATING

2.1 Glaciological characteristics

Holtedahlfonna ice field is the largest ice field (300 km^2) in northwestern Spitsbergen island (Svalbard, Norway), 40 km from the Ny-Ålesund and Zeppelinfjellet stations and 100 km northwest from Lomonosovfonna ice cap (1255 m a.s.l.) (Figure 1). A 125 m long ice core was drilled using an electromechanical corer in April 2005 on Holtedahlfonna (13°16'20"E and 79°8'15" N, 1150 m a.s.l.) from a saddle point where the horizontal ice flow velocity is expected to be minimal (Lefauconnier et al., 2001; Sjögren et al., 2007). The ice core did not reach bedrock. Ice depths around the core site were obtained by radar sounding using a pulse-radar with a center frequency of 10 MHz. The basal topography at the core site is extremely rugged (Figure 2a), with radar-derived ice depths varying from about 100 m to 250 m for data within 50 m of the core site (Figure 2b). The imprecisely known depth complicates the dating of the ice core (see section 2.3). The bottom temperature in the borehole was -3.3 °C, hence the whole core is cold ice (Figure 3). Ice temperature measured in the borehole features a maximum of -0.4 °C at 15 m depth (Sommer, 2005). Latent heat from refreezing of percolating meltwater is assumed to produce the thermal maximum at 15 m and is expected to impact chemistry as discussed in section 3.2.

2.2 Sampling and analysis

On average 60 cm long ice core pieces were retrieved and packed in clean plastic bags, placed in insulated boxes and transported under frozen conditions to the Norwegian Polar Institute (Tromsø, Norway) where DEP and high resolution density measurements were performed along the entire core (Sjögren et al., 2007) before subsampling for chemical measurements.

In a cold room, parallel-sided sections of the core were cut and split between tritium (van der Wel et al., 2011), oxygen isotopes (Divine et al., 2011), organic contaminants (Ruggirello et al., 2010) and ion measurements (this study) for which rectangular sections were collected from the inner part of the core. At the Finnish Forest Institute (Rovaniemi research station) the core pieces as well as blanks made from ultra-pure MilliQ© water were subsampled into 10 to 20 cm long increments. A total of 740 samples were melted at room temperature in a clean room just before being analyzed for major water soluble ions (Na^+, NH_4^+, K^+, Mg^{2+}, Ca^{2+}, $CH_3SO_3^-$, Cl^-, SO_4^{2-}, NO_3^-) via Dionex ion suppressed chromatography (DX-120 series) equipped with Dionex Ionpack CS12 columns for the cation channel and with Dionex Ionpack AS15 columns for the anion channel. Kekonen et al. (2002, 2004) and Virkkunen (2004) described the analytical methods in details. Mean blank values (12 samples) obtained were 0.09 ± 0.8 $ng.g^{-1}$ for Na^+, 0.8 ± 1.5 $ng.g^{-1}$ for NH_4^+, 0.2 ± 0.1 $ng.g^{-1}$ for K^+, 0.08 ± 0.09 $ng.g^{-1}$ for Mg^{2+}, 0.5 ± 0.7 $ng.g^{-1}$ for Ca^{2+}, 0.03 ± 0.09 $ng.g^{-1}$ for $CH_3SO_3^-$, 1.01 ± 0.7 $ng.g^{-1}$ for Cl^-, 0.9 ± 0.6 $ng.g^{-1}$ for SO_4^2, and 0.2 ± 0.9 $ng.g^{-1}$ for NO_3^-. Non-sea-salt (nss) fractions of calcium, sulfate, magnesium and chloride were calculated using a conservative sea-salt species, i.e. sodium, as the sea-salt indicator (Keene et al., 1986).

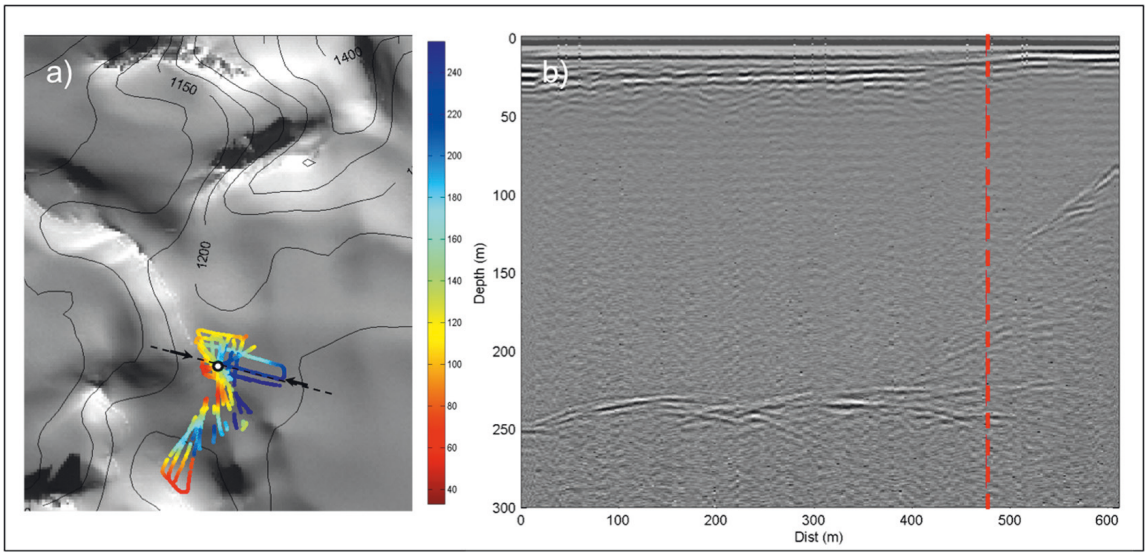

Figure 2.

a) Topographical map of the drilling site (white circle) area showing radar survey tracks. The black arrows and the dashed black line point the track corresponding to the radargram shown in b);

b) radar profile passing over the drilling site (dashed red line).

2.3 Dating

Previous studies using the Holtedahlfonna ice core data (Sjögren et al., 2007; Ruggirello et al., 2010; van der Wel et al., 2011) used an age-depth scale based on the Nye thinning model (Nye, 1963) constrained by the depth of the 1963 radioactivity fallout layer at 28.5 m depth (van der Wel et al., 2011), giving a constant accumulation rate (0.50 m w e yr^{-1} for 1963-2005) together with a range of plausible ice thicknesses (Figure 4). Divine et al. (2011) used automated counting of annual $\delta^{18}O$ (Pohjola et al., 2002b) layers to derive variable accumulation rates. The rate of thinning of layers is best matched with Nye age depth model having a glacier thickness of 300 m, which is 150 m more than the ice thickness estimation used in earlier studies (Sjögren et al., 2007). Ice thicknesses up to 250 m are found within tens of meters to the drilling site (Figure 2). Recently a dating method based on statistical extraction of historically known volcanic eruptions was used (Moore et al., 2012). To do this, the sulfate profile is fitted to all other ion species measured in the core using a multiple linear regression with moving windows in logarithmic concentration space (Moore et al., 2006). This allows the contributions of the several possible time-varying sulfate sources (other than volcanic) as well as the melt-induced relocation of ions and the heteroscedastic ion chromatography errors to be taken into account. In the sulfate residual obtained, peaks can only be related to stochastic sources (i.e. mainly volcanic). The significance of these peaks in the residual is found by assessing the variance within the sliding window used in the empirical regression. The chemical fingerprints of 5 volcanic eruptions were found (at 95% confidence level) and among them a peak could be assigned to the Laki eruption (1783) at 103.6 m depth. The volcanic signatures could be used as reference horizons in a stacked Nye thinning model. Figure 4 shows that the Nye ice thickness

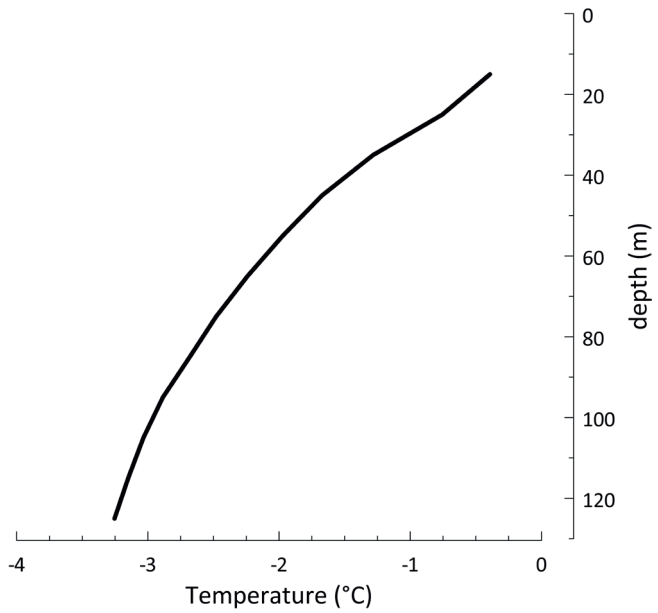

Figure 3. Temperature profile measured along the borehole (Sommer, 2011).

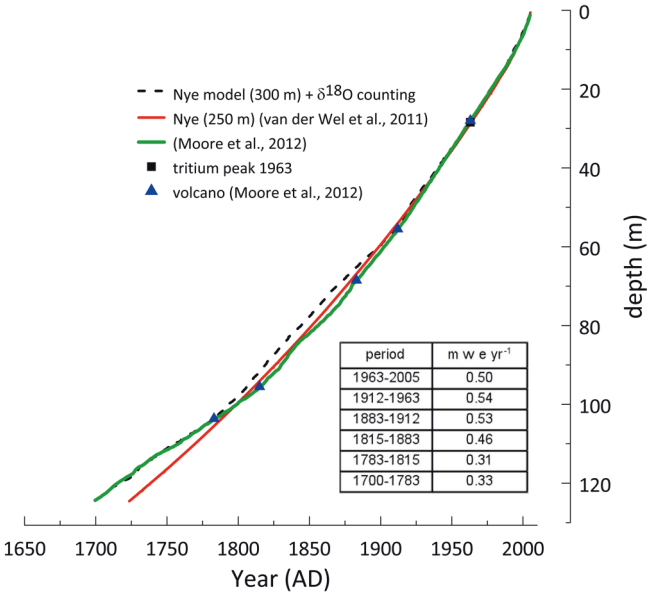

Figure 4. Age depth scale combining the Nye age scale assuming a glacier thickness of 300 m with an automated $\delta^{18}O$ cycle counting (dashed line). Nye age scale (for a glacier thickness of 250 m) used in van der Wel et al. (2011) (red line). Age scale developed by Moore et al. (2012) (green line) using five volcanic reference horizons (blue triangles) with cycle counting and employed in this study. The table (insert) shows the average accumulation rates calculated for intervals between volcanic reference horizons and decompressed using a Nye model with 300 m ice depth.

makes little difference to the dating except below 100 m depth. The closest fit to the volcanic reference layers is with a Nye depth of 300 m. This is deeper than the depth from the radar (Figure 2), it is however consistent with the temperature profile (Figure 3) (Sommer, 2005). The extremely rugged topography will lead to ice dynamic flow far different from that assumed in the simple Nye model. So we use a thinning model with 300 m depth because the resulting ice column at the time of the ice coring has been vertically shortened by higher shear to the same length as a column of originally 300m would have been shortened by only considering normal compression of the column. As described in sections 3.3 and 3.4, Holtedahlfonna chemistry is dominated by ions originating mostly from the marine and anthropogenic sources with the volcanic sulfate fraction representing only 1.4 % of the total sulfate budget (Moore et al., 2012). This rather weak volcanic signal explains why none of the 5 volcanic peaks could be previously detected with DEP measurements. For each horizon, the dating uncertainty, that is the difference between the eruption date and the dating model based on cycle counting (Divine et al., 2011), ranges from -0.9 years (for Agung, 1963) to + 9.6 years (for Krakatau, 1883).The core age depth scale calculated by Moore et al. (2012) shows that the core covers a period of 305 years with a mean accumulation rate of 0.38 m w e yr^{-1}.

3 RESULTS AND DISCUSSION

3.1 Snow accumulation and source of moisture

For the 1963-2005 period, i.e. for the upper 28.5 m of the Holtedahlfonna core, van der Wel et al. (2011) calculated an average annual accumulation rate on Holtedahlfonna of 0.50 m w e yr^{-1} which is somewhat higher than the rate given by Kekonen et al. (2005) for the 1963-1997 interval on Lomonosovfonna (0.41 m w e yr^{-1}) and attributed this difference to Holtedahlfonna being located first on the trajectory of westerly storm tracks. For the earlier period 1783-1963, we found little difference in accumulation at Holtedahlfonna in contrast with Lomonosovfonna where average snow annual accumulation rates are about 20% larger for over the recent period compared with the pre-1963 period. This result suggests a substantial difference in response of western and eastern Spitsbergen concurrent with warming and increased moisture content of the Arctic troposphere (Morison et al., 2000; Groves and Francis, 2002). We shall show this is likely due to different sea ice histories on western and eastern Spitsbergen which in turn impacts moisture availability, water isotopes and chemistry for Lomonosovfonna and Holtedahlfonna.

The oxygen isotope ratio in ice cores is commonly used as a tracer for the water cycle and Divine et al. (2011) show that the $\delta^{18}O$ of Svalbard ice cores is a useful proxy for regional winter air temperatures, most of $\delta^{18}O$ signal is preserved in the annual layer despite percolation and refreezing (Van der Wel et al., 2011). The 10-year running mean of the $\delta^{18}O$ time series for Holtedahlfonna and Lomonosovfonna ice cores are plotted in Figure 5. Although the amplitude of the isotopic variations is similar at both sites (between 1 and 3 ‰ on average), the smoothed $\delta^{18}O$ values are less negative in the Holtedahlfonna core and average -14 ‰ over the whole period spanned by the core (-16 ‰ for Lomonosovfonna). The similar altitude and latitude of Holtedahlfonna and Lomonosovfonna suggests similar cloud and surface temperatures, hence the difference in isotope values suggests either depletion due to longer transport pathways from a common source, or two different moisture sources. The short distance to the mostly non-sea ice covered Greenland Sea provides an obvious source for that would travel 100 km further to reach Lomonosovfonna. In the Canadian Arctic, 200 km difference in snow from a moisture source produces a 3‰ change in $\delta^{18}O$ (Koerner, 1979), which compares with the 2 ‰ average difference between Holtedahlfonna and Lomonosovfonna for a 100 km distance to open water difference. Of course the Barents Sea will also provide a moisture source for both drill sites on some occasions, though in that case we would expect the deposition at Holtedahlfonna to be more depleted relative to Lomonosovfonna, hence this must be a relative infrequent moisture source for Holtedahlfonna. An alternative explanation for the relatively higher $\delta^{18}O$ values in Holtedahlfonna ice may be that part of the winter snow is removed at the coring site by wind scouring with resulting mean $\delta^{18}O$ biased toward heavier values (Fisher et al., 1983, 1998). There is no direct data on seasonal distribution of snow accumulation and wind regime on Holtedahlfonna. However data from radioisotope deposits suggests that wind scouring is not significant in these locations, as we discuss in the next section.

3.2 Post-depositional processes impact on glaciochemistry

Experience from Lomonosovfonna ice core leads us to expect that the Holtedahlfonna chemical records will be affected by significant seasonal surface melting, melt water percolation and refreezing.

In fact, for Lomonosovfonna, van de Wal et al. (2002) reported a firn temperature of -2.8 °C at 15 m depth which, considering the mean annual air temperature at the drilling site is -12.5°C (Pohjola et al. 2002a), principally results from transfer and release of latent heat by melt water refreezing at depth. In his detailed stratigraphic study of shallow cores from Lomonosovfonna, Samuelsson (2001) found that melt water normally does not penetrate further than 4 or 5 m depth. This is consistent with Kekonen et al. (2005) who found that during the warmest years on Lomonosovfonna the percolation length ranges from 2 to 8 annual layers. Holtedahlfonna borehole measurements (Sommer, 2005) reveal a firn temperature of -0.4°C at 15 m depth (Figure 3) suggesting a greater impact of refreezing than on Lomonosovfonna. This is also reflected in the presence of more thin icy layers and, a shallower firn-ice transition depth in Holtedahlfonna, as shown by the detailed density profiles of two shallow firn cores extracted in the same year (2008) from the two ice caps (Figure 6). Grumet et al. (1998) and Fisher et al. (1998) showed that higher infiltration layer frequency generally implies the chemical signals are more affected by elution for Penny ice cap (Canadian Arctic). However, the opposite effect of ice layer formation, i.e. limiting the diffusion of the chemical signal, was shown by van der Wel et al. (2011) using high resolution tritium profiles from

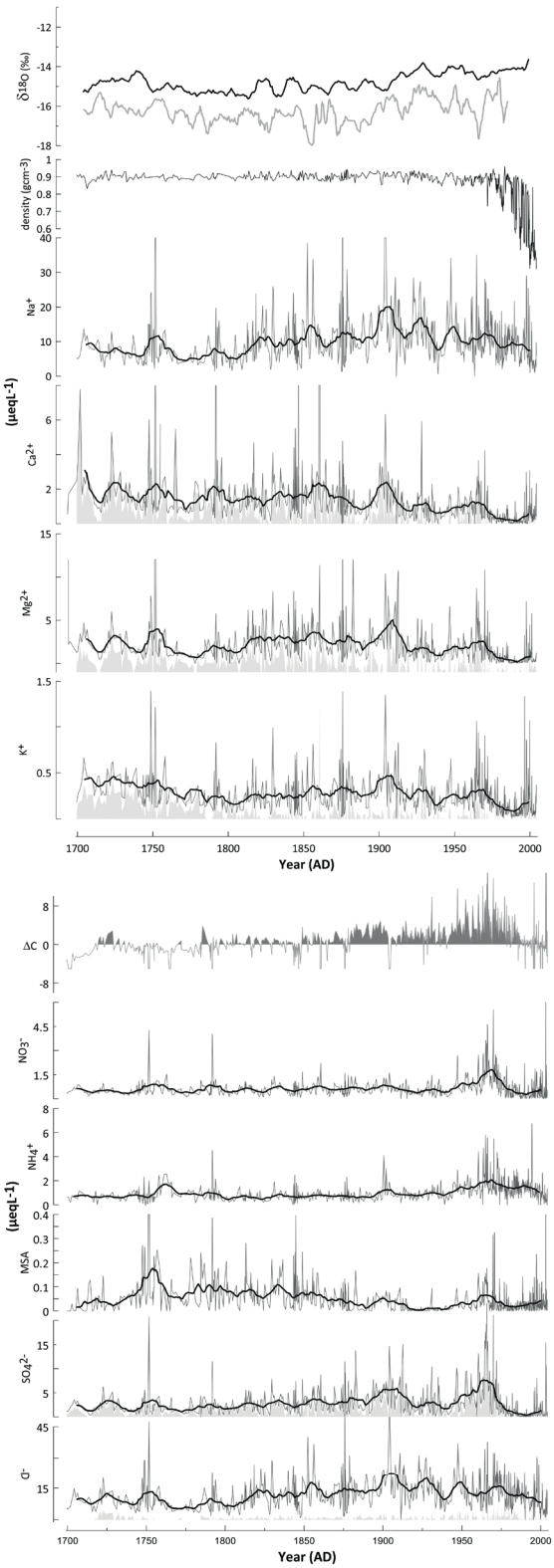

Figure 5. High resolution Holtedahlfonna glaciochemical records (grey lines) with 10-year running average (black line) and non-sea-salt fraction (light grey shaded area). Lomonosovfonna $\delta^{18}O$ curve (10-year running average) is shown in grey. The dark grey shaded area displays the acidic portion of Holtedahlfonna core ($\Delta C>0$ with $\Delta C = \sum$anions - $\sum$cations) on panel 2.

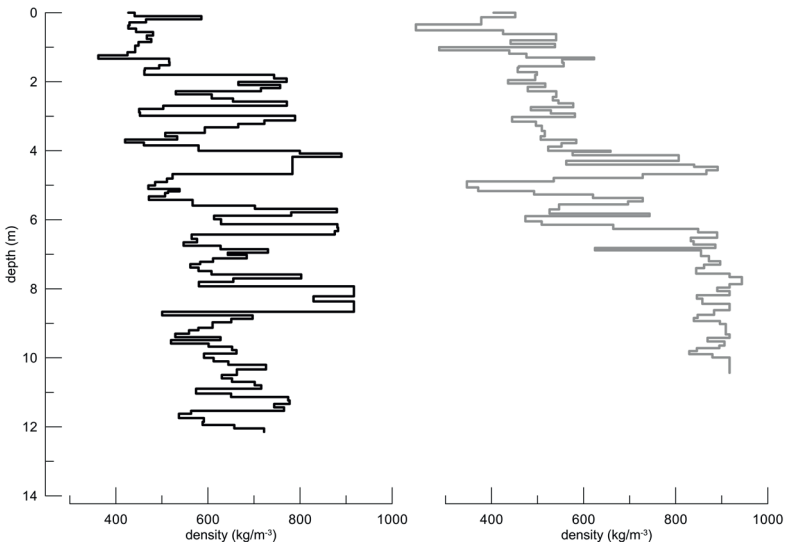

Figure 6. Density (kgm^{-3}) profiles with depth (m) of a) Holtedahlfonna shallow core and b) Lomonosovfonna shallow core. Both shallow cores were extracted in 2008. Their respective drill sites are close to the deep Holtedahlfonna (within 2.3 km) and deep Lomonosovfonna (within 100 m) cores discussed in this article.

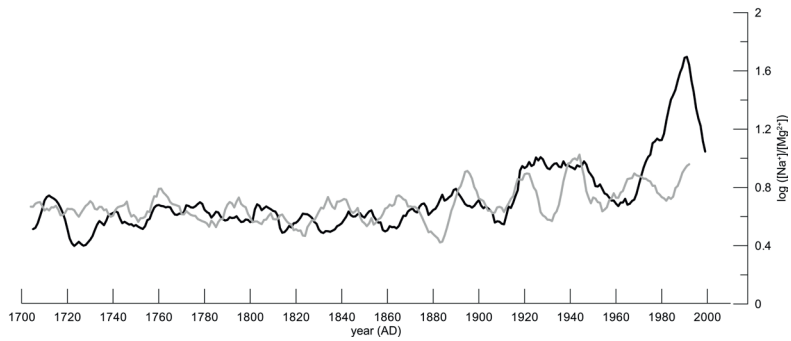

Figure 7. 10-year running average of the melt indicator (log ([Na^+]/[Mg^{2+}])) for Holtedahlfonna (black curve) and Lomonosovfonna (grey curve).

Holtedahlfonna and Lomonosovfonna. The same study also indicates the 1963 tritium peak has the same amplitude in both ice cores and is consistent with other radioactivity measurement from other Svalbard ice cores (Pinglot et al., 1999). More particularly, ^{137}Cs on Lomonosovfonna has the same mean value at the summit drill site and at much lower altitudes on the glacier ruling out any strong removal of snow or high magnitude spatial noise induced by wind scouring (Pinglot et al., 1999).

As an overview of the role of melting and percolation in the post-depositional processes over the entire record, we plot in Figure 7 log ([Na^+]/ [Mg^{2+}]) which was defined as a good index of ion elution in Svalbard, (Iizuka et al., 2002, Grinsted et al., 2006). Holtedahlfonna and Lomonosovfonna melt signals (10-year running average) show some interesting dissimilarities (Figure 7): variations in amplitude and frequency are larger for Holtedahlfonna. These differences are especially visible for

		HOLTEDAHLFONNA		LOMONOSOVFONNA	
		EOF 1	EOF 2	EOF 1	EOF 2
HF	Cl^-	**0,33**	**0,48**		
	NO_3^-	**0,37**	0,06		
	SO_4^{2-}	**0,43**	-0,05		
	MSA	0,16	**-0,34**		
	NH_4^+	0,07	**0,44**		
	K^+	**0,37**	-0,12		
	Ca^{2+}	**0,36**	**-0,41**		
	Mg^{2+}	**0,41**	**-0,22**		
	Na^+	**0,33**	**0,47**		
LF	Cl^-			**0,37**	0,09
	NO_3^-			**0,31**	**-0,55**
	SO_4^{2-}			**0,34**	**-0,27**
	MSA			**0,30**	**0,20**
	NH_4^+			0,17	**-0,66**
	K^+			**0,35**	0,21
	Ca^{2+}			**0,33**	0,16
	Mg^{2+}			**0,40**	**0,23**
	Na^+			**0,37**	0,16
variance (%)		49,32	18,49	54,22	13,61
cum variance (%)		49,32	67,81	54,22	67,83

Table 1. EOF analysis Holtedahlfonna and Lomonosovfonna major ion dataset for the period 1700-1997.

the 20th century showing that Holtedahlfonna was more sensitive to melt than Lomonosovfonna. We found a significant correlation ($r = 0.41$, $p \leq 0.05$) between the Holtedahlfonna melt index and the summer air temperatures (June, July, August) recorded at the Svalbard airport (Longyearbyen) since 1911; for Lomonosovfonna the correlation coefficient is only 0.01. Virkkunen et al. (2007) found that for Spitsbergen glaciers, daily peak air temperature affects the amount of melting more than, for example, the length of the summer or the number of positive-degree-days.

The sharp rise in the melt indicator log ($[Na^+]/[Mg^{2+}]$) in the 1980s (Figure 7) is closely matched with a decrease in concentration for the NO_3^- and SO_4^{2-} (Figure 5), both of which are easily eluted (Moore et al., 2005) components. Prior to 1980 the temporal evolution of these ions was similar as found for Lomonosovfonna (Kekonen et al., 2002; Kekonen et al., 2005). Hence it is consistent with the recent warming recorded by the melt index that some of the more mobile ions species appear to have been lost in recent decades.

Moore et al. (2005) performed an empirical orthogonal function (EOF) analysis on Lomonosovfonna ice core samples to investigate the roles of precipitation and post-depositional movement of species in ice. Monte Carlo testing the EOF factors (Moore and Grinsted, 2009) showed that the first 8 EOFs were significant. Moore et al. (2005) found that 60% of the variation in Lomonosovfonna data is due to elution and is the leading EOF. We use a similar approach for the Holtedahlfonna core, using log-transformed and standardized concentrations. The first 6 EOF each correlate with at least one of the chemical species and account for a total of 95% of the variance (we would expect about 5% measurement noise errors, so no more than 95% variance can be expected to be physically

Table 2. Average concentrations (x) in μeqL^{-1} (but MSA in ηeqL^{-1}) and standard errors (σ_x) in a) Holtedahlfonna and b) Lomonosovfonna (Kekonen et al., 2005) in different time periods (n is the number of samples, % nss is the non-sea-salt fraction over the 1700-1997 period calculated using sodium as a reference.

a)

	$CH_3SO_3^-$		Cl^-		SO_4^{2-}		NO_3^-		Na^+		NH_4^+		K^+		Mg^{2+}		Ca^{2+}		n
average/sdt error	x	σ_x	x	σ_x	x	σ_x	x	σ_x	x	σ_x	x	σ_x	x	σ_x	x	σ_x	x	σ_x	
whole core	47,97	2,5	11,95	0,3	2,66	0,1	0,66	0,0	9,89	0,3	1,06	0,0	0,25	0	1,90	0,1	1,30	0,1	739
1700-1815	79,44	8,3	8,86	0,5	2,16	0,2	0,61	0,0	7,37	0,4	0,82	0,0	0,33	0	2,17	0,2	1,84	0,2	146
1815-1880	63,33	4,7	12,83	0,7	2,78	0,2	0,59	0,0	10,91	0,7	0,72	0,0	0,28	0	2,84	0,2	2,28	0,6	166
1880-1920	27,09	4,3	15,38	1,0	4,08	0,4	0,62	0,0	12,69	1,1	0,85	0,1	0,32	0	2,89	0,3	1,26	0,1	66
1920-1950	10,87	2,1	15,79	0,9	2,56	0,3	0,54	0,0	13,12	0,8	0,99	0,1	0,25	0	1,49	0,2	0,88	0,1	69
1950-1970	57,44	6,9	12,73	0,9	6,92	0,6	1,45	0,1	10,48	0,7	1,80	0,1	0,29	0	2,35	0,2	1,18	0,1	64
1970-1997	25,27	2,8	12,32	0,5	1,29	0,2	0,58	0,1	9,68	0,4	1,52	0,1	0,14	0	0,67	0,1	0,33	0,0	165
1997-2004	45,72	12	7,39	0,8	1,38	0,3	0,59	0,1	6,65	0,7	0,83	0,1	0,20	0	0,95	0,2	0,70	0,1	65
% nss			2,2		55,7								15,2		22,8		67,7		

b)

	$CH_3SO_3^-$		Cl^-		SO_4^{2-}		NO_3^-		Na^+		NH_4^+		K^+		Mg^{2+}		Ca^{2+}		n
average/ sdt error	x	σ_x	x	σ_x	x	σ_x	x	σ_x	x	σ_x	x	σ_x	x	σ_x	x	σ_x	x	σ_x	
whole core	115,12	5,20	8,06	0,2	3,80	0,2	0,88	0,0	5,03	1,0	0,89	0,0	0,18	0,0	1,63	0,1	1,72	0,1	787
1700-1815	124,81	6,73	7,39	0,3	3,07	0,3	0,68	0,0	2,67	0,9	0,06	0,0	0,18	0,0	1,60	0,1	1,59	0,1	214
1815-1880	143,90	10,80	8,28	0,4	2,90	0,2	0,86	0,1	3,47	0,8	1,24	0,0	0,23	0,0	1,82	0,1	2,07	0,2	222
1880-1920	144,26	24,53	10,38	0,7	3,71	0,3	0,80	0,1	4,00	1,0	1,21	0,1	0,22	0,0	2,06	0,2	1,70	0,2	103
1920-1950	63,88	9,76	9,17	0,7	5,15	0,6	0,71	0,1	8,94	2,9	0,82	0,1	0,11	0,0	1,79	0,2	2,57	0,4	88
1950-1970	92,51	11,45	7,56	0,7	7,49	1,0	1,46	0,1	17,57	11,1	1,52	0,3	0,15	0,0	1,54	0,3	1,03	0,1	63
1970-1997	58,12	7,39	5,90	0,5	3,95	0,4	1,20	0,1	3,18	0,7	1,20	0,1	0,07	0,0	0,70	0,1	0,88	0,2	97
% nss			26,4		84,3								37,3		29,7		87,5		

explainable). Table 1 displays only the 2 first eigenvectors that together account for 68% of the variance; the first eigenvector (EOF 1) describes 49.3% of variance in the dataset. EOF 1 is loaded in all ions except ammonium and, to a lesser extent, MSA. Virkkunen et al. (2007) showed that ammonium is the least mobile ion within the snow pack and has the lowest elution rate (Pohjola et al., 2002) due to its solubility within the ice crystal. MSA has a higher elution rate than ammonium, (Pohjola et al., 2002; Moore et al., 2005) as it is a highly soluble acid that can moves in the liquid or vapor phase along firn grain boundaries (Mulvaney et al., 1992) even in snow pack and firn well below the melting point (Kreutz et al., 1998; Pasteur and Mulvaney, 2000; Curran et al., 2002). However at sites with seasonal melting, provided melting rate does not lead to ion loss by runoff, eluted ions are trapped by refrozen ice layers and prevented from longer diffusion and relocation. Furthermore, MSA variations in Lomonosovfonna core were found to significantly correlate with Barents Sea surface temperatures (O'Dwyer et al., 2000), showing meaningful signals are preserved in the MSA record. Hence, as for Lomonosovfonna, about half of the variance of Holtedahlfonna chemical dataset is due to post-depositional movement of ions, with the other half likely related to climatic factors. Therefore to improve the signal to noise ratio and to take into account the signal fractionation due to elution, we use 10-year running means of the ion time series.

3.3 Chemical composition of Holtedahlfonna ice core

Basic statistical properties of each ion and their non-sea-salt fraction at different periods on Holtedahlfonna and Lomonosovfonna are summarized in Table 2. The concentration of measured ions in both cores averaged over the period 1700-1997 is shown in Figure 8 as anion and cation stacks. Since we have no concrete evidence of the bedrock depth or layer thinning as a function of depth in the complex ice flow regime around the drill site, we do not attempt to calculate fluxes of ions. Therefore, it is not possible to thoroughly conclude that ion concentrations in Holtedahlfonna ice core are not controlled by accumulation or dry deposition. However, Figure 4 shows that accumulation rates vary little of most of the core and in order to ease the comparison with Lomonosovfonna ice core dataset (Kekonen et al., 2005) we will use concentrations rather than fluxes in the discussion of our results.

Almost all ion (chloride, sulfate, nitrate, ammonium, sodium, potassium, magnesium) concentration profiles (Figure 5) display an increase from 1815. Calcium and MSA are exceptions and their average concentration during the period 1700-1815 were about 50% higher than after 1815 (Table 2). Sodium, chloride and potassium do not show significantly higher concentrations during the coldest part of the LIA culminating about 1850 in Svalbard (Divine et al., 2011), and between 1800 and 1840 in the Arctic as a whole (Overpeck et al., 1997). In contrast, magnesium concentrations are more than 50% higher during 1750-1880 and are dominated by the terrestrial fraction (Figure 5), as was also observed in Canadian Arctic and Greenland ice cores (Kang et al., 2003).

Anions outweigh the cations in the mean ionic ice composition (Figure 8). The ice is distinctly acidic from 1850 which corresponds with the onset of the industrial revolution in Europe (Figure 5) and even more between 1940 and 1980 when human activity (fossil fuel burning) significantly enhanced the level of acidic species such as nitrate, non-sea-salt sulfate, non-sea-salt chloride; probably deposited as HNO_3^-, H_2SO_4 and HCl brought by Arctic haze (Virkkunen et al., 2004). Sulfate concentrations have risen by a factor of 1.7 since 1880. The major part of the increase occurred after 1940. Peak levels are reached during the 1960's which is consistent with ice core records from Snøfjellafonna (Goto-Azuma et al., 1995) and from Severnaya Zemlya (Weiler et al., 2005) but contrasts with Greenland and the Canadian Arctic (Grumet et al., 1998), which display a more gradual sulfate rise over the 20th century. It is likely that these ice cores from Greenland and Canada are more representative

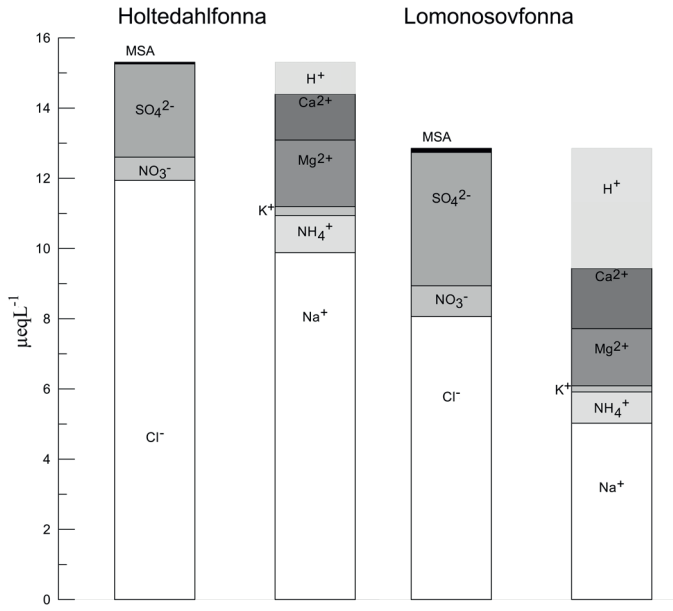

Figure 8. Mean concentrations of measured ions in the Holtedahlfonna and Lomonosovfonna cores separated in anion and cation stacks.

of the northern hemisphere tropospheric concentration (Fisher et al., 1998). In Holtedahlfonna core, the average concentration of ammonium is 2.2 times higher during the 20th century than during the 18th century (Table 2). On the contrary, the mean calcium concentration is more than 2 times lower for the industrialized period (0.87 μeqL^{-1}) than between 1700 and 1880 (1.85 μeqL^{-1}) when the ice is alkaline. Alkalinity peaks ($\Delta C<0$, Figure 5) are systematically related to higher excess calcium suggesting the ice could contain un-neutralized carbonate. 1750-1780 is the longest "alkaline" period during which sea-salt is also notably less fractionated and nssCl (HCl) concentration is close to zero.

3.4 Comparison with Lomonosovfonna ice core

Since ion chromatograph data are heteroscedastic (in this case errors are proportional to concentration), and post-depositional processes affect ion elution rates (Moore et al., 2005), calculation of statistics assuming normality and non-sea-salt ratios are suspect; however these measures are still commonly used, and may be useful for comparison purposes between similar cores providing all concentration data are log-transformed. On average over the last 3 centuries, the proportion of species with a dominant sea-salt source (Na^+, Cl^-, K^+, Mg^{2+}; Table 2) is larger in Holtedahlfonna (80%) than Lomonosovfonna (70%) with chloride and sodium being the two major sea-salt species (respectively 40% and 33%). Throughout all periods reported in Table 2 and Figure 5, the mean concentrations for sea-salt ions are systematically higher in Holtedahlfonna (Table 2a) ice than in Lomonosovfonna (Table 2b), except the period 1920-1950 when magnesium was slightly less abundant in Holtedahlfonna (1.49 μeqL^{-1}) than in Lomonosovfonna (1.79 μeqL^{-1}).

At both sites, sulfate is the third largest contributor to the ion budget although its proportion of the sum in Holtedahlfonna ice (9%) is only half of that in Lomonosovfonna (17%). The non sea salt (nss) SO_4 contribution to the total SO_4^{2-} concentration is also on average much smaller on Holtedahlfonna (55%) than on Lomonosovfonna (74%). Moore et al. (2012) estimate that the volcanic sulfate fraction on Holtedahlfonna is less than half that on Lomonosovfonna. The greater total amount of sea-salt as well as the smaller fraction of non-sea-salt sulfate at Holtedahlfonna may reflect the shorter distance from the marine aerosol source to Holtedahlfonna summit compared with Lomonosovfonna. The marine biogenic fraction of sulfate, estimated by MSA concentrations, is surprisingly low at Holtedahlfonna with an average concentration less than half that of Lomonosovfonna (0.05 and 0.12 μeqL^{-1} respectively). This probably points to a difference in the primary productivity of the marine source implying two different marine origins with respectively low and high primary productivity. This latter point is further discussed in section 3.5.

The difference in the calcium budget and the relative proportion of terrestrial calcium in the two ice cores also reveals the more proximal and influential sea-salt source for Holtedahlfonna ice cap. In the Holtedahlfonna core, calcium accounts for 4.4% of all ions (7.7% in Lomonosovfonna) and is only the 5th (4th in Lomonosovfonna) most abundant species after sea-salt, sulfate and magnesium (6.4%). Furthermore, while Kekonen et al. (2005) report that 88% of calcium over the common period 1700-1997 between the cores in Lomonosovfonna ice is of terrestrial origin, we calculate that on Holtedahlfonna this fraction represents only 68%. This means that not only the oceanic contribution is enhanced for Holtedahlfonna but also the terrestrial contribution to Ca^{2+} is limited for Holtedahlfonna. This observation should nevertheless be moderated when comparing the different periods. For example, Holtedahlfonna received on average about the same amount of terrestrial calcium than

Lomonosovfonna during most of the 18th century (1700-1780) (1.52 and 1.56 μeqL^{-1} respectively) and twice as much between 1950 and 1970 (0.72 and 0.36 μeqL^{-1} respectively).

Ammonium and nitrate represents respectively 3.5% and 2.2% of total ions which are slightly smaller contributions than in Lomonosovfonna for the same period.

3.5 Biogenic source productivity

As an oxidation product of gaseous biogenic dimethylsulfide (DMS) emissions (Dacey and Wakeham, 1986), MSA is commonly used as a proxy for marine biogenic productivity. Isaksson et al. (2006) suggested that sea ice extent was likely the dominant effect on MSA concentrations variability in Lomonosovfonna ice and also hypothesized that the higher MSA concentration during the colder 19th century could be a result from a change of source and/or from more favorable growing conditions for the DMS producing phytoplankton during the colder conditions prevailing. For the 20th century, O´Dwyer et al. (2000) found that Lomonosovfonna MSA better correlated with Barents Sea surface temperature and ice cover than with the Greenland Sea conditions indicating that the amount of MSA deposited on Lomonosovfonna is very much influenced by the conditions in the Barents Sea.

Similarly to Lomonosovfonna, the Holtedahlfonna core contains more MSA on average during part of the cold period 1700-1880 (0.07 ± 0.08 μeqL^{-1}) than during the 20th century (0.03 ± 0.05 μeqL^{-1}). The MSA concentrations in Holtedahlfonna remain lower than those in Lomonosovfonna throughout the last 3 centuries, suggesting a different and/or less productive marine source influencing western Spitsbergen. The transition from the LIA to the warmer 20th century is more marked in Holtedahlfonna records, with 20th century concentrations being 43% of LIA values, than at Lomonosovfonna when MSA concentrations dropped to 66% of earlier levels (Figure 9a). These sharp decreases coincide with the drastic sea ice cover change in the Greenland Sea around 1880 (Divine et al., 2008) creating on the western side of Spitsbergen year-round open water conditions. Figure 9b displays the maximum (April) and the minimum (August) seasonal sea ice extent anomalies for the Greenland Sea and shows the larger seasonal ice extent before 1880 compared to the 20th century. The reduction in seasonal sea ice variability corresponds with the decline in MSA concentrations in Holtedahlfonna. Correlation between the 10-year running average time series of MSA and Greenland Sea April ice extent anomaly for the period 1762-1880 is higher than with Barents Sea ice extent anomaly and coefficients are significantly different (0.46 ($p < 0.05$), and 0.10 respectively) and suggestive of a connection between positive Greenland Sea ice anomalies and high MSA levels at Holtedahlfonna during the LIA. Such results are expected as the more extensive seasonally ice covered part of the western side of Svalbard lead to increased production of meltwater, thereby stabilizing the water column in spring and summer which may have favored biomass production in the euphotic zone and thus enhanced release of DMS in the atmosphere (Sakshaug and Walsh, 2000; Strass and Nothig, 1996). A similar process might have also taken place in the Barents Sea (Isaksson et al., 2006) with a wider seasonally ice free area creating a stronger DMS source on eastern Svalbard being recorded in Lomonosovfonna ice. Records of higher MSA concentration for the 19th century in Holtedahlfonna are in accordance with those from Greenland ice cores. A negative relationship between the Greenland Sea surface temperature and MSA concentrations in 20D ice core (Southern Greenland) was found by Whung et al. (1994) over the 1870-1950 time period and Legrand et al. (1997) suggest that such a correlation, also demonstrated for MSA records from Summit (Central

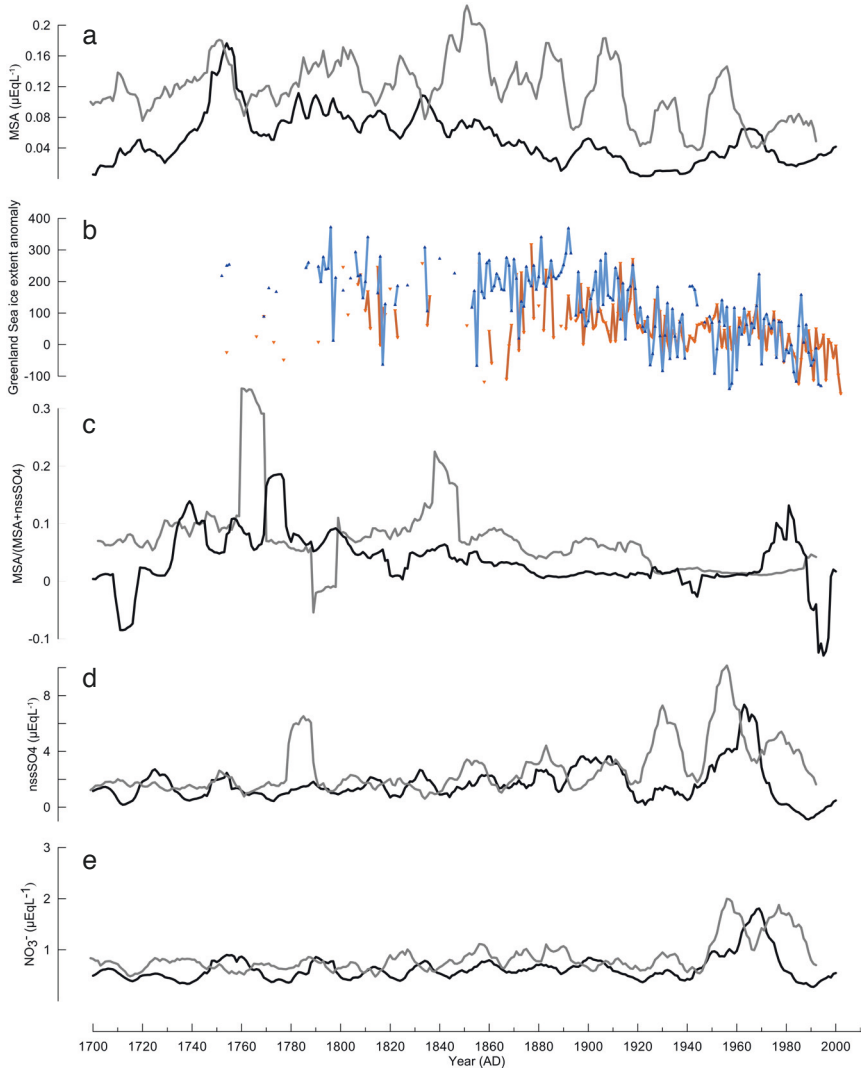

Figure 9. 10-year running average for Holtedahlfonna (black) and Lomonosovfonna (grey) of a) MSA concentrations; b) April sea ice extent anomaly (blue) and August sea ice extent anomaly (orange) for the Greenland Sea ice (Divine and Dick, 2006 – data are not available for every year), note the decrease in amplitude of seasonal variability in sea ice extent around 1880; c) MSA fraction, with a mean of 8% Holtedahlfonna prior to 1880 and 1% after that; d) $nssSO_4$ concentrations; e) NO_3^-, note that the profiles are uncorrelated with MSA.

Greenland), may result from increased sea ice extent during cold period causing higher DMS emissions in the atmosphere.

The relationship between MSA and Greenland Sea ice extent as well as the MSA concentration difference between Holtedahlfonna and Lomonosovfonna seem to imply that the Greenland Sea biogenic productivity was weaker than that of the Barents Sea during the 19th century. However this does not rule out the possible contribution of lower latitude air masses to Holtedahlfonna MSA budget. The MSA fraction of non-sea-salt sulfur is known to increase with latitude and has often been used

to investigate the possible origin of marine air masses (Bates et al., 1992). This is based on the fact that DMS oxidation by ·OH radicals (the dominant oxidant in a clean atmosphere) is temperature dependent as the addition pathway producing MSA is favored at low temperature (Hynes et al., 1986; Seinfeld and Pandis, 1998). Between 1700 and 1920 the MSA fraction, i.e. MSA/(MSA+nssSO_4) (Figure 9c) in Holtedahlfonna is fairly consistently 3% lower than that of Lomonosovfonna. While Greenland MSA fraction is (10-20%) (Legrand et al., 1997) is more similar to Lomonosovfonna in the LIA than Holtedahlfonna. The MSA fraction shows marked variability during the LIA compared with the 20th century at Holtedahlfonna, which is also consistent with the much reduced sea ice cover in the Greenland Sea, and especially the reduced amplitude of seasonal variations. After 1920 Lomonosovfonna and Holtedahlfonna have very similar MSA fraction, which is linked to the retreat of the sea ice margin in the Barents Sea at that time (Divine et al., 2008). The loss of ions through runoff is responsible for the negative fraction seen after 1980 at Holtedahlfonna. The generally lower MSA fraction compared with Lomonosovfonna either constitutes more evidence for a different marine biogenic source influencing western Spitsbergen or point to an additional source of nssSO_4 for Holtedahlfonna that could be terrestrial biogenic, continental (gypsum dust) or volcanic. Any significant volcanic contribution is unlikely as the fraction of volcanic sulfate in Holtedahlfonna is very low (1.4 %) in comparison with that of Lomonosovfonna (4.5%) (Moore et al., 2006, 2012) or Greenland (57%) (Legrand et al., 1997). We can use wavelet coherence (WTC, Grinsted et al., (2004) to investigate the relationship between MSA and nssSO_4 (Figure 9d) variations. Between 1700 and 1880 (Figure 10) the time series are highly coherent (WTC > 0.8) and in-phase at almost all periods. This contrasts with a smaller and more disjoint significant area in the WTC plot for nssCa and nss-SO_4

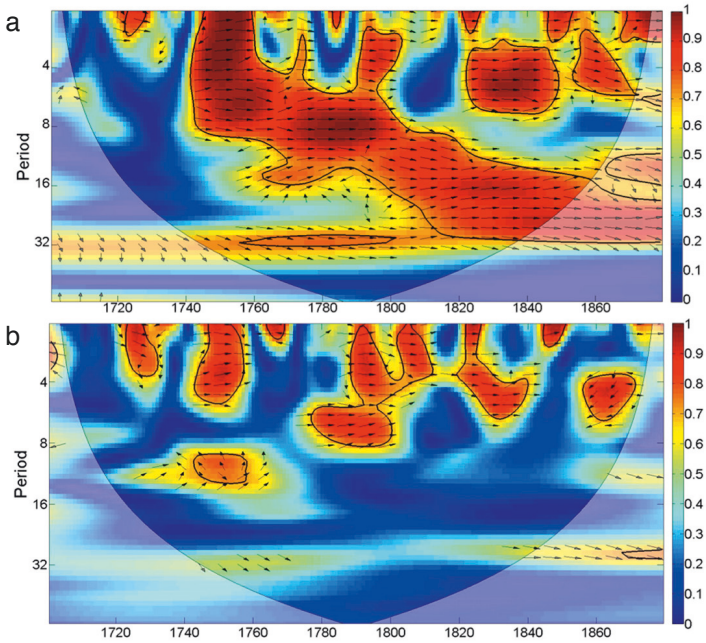

Figure 10. Wavelet coherency and phase between a) MSA and nssSO_4; b) nssCa and nssSO_4. The thick black contour designates the 5% significance level against red noise and the thin black curve is the cone of influence. Arrows pointing to the right indicate in-phase relative relationship.

(Figure 10). The correlation between MSA and nssSO_4 argues in favor of a dominant biogenic source of nssSO_4 in Holtedahlfonna during the 18th and 19th centuries. Since DMS can also be oxidized by radicals other than OH^- (such as NO_3^-, BrO, IO, H_2O_2) producing sulfur dioxide (SO_2) or SO_4^{2-} instead of MSA, the interpretation of the MSA fraction in terms of the biogenic source latitude (or temperature) is not straightforward when the oxidative capacity of the atmosphere changes. Yet, Whung et al. (1994) argue that NO_3^- oxidant, despite the substantial NO_x levels in the Arctic atmosphere during the industrial period, does not control the MSA concentration in Greenland ice core because NO_3^- is photolyzed before DMS emissions reach their maximum in spring-summer. Similarly, in Holtedahlfonna core, the sharp increase of NO_3^- (NO_x) (Figures 9e) did not lead to a decrease of MSA, therefore we also suggest that the variation of MSA concentration during the 20th century still reflect those of marine biota. Additionally, the increases of nssSO_4 are similar at Holtedahlfonna and Lomonosovfonna (Figure 9d, Table 2), and so we ascribe the sharp change of MSA in Holtedahlfonna around 1880 to the rapid sea ice cover decline in the Greenland Sea and its relatively larger temperature rise at the end of the LIA than occurred in the wider North Atlantic (Engelsen et al., 2002).

3.6 Ammonium variability

Lomonosovfonna and Holtedahlfonna display divergent behavior of ammonium around the end of the LIA (Figure 5). The 10-year running mean NH_4^+ values in the Lomonosovfonna core follow a decreasing trend from 1900 to 1940 before reflecting the impact of anthropogenic pollution in the 1950's (Figure 11a) (Kekonen et al., 2002). In contrast, Holtedahlfonna ammonium concentrations rise by a factor of 3 starting in 1880. Explanations for the earlier rise of ammonium concentration could be that it either reflects a more efficient ammonium transport to Holtedahlfonna or that during the period 1880-1940 Holtedahlfonna received an additional source of ammonium than Lomonosovfonna. In relation to the regional climate component discussed section 3.1, local wetland formed by the reduction of snow covered area at the end of LIA might have constituted a source of local gaseous ammonia (NH_3, a precursor of ammonium) influencing the Holtedahlfonna NH_4^+ budget. However, the lack of data on wetland for the Svalbard region makes it impossible to verify this hypothesis.

Jickells et al. (2003) uses stable N isotopes in ammonium to derive sources of ammonium. However we have only ion concentration data, so we use an indirect approach. To investigate the temporal evolution of the contributions to the ammonium budget along the core we performed a multiple linear regression (MLR) between ammonium and other ions (Figure 11b). The procedure is essentially the same as used to evaluate the sulfate budget in Lomonosovfonna described by Moore et al (2006), and the first steps of finding the volcanic sulfate residuals (Moore et al., (2012) and Section 2.3), but rather than modeling sulfate as function of the other ions, here we target ammonium by fitting the other ions. During the pre-industrial period until 1880, nitrate is the most significant co-factor with ammonium indicating the existence of natural ammonium nitrate (NH_4NO_3) - a compound formed more favorably in cold conditions (Teinilä et al. 2003; Battye et al. 2003). The North American soil and vegetation and biomass burning NH_3 emissions constitute the main pre-industrial source of ammonium for Greenland and reflect the propensity of polar ice sheets to sample the free troposphere where NH_3 and NH_4^+ resident times allows their long range transport (Fuhrer et al., 1996). Yet, the oceanic source of NH_3 in the Arctic is considered as non-negligible, especially in winter (Fisher et al., 2011). Jickells et al. (2003) provided evidence for a substantial marine ammonia winter source. The ocean constitutes a net source

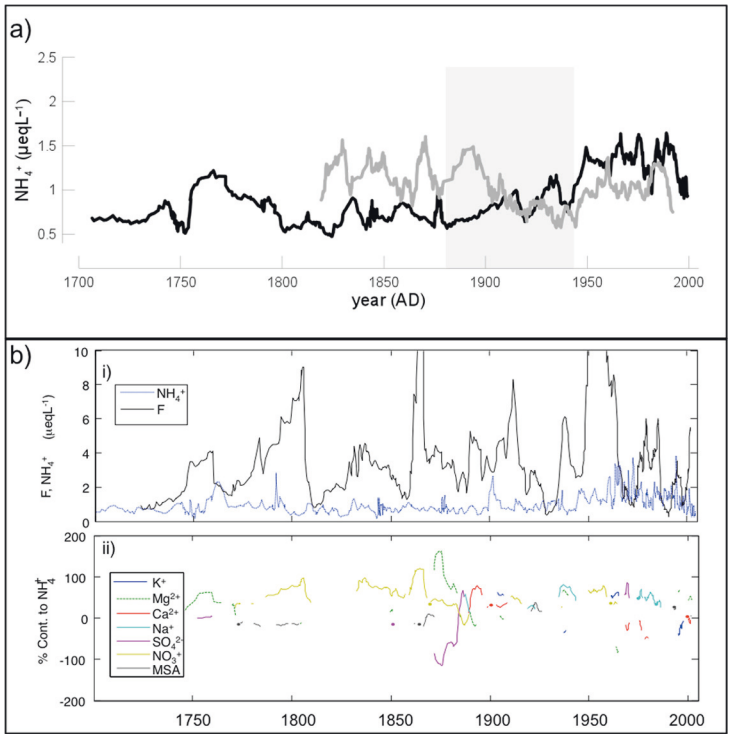

Figure 11. a) 10-year running average concentrations of NH_4^+ (μeqL^{-1}) in Holtedahlfonna (black) and Lomonosovfonna (grey) cores. The shaded area indicate the LIA (Little Ice Age) termination; b) Ammonium multiple linear regression (MLR): i) sample-by-sample ammonium ion concentration profile (blue dotted curve) and the F statistic for the 100 points windowed MLR; ii) contributions of each species in the MLR to the ammonium concentration (see Moore et al., (2006) for method details), the ion curves are only plotted when their contribution is significant at the 95% level. Most of the record is dominated by co-variation with NO_3^- (light green). Post 1880, no ion stands out as generally co-varying with NH_4^+, though sometimes both Na^+ (turquoise), and SO_4^{2-} (purple) are important factors.

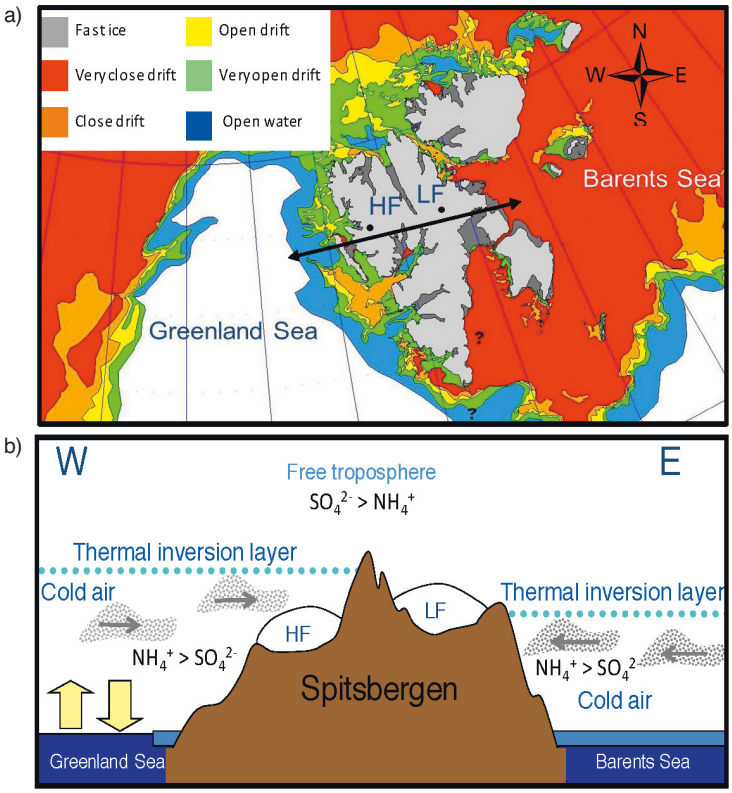

Figure 12. a) Map of Svalbard and surrounding seas showing present day typical sea ice conditions in winter (source: http://retro.met.no/kyst_og_hav/iskart.html). The black double arrow marks the W-E profile section of Spitsbergen through Holtedahlfonna (HF) and Lomonosovfonna (LF) represented in b) winter-spring Arctic haze situation and the vertical stratification of aerosol acidity (Fisher et al., 2011).

of NH_x (i.e. NH_3 and NH_4^+) to continent during pre-industrial times with smaller sea-water NH_x concentrations in regions of low primary productivity (nutrient-limited communities being more efficient at utilizing recycled nitrogen and thus maintaining a lower ambient concentration) (Spokes et al., 2000; Johnson et al., 2008 and references therein). Depending on which of the natural sources (oceanic or continental) dominates Svalbard ammonium budget, the lower pre-industrial NH_4^+ concentration measured in Holtedahlfonna ice compared to Lomonosovfonna could: 1) be an additional argument in favor of a cold and low-productive marine source for western Spitsbergen compared with eastern Spitsbergen which is more influenced by the North Atlantic where NH_3 sea-air fluxes are one order of magnitude higher (Johnson et al., 2008) or 2) indicate that Holtedahlfonna is less influenced by the free troposphere than Lomonosovfonna. After 1880, the nitrate co-variation and fractional contribution to ammonium becomes insignificant and none of the other ions becomes a consistent replacement in the MLR (Figure 11b). Over a period when melting impact rises constantly, this probably reflects the specific elution resistant behavior of NH_4^+ (Table 1). This may be the case during the 1980's when higher NH_4^+ concentrations are not correlated with nitrate or sulfate (Figure 5).

Virkkunen et al. (2007) showed that the chemical fingerprint of anthropogenic ammonia (NH_3), sulfur dioxide (SO_2) and nitrogen oxides (NO_x) (the main constituents of the Arctic haze) was present in 2001/02 snowpack on Holtedahlfonna but absent on Lomonosovfonna. The rise of NH_4^+ in Holtedahlfonna records starting in 1880 could result from mid-latitude pollution reaching the Arctic in late winter when meridional transport intensifies (Iversen and Joranger, 1985). The global NO_x emissions started to rise in the 1860s (Klimenko et al., 2000). Anthropogenic ammonium pollution is also detected from 1870 in Colle Gnifetti ice core (Döscher et al., 1996), at least from 1920 in Col du Dôme (Fagerli et al., 2007) while no increasing trend is visible before 1940-50's in Greenland (Fuhrer et al., 1996), Everest (Shugui et al., 2003) or Lomonosovfonna (Kekonen et al., 2005) records. To account for the absence of Arctic haze from Lomonosovfonna snow, Virkkunen et al. (2007) invoked geographical factors such as the orientation of the surrounding fjords. Rather here we advocate the two glaciers respective position relative to the top of the atmospheric boundary layer within which neutralized pollutants are transported from continental source area in late winter. The acidity of Arctic haze aerosols depends on the availability of ammonia to neutralize sulfate. Using aircraft and surface aerosol data (including data from Zeppelin station), Fisher et al., (2011) investigated the source contributing to ammonium, sulfate and aerosol acidity through the depth of the Arctic troposphere over the winter-spring season. For the winter season, they found that sulfate and ammonium sources are more stratified than later in spring. Aerosols in the free troposphere are more acidic and are dominated by sulfate (originating mostly from East Asia), whereas more abundant and neutralized aerosols (from West Asia and Europe) remain within the boundary layer. As shown in Figure 12, the shorter distance of Holtedahlfonna to the quasi-permanent open sea (the Greenland Sea) could facilitate oceanic heat advection to the ice cap in summer and allow, in winter, some vertical convection thereby weakening the temperature inversion gradient and slightly raising its upper boundary, placing Holtedahlfonna within the inversion layer (Solberg et al. 1996; Treffeisen et al. 2007). Conversely, the presence of ice covered sea on the eastern side of Spitsbergen would provoke an intensive radiative cooling of the lower troposphere leading to the formation of a very stable and hence thin inversion layer during the polar night (Wu et al. 2004; Koenigk et al. 2009). In those conditions Lomonosovfonna would be located above the thermal inversion layer and would most likely collect pollution from the more acidic free troposphere in winter. The atmospheric vertical stratification of acidity could then explain Svalbard's highest sulfate and greater acidity levels recorded in Lomonosovfonna (Kekonen et al., 2005) (Figure 7).

4 CONCLUSIONS

We present the ion chemical data for the past 300 years from Holtedahlfonna and compare them with records extracted from the Lomonosovfonna core to illustrate site-specific climatic and glaciological factors and better estimate the local influence of environmental factors on ice records in the Svalbard setting. Despite that a melt indicator is on average higher in Holtedahlfonna, melting is responsible for only 49% of the variance in ion concentration which is almost the same as estimated for the Lomonosovfonna ice core (55%). This is likely because of the formation of thin layers of ice in the annual snowpack which act as a barrier to the deeper elution of ions, helping to preserve a multi-year resolution environmental record. Holtedahlfonna chemical melt indicator (log ($[Na^+]/[Mg^{2+}]$)) is a better proxy for Svalbard 20th century summer air temperatures than provided by other ice cores from the archipelago.

A strong local response is also shown in the spatial and temporal variability of chemical species. As expected, it was found that Holtedahlfonna ice contains more sea-salt due to its proximity to the Greenland Sea which is ice-free almost throughout the year. The lower MSA and NH_4^+ levels measured for the LIA period than that measured in Lomonosovfonna also argue in favor of the influence of a local marine source with lower primary productivity (a cooler source) during this period. The good correlation between Greenland Sea ice extent and Holtedahlfonna biogenic sulfur record (MSA) confirms this hypothesis and reveals in itself the complex air-sea-ice interactions that characterize the Greenland Sea compared with other Nordic Seas (Kvingedal, 2005). In addition to providing a proximal source of warmth, moisture, sea-salt and biogenic sulfur to western Svalbard, the low Greenland Sea ice concentration favors the altitudinal dispersal of tropospheric pollution. The study of the ammonium budget suggests either the open sea provides a winter source of ammonium, or just a consistently that the glaciers of the western part of Spitsbergen, such as Holtedahlfonna, may better reflect the tropospheric boundary layer pollution burden than eastern glaciers, which are more representative of the free troposphere in winter. The low sea ice extent in the Greenland Sea strongly influences the height of the winter inversion layer and thus the delivery of more neutralized Arctic haze aerosols to the glacier. As Arctic warming progresses we may expect the drastic retreat of the Barents Sea seasonal ice cover, the analysis of Holtedahlfonna ice core foretells how glaciochemical signals from eastern Svalbard glaciers (such as Lomonosovfonna) could be altered and how winter-spring pollution would be mixed higher in the Arctic troposphere.

ACKNOWLEDGEMENT

The comments of referees improved the manuscript considerably. We wish to thank the Norwegian Polar Institute, the Dutch Science Foundation (NWO) and the Swedish Science Council (VR) for funding the ice core drilling. We thank Kristiina Virkkunen and Venkata Gandikota for the primary cutting of the ice core. We are also grateful to the Finnish Forest Research Institute, Rovaniemi Research Unit for the use of the laboratory facilities and to the Academy of Finland and the ARKTIS graduate school which provided financial support for sample analysis. This research is partially supported by China's National Key Science Program for Global Change Research (No: 2010CB950504) and NSFC grant No. 41076125.

REFERENCES

Bates, T. S., J. A. Calhoun, and P. K. Quinn (1992), Variations in the Methanesulfonate to Sulfate Molar Ratio in Submicrometer Marine Aerosol Particles Over the South Pacific Ocean, J. Geophys. Res., 97(D9), 9859–9865, doi:10.1029/92JD00411.

Battye, W., V.P. Aneja, P.A. Roelle (2003), Evaluation and improvement of ammonia emissions inventories, Atmos. Environ., 37, 3873-3883, doi:10.1016/S1352-2310(03)00343-1.

Bengtsson, L., V. A. Semenov, and O. M. Johannessen (2004), The early twentieth-century warming in the Arctic- A possible mechanism, J. Clim., 17, 4045-4057.

Curran, M. A. J., A. S. Palmer, T. D. Van Ommen, V. I. Morgan, K. Phillips, A. J. McMorrow, and P. A. Mayewski (2002), Post-depositional movement of methanesulphonic acid at Law Dome, Antarctica, and the influence of accumulation rate, Ann. Glaciol., 35, 333– 339.

Dacey, J.W.H., and S.G. Wakeham (1986) Oceanic Dimethylsulfide: Production During Zooplankton Grazing on Phytoplankton, Science, 223 (4770), 1314-1316, doi: 10.1126/science.233.4770.1314.

Divine, D. and C. Dick (2006), Historical variability of sea ice edge position in the Nordic Seas, J. Geophys. Res., 111. C01001, doi:10.1029/2004JC002851.

Divine, D., E. Isaksson, V. Pohjola, H. A. J. Meijer, R. S. van de Wal, T. Martma, J. C. Moore, B. Sjögren, and F. Godtliebsen (2008), Deuterium excess record from a small Arctic ice cap, J. Geophys. Res., 113, D19104, doi:10.1029/2008JD010076

Divine, D., E. Isaksson, F. Godtliebsen, T. Martma, H. A. J. Meijer, J. C. Moore, V. Pohjola, and R. S. van de Wal (2011), Thousand years of winter surface air temperature variations in Svalbard and northern Norway reconstructed from ice core data, Polar Res. 30, 7379, doi: 10.3402/polar.v30i0.7379

Döscher, A., H. W. Gäggeler, U. Schotterer, and M. Schwikowski (1996), A historical record of ammonium concentrations from a glacier in the Alps, Geophys. Res. Lett., 23(20), 2741–2744, doi:10.1029/96GL02615.

Duce, R. A., et al. (1991), The atmospheric input of trace species to the world ocean, Global Biogeochem. Cycles, 5(3), 193–259, doi:10.1029/91GB01778.

Engelsen, O., E. N. Hegseht, H. Hop, E. Hansen, and S. Falk-Petersen (2002), Spatial variability of chlorophyll-a in the Marginal Ice Zone of the Barents Sea, with relations to sea ice and oceanographic conditions, J. Marine Syst., 35, 70-97.

Fagerli, H., M. Legrand, S. Preunkert, V. Vestreng, D. Simpson, and M. Cerqueira (2007), Modeling historical long-term trends of sulfate, ammonium, and elemental carbon over Europe: A comparison with ice core records in the Alps, J. Geophys. Res., 112, D23S13, doi:10.1029/2006JD008044.

Fisher, D. A., R. M. Koerner, W. S. B. Paterson, W. Dansgaard, N. Gundestrup, and N. Reeh (1983), Effect of wind scouring on climatic records from ice-core oxygen-isotope profiles, Nature, 301, 205 – 209, doi:10.1038/301205a0.

Fisher, D. A., R. M. Koerner, J. C. Bourgeois, G. Zielinski, C. Wake, C. U. Hammer, H. B. Clausen, N. Gundestrup, S. Johnsen, K. Goto-Azuma, T. Hondoh, E. Blake, M. Gerasimoff (1998), Penny Ice Cap Cores, Baffin Island, Canada, and the Wisconsinan Foxe Dome Connection: Two States of Hudson Bay Ice Cover, Science, 279 (5351), 692-695, doi: 10.1126/science.279.5351.692.

Fisher, J.A., D. J. Jacob, Q. Wang, R. Bahreini, C. C. Carouge, M. J. Cubison, J. E. Dibb, T. Diehl, J. L. Jimenez, E. M. Leibensperger, Z. Lu, M. B. J. Meinders, H. O. T. Pye, P. K. Quinn, S. Sharma, D. G. Streets, A. van Donkelaar, R. M. Yantosca (2011), Sources, distribution, and acidity of sulfate-ammonium aerosol in the Arctic winter-spring, Atmos. Environ., 45, 7301-7318, doi:10.1016/j.atmosenv.2011.030.

Fischer, H., D. Wagenbach and J. Kipfstuhl (1998), Sulfate and nitrate firn concentrations on the Greenland ice sheet. 2. Temporal anthropogenic deposition changes. J. Geophys. Res.,103(D17), 21,935–21,942.

Fuhrer, K., A. Neftel, M. Anklin, T. Staffelbach, and M. Legrand (1996), High-resolution ammonium ice core record covering a complete glacial-interglacial cycle, J. Geophys. Res., 101(D2), 4147–4164, doi:10.1029/95JD02903.

Grinsted, A., J.C. Moore and S. Jevrejeva (2004), Application of the cross wavelet transform and wavelet coherence to geophysical time series, Nonlinear Processes Geophys., 11, 561-566.

Grinsted, A., J. C. Moore, V. Pohjola, T. Martma, and E. Isaksson (2006), Svalbard summer melting, continentality and sea ice extent from the Lomonosovfonna ice core, J. Geophys. Res., 111, D07110, doi:10.1029/2005JD006494.

Goto-Azuma, K., S. Koshima, T. Kameda, S. Takahashi, O. Watanabe, Y. Fujii, and J.-O. Hagen (1995), An ice-core chemistry record from Snøfjellafonna, northwestern Spitsbergen, Ann. Glaciol., 21, 213-218.

Goto-Azuma, K., and R.M. Koerner (2001), Ice core studies of anthropogenic sulfate and nitrate trends in the Arctic, J. Geophys. Res., 106, 4959-4969.

Groves, D. G., and J. A. Francis (2002), Variability of the Arctic atmospheric moisture budget from TOVS satellite data, J. Geophys. Res., 107(D24), 4785, doi:10.1029/2002JD002285.

Grumet, N. S., C. P. Wake, G. A. Zielinski, D. Fisher, R. Koerner, and J. D. Jacobs (1998), Preservation of glaciochemical time-series in snow and ice from the Penny Ice Cap, Baffin Island, *Geophys. Res. Lett.*, 25(3), 357-360, doi:10.1029/97/GL03787.

Iizuka, Y., M. Igarashi, K. Kamiyama, H. Motoyama, and O. Watanabe (2002), Ratios of Mg^{2+}/Na+ in snowpack and an ice core at Austfonna ice cap, Svalbard, as an indicator of seasonal melting, *J. Glaciol.*, 48(162), 452-460.

Isaksson, E., V. A. Pohjola, T. Jauhiainen, J. C. Moore, J-F. Pinglot, R. Vaikmaäe, R. S. W. van de Wal, J-O. Hagen, J. Ivask, L. Karlöf, T. Martma, H.A.J. Meijer, R. Mulvaney, M. Thomassen, M. van den Broeke (2001), A new ice core record from Lomonosovfonna, Svalbard: Viewing the data between 1920– 1997 in relation to present climate and environmental conditions, *J. Glaciol.*, 47(157), 335– 345, doi:10.3189/172756501781832313

Isaksson, E., J. Kohler, V. Pohjola, J. C. Moore, M. Igarashi, L. Karlöf, T. Martma, H. A. J. Meijer, H. Motoyama, R. Vaikmäe, and R. S. van de Wal (2005), Two ice-core $\delta^{18}O$ records from Svalbard illustrating climate and sea-ice variability over the last 400 years, *The Holocene,* 15(4), 501-509.

Isaksson, E., T. Kekonen, J. C. Moore, and R. Mulvaney (2006), The methansulfonic acid (MSA) record in a Svalbard ice core, *Ann. Glaciol.,* 42(1), 345-351.

Iversen, T. and E. Joranger (1985), Arctic air pollution and large scale atmospheric flows, *Atmos. Environ.,* 19, 2099-2108.

Jickells, T. D., S. D. Kelly, A. R. Baker, K. Biswas, P. F. Dennis, L. J. Spokes, M. Witt, and S. G. Yeatman (2003), Isotopic evidence for a marine ammonia source, *Geophys. Res. Lett.*, 30(7), 1374, doi:10.1029/2002GL016728.

Johnson, M. T., P. S. Liss, T. G. Bell, T. J. Lesworth, A. R. Baker, A. J. Hind, T. D. Jickells, K. F. Biswas, E. M. S. Woodward, and S. W. Gibb (2008), Field observations of the ocean-atmosphere exchange of ammonia: Fundamental importance of temperature as revealed by a comparison of high and low latitudes, *Global Biogeochem. Cycles*, 22, GB1019, doi:10.1029/2007GB003039.

Kameda, T., S. Takahashi, K. Goto-Azuma, S. Kohshima, O. Watanabe, and J.-O. Hagen (1993), First report of ice core analyses and borehole temperatures on the highest ice field on western Spitsbergen in 1992, *Bull. Glac. Res.*, 11, 51-62.

Kang, S., P. A. Mayewski, Y. Yan, D. Qin, T. Yao, and J. Ren (2003), Dust records from three ice cores: Relationships to spring atmospheric circulation over the Northern Hemisphere, *Atmos. Environ.,* 37, 4823–4835.

Keene, W. C., A. A. P. Pszenny, J. N. Galloway, and M. E. Hawley (1986), Sea-Salt Corrections and Interpretation of Constituent Ratios in Marine Precipitation, *J. Geophys. Res.*, 91(D6), 6647–6658, doi:10.1029/JD091iD06p06647.

Kekonen, T., J. C. Moore, R. Mulvaney, E. Isaksson, V. Pohjola, and R. S. van de Wal (2002), A 800 year record of nitrate from the Lomonosovfonna ice core, Svalbard, *J. Glaciol.,* 35, 261-265.

Kekonen, T., P. Perämäki, and J. C. Moore (2004), Comparison of analytical results for chloride, sulfate and nitrate obtained from adjacent ice core samples by two ion chromatograph methods, *J. Environ. Monit.*,6, 147-152.

Kekonen, T., J. C. Moore, P. Perämäki, R. Mulvaney, E. Isaksson, V. Pohjola, and R. S. W. van de Wal (2005), The 800 year long ion record from the Lomonosovfonna (Svalbard) ice core, *J. Geophys. Res.*, 10, doi:1029/2004JD005223.

Klimenko, V. V., A. V. Klimenko, and A. G. Tereshin (2000), Reducing emissions of trace greenhouse gases as an alternative to reducing emissions of carbon dioxide: Part II, *Thermal. Eng.*, 47(6), 476-493.

Koenigk, T., U. MikolajewiczJ. H. Jungclaus, A. Kroll (2009), Sea ice in the Barents Sea: seasonal to interannual variability and climate feedbacks in a global coupled model, *Clim. Dyn.*, 32, 1119–1138, doi: 10.1007/s00382-008-0450-2.

Koerner, R.M. (1979), Accumulation, ablation, and oxygen isotope variations of the Queen Elisabeth Island ice caps, Canada, *J. Glaciol.*, 22, 86, 25-41.

Kreutz, K. J., P. A. Mayewski, S. I. Whitlow and M. S. Twickler (1998), Limited migration of soluble ionic species in a Siple Dome, Antarctica, ice core. *Ann. Glaciol.*, 27, 371-377.

Kvingedal, B. (2005), Sea Ice Extent and variability in the Nordic Seas 1967-2002, The Nordic Seas: an integrated perspective, Helge Drange, AGU, ISBN-13:978-0-87590-423-8.

Hynes, A.J., P.H. Wine, and D.H. Semmes (1986), Kinetics and mechanism of OH reactions with organic sulfides, *J. Phys. Chem.*, 90, 4148-4156.

Lefauconnier, B., J.-O. Hagen, and J.-P. Rudant (2001), Flow speed and calving rate of Kongsbreen glacier, Svalbard, using SPOT images, *Polar Res.,* 59-65.

Legrand, M., C. Hammer, M. De Angelis, J. Savarino, R. Delmas, H. Clausen, and S. J. Johnsen (1997), Sulfur-containing species (methanesulfonate and SO_4) over the last climatic cycle in the Greenland Ice Core Project (central Greenland) ice core, *J. Geophys. Res.*, 102(C12), 26,663–26,679, doi:10.1029/97JC01436.

Matoba, S., H. Narita, H. Motoyama, K. Kamiyama, and O. Watanabe (2002). Ice core chemistry of Vestfonna ice cap in Svalbard, Norway. *J. Geophys. Res.*,107, doi:10.1029/2002JD002205.

Moore, J. C., A. Grinsted, T. Kekonen, and V. Pohjola (2005), Separation of melting and environmental signals in an ice core with seasonal melt, Geophys. Res. Lett., 32, L10501, doi:10.1029/2005GL023039.

Moore, J. C., T. Kekonen, A. Grinsted, and E. Isaksson (2006), Sulfate source inventories from a Svalbard ice core record spanning the Industrial Revolution, J. Geophys. Res., 111, D15307, doi:10.1029/2005JD006453.

Moore, J. C. and A. Grinsted (2009), Ion fractionation and percolation in ice cores with seasonal melting, Physics of Ice Core Records II, Supplement Issue of Low Temperature Science, 68.

Moore, J. C., E. Beaudon, S. Kang, D. Divine, E. Isaksson, V.A. Pohjola, R .S.W. van de Wal (2012), Dating ice cores using statistical extraction of volcanic sulfate, J. Geophys. Res., 111, D15307, doi:10.1029/2005JD006453.

Morison, J., K. Aagaard, M. Steele (2000), Recent environmental changes in the Arctic: A Review, Arctic, 53, 4, 359-371.

Mulvaney, R., E. C. Pasteur, D. A. Peel, E. S. Saltzman and P.-Y. Whung (1992) The ratio of MSA to non-sea-salt sulphate in Antarctic Peninsula ice cores. Tellus, 44B(4), 295–303.

Nye, J. F. (1963), Correction factor for accumulation measured by the thickness of the annual layers in an ice sheet, J. Glaciol., 4(36), 785-788.

O'Dwyer, J., E. Isaksson, T. Vinje, T. Jauhiainen, J. C. Moore, V. Pohjola, R. Vaikmäe, and R. S. van de Wal (2000), Methansulfonic acid in a Svalbard ice core as an indicator of ocean climate, Geophys. Res. Lett., 27(8), 1159-1162.

Overpeck, J., K. Hughen, D. Hardy, R. Bradley, R. Case, M. Douglas, B. Finney, K. Gajewski, G. Jacoby, A. Jennings, S. Lamoureux, A. Lasca, G. MacDonald, J. Moore, M. Retelle, S. Smith, A. Wolfe, and G. Zielinski (1997), Arctic environmental changes of the last four centuries. Science, 278, 1251–1256.

Pasteur, E. and R. Mulvaney (2000), Migration of methane sulphonate in Antarctic firn and ice. *J. Geophys. Res*., 105(D9),11,525-11,534.

Pohjola, V.A., J. C. Moore, E. Isaksson, T. Jauhiainen, R. S. van de Wal, T. Martma, H. A. J. Meijer, and R. Vaikmäe (2002a), Effect of periodic melting on geochemical and isotopic signals in an ice core from Lomonosovfonna, Svalbard, *J. Geophys. Res.,* 107(04), 1-14.

Pohjola, V.A., T .Martma, H. A. J. Meijer, J. C. Moore, E. Isaksson, R. Vaikmäe and R. S. W. van de Wal (2002b), Reconstruction of three centuries of annual accumulation rates based on the record of stable isotopes of water from Lomonosovfonna, Svalbard. *Ann. Glaciol.*, 35, 57-62.

Pinglot, J. F., M. Pourchet, B. Lefauconnier, J. O. Hagen, E. Isaksson, R. Vaikmaë, and K. Kamiyama (1999), Investigations of temporal change of the accumulation in Svalbard glaciers deducted from nuclear tests and Chernobyl reference layers, *Polar Res.*, 18, 315– 321, doi:10.1111/j.1751-8369.1999.tb00309.x.

Ruggirello, R. M., M. H. Hermanson, E. Isaksson, C. Teixeira, S. Forsström, D. C. G. Muir, V. Pohjola, R. S. van de Wal, and H. A. J. Meijer (2010), Current-use and legacy pesticide deposition to ice caps on Svalbard, Norway, *J. Geophys. Res.*, 115 (D18308), doi:10.1029/2010JD014005.

Sakshaug, E. and J. Walsh (2000), Marine biology: biomass, productivity distribution and their variability in the Barents and Bering Seas, *Nuttall, M. and T.V. Callaghan, eds. The Arctic: environment, people, policy. Amsterdam, etc., Harwood Academic Publisher.:* 161-196.

Samuelsson, H. (2001), Distribution of melt layers on the ice field Lomonosovfonna, Spitsbergen, M.S. thesis, Dep. of Earth Sciences, Uppsala Univ., Uppsala, Sweden.

Shugui, H., Q. Dahe, Z. Dongqi, K. Shichang, P. A. Mayewski, and C. P. Wake (2003), A 154a high-resolution ammonium record from the Rongbuk Glacier, north slope of Mt. Qomolangma (Everest), Tibet-Himal region, *Atmos. Environ.*, 37, 721–729 doi:10.1016/S1352-2310(02)00582-4.

Sjögren, B., O. Brandt, C. Nuth, E. Isaksson, V. Pohjola, J. Kohler, and R. S. van de Wal (2007), Determination of firn density in ice cores using image analysis, *J. Glaciol.*, 53(182), 413-419.

Solberg, S., N. Schmidbauer, A. Semb, F. Stordal and Ø. Hov (1996), Boundary-layer ozone depletion as seen in the Norwegian Arctic in spring, *J. Atm. Chem.*, 23(3),301-332, doi:10.1007/BF00055158.

Sommer, W. (2005), Reconstruction of surface temperature variations from temperature measurements along a medium-depth borehole at Holtedahlfonna, Svalbard, bachelor thesis, Institute for Marine and Atmospheric research Utrecht, Utrecht University, The Netherlands.

Spokes, L.J., Yeatman, S.G., Cornell, S.E., Jickells, T.D., (2000), Nitrogen deposition to the eastern Atlantic Ocean. The importance of south-easterly flow. *Tellus* 52B, 37–49.

Strass, V. H., and E-M. Nöthig (1996), Seasonal shifts in ice edge phytoplankton blooms in the Barents Sea related to the water column stability, *Polar Biol.*, 16(6), 409-422, doi: 10.1007/BF02390423.

Teinilä, K., R. Hillamo, V.-M. Kerminen, and H. J. Beine (2003), Aerosol chemistry during the NICE dark and light campaigns, Atmos. Environ., 37, 563–575. doi:10.1016/S1352-2310(02)00826-9.

Treffeisen, R., R. Krejci, J. Ström, A. C. Engvall, A. Herber, and L. Thomason (2007) Humidity observations in the Arctic troposphere over Ny-Ålesund, Svalbard based on 15 years of radiosonde data, *Atmos. Chem. Phys.*, 7, 2721–2732.

Virkkunen, K. (2004), Snowpit studies in 2001-2002 in Lomonosovfonna, Svalbard, M.S. thesis, Dep. of Chem., Oulu Univ., Oulu, Finland.

Virkkunen, K., J. C. Moore, E. Isaksson, V. Pohjola, P. Perämäki, A. Grinsted, and T. Kekonen (2007), Warm summers and ion concentrations in snow: comparison of present day with Medieval Warm Epoch from snow pits and an ice core from Lomonosovfonna, Svalbard, *J. Glaciol.,* 53(183), 623-634.

van de Wal, R. S. W., R. Mulvaney, E. Isaksson, J. C. Moore, J.-F. Pinglot, V. Pohjola, and M. P. A. Thomassen (2002), Reconstruction of the historical temperature trend from measurements in a medium-length borehole on the Lonomosovfonna Plateau, Svalbard, *Ann. Glaciol.*, 35, 371–378.

van der Wel, L. G., H. J. Streurman, E. Isaksson, M. M. Helsen, R. S. van de Wal, T. Martma, V. Pohjola, J. C. Moore, and H. A. J. Meijer (2011), Using high resolution tritium profiles to quantify the effects of melt on two Spitsbergen ice cores, *J. Glaciol.,*57(206),1087-1096.

Watanabe, O., H. Motoyama, M. Igarashi, K. Kamiyama, S. Matoba, K. Goto-Azuma, H. Narita, T. Kameda (2001), Studies on climatic and environmental changes during the last few hundred years using ice-cores from various sites in Nordaustlandet, Svalbard, *National Institute of Polar Research Memoirs*, 54 (special issue), 227–242.

Weiler, K., H. Fischer, F. Diedrich, U. Ruth, F. Wilhelms, H. Miller (2005), Glaciochemical reconnaissance of a new ice core from Severnaya Zemlya, Eurasian Arctic. J. Glaciol., 51 (172), 64-74(11), doi:10.3189/172756505781829629.

Whung, P.-Y., E. S. Saltzman, M. J. Spencer, P. A. Mayewski, and N. Gundestrup (1994), Two-hundred-year record of biogenic sulfur in a south Greenland ice core (20D), *J. Geophys. Res.*, 99(D1), 1147–1156, doi:10.1029/93JD02732.

Wu, B., J. Wang, J. Walsh (2004), Possible Feedback of Winter Sea Ice in the Greenland and Barents Seas on the Local Atmosphere, *Mon. Wea. Rev.*, 132, 1868–1876, doi: 10.1175/1520-0493(2004)132<1868:PFOWSI>2.0.CO;2